SYNTHETIC STUDY OF A PHOTOGATED ION CHANNEL

by

Gordon Grant Cross
B.Sc., University of Toronto, 1973
M.Sc., University of Alberta, 1979

A Dissertation Submitted in Partial Fulfillment of the
Requirements for the Degree of

DOCTOR OF PHILOSOPHY

in the Department of Chemistry

We accept this thesis as conforming
to the required standard

Dr. T.M. Fyles, Supervisor (Department of Chemistry)

Dr. G.A. Poulton, Departmental Member (Department of Chemistry)

Dr. P.C. Wan, Departmental Member (Department of Chemistry)

Dr. W.W. Kay, Outside Member (Department of Biochemistry)

Dr. B.A. Keay, External Examiner (University of Calgary)

© GORDON GRANT CROSS, 1994

University of Victoria

All rights reserved. Dissertation may not be reproduced in whole or in part, by
photocopying or other means, without the permission of the author.

Supervisor: Dr. Thomas M. Fyles

ABSTRACT

The project target was a photogated unimolecular ion channel, derived from a previously prepared ion transporter which is comprised of an 18-crown-6 tetracarboxylate core bearing four identical amphiphilic wall / polar head units. The target structure has one of the four groups replaced by an azobenzene moiety linked via a tertiary amide to the crown ether core. In the thermally stable *trans* configuration a pendant ammonium group should occupy the central cavity of the crown ether.

The azobenzene component was prepared by coupling the aromatic diazonium salt derived from *t*BOC protected 4-(2-aminoethyl)aniline to resorcinol mono-*O*-substituted with a THP-protected ethylene glycol arm ultimately intended to link to the crown ether. The regiochemistry of this reaction could not be proven by normal spectral methods, but was established by both an unambiguous synthesis and an NMR ^{13}C - ^{13}C correlation spectrum. Careful acid hydrolysis removed the THP group in the presence of the *t*BOC group. Addition of a wall unit bearing a glycol head group, protected as its isopropylidene derivative, afforded the target photogate ready for coupling to the crown ether component.

The original strategy to substitute a tertiary amide group at only one of the four identical crown ether carboxylate positions was an intramolecular capping reaction across the dianhydride derived from the crown tetracarboxylate, followed by selective cleavage of one end of the cap, but this approach was completely unsuccessful. Simple addition of one equivalent of amine to the crown ether dianhydride produced predominantly the diamide. Reaction of the dianhydride with one equivalent of water followed by one equivalent of benzylamine gave the desired monoamide in good yield, but this result was far from general. In the comparable reaction using even a simple aliphatic secondary amine epimerization at the α carbon of the crown ether was a significant competing reaction. In the comparable reactions of the dianhydride with functionalized amines, secondary or primary, both epimerization and other undetermined side reactions led to inseparable complex mixtures of products. These results call into question the future of the 18-crown-6 tetracarboxylate as a molecular framework.

Examiners:

Dr. T.M. Fyles, Supervisor (Department of Chemistry)

Dr. G.A. Poulton, Departmental Member (Department of Chemistry)

Dr. P.C. Wan, Departmental Member (Department of Chemistry)

Dr. W.W. Kay, Outside Member (Department of Biochemistry)

Dr. B.A. Keay, External Examiner (University of Calgary)

TABLE OF CONTENTS

TITLE PAGE i

ABSTRACT ii

TABLE OF CONTENTS iv

LIST OF TABLES vi

LIST OF FIGURES vii

LIST OF SCHEMES x

LIST OF ABBREVIATIONS xii

ACKNOWLEDGEMENTS xiii

CHAPTER 1 INTRODUCTION 1

- 1.1 Transmembrane Ion Transport 1
  - 1.1.1 Natural Ion Transporters 1
  - 1.1.2 Artificial Ion Transporters 4
- 1.2 Proposed Project 23
  - 1.2.1 General Considerations 23
  - 1.2.2 Monofunctionalized Crown Ether 27
  - 1.2.3 Photogate 30
  - 1.2.4 Target Compound 40
  - 1.2.5 Evaluation 43

CHAPTER 2 RESULTS AND DISCUSSION 44

- 2.1 Synthesis of the Photogate 44
  - 2.1.1 Azo Coupling Reaction 46
  - 2.1.2 Regiochemistry of Azo Coupling Reaction 49
  - 2.1.3 Blocking Group Manipulation 66
- 2.2 Monofunctionalized Crown Ether 76
  - 2.2.1 Capping Reaction 76
  - 2.2.2 Bulk Addition 80
  - 2.2.3 Reactions of the Crown Ether Dianhydride with Simple Amines 83

2.2.4 Bulk Addition Preceded by Water 89
    i) benzylamine 89
    ii) di-n-butylamine 90
    iii) target amine **44** 95
    iv) excess benzylamine 103
    v) other primary amines 105
2.2.5 Reaction Using DCC 105

2.3 Summary and Prospects 106

CHAPTER 3 EXPERIMENTAL 110

APPENDIX ^{13}C NMR spectra of new compounds 146

REFERENCES 166

LIST OF TABLES

Table 1 Normalized ion transport rates for candidate transporters 17

Table 2 Optical rotation values for recovered tetraacid 99

Table 3 Optical rotation values for products of the monofunctionalization reaction 99

LIST OF FIGURES

Figure 1 Ion transport mechanisms 2

Figure 2 Structures of gramicidin A and amphotericin B 6

Figure 3 Examples of artificial ion channels 9

Figure 4 A Lehn "bouquet" molecule 10

Figure 5 Schematic and chemical structure of an ion channel mimic 11

Figure 6 Components of candidate transporters with assigned mechanisms 17

Figure 7 Typical pH-stat plot 18

Figure 8 Cartoon of possible gating mechanisms 24

Figure 9 Schematic structure of target compound 26

Figure 10 Cyclic imide formation from secondary amide 29

Figure 11 Twisted intramolecular charge transfer compound 31

Figure 12 Spiropyran / merocyanine photochemical switch 31

Figure 13 The *trans* - *cis* isomerization of azobenzene 32

Figure 14 Possible *trans* - *cis* isomerization mechanisms 33

Figure 15 Azobenzene and azopyridine capped crown ethers 37

Figure 16 The Shinkai "butterfly" compound and the compound using phenoxide assisted binding 38

Figure 17 The Shinkai "tail-biting" compound 39

Figure 18 Proposed target compound 41

Figure 19 Photogate target 44

Figure 20 Resonance structure of the diazonium ion 46

Figure 21 S_E2 reaction mechanism 48

Figure 22 Diazotate formation 48

Figure 23 Predicted and observed ^{13}C NMR chemical shifts 52

Figure 24 Heteronuclear 2D NMR spectrum (J = 130 Hz) of **20** 54

Figure 25 Heteronuclear 2D NMR spectrum (J = 130 Hz) of **19** 55

Figure 26 Heteronuclear 2D NMR spectrum (J = 7 Hz) of **20** 56

Figure 27 Proposed mechanism for the Wallach rearrangement 59

Figure 28 ^{13}C - ^{13}C INADEQUATE spectrum of **23** 63

Figure 29 Mechanism proposed for loss of the six-carbon arm 69

Figure 30 Amide hydrolysis by *cis* $[Co(trpn)(H_2O)_2]$ 70

Figure 31 ^{13}C NMR spectrum of **38** 74

Figure 32 ^{13}C NMR spectrum of photogate target **13** 75

Figure 33 ^{13}C NMR spectrum of typical capping reaction product 78

Figure 34 Alcohol / amine capping substrates 79

Figure 35 ^{13}C NMR spectrum of **42** 82

Figure 36 Expanded methine region of the ^{1}H NMR spectrum of **48** 85

Figure 37 ^{13}C NMR spectrum of monoamide **53** 91

Figure 38 Expanded methine and carbonyl regions of ^{13}C NMR spectrum of **53** 92

Figure 39 ^{1}H NMR spectrum of monoamide **53** 93

Figure 40 Expanded methine region of the ^{1}H NMR spectrum of **53** 94

Figure 41 Expanded methine region of the ^{13}C NMR spectrum of purported **10** 97

Figure 42 Expanded methine region of the ^{1}H NMR spectrum of **48** **104**

Figure 43 Rate of thermal back reaction from *cis* to *trans* isomer 122

Figure 44 ^{13}C NMR spectrum of mono-*O*-*t*-butyldimethylsilyl resorcinol 147

Figure 45 ^{13}C NMR spectrum of compound **18** 148

Figure 46 ^{13}C NMR spectrum of compound **20** 149

Figure 47 ^{13}C NMR spectrum of compound **19** 150

Figure 48 ^{13}C NMR spectrum of compound **21** 151

Figure 49 ^{13}C NMR spectrum of compound **22** 152

Figure 50 ^{13}C NMR spectrum of compound **24** 153

Figure 51 ^{13}C NMR spectrum of compound **23** 154

Figure 52 ^{13}C NMR spectrum of compound **29** 155

Figure 53 ^{13}C NMR spectrum of compound **30** 156

Figure 54 ^{13}C NMR spectrum of compound **28** 157

Figure 55 ^{13}C NMR spectrum of compound **33** 158

Figure 56 ^{13}C NMR spectrum of compound **34** 159

Figure 57 ^{13}C NMR spectrum of compound **37** 160

Figure 58 ^{13}C NMR spectrum of compound **40** 161

Figure 59 ^{13}C NMR spectrum of compound **41** 162

Figure 60 ^{13}C NMR spectrum of compound **8** 163

Figure 61 ^{13}C NMR spectrum of compound **44** 164

Figure 62 ^{13}C NMR spectrum of compound **47** 165

LIST OF SCHEMES

Scheme 1	Coupling using the Me_4N^+ carboxylate method	14
Scheme 2	Capping reaction to make photoionophores	28
Scheme 3	Proposed capping / hydrolysis route	29
Scheme 4	Diazonium salt coupling to monosubstituted resorcinol	46
Scheme 5	Hydrolysis of reaction mixture to a single product	50
Scheme 6	Model azo coupling reaction	51
Scheme 7	Azo coupling reaction with acetyl-protected amine	58
Scheme 8	Synthesis of substrate for Wallach rearrangement	60
Scheme 9	Photochemical Wallach rearrangement	60
Scheme 10	Addition of second arm in model series	65
Scheme 11	Synthesis of the six-carbon wall / head unit	67
Scheme 12	Synthesis of the fully protected photogate	67
Scheme 13	Proposed selective blocking route	68
Scheme 14	Azo coupling reaction with tBOC-protected amine	71
Scheme 15	Complete synthesis of photogate target	72
Scheme 16	Preliminary bulk addition reaction	80
Scheme 17	Proposed bulk additon of amine **44**	81
Scheme 18	Bulk addition of benzylamine	84
Scheme 19	Proposed bulk addition of di-n-butylamine	88

Scheme 20 Bulk addition preceded by water to give monoamide **53** 89

Scheme 21 Bulk addition of di-n-butylamine preceded by water 95

Scheme 22 Bulk addition of amine **44** preceded by water 96

LIST OF ABBREVIATIONS

Ac	acetyl
Ar	aromatic
DCC	N,N'-dicyclohexylcarbodiimide
DMA	N,N-dimethylacetamide
DMF	N,N-dimethylformamide
DMSO	dimethylsulfoxide
ESR	electron spin resonance
FCCP	carbonylcyanide 4-(trifluoromethoxy)phenylhydrazone
IR	infrared
HPLC	high pressure liquid chromatography
mp	melting point
MS	mass spectrum
NMR	nuclear magnetic resonance
tBOC	*tert*-butyloxycarbonyl
THF	tetrahydrofuran
THP	2-tetrahydropyranyl
TLC	thin layer chromatography
TMS	tetramethylsilane

Mass spectral data

CI	chemical ionization
EI	electron impact
FAB	fast atom bombardment

NMR spectral data

Ar	aromatic
br	broad
d	doublet
FT	Fourier transform
m	multiplet
q	quartet
s	singlet
t	triplet

ACKNOWLEDGEMENTS

I would like to express my thanks to Dr. Tom Fyles for his help and guidance throughout this project. Many thanks are due to many co-workers, past and present, for their support and advice, and for a good working environment. I would like to acknowledge the assistance of the technical staff of the University of Victoria Chemistry department, in particular Mrs. Christine Greenwood. Financial assistance in the form of awards from the B.C. Science Council and the University of Victoria was much appreciated. And finally, I am grateful to my family for their support throughout the long course of my education.

CHAPTER 1 INTRODUCTION

1.1 Transmembrane Ion Transport

1.1.1 Natural Ion Transporters

An essential feature of living cells and the organelles within them is a separate internal environment created and maintained across the surrounding phospholipid bilayer and, among other things, metal ions must constantly be moved in and out in a controlled way[1]. This must be facilitated by some sort of transporter as the energy barrier is large - about 155 kcal/mole to move a Na^+ ion from water to the middle of a 30 Å thick bilayer[2] - and obviously just opening a hole would indiscriminately empty the cell. The basic mechanistic possibilities for transport are illustrated in Figure 1 as a carrier, a channel and a stepwise relay mechanism between multiple sites. A carrier would be an encapsulating or complexing molecule which moves with respect to the membrane so it is exposed alternately to the two aqueous phases. For good mobility it should be relatively small. Many naturally occurring ion carriers are known but not as mediators of normal metabolism; along with nonspecific membrane disrupting compounds they arise as agents of chemical warfare among microorganisms and so have found wide use as antibiotics[3]. As carriers tend to be small, structural and functional mimics are more easily synthesized so that a large number have been made and structure / activity relationships established. This broad subject has recently been reviewed by Fyles[4] and Tsukube[5]. A channel (or a pore - in general a less specific aggregate structure) would be a long tubular or helical molecule which does not move with respect to the membrane and is exposed simultaneously to both aqueous phases, so it must have at least one control point or "gate"

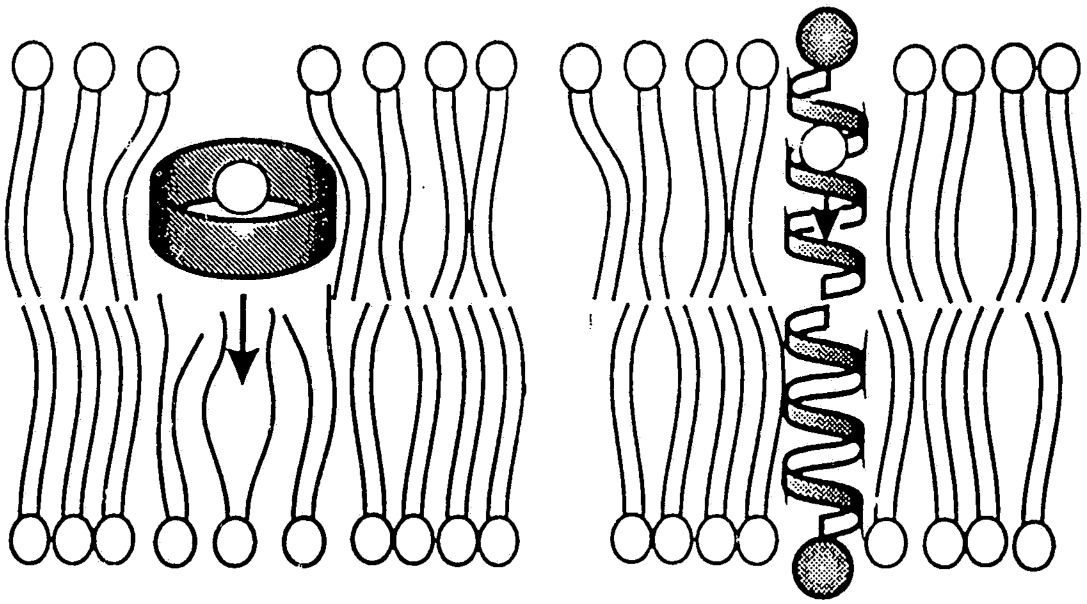

Carrier

Channel

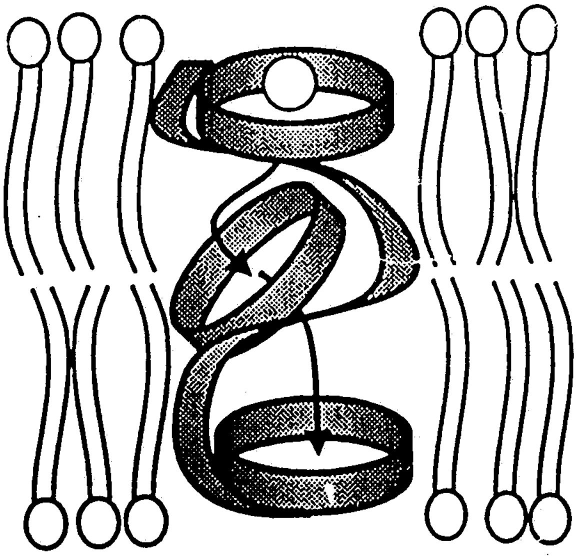

Relay

Figure 1. Ion transport mechanisms.

to prevent wholesale leakage and to impose selectivity.

It can be shown that kinetically these simplistic models are not distinct but are the limiting cases of a continuum of mechanistic possibilities. This continuum is best modelled as a channel which can assume a number of states, each with a distinct free energy profile[6]. This makes sense intuitively considering that as soon as an ion moves to occupy a different site in the channel the entire system is in a different state with a different free energy profile. Whether the kinetic behavior resembles a carrier or channel depends on the energy profile of each significant state and the rate of flipping between states relative to the rate of ion movement. For instance simplistic carrier behavior is approached by a two state channel where in one state there is a very large energy barrier at one interface and a very small barrier at the other interface, and in the other state the barriers are reversed. A simplistic channel is approached by having a large number of small energy barriers in each state, with state changes being very fast with respect to ion movement (when state changes are very slow with respect to ion movement then observed behavior is just a weighted average of the behaviors in all states). Clearly the stepwise mechanism falls somewhere between these two limiting cases. This model is appropriate to describe real ion transporting proteins, many of which have been shown to fluctuate between multiple conformational states although intimate mechanistic details are not yet known for any real proteins. The most thoroughly studied is probably the proton transporter bacteriorhodopsin which undergoes several protein conformational changes in concert with changes in the rhodopsin chromophore during the transport cycle. It is thought that proton transport through the restrictive part of the bacteriorhodopsin channel is done by hopping between side chain and channel-bound water sites although confirmation of this idea awaits a more detailed structure of the protein[7]. It is easy enough to picture a metal ion moving by hopping between adjacent sites along a stationary channel with ligand-metal interactions at each site replacing some (probably not all) of the ion hydration sphere. The rate of transport would depend on metal ion concentration in a complex way since ion concentration affects both the distribution between states and the kinetic behavior of each state. As mentioned above the relative rates of fluctuation between states and ion movement are important and in the case of real transport proteins the time scale of the former varies from the second to the picosecond range so a variety of complex kinetic behaviors is expected. Note that any mechanism on the continuum can involve ion pumping, where externally supplied energy raises the transporter to a state of higher energy and this energy ultimately drives the ion transport against a gradient. Note also that any mechanism is amenable to gating; in the case of a simple carrier this most easily visualized as a change in the ion-binding characteristics of the carrier while for a simple channel it would just be plugging the hole.

1.1.2 Artificial Ion Channels

Natural ion channels are highly efficient and selective but are only stable within a very limited "natural" environment and this limits their use in practical devices such as sensors or molecular switches. There is therefore a need for more stable artificial mimics which could also be much smaller and simpler. These are *functional* mimics but of course a certain amount of *structural* mimicry is used in their design. Naturally occurring ion channels are generally proteins of very high molecular weight which transport ions between helical segments in a poorly defined way but the smaller channel-forming antibiotics can provide design suggestions. A widely studied example is gramicidin A, an oligopeptide of 15 amino acids of alternating D- and L- chirality which forms a β-helical structure with a 4 Å internal diameter[8]. As a hydrogen-bonded end-to-end dimer it is 26 Å long, the minimum to span a lipid bilayer membrane with the help of some "dimpling" of the membrane surface. The amide groups line the internal surface while hydrophobic side-chains face the outside; thus the structure interacts favorably with the membrane lipids while at the same time stabilizing ion transit along the helical axis[8]. A computational examination of a cation within the gramicidin channel[9] concluded that there are always at least two water molecules in the first hydration sphere of the ion during transit so the channel does not have to provide a full co-ordination sphere; in addition the partially hydrated species faces lower energy barriers than a naked cation.

Similar design suggestions are provided by amphotericin B, a macrocyclic antibiotic that forms pores in sterol containing bilayer membranes as aggregates of 12 - 20 molecules, again end to end dimerized to span the membrane[10]. The macrocycles each have one hydrocarbon edge which faces out towards the membrane lipids and one polar polyol edge which faces inwards to line the pore. A polar mycosamine head group interacts with the polar surface and serves to orient the amphotericin molecules perpendicular to the bilayer plane. These suggestions can be combined with chemical common sense to decide that an artificial channel should have[11]: i) the length to span a lipid bilayer membrane as either a single molecule or a dimer; a single molecule would then have a molecular weight of at least 3500 - 4000 ii) an internal hole of defined

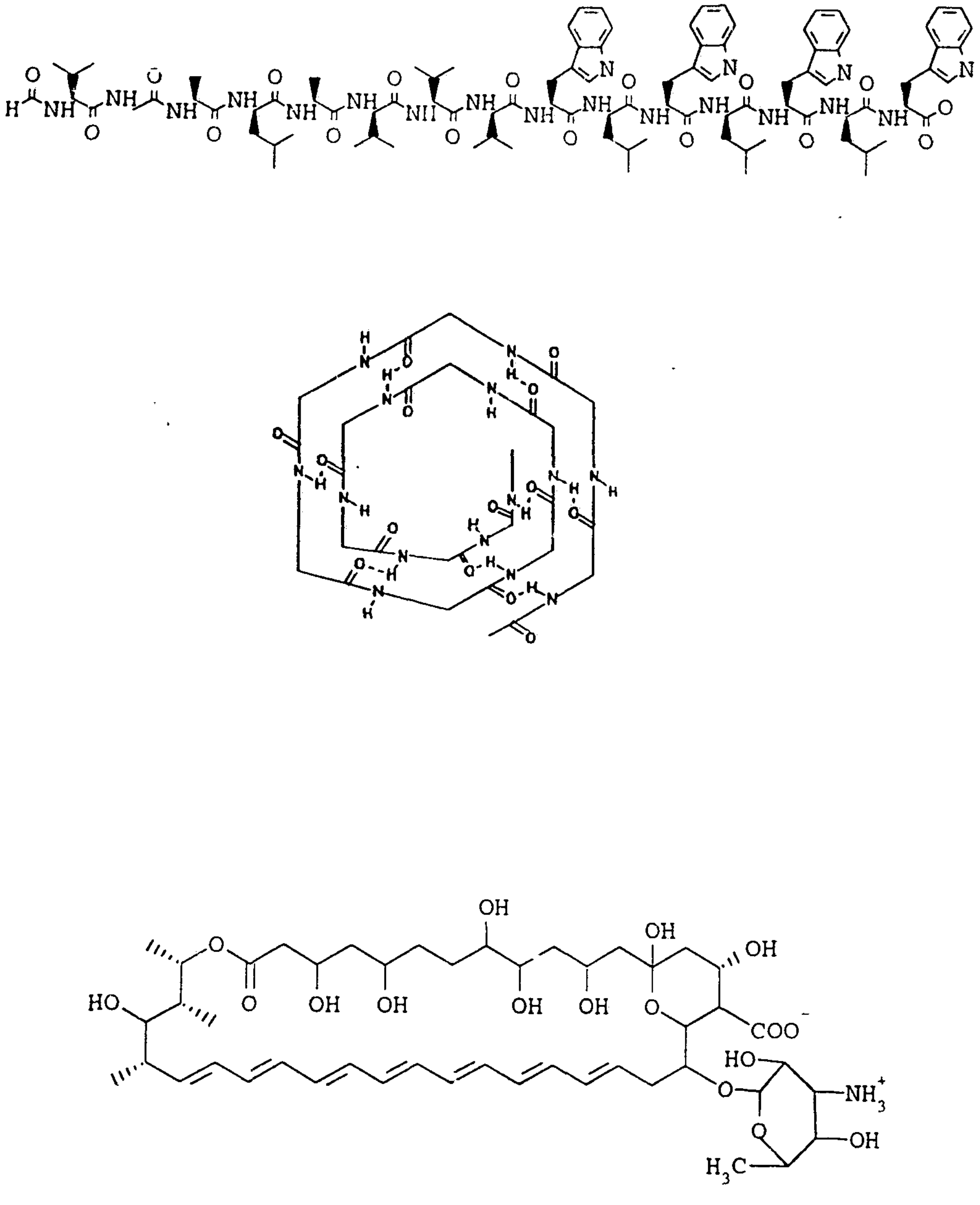

Figure 2. Top: Linear gramicidin A. Centre: Helical gramicidin. Bottom: Amphotericin B.

diameter to give selectivity; for a discreet channel molecule this implies a certain amount of rigidity and for an aggregate it implies an affinity for self-association iii) a hydrophobic outside to interact favorably with the membrane interior, a polar or amphiphilic interior to stabilize an ion in transit without binding it irreversibly, and polar head groups to interact with the membrane exterior and thus orient the long axis perpendicular to the membrane iv) the ability to insert into the membrane, which means for a single molecule channel that the head groups are only moderately polar so that they interact with the membrane exterior and the aqueous phase but are not so polar that insertion is energetically expensive; it also means a roughly cylindrical shape because a head group much larger than the tail promotes formation of micelles while a head much smaller than the tail favours reverse micelles[11] v) a feasible synthesis, as formidable problems in purification and characterization are inevitable with a molecule of this size.

Attempts to synthesize artificial ion channels have relied to some extent on structural mimicry, the most obvious strategy being that of Stankovic et.al.[12] who simply replaced the H-bonding interaction with a covalent link between two gramicidin monomers. This compound is of incidental interest to this thesis since it exhibited uncontrolled gating behavior as the dioxolane covalent link undergoes a conformational flip that temporarily blocks the channel. Some other gramicidin structural mimics[13] tended to form aggregates which allowed ion transport with poor selectivity, suggesting non-specific membrane disruption reminiscent of melittin, a component of bee venom[14]. Much work has gone into synthesizing helical peptides that are structural mimics of natural ion channels but this broad topic is beyond the scope of this discussion and the channel pathways are between the helices rather than within them[15].

Synthetic transporters from a number of research groups have been suggested to be aggregate pore formers, generally exhibiting poor ion selectivity and a kinetic order in transporter greater than one[16,17]. In these cases a unique well formed pore is less likely than a population of ion-compatible membrane defects with reproducible bulk properties. The structural themes suggested by amphotericin - the overall length, the polar head groups, the one hydrophobic edge and the other amphiphilic edge - emerge repeatedly. Perhaps our current state of knowledge in this area is symbolized by Menger[17e,17f] who achieved ion transport with synthetic precursors to his target pore-formers which were themselves inactive.

A synthetic unimolecular channel has the additional requirement of rigidity, hence pre-organization. The earliest example is from Tabushi[18] who used cyclodextrin as a rigid polar head, pendant alkyl chains compatible with the membrane lipids and amide groups at the end of these chains to encourage the end to end H-bonding dimerization needed to span a bilayer. This compound showed slow transport of Co^{+2} ions. Nolte[19] made use of an isocyanide polymer which has a strong tendency to form a rigid α-helix with one turn every four residues; he prepared a 10 turn / 40 monomer unit molecule in which pendant 18-crown-6 groups arrange in four face-to-face stacked columns with a 40Å overall length. This material was a more active transporter of Co^{+2} and since the activation energy for transport was comparable to the activation energy for transport by gramicidin in the same system a channel mechanism was proposed. Perhaps the minimal structure is represented by Gokel's tris-crown compound[20]. He proposes that one crown sits at each

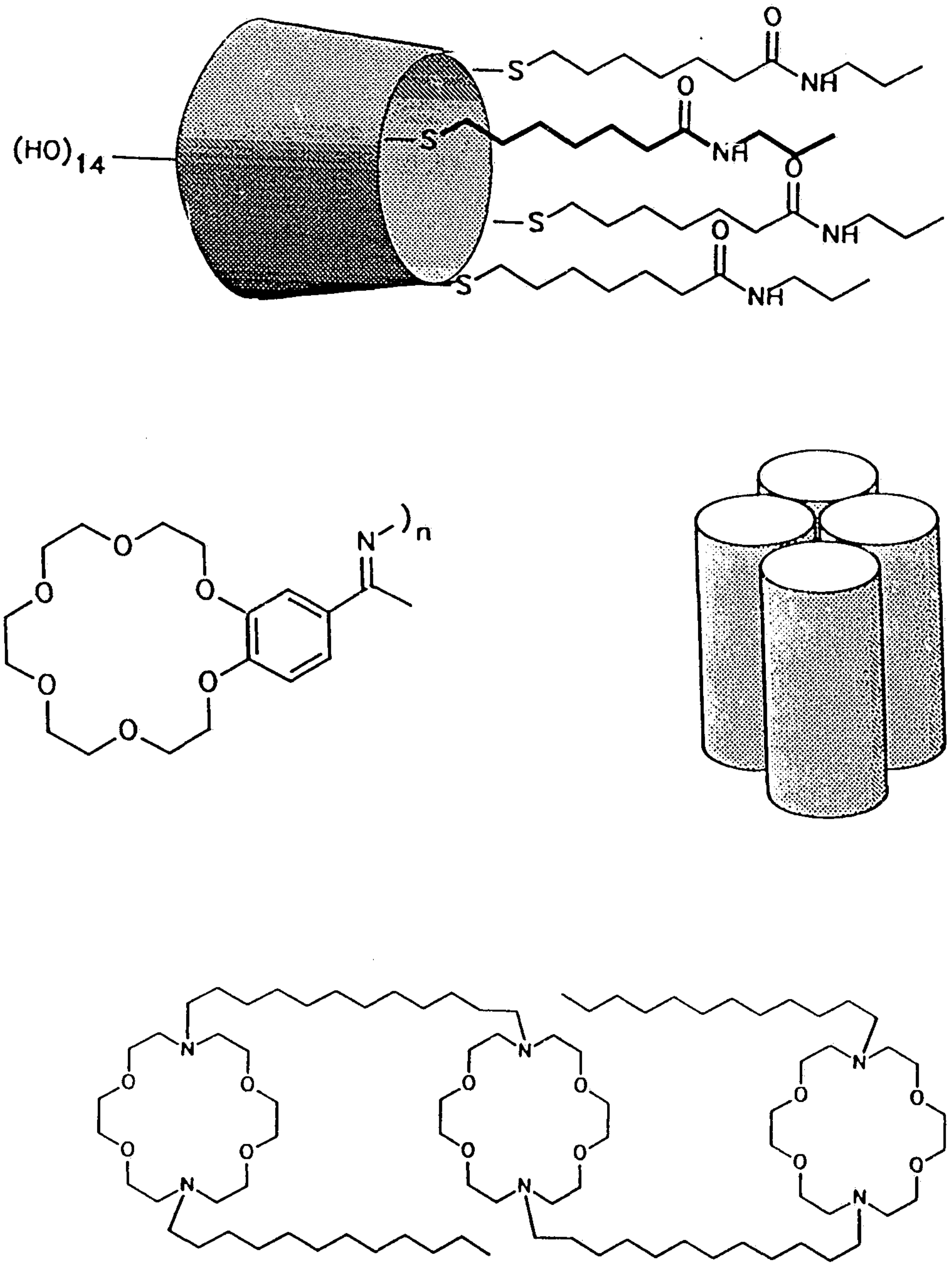

Figure 3. Top: The Tabushi cyclodextrin based channel.
Centre: The Nolte crown ether / isocyanide polymer channel.
Bottom: The Gokel *tris* macrocycle channel.

interface and one at the bilayer midplane and that transport occurs by ion hopping between crowns; the molecule appears to be insufficiently rigid but is in fact one of the more active artificial channels. The foregoing three compounds are illustrated in Figure 3. Lehn[21] proposed stacked arrays of crown ethers linked by short spacers but only a short stack of three crowns was reported, presumably because of synthetic problems. Following the work of Fyles[22], Lehn used tartarate crown ethers, as well as cyclodextrins, as well defined rigid structural units for his "bouquet" molecules[23], an example of which is shown in Figure 4. These structures follow the general guidelines for channel design in terms of overall size and polar head groups although the pendant chains were either all hydrocarbon or all polyether. They showed about equally slow transport rates with the two different chain types.

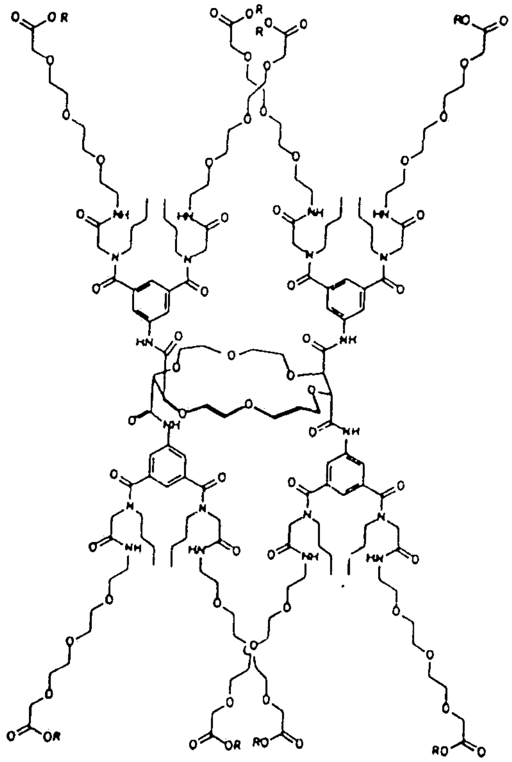

Figure 4. A Lehn "bouquet" molecule.

Synthetic channels in solid state media form another broad topic beyond the scope of this discussion but it bears mentioning that again the emphasis is on structural organization. For example the tendency of phthalocyanines to stack was used to direct face to face stacking by crown ethers although in the event many such compounds were inactive since the crowns stack in a staggered fashion[24]. Similarly Voyer has organized crowns using peptide scaffolds[25] and cyclic peptide and tetraphenyl porphyrin have been used as frameworks for bundles of peptide helices[26,27].

In 1989 Fyles et.al.[22] reported a functional synthetic ion channel mimic. The design derives from the guidelines discussed above; a rigid central crown ether unit bears partially rigid amphiphilic wall units topped by polar head groups. This structure is illustrated in Figure 5.

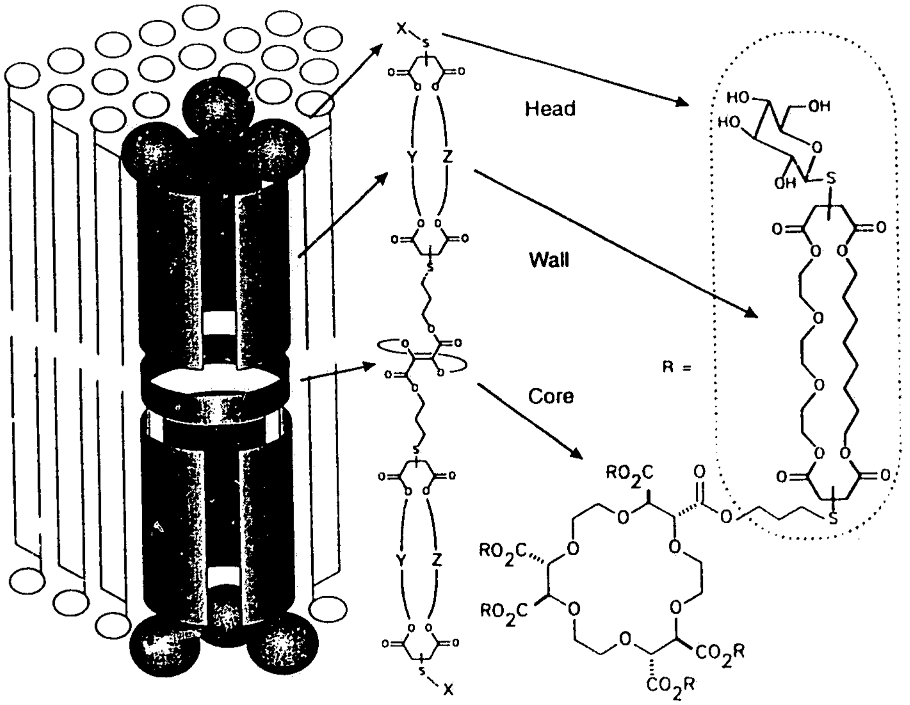

Figure 5. Schematic and chemical structure of ion channel mimic.

Subsequently a suite of 21 related compounds was prepared in order to evaluate 5 different crown components, 5 wall units, and 3 head groups[28-31]. With this approach there is a good chance of coming up with at least some active compounds and the resulting structure / activity relationships serve as guidelines both to mechanism and to improved designs. The synthesis followed a modular approach in which central crown, wall, and head groups were all made independently before final assembly; these pieces are informally referred to as the "tinker toy" set. With such a modular strategy improved designs are then easily accesible, mostly from existing pieces and via established chemistry. As well this synthetic scheme represents a convergent, rather than linear, overall route and this is inherently more efficient in terms of time and materials[32], a very important consideration in view of the size of the target. The size and shape of each modular construction piece should be roughly known but since the overall synthesis is property directed (as opposed to being final structure directed as is the case with most natural product syntheses) there is considerable flexibility with respect to the exact structure of the pieces. Synthetic efficiency thus becomes a more important consideration than exact structure so the construction set must be made suitable for simple reliable linkage reactions. It also bears mentioning that the flexibility with respect to final structure is essential to work around unforseen synthetic difficulties that are inevitable with a molecule of this size with as many functional groups. The modular components are:

i) a tartarate crown ether intended to sit at the bilayer midplane. The tartarate carboxylates provide points to attach wall units. The R,R,R,R-tetraacid crown gives two wall units on each side of the crown ring, probably the bare minimum requirement for an overall cylindrical shape. The most important consideration in the choice of R,R-tartarate crowns is the fact that they have been shown by X-ray[33,34], NMR[35a], and ESR[35b] data to have a strong preference both in the solid state and in solution for a trans-diaxial orientation of the carboxylate groups so that in the final structure the wall units would be perpendicular to the crown ring and pointed towards the outer surface of the membrane, establishing the desired cylindrical shape. Of course the crown also provides a hospitable environment for metal ions and possibly channel-bound water; tetra- and hexa-acid crowns derived from R,R-tartaric acid form crystalline complexes with a number of metal ions, all including bound water[33,34].

ii) a short spacer linking the crown to the walls. One end is a thiol for coupling to the wall unit via simple reliable Michael addition chemistry. The link to the crown was chosen to be ester rather than amide to avoid uncontrolled amide H-bond formation once the molecule is inserted into a membrane. The first functional channel prepared by Dutton[34] used thioethanol as the spacer, with reaction between the alcohol and the crown hexa-acid chloride giving the desired ester link. James[28] subsequently found that this resulted in some epimerization at the α-carbon, most likely through elimination of HCl by triethyamine present in the reaction mixture to give a ketene which is then susceptible to attack by the alcohol from either face. James avoided this problem by using the carboxylate nucleophile method of Kellogg[36] which had already been shown to be effective with tartarate diacid crowns[31]. This necessitates the use of a three carbon thiopropanol unit since as a mustard the thioethanol derivative is subject to elimination as a serious side reaction. Coupling using the Cs^+ tetracarboxylate, which follows Kellogg[36] and Cross et.al.[31], was unsuccessful since this salt was completely insoluble in all suitable solvents, but the Me_4N^+ salt was found to be soluble and coupling was accomplished.

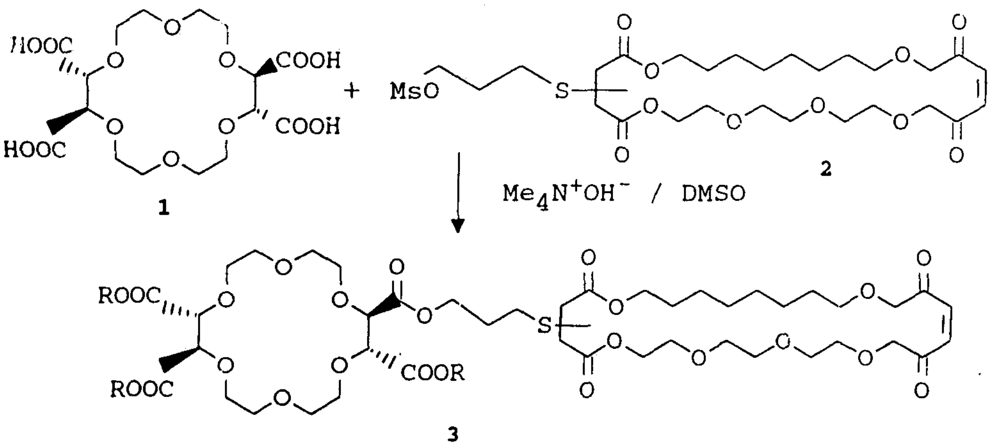

Scheme 1. Coupling using the Me_4N^+ carboxylate method[29,31].

iii) identical macrocyclic wall units which are coupled to the thiopropanol spacers by Michael addition then coupled simultaneously to the crown in the esterification step just described above. The wall unit structures are derived directly from the work of Furhop[37] who used them to form functional pores across artificial membranes designed to accomodate them. The Michael addition reaction does result in stereoisomerism and in the case of unsymmetrical macrocycles results in regioisomerism as well. The edges of the macrocycle are either hydrocarbon or polyether, and on the basis of the discussion above it would be expected that one of each would give the best functional wall unit. Molecular models predict that an eight membered edge represented by $(CH_2)_8$ or triethylene glycol is the optimum length to span a bilayer. In the event the synthesis of these wall units was far from satisfactory[28,38]. It proved to be impossible to completely remove side products (in particular small macrocycles), workups were tedious, and yields were mediocre at best. This result violates our design criteria and efforts are currently underway to produce wall units that are both symmetric to avoid stereo- and regioisomerism and accessible via more efficient routes[39].

iv) a polar head group. Polarity and size constraints were discussed briefly above. Again identical head groups are added simultaneously by Michael addition and again this introduces more stereo- and regioisomers. Head groups are added last because they give the whole molecule a pronounced amphiphilic character which tends to make purification exceptionally difficult; this makes a reliable efficient final coupling reaction all the more important. Fortunately at this late stage of the synthesis the size of the molecule actually becomes an advantage since it is now large enough to be purified by gel filtration techniques.

The activity of the set of 21 channel compounds was evaluated by a pH-stat technique. Large unilamellar vesicles (LUVs) 200 Å to 500 Å in diameter were prepared from egg phosphatidyl choline / egg phosphatidic acid / cholesterol (8:1:1) and characterized by electron microscopy and a melittin assay[40]. The vesicles have an entrapped volume of pH 6.6 buffer to provide H^+ ions for countertransport plus additional salt (choline sulfate) and mannitol to maintain osmotic pressure. They are then filtered through polycarbonate filters and a gel column to remove large aggregates and small fragments. In the pH-stat experiment the vesicles are dispersed in an external solution at pH 7.6, a proton carrier FCCP is added, and then metal ion is added. Once the synthetic transporter is added metal transport begins, accompanied by FCCP facilitated H^+ countertransport which maintains electric neutrality across the membrane. The H^+ efflux is monitored by the volume of OH^- added to maintain the external pH at 7.6, plotted as a function of time. In a typical experiment H^+ efflux levels off at a volume of added base less than that corresponding to complete release of all entrapped H^+ ions; addition of Triton detergent at this point rapidly lyses all intact vesicles to release all the remaining entrapped volume. The suite of 21 candidate channels is pictured in Fig **6** along with the transport mechanism ultimately assigned to each. Because of their size a semisystematic naming convention described in Reference 29 is used. Transport rates are summarized in Table **1**[31].

First of all control experiments determined the following:

- a melittin assay established that 95% of the entrapped volume was in LUVs and therefore available for transport

- electron microscope examination showed that transporters do not change the size or morphology of vesicles

- the unconnected modular subunits are inactive

- in the absence of transporter but with all other components present the leakage rate is very slow

- transporters are not active in the absence of FCCP, the proton countertransport carrier,

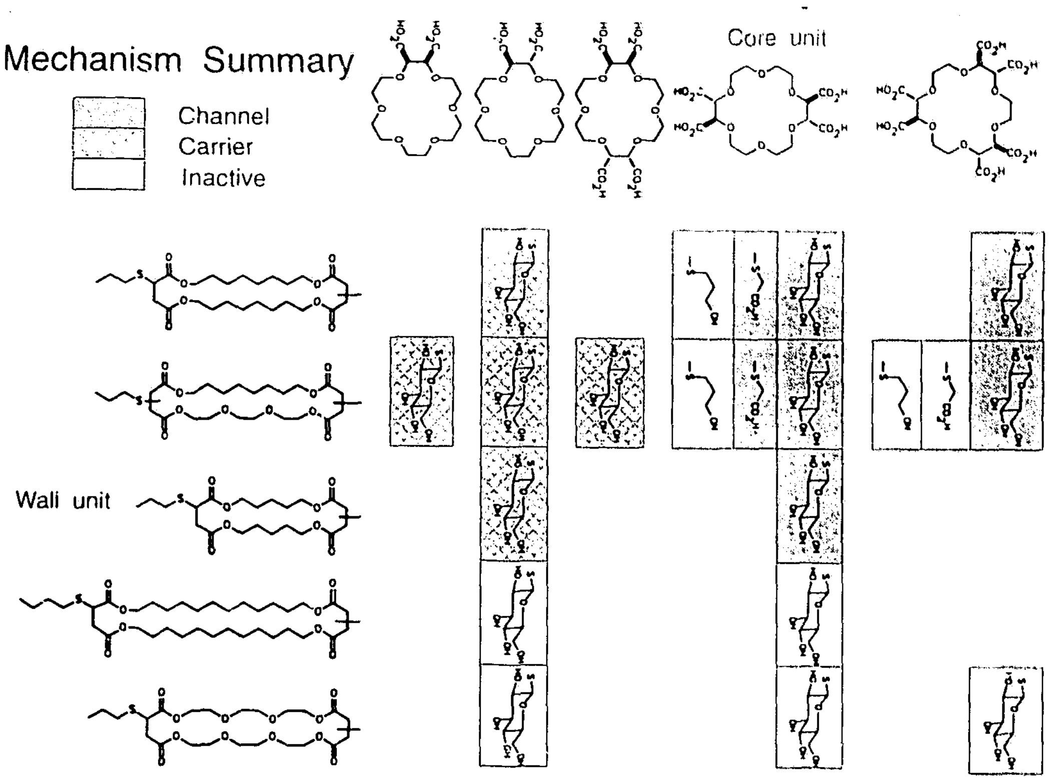
Mechanism Summary
Channel
Carrier
Inactive
Core unit
Wall unit

Figure 6. Components of candidate transporters with assigned mechanisms.

Transporter	Rate x 10^9 mol H^+ sec^{-1}	Transporter	Rate x 10^9 mol H^+ sec^{-1}
gramicidin	14.9	$(G8_2P)_6$Hex	0.8
$(G8TrgP)_4$Tet	8.2	$(G8TrgP)_2$mDi	0.7
$(G8TrgP)_4$mTet	6.5	$(GTrg_2P)_2$Di	0.4
$(G8_2P)_2$Di	5.8	$(P8TrgP)_4$Tet	0.4
valinomycin	3.6	$(GTrg_2P)_6$Hex	0.3
$(G8TrgP)_2$Di	2.1	$(A8TrgP)_6$Hex	0.3
$(G8_2P)_4$Tet	1.8	$(G12_2P)_4$Tet	0.2
$(A8TrgP)_4$Tet	1.7	$(P8TrgP)_6$Hex	0.2
$(A8_2P)_4$Tet	1.7	$(GTrg_2P)_4$Tet	~0
$(G5_2P)_2$Di	1.6	$(G12_2P)_2$Di	~0
$(G8TrgP)_6$Hex	1.3	$(P8_2P)_4$Tet	~0
$(G5_2P)_4$Tet	1.1		

Table 1. Normalized ion transport rates for candidate transporters.

so the transporters are not simply lysing the membrane.

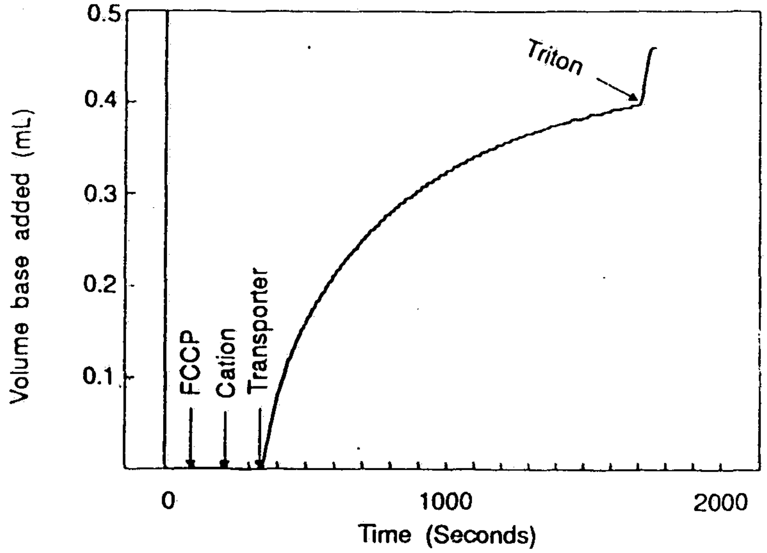

Figure 7. Typical pH-stat plot. This particular plot was recorded using the most active transporter - designated $(G8TrgP)_4Tet$.

A typical transport experiment plot of volume of added base (= proton efflux) vs. time is shown in Figure 7. Transporters were classified as "inactive" if the normalized transport rate was less than 0.5×10^{-9} mol H^+ sec^{-1} (see Table 1).

The traditional way to establish a channel mechanism for an ion transporter is by a bilayer conductivity experiment. A bilayer incorporating the transporter is formed across the tip of a capillary electrode or across an orifice in a Teflon barrier then a voltage applied across the bilayer and electrical current, the result of ion transport, plotted as a function of time[41]. A channel is in an "all or nothing" open or closed state so if the transporter is a channel a step function is plotted; carriers give rise to smooth continuous plots. This method unambiguously assigns a mechanism but is not well suited to our structure / activity study as it requires a specialized experimental setup and the data analysis requires a great deal of work. The first channel compound prepared by Dutton was tested in such an experiment performed elsewhere, and the result was the step function characteristic of a channel[42]. This same compound was also assigned a channel mechanism on the basis of the transport E_{act} value determined by Kaye[40] which was about the same as the E_{act} of the channel gramicidin but far lower that that of the carrier valinomycin. Another guideline to transporter mechanism is its behavior in the gel and crystalline phases of a black lipid membrane (BLM); both channel and carrier should function in the gel phase but only a channel would function in the crystalline phase. This method is inappropriate once the decision to use a vesicle system was made as the vesicles are somewhat fragile, and as well preparation of a uniform batch is still something of a black art - to the extent that valid comparisons between transporters must be made using the same batch of vesicles and within a couple of days of preparing them[40]. Another criterion was proposed by Gary-Bobo[43] as a result of studies on gramicidin and valinomycin. He observed that in vesicle experiments using valinomycin the *extent* of transport always reached 100% independent of valinomycin concentration whereas in experiments with gramicidin the extent of transport was dependent on the channel concentration. This is easily rationalized: gramicidin only inserts into some of the vesicles, with the number being dependent on gramicidin concentration, but once the channel has collapsed the gradient across a vesicle membrane it remains in that vesicle membrane and does not migrate to a fresh vesicle at any significant rate; valinomycin on the other hand migrates rapidly between vesicles so all gradients are eventually collapsed regardless of valinomycin concentration. From our own studies[28,30,38] it is clear that these examples are limiting cases of a continuum, with gramicidin representing the case where transport is much faster than migration and valinomycin representing migration being much faster than transport, and for the active compounds among the 21 assembled for this study the rates of transport and migration are close enough to each other that a concentration dependence for extent of transport is seen regardless of the mechanism of action[30]. James[28,30] performed "add-back" experiments in which a fraction of the vesicles was removed from the experiment before transporter was added and then added back once transporter had been added and the extent of transport had reached a plateau. Comparing transport rates before and after add-back gives an indication of how readily the transporter migrates between vesicles. In this case the compounds ultimately identified as channels did tend to migrate more slowly, particularly the one based on the tartarate crown hexa-acid, but there was no clear cut distinction that could be used as evidence for mechanism. The slow migration rates however are an encouraging sign that the compounds do effectively penetrate the membrane.

The initial rates for most active transporters were first order in transporter which rules out an aggregate pore as a mechanism but does not distinguish between channels and carriers. Consider the two limiting cases, for a carrier or a channel. In both cases the collapse of the ion concentration gradient does not have a large effect until the extent of transport is well advanced. In the case of channels which insert into a vesicle, collapse the gradient with a single random "all or nothing" channel opening, and then remain within the same vesicle the first order kinetics reflect the exponential decay of the number of intact vesicles. In the case of carriers which may partially collapse a gradient and then at random rapidly migrate to another vesicle the kinetics still reflect an exponential decay in the number of intact unemptied vesicles. A few compounds were classified as channels on the basis of zero order behavior. Their behavior cannot be shifted to first order by changing the metal or its concentration or the concentration of transporter. The fact that they cannot be driven to first order behavior by increased transporter concentration eliminates the possibility that the behavior results simply from poor partitioning of the transporter from the aqueous phase into the membrane. A zero order behavior by a carrier is only possible in the highly unlikely event that back-diffusion of the empty carrier dominates the kinetics, which requires it to be much slower than diffusion of the carrier-metal complex. Zero order behavior by a channel is possible but is not consistent with the "all or nothing" opening postulated for most channels. It would require a model in which the vesicle is only partially emptied during repeated short channel opening events, with several openings required to completely empty the vesicle. Studies are currently under way to confirm this short opening event model with bilayer conductivity experiments.

Another criterion for distinguishing channels and carriers is ion selectivity among the alkali metals. In examining rate as a function of metal ion concentration the transporters were seen to exhibit saturation behavior which is amenable to a Michaelis-Menten type analysis, which yields values for the maximum (saturation) rate and the concentration at which saturation is approached[44]. These values lent assurance that the ion selectivity experiments were run at concentrations well into the saturation range. Some transporters showed Eisenmann type III or type IV selectivity[45] characteristic of an equilibrium between metal in aqueous solution and complexed in an environment of oxygen donors so this indicates that for these transporters ion complexation is involved in the rate limiting step and suggests a carrier mechanism. Other transporters showed ion selectivity unrelated to any Eisenmann sequence so in these cases ion binding considerations do not govern the rate limiting step and this suggests a channel mechanism. Inhibition by Li^+ ion was another criterion to distinguish channels and carriers since Li^+ transport rates were essentially zero for all compounds studied. Presumably in the case of a carrier this reflects a very low binding constant so Li^+ would not be expected to inhibit a carrier, but it could conceivably block a channel without being transported and inhibition by Li^+ was taken as evidence of a channel mechanism.

On the basis of these criteria the 21 compounds in Figure **6** have been classified with respect to mechanism as shown and these results validate the design guidelines. The R,R-diacid, *meso* diacid, and *meso* tetraacid crowns cannot form a cylindrical structure and so when their compounds are active it is via a carrier mechanism while on the other hand the R,R,R,R-tetraacid and R,R,R,R,R,R-hexaacid crown compounds are designed to be cylindrical and can act as channels. Clearly thiopropanol is unsuitable as a head unit possibly because it is not polar enough to effectively partition to the membrane surface. The wall unit in which the succinate units are joined via two $(CH_2)_{12}$ chains (designated as **1212** in Fig. **6**) is too long for its compounds to span the bilayer in a roughly straight conformation and some sort of unproductive conformation must be assumed. The arm with two $(CH_2)_5$ units (designated **55** in Fig. **6**) is too short but the membrane can "dimple" to accomodate a shorter molecule as it does for the gramicidin dimer (26 Å long across a 35 - 40 Å bilayer). All compounds with the wall in which the succinate units are joined by two triethylene glycol fragments (designated **TrgTrg** in Fig. **6**) were inactive, most likely reflecting poor partitioning from the aqueous into the membrane phase. This is consistent with Lehn's observation that his bouquet channels bearing four polyether arms were not incorporated into a membrane to as great an extent as those bearing four hydrocarbon arms[23]. The channels showing zero order behavior are the three using the wall unit in which the succinate units are joined by two $(CH_2)_8$ chains (designated **88** in Fig. **6**) and this is consistent with a distinct mechanism, such as the multiple short lived channel opening one proposed above.

In summary: design guidelines from natural and synthetic ion transporters have succeeded in producing functional ion transporters exhibiting channel-like behavior, and function and mechanism can be controlled through structure in a rational way. This is the first step beyond molecules that indiscriminately poke holes in membranes - now the next step is external control of the transport through gating, so that we can control both what goes through the membrane and when.

1.2 Proposed Project

1.2.1 General Considerations

The goal of this project is to synthesize and evaluate a functional ion channel with an externally controlled gate. Logically the target would closely resemble the most active of the channels shown in Figure **6**. This is the compound bearing thioglucose head groups on wall units in which the succinate groups are linked by one 8-carbon chain and one triethylene glycol unit, with the other end of the wall linked by thiopropanol to an R,R,R,R-tetraacid crown ether (designated $(G8TrgP)_4Tet$ in Table **1**). It remains for a suitable gate to be chosen. The accompanying Figure 8 is from Hille[46] and depicts in cartoon fashion an electrophysiologist's view of possible gating mechanisms.

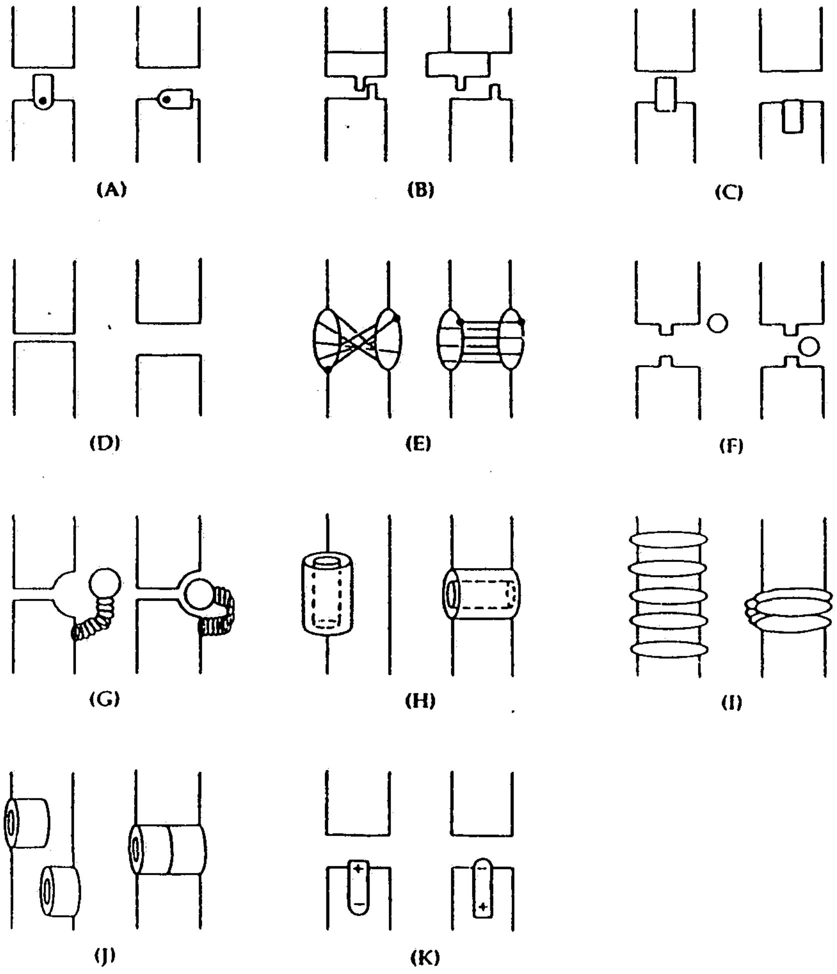

Figure 8. Cartoon of possible gating mechanisms.

Of these possibilities mechanism (G) in particular appeals to a chemist from both mechanistic and synthetic perspectives. It is inherently simple in that an intramolecularly bonded plug undergoes a single specific interaction (the "ball" with the "socket") to block the channel and this is brought about by a simple conformational change (of the "spring") moving a relatively small structure through space. Many of the mechanisms illustrated have large structures sliding across surfaces or through the membrane and are likely to be mechanistically complicated and energetically expensive. Synthetically the architecture of (G) is amenable to modular assembly, giving the flexibility necessary in a property directed synthesis; in other words the ball, socket, and spring components can be structurally fine-tuned with the minimum synthetic effort. The gating event could be driven either by a conformational change of the spring or by a change in the ball and socket interaction. At this stage of development the gating does not need to be reversible although this would be preferable. Within the strict definition of a gate it should be energetically independent of the transport event and ideally the energy to open the gate would be trivial. When gating and transport events are energetically separate then the gate can be applied to different transport systems, and any such system is subject to two independent levels of control.

A variety of stimuli could be used to drive the gating event - an applied voltage, temperature, light, pH gradient, metal ion gradient, or a redox reaction. We settled on a photochemical gate since several photoresponsive groups are already known which use light to drive a well defined conformational change. Applying light as a stimulus is very simple experimentally and it does not affect either the membrane or the aqueous phases in any way. The proposed channel thus has the general structure illustrated in Figure 9 where the central ring is the tetraacid crown and the three identical substituents are the thioglucose head - "**8Trg**" (see Figure 6) wall unit - propyl spacer combination from the most active channel compound. The synthesis and coupling of these units is already established. Figure 9 shows the gating event as a conformational change in the "spring", specifically the *trans* - *cis* isomerization of an azo compound. This is in fact the mechanism that was chosen, as described in section **1.2.3** (page 30). The "plug" will be an aliphatic ammonium group; it binds well to this type of crown (with 18-crown-6 log K ≈ 1.2 in water) as is evident from the work of Shinkai (see below) and from a synthetic point of view the protection and deprotection of amines has been thoroughly studied[47]. The synthetic problem then breaks down to two major components - design and synthesis of the photogate arm and selective functionalization of only one of four identical crown carboxylate sites.

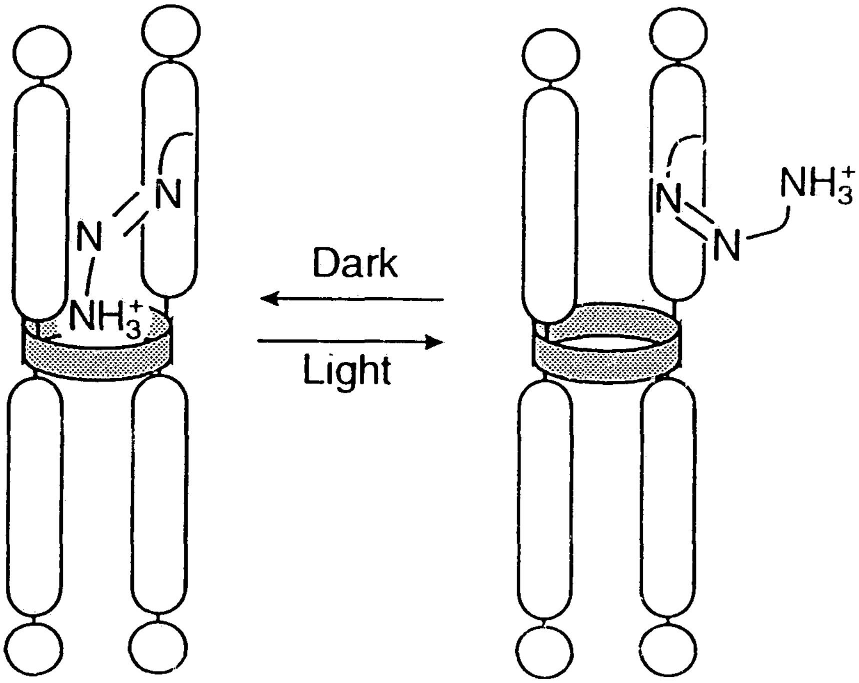

Figure 9. Schematic structure of target compound.

1.2.2 Monofunctionalized Crown Ether

Tartarate tetraacid crowns are prepared from R,R-tartaric acid and during the macrocyclization reaction pains are taken to ensure that no epimerization occurs so that all four carboxylates are identical[48]. As a result only one product isomer is possible so the formidable task of separating stereoisomers is avoided. The product has two arms on either side of the crown ring allowing a cylindrical shape for the channel compound. The problem in constructing the desired gated channel is to functionalize one and only one of these identical positions. We decided that this single functionality should be a carboxylic amide as this would be stable enough to withstand the variety of reaction conditions that will be encountered during the entire assembly; then once the photogate arm has been attached the other three arms can be coupled as esters using the established methodology (the Me_4N^+ carboxylate as nucleophile). Bulk addition of one equivalent of amine to the tetraacid chloride crown should statistically give about 42% monoamide in a mixture with diamide, triamide, tetraamide, and unsubstituted tetraacid products. Using the dianhydride derived from the tetraacid crown with one equivalent of amine would statistically give 50% monoamide mixed with diamide and the unsubstituted tetraacid. These yields are not prohibitively low but we would hope to do better, particularly since crown ether mixtures are notoriously difficult to purify.

It would be possible to make a monoamide from reaction of tartaric acid anhydride with an equivalent of amine and then use this fragment to build the desired monoamide crown in a stepwise route. This tack would involve a lot of blocking / deblocking chemistry particularly as the monoamide moiety must carry an additional functional group that will ultimately be used to couple with the photogate moeity. As a result of years of experience with this type of compound and a survey of Dutton's synthesis of the hexa-acid crown[34] by such a route this option was never seriously considered. Even to make a single compound the strategy would probably be unacceptable because of purification problems but here it was hoped to establish a general route to a whole class of monofunctionalized crowns for structure / activity evaluation and ultimately for using other gating mechanisms. Fortunately a simple elegant alternative was evident. As part of a project to make photoionophores Fyles and Suresh[49] used the reaction of *meta* or *para* xylylene diamine with tetraacid chloride **6** and tetraacid dianhydride **4** to give the bis-capped tetraamide **7** and mono-capped diamide diacid **5** respectively as shown in Scheme 2.

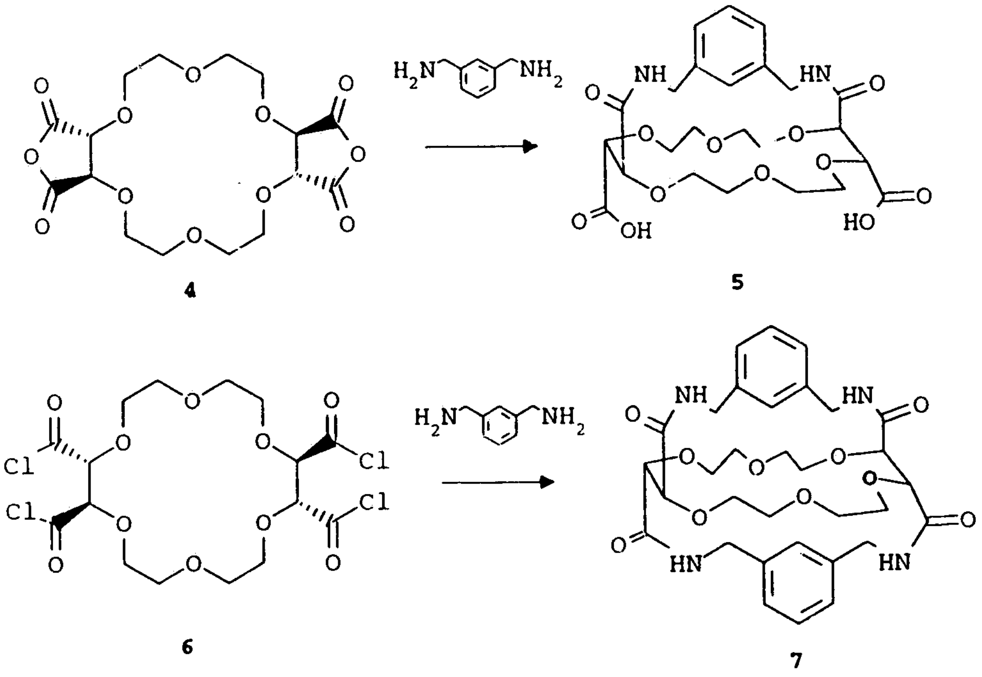

Scheme 2. Capping reaction to make photoionophores.

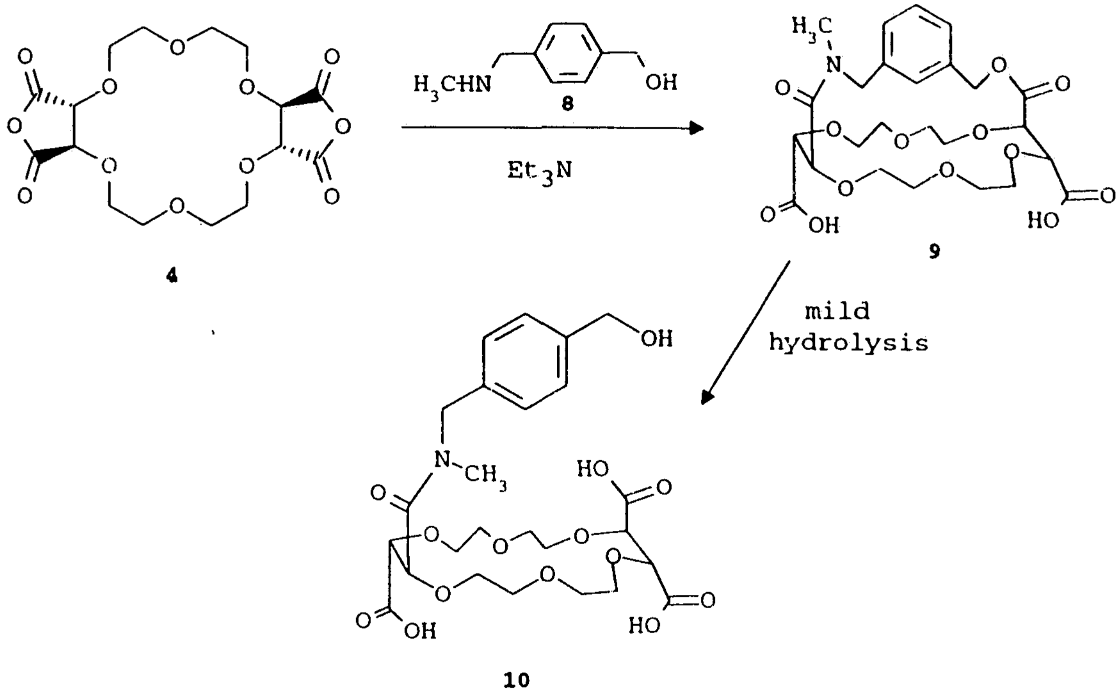
4
H3CHN
OH
8
Et3N
H3C
N
OH
HO
9
mild
hydrolysis
OH
N
CH3
HO
OH
HO
10

Scheme 3. Proposed capping / hydrolysis route for monofunctionalization of the crown ether tetracarboxylate.

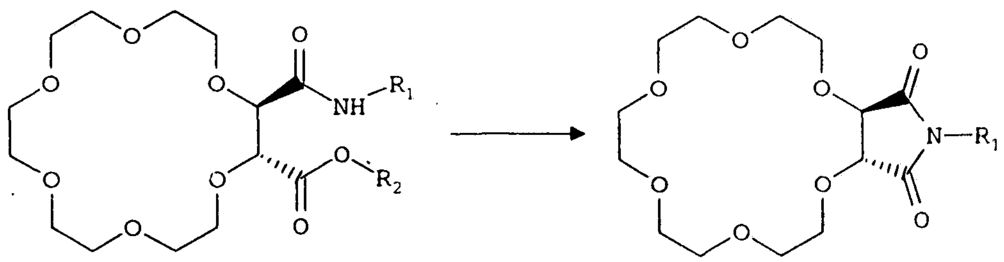

Figure 10. Cyclic imide formation from secondary amide.

If an analogous capping reaction could be achieved between the dianhydride and an analogous aromatic amine / alcohol **8** then selective hydrolysis could be used to cleave only the ester linkage of the resulting amide / ester **9** and the monofunctionalization would be accomplished. The amine would be expected to react rapidly with an anhydride but the esterification to complete the cap could be slow so that very high dilution conditions would be needed. The additional restriction is that the amine must be secondary; the amide will have a vicinal ester group in the ultimate target channel and in the 18-crown-6 tartarate diacid series vicinal secondary amide / esters readily and irreversibly form cyclic imides[31]. The proposed reaction route and cyclic imide formation are depicted in Scheme **3** and Figure **10** respectively.

1.2.3 Photogate

The general requirements for a photogate are that it be chemically stable and that excitation produce a significant geometry change with a reasonable quantum yield. It does not have to be reversible although this would provide an additional level of control. There are three organic photoisomerizations commonly used as gates or switches.

Twisted intramolecular charge transfer (TICT) compounds are aromatic molecules with a weakly coupled strong donor / strong acceptor pair of substituents[50] which have two intramolecular charge transfer states, one planar and the other twisted at 90°. The two states have substantially different λ_{max} values, geometries, and dipole moments. The properties can also be manipulated by additional substituents on the aromatic ring.
A simple example is shown in Figure **11**.

The spiropyran merocyanine pair shown in Figure **12** exist in an equilibrium whose position can be controlled by irradiation at the appropriate wavelength of uv or visible light[51]. Again λ_{max} values, geometries and dipole moments are generally very different, and can be altered by the presence of substituents.

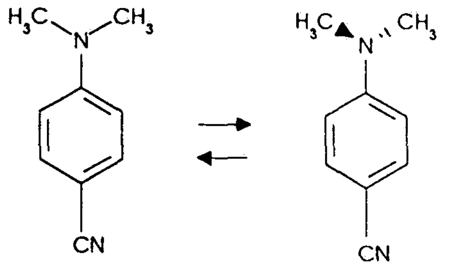

Figure 11. Twisted intramolecular charge transfer compound.

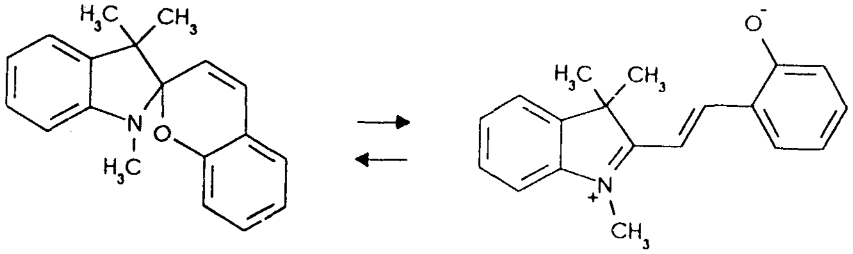

Figure 12. Spiropyran / merocyanine photochemical switch.

Azobenzene compounds (the formal IUPAC name is diphenyl diazenes but this is not commonly used) have been used as commercial dyes for a long time but more recently the *cis* - *trans* isomerization has been widely used as a photochemical switch. The photochemistry has been studied extensively because of these practical uses and because they are similar to stilbene[52]. The isomerization is accompanied by a large and well defined geometry change and can be reversed by changing the wavelength of the light. A feature which makes this system attractive as a molecular device is the photochemical stability; the *cis-trans* isomerization is the only readily accessible photochemical pathway so there are no side reactions and the isomerization may be repeated through many cycles without appreciable decomposition[52]. Features that limit its practical application are the fact that at room temperature there is a slow thermal *cis* to *trans* isomerization and the fact that isomerization gives a significant change in ε more than in λ_{max}, but for our purposes these are not a problem. An important factor in our choice of this switch is its chemical stability under a wide variety of conditions as during the synthesis it will have to withstand several coupling, blocking, and deblocking reactions. In addition it should be fully compatible with a phospholipid bilayer and the fact that it is coloured facilitates purification by column chromatography.

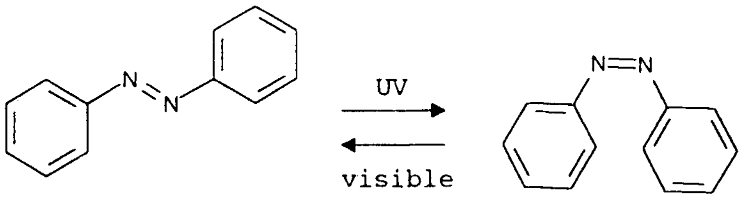

Figure 13. The *trans* - *cis* isomerization of azobenzene

The *trans* isomer of azobenzene is planar and characterized by a π-π^* transition at λ_{max} 323 nm (ε=22,000) and an n-π^* transition at λ_{max} 449 nm (ε=405). The *cis* isomer has a planar azo group with the phenyl rings parallel to each other but twisted at 56° from the plane containing the azo group and the two carbons bonded directly to it. It has a π-π^* transition at 278 nm (ε=9,000) and an n-π^* transition at 440 nm (ε=1250). Optical pumping in the uv range (π-π^*) drives the equilibrium towards the *cis* isomer while in the visible range (n-π^*) the equilibrium is driven towards the *trans* isomer, so it is a reversible switch. The *cis* isomer is ~12 kcal/mole higher in energy so the molecule is exclusively *trans* at thermal equilibrium. For the thermal *cis* to *trans* isomerization the E_a is 22.7 kcal/mole for the parent azobenzene and 20 - 24 kcal/mole for various substituted azobenzenes so the thermal reaction is slow at room temperature and *cis* isomers are isolable. Photochemically the molecule is characterized by a pronounced "floppiness", meaning large distortions are possible in both the ground and excited states so there is extensive spin-orbit and vibrational coupling of states. Hence the spectra show no vibrational fine structure, changes in substitution or solvent polarity have only a moderate effect, and emission has never been observed from either singlet or triplet states (i.e. decay from all excited states is via non-radiative pathways). Triplet states are not accessible from direct irradiation and must be reached through triplet sensitizers.

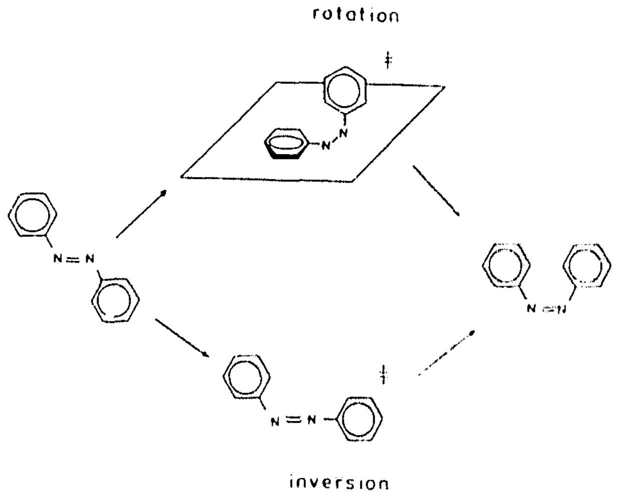

Figure 14. Possible *trans* - *cis* isomerization mechanisms[52].

There are two possible mechanisms for the isomerization of azobenzenes: rotation, in a manner analogous to stilbene, and inversion, via a planar transition state with an sp-hybridized nitrogen. Inversion is widely accepted as the mechanism for the thermal isomerization[53], and this accounts for the thermal reaction being so much faster than it is for stilbene. *Ab initio* calculations to this point are inconclusive as azobenzene is rather large for such methods but they do eliminate a fully linear transition state in favor of the semi-linear one shown[54]. The photochemical mechanism is more elusive, as it clearly involves participation by more than one state. Again *ab initio* calculations are inconclusive but they do agree that the molecule is floppy so that near either transition state geometry, which would be a 90° twist for rotation or the semi-linear structure shown for inversion, singlet and triplet excited states and the ground state are close enough in energy that radiationless decay is favored[52]. Results from a number of authors[52, 54] have established quantum yield values for the *trans* to *cis* reaction as .25 for for excitation at 436 nm (n-π^* transition to S_1) and .11 for excitation at 313 nm (π-π^* transition to S_2); note that the much lower quantum yield from S_2 is atypical of organic photoreactions as there is normally very rapid internal conversion to S_1 but in this case because of the floppiness of azobenzene there may be a facile radiationless decay from S_2 back to the ground state. Rau[54] synthesized azobenzenes for which rotation was impossible and found quantum yields to be the same (.24) for excitation to either S_1 or S_2, implying that all molecules reach the same state (S_1) and then react via the same mechanism. He concluded that in normal azobenzenes isomerization from the S_1 (n-π^*) state goes by inversion whereas from the S_2 state (π-π^*) it proceeds via rotation[55]. This is not unreasonable as the S_2 state of azobenzene is similar to the S_2 state of stilbene which must isomerize by rotation. The argument requires that internal conversion from S_2 to S_1 be relatively slow but this is possible. On the other hand Monti et.al.[56] draw a substantially different energy level diagram for the rotation pathway. They conclude from the same data that again isomerization from S_1 is via inversion, but that from the S_2 state the molecule rotates to a distorted excited state energy minimum, perhaps similar to the "phantom singlet" proposed for the rotation of stilbene. This represents a bifurcation point from which about half the molecules decay to the ground state without isomerizing and the other half back-rotate to the S_1 state which then isomerizes by inversion; in short, there is no isomerization by rotation. Quantum yield values for the *cis* → *trans* reaction are much less accurate but the average values from several authors are .55 from S_1 and .40 from S_2[52]. Results from this *cis* → *trans* reaction do not distinguish between the two mechanistic possibilities but this is expected since the *cis* ground state is distorted from planarity and the Franck-Condon states should have significant mixing of the S_1 and S_2 states, and this is reflected in the quantum yield values from either state being similar.

A complete survey of azobenzene-containing photoresponsive compounds is far beyond the scope of this thesis but I will describe a few illustrative examples. Azobenzenes are widely used because they meet the basic requirements for a photoswitch; they are chemically and photochemically stable and they react with reasonable quantum yields to give a large well defined geometric change. This results in a change in dipole moment - for *trans* azobenzene the dipole moment is 0, for the *cis* isomer it is about 3 DB[52]. Note that the geometry change could also result in significant secondary effects, for example changes in H-bonding or electrostatic interactions. Azobenzene units have been incorporated into polymers both as part of the main chain and as pendant groups[57], and the isomerization reaction causes significant changes in solution properties such as aggregation or viscosity and in solid state properties such as gel transition temperature, swelling or helical content. These changes result from unspecific steric effects. Azobenzene-containing lipids with polar heads will insert into bilayer membranes and facilitate water[58] and ion[59] transport on irradiation with uv light; again this is an unspecific steric effect, the reasonable assumption being that the flat *trans* isomer can fit snugly into the bilayer while the *cis* isomer occupies more space and disrupts the bilayer enough to allow water or ion leakage. Shinkai published a number of papers describing compounds in which azobenzene was linked to crown ethers in a variety of architectures and this represents the next level of sophistication in that the structures are designed so that the *cis* ⇌ *trans* isomerization promotes or inhibits *specific* ion binding interactions. For example he synthesized a polymer with an azo-crown-azo crosslink[60] and ion binding studies were consistent with his prediction that with the azo groups in the *cis* configuration the crown ether ion binding pocket would collapse. Shinkai was able to use the azobenzene isomerization to alter ion binding properties of crown ethers in a systematic way. Azobenzene incorporated into the crown ether ring itself[61] or used to form pillars linking stacked crowns[62] could open or collapse the crown cavity resulting in "all or nothing" ion binding. Crowns capped with azobenzene had much higher ion affinities as the *cis* isomer because of the shape of the cavity[63] while azopyridine capped crowns bound ions better as the *trans* isomer because its conformation allowed the pyridine nitrogens to assist the binding[64]. Note that in the latter case there is an additional level of control with changes in pH. A compound was also synthesized in which the trans configuration simply blocks the crown ether cavity with a large non-polar pendant group[65].

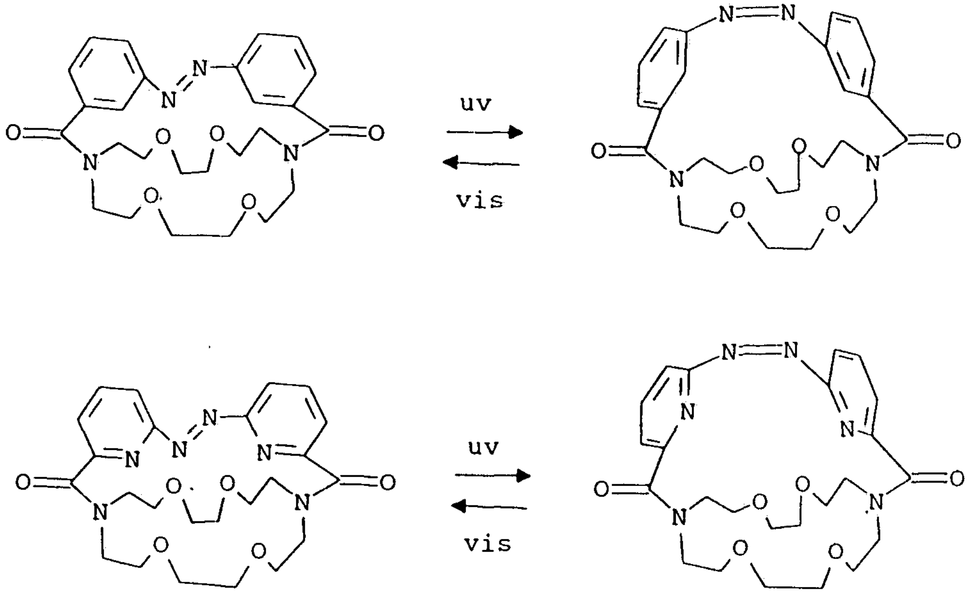

Figure 15. Azobenzene and azopyridine capped crown ethers.

These concepts were extended to ion transport through liquid membranes both with his "butterfly" compounds in which the *cis* isomers allow two crowns to form a sandwich complex with large ions[66] and with compounds in which a pendant phenoxide oxygen can assist metal ion binding[67]. Transport was achieved by irradiating one interface, the one between the membrane and the more concentrated aqueous phase, with uv light thus driving the equilibrium at that interface towards the ion-binding *cis* isomer. These experiments achieved passive transport only, i.e. metal ion transport and proton countertransport were both down their concentration gradients. These experiments also

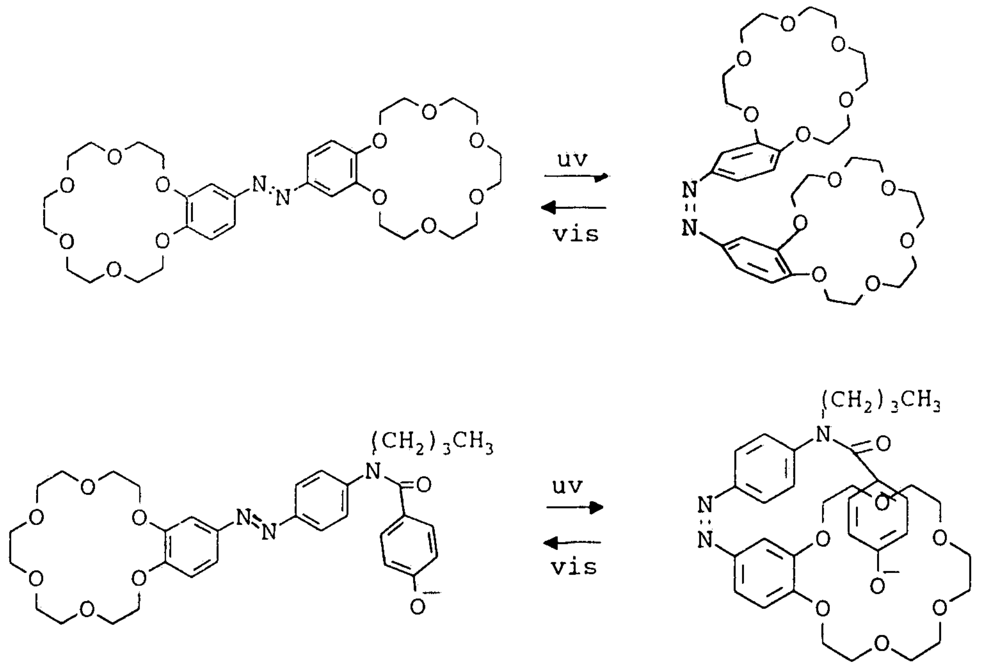

Figure 16. Shinkai "butterfly" compound and compound using phenoxide assisted binding.

introduced two additional methods of control; alternating uv and visible light irradiation to adjust the amounts of the two isomers, and anion control in which increased anion hydrophobicity changes the rate limiting step from ion complexation to ion release so that uv irradiation can either accelerate or inhibit transport depending on the anion[68].

The idea to use an aliphatic ammonium group to block the crown ether cavity, which I propose to incorporate into my target channel compound, derives from Shinkai's "tail biting" molecules in which a pendant ammonium group binds within the crown cavity of the *cis* isomer and thus prevents metal ion binding[69]. Once more there is an added element of pH control and transport could be regulated by uv or alternating uv / visible irradiation. There is a limit to crown carrier concentration in these experiments

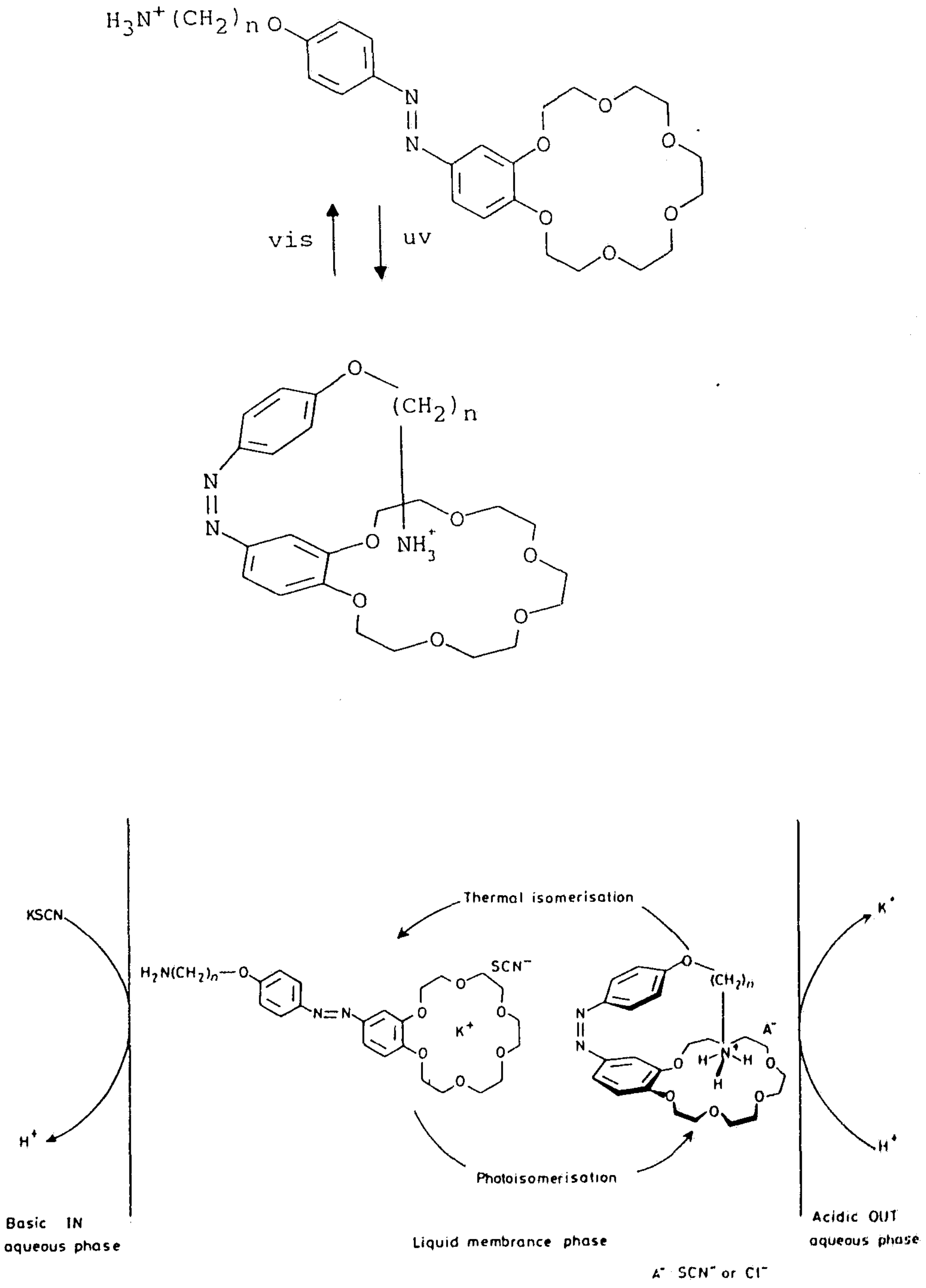
$H_3N^+(CH_2)_nO$
vis
uv
$(CH_2)_n$
NH_3^+
Thermal isomerisation
KSCN
$H_2N(CH_2)_n$—O
SCN^-
K^+
$(CH_2)_n$
A^-
K^+
H^+
H^+
Photoisomerisation
Basic IN aqueous phase
Liquid membrance phase
Acidic OUT aqueous phase
A^- SCN^- or Cl^-

Figure 17. Top: The Shinkai "tail-biting" compound. Bottom: Schematic picture of the transport experiment[69].

since at higher concentrations intermolecular tail biting becomes dominant. Since the ion binding to the tail biting *cis* isomer is essentially zero Shinkai was able to accomplish *active* transport with these carriers, that is transport of the metal against its concentration gradient[69c].

This is an opportune place to comment on the coupling of the gating and transport events. As stated above strictly speaking a gate should be energetically independent of the transport event and ideally the energy to open it is small. The target compound for this project is designed to have the gating event independent of the transport event although the energy to open the gate is not trivial (λ_{max} for the *trans* isomer is 323 nm corresponding to 90 kcal/mole). Shinkai's butterfly compounds transported along the concentration gradient but transport was energetically linked to the gating event, that is the light absorption contributed by driving the equilibrium at one interface. Active transport by the tail-biters was driven partly by the shift in equilibrium resulting from light absorption and partly by proton countertransport down a gradient. At the opposite extreme to ideal gating is the limiting case represented by bacteriorhodopsin where absorption of light is the single source of energy for both the gating event and the transport event, which is moving a proton against its gradient.

1.2.4 Target Compound

The specific structure proposed as a target is illustrated in Figure **18**. The short arm between the azobenzene moeity and the amine group allows for some flexibility so the molecule should always be able to find a stable conformation with the amine in the crown ring, and 4-(2-aminoethyl)aniline is a commercially available material which can be used as its aliphatic amine-protected derivative to form the azo link. Resorcinol is a good nucleophilic component for the azo coupling reaction and serves to attach both the link to the monofunctionalized crown and the wall unit / head group arm via simple conventional chemistry. In addition the regiochemistry of the azo coupling reaction to resorcinol is known[70]. The ethylene glycol link to the crown is also accessible via simple chemistry starting with the THP (tetrahydropyranyl) protected derivative of 2-bromoethanol. Coupling between this ethylene glycol hydroxide and the hydroxide on the aromatic capping moiety could be done with either oxygen as nucleophile and the other

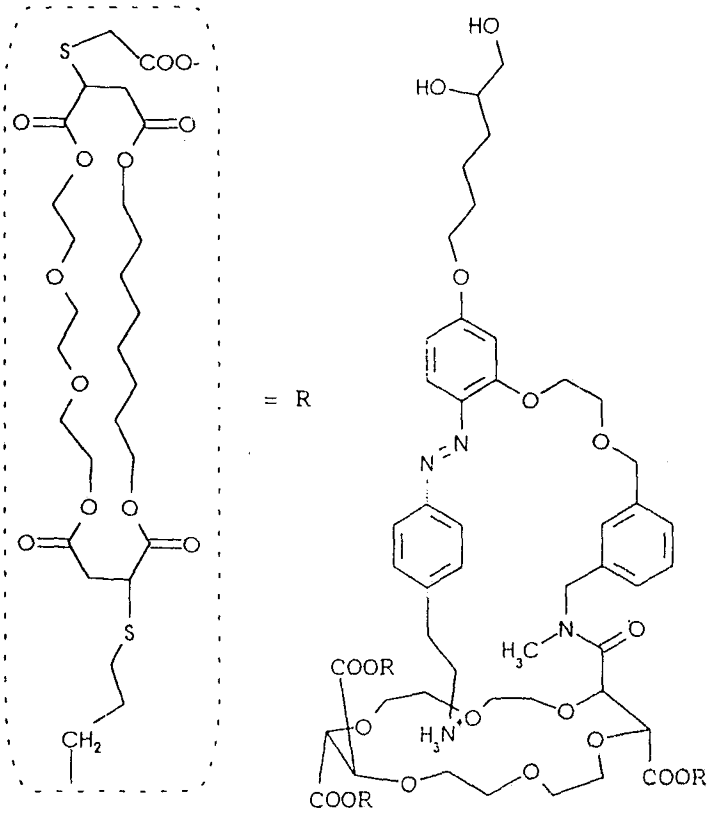

Figure 18. Proposed target compound. **11**: R = H. **12**: R as shown.

as a tosylate or mesylate leaving group. The length of the six carbon arm was arrived at from space filling models, and the structure / activity studies described above suggest that glycol would be a suitable head group. The glycol is easily protected as a ketal and the whole structure is synthetically accessible.

The target compounds with either a *meta* or a *para* aromatic cap were compared by the PCMODEL molecular modelling programme since either can be used to form a cap[49]. The energies of the minimum energy structures of the *trans* azo compound with either *meta* or *para* were approximately equal although the *para* generated more low energy structures. The *cis* azo compounds were also evaluated; since the programme evaluates structures from heats of formation in order to compare *trans* and *cis* structures the latter must be considered with the ammonium group still bound in the crown ring. The *trans para* isomer is more stable than the *cis para* by about 30 kcal/mole and the *trans meta* more stable than the *cis meta* by about 34 kcal/mole, so it appears that either would be suitable. Both *meta* and *para* aminoalcohol capping components were in fact prepared and the latter proved to be the easier target. Aromatic caps were made by Fyles and Suresh[49] for their fluorescence properties but may in fact also form the cap more readily than a comparable aliphatic compound. The "rigid group principle" holds that the transition state for a cyclization reaction is product-like and is formed with considerable loss of entropy, so that by using a more rigid component which is already conformationally resticted this entropy loss is reduced and the cyclization is faster. Lehn[71] was able to cap the crown tetraacid chloride with $H_2N(CH_2)_2O(CH_2)_2NH_2$ although with this length he got both *syn* and *anti* capping. Aliphatic caps are not directly comparable to aromatic ones or to each other by PCMODEL but it appears that a three carbon aminoalcohol would be the best length since the low energy structures of the target compound with longer aliphatic cap moieties had conformations with the photogate component sticking out to the side rather than above the crown ring, and this would disrupt the desired overall columnar shape. As a minor consideration this may also affect the optimum length of the wall / head arm.

1.2.5 Evaluation

Once the target **11** (R=H) is made then it will be evaluated by measuring the ion binding constant of the *trans* isomer with a suitable metal such as K^+, then irradiating with uv light and measuring the new binding constant of the *cis* isomer. If $K_{cis} > K_{trans}$ then the target will be converted to the ion channel **12** (R=G8TrgP) by attaching the wall / head group arms via the carboxylate nucleophile procedure of James[28]. This can then be evaluated by measuring ion transport rates[30,40] before and after irradiation with uv light.

1.2.6 Summary

In summary this is an exercise in biomimetics, attempting to duplicate the function of a natural ion transporter with a simpler more stable artificial one. Transport studies of this target will provide additional evidence with respect to the mechanism of action of these artificial transporters, and both the photogate and the monofunctionalised crown are versatile additions to the modular molecular construction set. The project thus contributes to the overall goal of predictable control of molecular function through structure, ultimately leading to practical devices.

CHAPTER 2 RESULTS AND DISCUSSION

2.1 Synthesis of the Photogate

The structure of the photogate component of the target was set out in the introduction, and the compound **13** is projected as the fully assembled photogate suitably blocked for coupling to the crown and for subsequent coupling to the wall / head units to give the ion channel. The synthesis of this component breaks down into two principal problems: proving and possibly directing the regiochemistry of the azo-coupling reaction, and manipulation of the blocking groups during assembly.

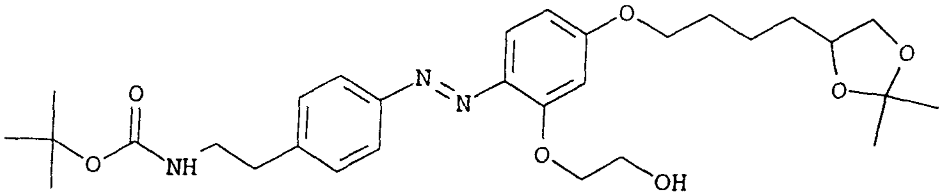

13

Figure 19. Photogate target.

The azo coupling reaction must be done with one oxygen substituent of the resorcinol ring as phenoxide in order for the ring to be sufficiently electron rich to be an effective nucleophile, and this substituent serves as the primary directing group with respect to the regiochemistry of the reaction. According to the literature[70] azo coupling to mono-*O*-substituted resorcinols is predominantly *para* to the phenoxide position but in this synthesis the correct regiochemistry is critical and product structure must be proved unequivocally. It would not matter if the anticipated minor product, of coupling *ortho* to phenoxide, turned out to be the major product so long as its identity was certain, since both arms are added to the resorcinol by the same chemistry and the regiochemical preference just determines which arm is added before the azo coupling and which is added after. If the regiochemical preference is not strong then there is the possibility of directing it towards the *ortho* product by using a very bulky substituent on the one oxygen.

Blocking group manipulation is necessary because the primary aliphatic amine must be protected throughout the synthesis. The first step generates an aromatic diazonium ion and these react with primary amines to give triazenes[72], and then later during nucleophilic coupling to the wall / head arm the amine would compete with the alkoxide O^-. In addition the ionization level of this group would constantly be changing with pH causing problems with respect to solubility, extractability, and chromatographic mobility. The glycol head group must be blocked during coupling to the crown component and the resultant product again is far easier to extract and chromatograph as the blocked compound. The choice of amine blocking group is not obvious. During the synthesis it has to withstand both acidic and basic conditions; a group such as benzyl is stable to these conditions but is normally removed by hydrogenolysis, which would attack the azo group. There are a number of photolabile amine protecting groups but they are unsuitable since their absorbtion maxima tend to be very close to the intensely absorbing ($\varepsilon \approx 20{,}000$) azo group band at $\lambda_{max} \approx 360$ nm.

2.1.1 Azo Coupling Reaction

This reaction involves initially preparing the aromatic diazonium ion then reacting it with a monosubstituted resorcinol anion as shown in Scheme 4, which also shows the anticipated regiochemical result.

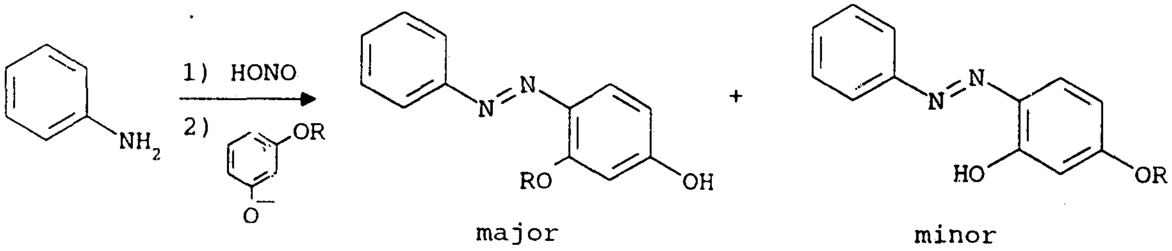

Scheme 4. Diazonium salt coupling to monosubstituted resorcinol.

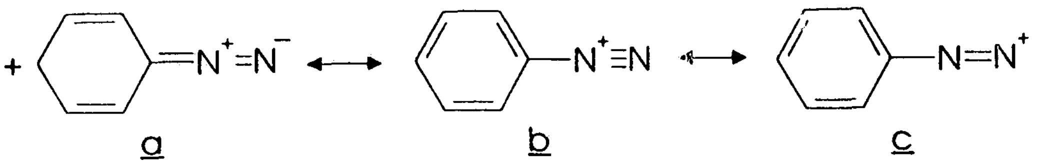

Figure 20. Resonance structure of the diazonium ion.

Aromatic diazonium salts have the resonance structure shown in Figure 20 and are normally written as b, which is the major resonance contributor according to IR stretching frequencies, although a is invoked to justify the greater stability of aromatic diazonium salts relative to their aliphatic analogues and c represents the structure that reacts with electrophiles. They are usually prepared using what is nominally referred to as nitrous acid (HONO - generated *in situ* from $NaNO_2$ and HCl) although it actually represents a set of complex equilibria involving several nitrosating species, the strongest of which is NO^+. Despite the acidic conditions it is considered that the free amine reacts with NO^+ in what is normally the rate limiting step to give $Ar\text{-}NH_2^+\text{-}N{=}O$ which then tautomerizes and dehydrates[73] to give $Ar\text{-}N_2^+$. The overall reaction is $2HCl + NaNO_2 + ArNH_2 \rightarrow ArN_2^+Cl^- + NaCl + 2H_2O$. At $pH \leq 3$ aliphatic amines do not form diazonium salts but the primary aliphatic amine here must be protected since it is expected to react with the product aromatic diazonium salt to give a triazene[72]. I found this to be the case as adding the unprotected diazonium salt to a basic buffer in methanol / water immediately gave an intense orange colour. This reaction was used as a crude preliminary experiment to determine the length of time for the diazotization to go to completion, and it was found to be complete within five minutes. The overall reaction requires two equivalents of HCl, assuming the amine is already as its HCl salt, and so three equivalents were used which in the small volume ultimately used for the reaction gives initially ≈1.5 M HCl. In more dilute solutions the reaction was slow, which is undesirable since the diazonium salt product is rather unstable.

The coupling of the diazonium salt to the monoprotected resorcinol anion is thought to follow a S_E2 mechanism[74] shown in Figure **21**. Either step can be rate limiting depending on the amount of crowding in the intermediate ArN_2R^+H and the structure of the base B but in aqueous OH^- with relatively unhindered substrates k_1 is most likely rate limiting. The pH must be high enough to give the anion of resorcinol in order for it to be sufficiently nucleophilic; I did attempt a reaction with the neutral dimethyl ether of resorcinol but there was no reaction whatsoever. Under such aqueous basic conditions

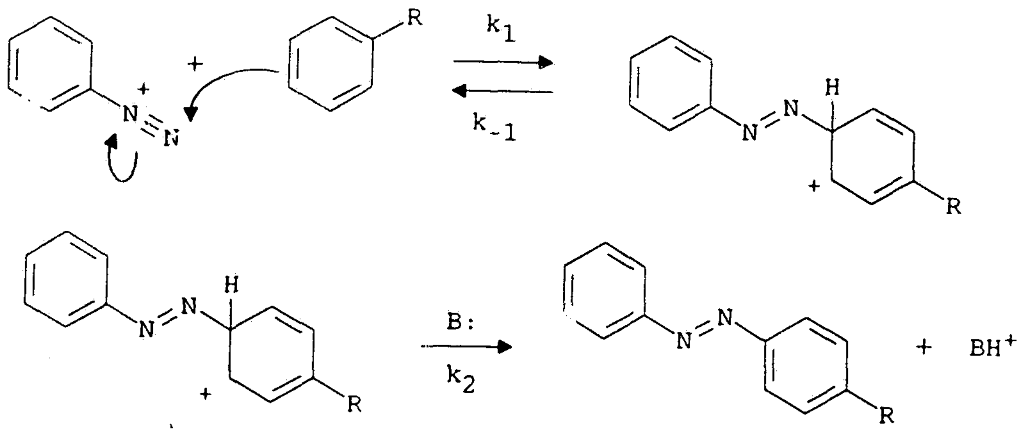

Figure 21. S_E2 reaction mechanism.

diazonium salts can form diazotates according to the equation shown in Figure 22. The equilibrium shifts farther to the right with increasing pH and the *anti* form is relatively unreactive so this side reaction is a potential problem if the pH is too high or the desired azo coupling reaction slow.

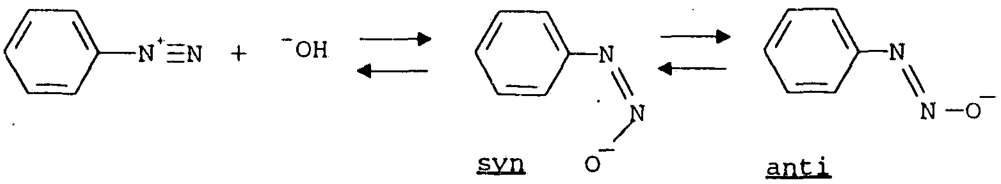

Figure 22. Diazotate formation.

Another potential problem concerning the pH is that although the new electron withdrawing ArN_2- substituent on the resorcinol ring makes the product less reactive towards a second molecule of the diazonium salt it also makes the phenoxide more acidic and at pH ≈ pK_a of the product the higher concentration of monosubstituted product anion may result in the bis-azo adduct being a significant byproduct. This compound can form as seen in an experiment in which there was an accidental excess of diazonium salt resulting in the bis-adduct as the only isolated product. In the event, the reaction carried out at either "pH 8" or "pH 11" (in fact 1:1 mixtures of the appropriate buffers with methanol for solubility reasons), which lie to either side of the expected pK_a of the product, gave identical good results with the bis-azo adduct as a very minor byproduct.

2.1.2 Regiochemistry of the Azo Coupling Reaction

As an electrophilic aromatic substitution reaction the attack by the diazonium salt should be to the site of highest electron density which is normally *para* to the primary activating / directing O^- group[70]. Steric effects have also been discussed in the literature although most of the work concerned sulfonated naphthols of interest to the dye industry[75] and is not particularly relevant to this study. In addition any discussion of steric effects in my system involves an estimation of the relative sizes of the OR substituent and the O^- substituent solvated in methanol / aqueous buffer, which is open to debate. The primary *para* direction is an empirical observation with mono-*O*-substituted resorcinols and I had no reason to think that my system would be any different, but since the correct regiochemistry is essential for the target it had to be proved. It bears repeating that it didn't really matter which regioisomer predominated as long as it was strongly predominant for overall efficiency and as long as its identity was certain. A preliminary reaction between the diazonium salt from unsubstituted aniline and the mono-*O*-acetate of resorcinol (Scheme 5) was very rapid as shown by an immediate intense orange colour.

The product NMR spectra were not completely assigned but it was clear that there were about equal amounts of two major products (**15** and **16**). Room light or sunlight should not be intense enough for this to be a mixture of *cis* and *trans* isomers rather than regioisomers but this was proved by re-recording the NMR spectra after the sample had been in the dark for several days and finding them to be identical, and by hydrolysing the acetate blocking group to yield a single compound (**17**).

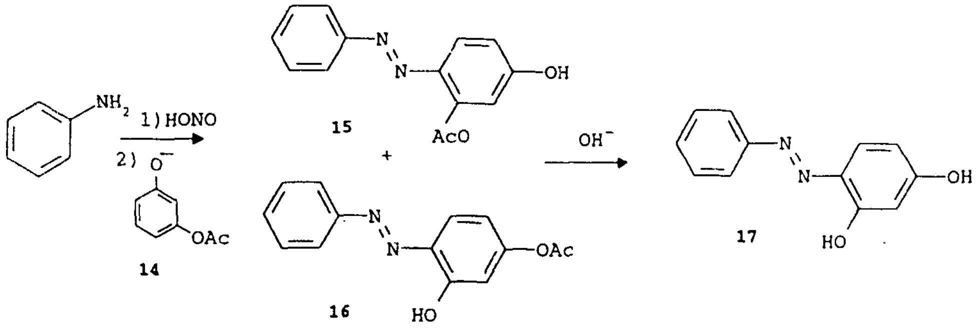

Scheme 5. Hydrolysis of reaction mixture to a single product.

Another preliminary reaction was carried out between the diazonium salt from unsubstituted aniline and resorcinol mono-*O*-substituted with the bulky TBDMS (t-butyldimethylsilyl) group to see if TBDMS is large enough to cause substitution *ortho* to O^- to predominate. Again the NMR spectra were not completely assigned but about equal amounts of the two isomers were evident. In any case the TBDMS group turned out to be unsuitable as it hydrolysed significantly even under the mild conditions of workup.

A model reaction, pictured in Scheme 6 was carried out to provide products to determine the regiochemistry. Note that the numbering scheme shown differs from the numbering used in naming the compounds (see Experimental chapter), which formally are substituted diphenyl diazenes. The numbering scheme shown here is used for convenience in comparing regioisomers throughout this thesis. At either "pH 8" or "pH 11" there were two significant products, 15% (chromatographed yield) of the fast-running (by tlc and silica gel column) minor isomer and 76% of the slow-running major isomer, along with a number of trivial byproducts. The two products were readily purified by column chromatography and from ^1H NMR, ^{13}C NMR, and mass spectra they were clearly the two regioisomers of the desired product. In many such cases the regiochemistry can be assigned on the basis of the ^{13}C NMR chemical shifts of the carbon atoms in the resorcinol ring; tables are available[76] giving the effects of all the substituents involved and their effects are roughly additive. In this case, however, the resorcinol ring bears three substituents all involved in resonance to some extent, and at this point the additive

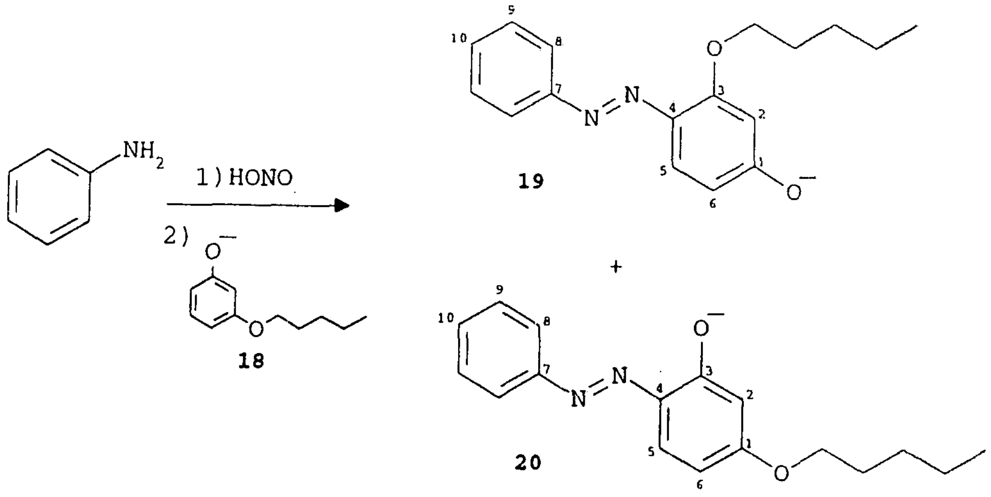

Scheme 6. Model azo coupling reaction.

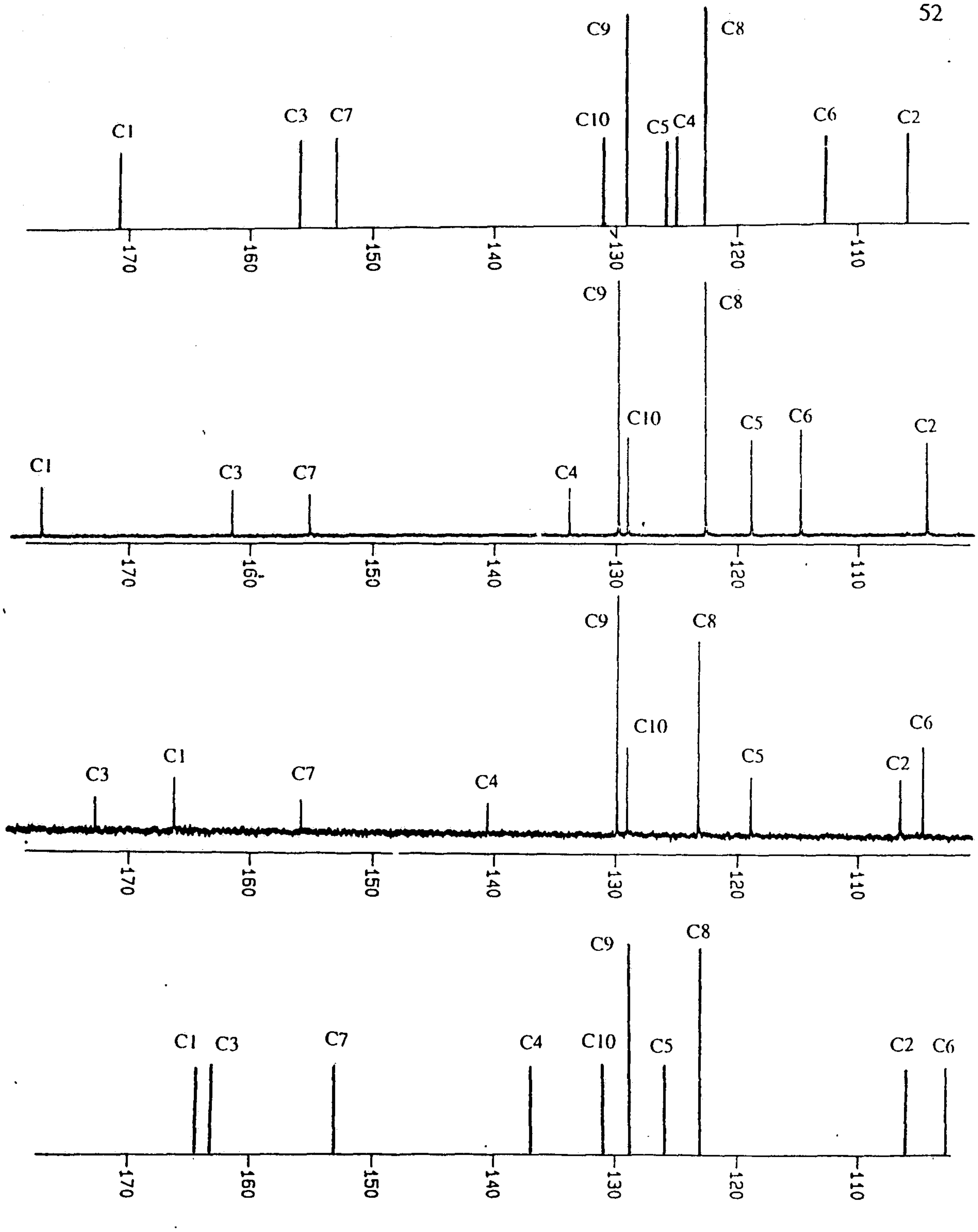

Figure 23. Predicted and observed ^{13}C NMR chemical shifts. Top: predicted for *para* coupled isomer. Top Centre: compound **19**. Bottom Centre: compound **20**. Bottom: predicted for *meta* coupled isomer.

substituent effects begin to break down. The ^{13}C-^{1}H coupling constants observed in the undecoupled ^{13}C spectrum are also somewhat atypical. Figure **23** gives the predicted and observed aromatic regions of the spectra of the anions and although it appears more likely that the major isomer is the *para* coupling product the assignment is by no means decisive. The recorded spectra are in CD_3OD / CD_3O^- solution primarily so that the two O-bearing carbon signals are distinct but it also turns out that as the neutral species in $CDCl_3$ the major isomer gives a spectrum with line broadening and extra peaks. This sort of appearance is usually associated with the formation of aggregates, although the sample here appears as a clear solution. All samples gave sharp spectra in CD_3OD / CD_3O^- solution and were found to be stable in this solution for weeks at least. It was shown that the chemical shift differences between the isomers in this solvent were not a result of complexed Na^+ counterion by adding 18-crown-6 to the NMR sample tube and observing no change in any chemical shift values.

The ^{1}H NMR spectra will not distinguish between these two regioisomers but the ^{1}H signals are easily assigned so that a heteronuclear (^{1}H and ^{13}C) 2D NMR allows unambiguous assignment of all ^{13}C signals, except to distinguish between the regioisomers. There is a delay time component of the pulse sequence used for the 2D experiment which selects for coupling constant and most assignments were made using the spectra shown as Figures **24** and **25** selecting for J=130 Hz, a typical $^{1}J_{H\text{-}C}$ value, for compounds **20** and **19** respectively. The spectrum of **19** selecting for J=7 Hz, intended to show *meta* $^{3}J_{H\text{-}C}$ coupling (although in this system some J values were unusual), shown in Figure **26** confirms the assignments of all ^{13}C signals; also the correlation between one

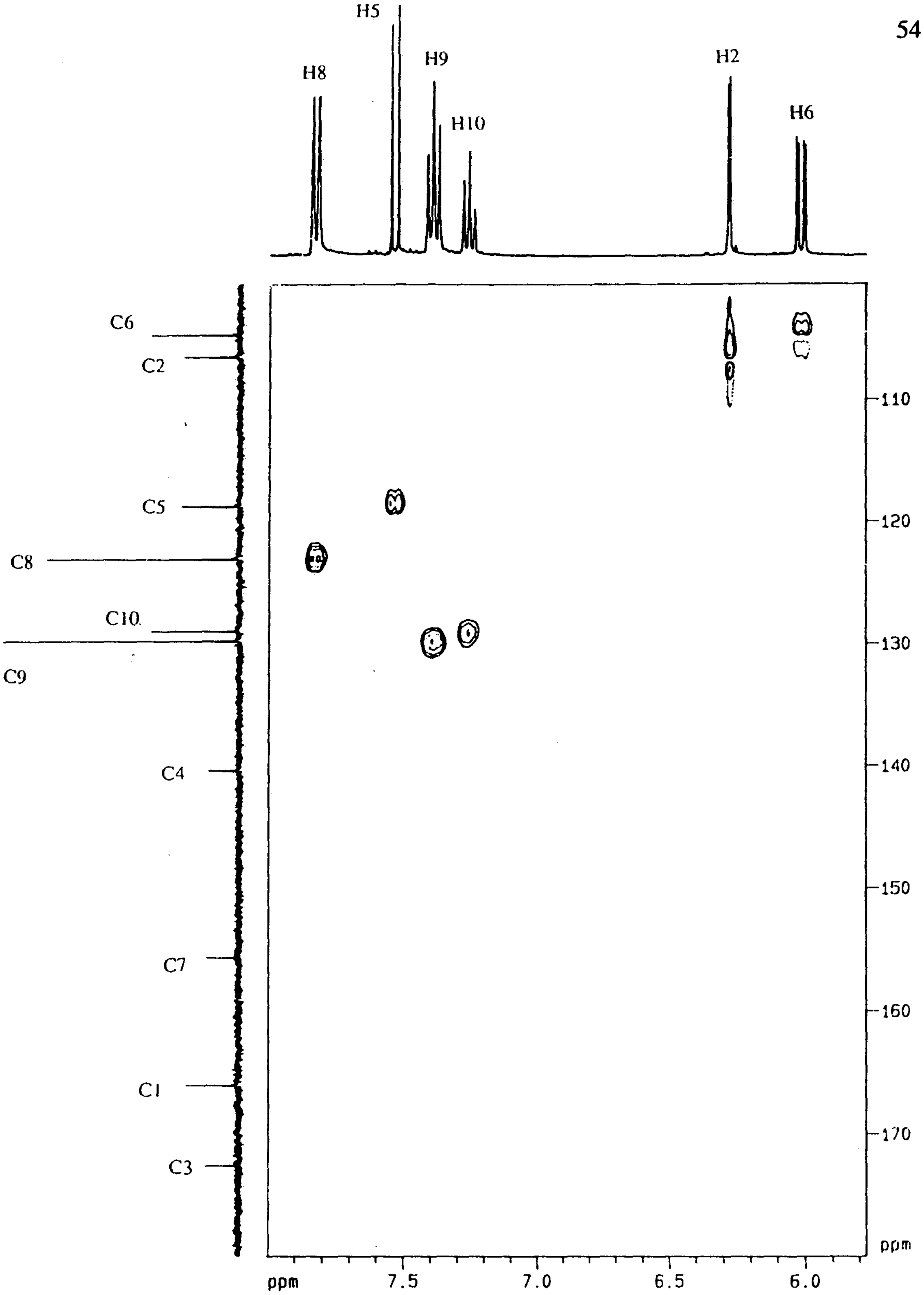

Figure 24. Aromatic region of heteronuclear 2D NMR spectrum (J = 130 Hz) of the minor isomer **20**.

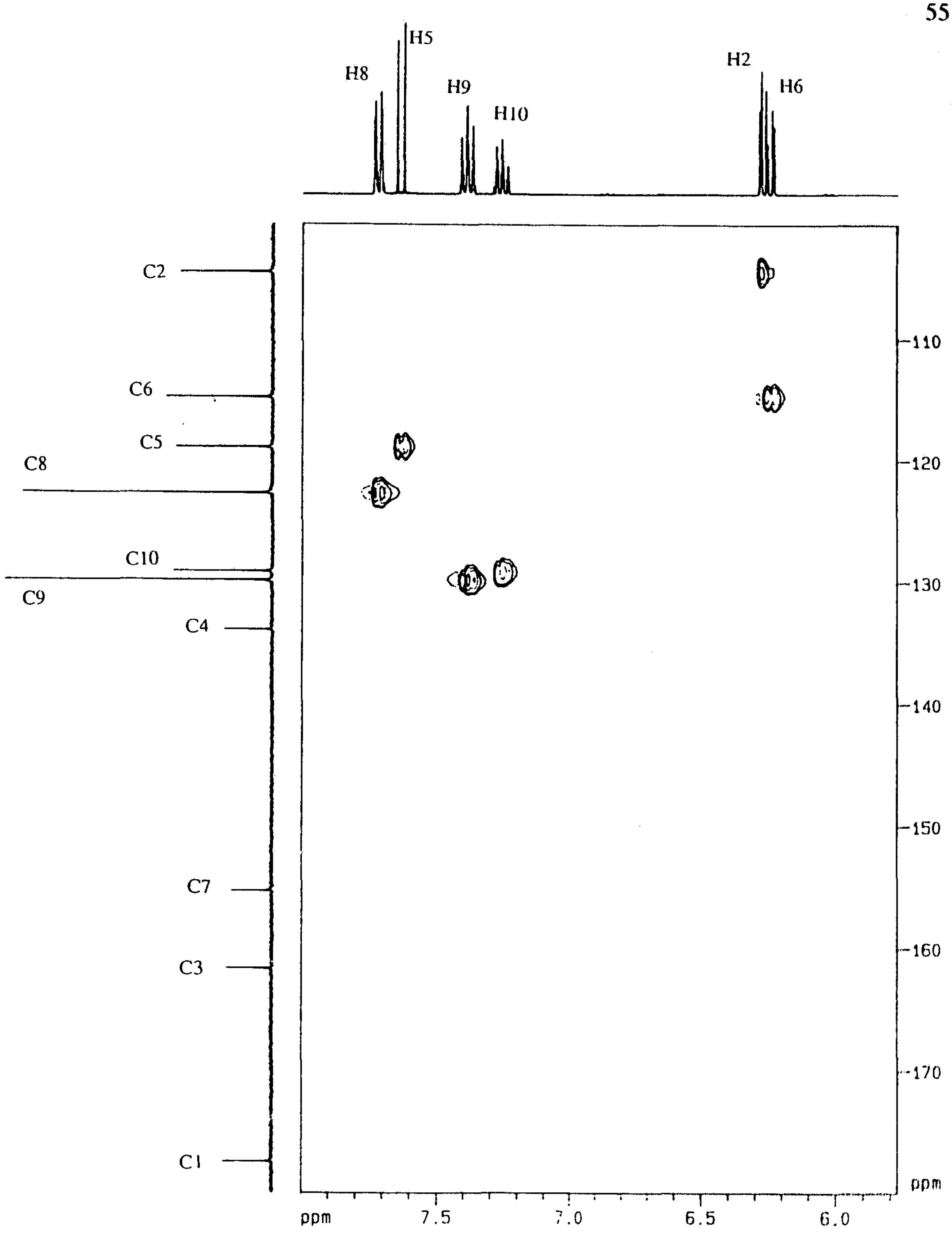

Figure 25. Aromatic region of the heteronuclear 2D NMR spectrum (J = 130 Hz) of the major isomer **19**.

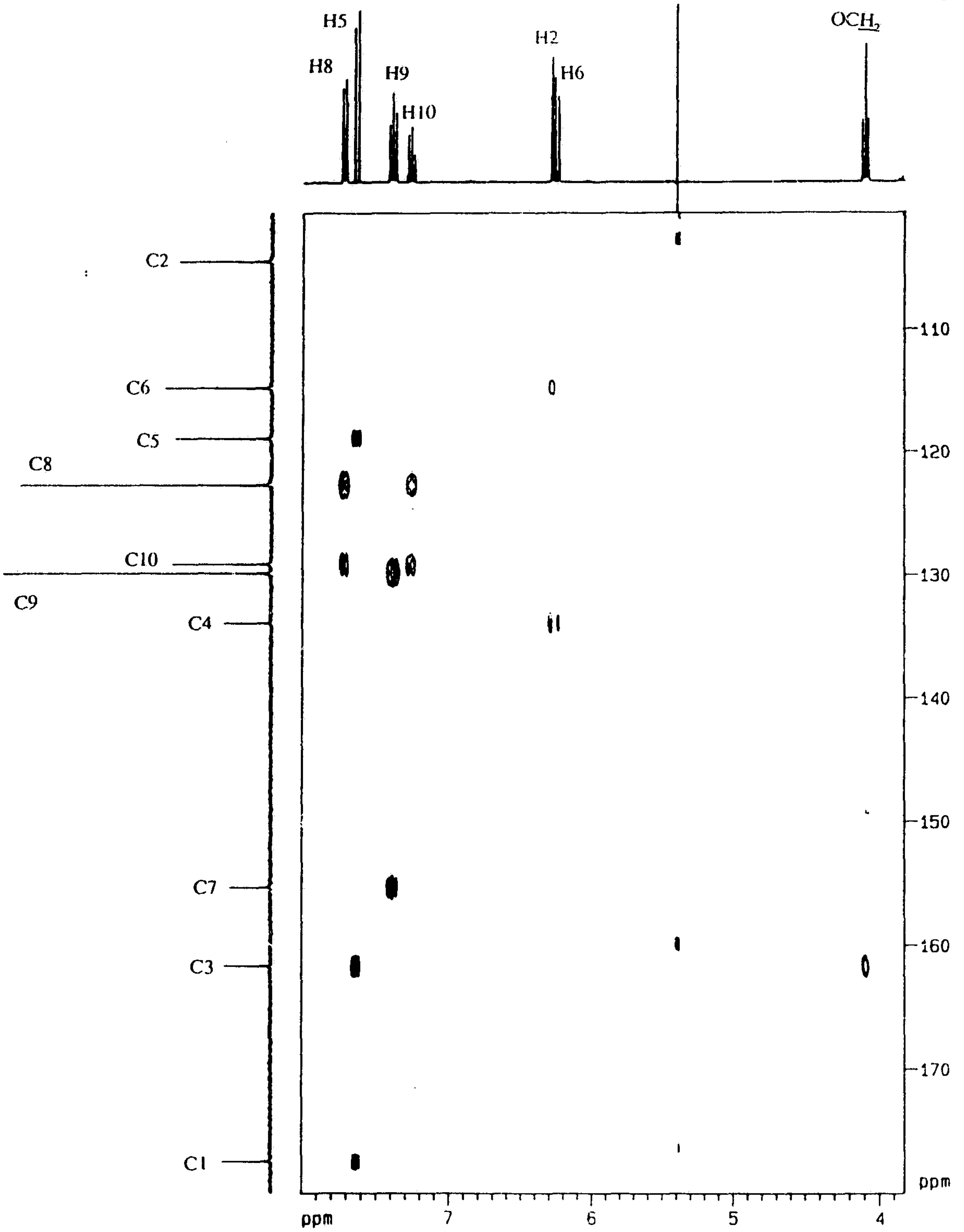

Figure 26. Aromatic region of the heteronuclear 2D NMR spectrum (J = 7 Hz) of the major isomer **19**.

of the ring carbons (C3) and the side chain O-CH_2 signal in Figure **26** confirms that the carbon bearing -O^- is the most downfield signal in the spectra of both isomers as expected, but this still does not establish which isomer has it *para* to the azo group and which has it *ortho*. One proton, H6 in Scheme **6**, might be in a position to distinguish the regioisomers because it is *ortho* to one oxygen-bearing carbon and *para* to the other but a typical *ortho* $^2J_{H\text{-}C}$ is 1-4 Hz and a typical *para* $^4J_{H\text{-}C}$ is 0.5-2 Hz so it would be dangerous to base an important assignment on this basis. Furthermore coupling constants within this ring system are not typical; for example the O-bearing carbons in this ring should each show one *meta* coupling and two *ortho* / *para* couplings in the undecoupled ^{13}C spectrum, but in fact in the spectra of both isomers the C-O^- carbon shows the *meta* coupling and one *ortho* / *para* coupling of 2.6-2.8 Hz, while the C-OR carbon shows the *meta* coupling only. Similarly although it has been reported that an OH proton adjacent to an azo group gives a ^1H NMR signal at very low field[77], I would be reluctant to base an important assignment on the chemical shift of an OH proton particularly since this result was reported for spectra in CCl_4, a solvent in which one of my isomers gives a complex line-broadened spectrum.

At this point the reaction using the *para* substituted diazonium ion shown in Scheme **7** was carried out with results virtually identical to the model series - about 15% of a fast-running minor isomer and 75% of a slow-running major isomer. The ^{13}C spectrum of the resorcinol ring of the major isomer was superimposable on the spectrum of the resorcinol ring of the major product of the model reaction. Similarly the spectra of the resorcinol rings of the minor isomers from both reactions were superimposable. The chemistry to add the second arm at the O$^-$ position was explored using both the model and target substrates and it was found that the aromatic regions of the spectra of all compounds arising from the major isomers were superimposable, and similarly the spectra of all compounds arising from the minor isomers were superimposable; in short, unambiguously assigning the regiochemistry of any one of these compounds would serve to identify them all.

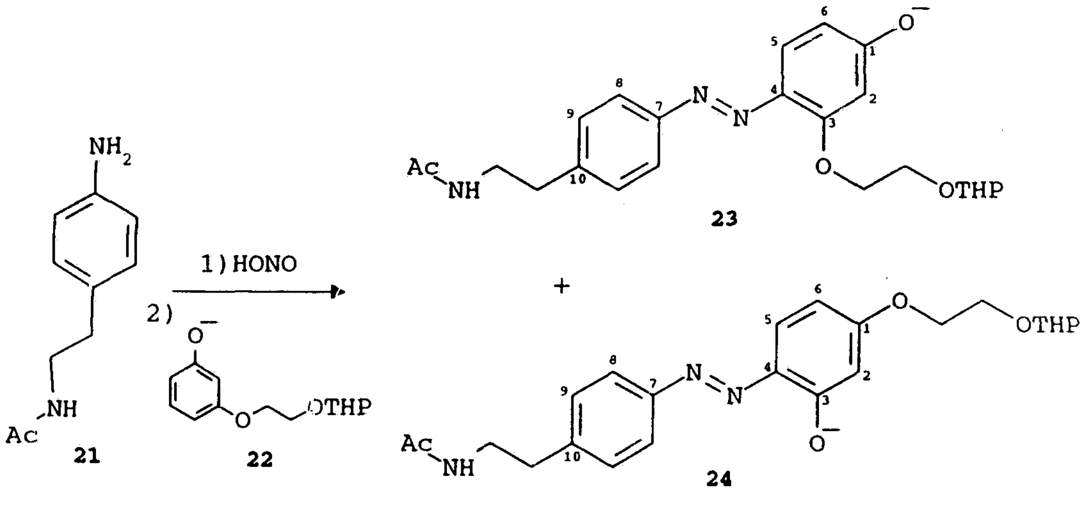

Scheme 7. Azo coupling reaction with acetyl-protected amine.

There has been a report of the mass spectra of azobenzenes[78] but this did not seem to be a promising method; prominent peaks were from M$^+$, loss of either aromatic moeity to give both Ar-N$_2^+$ ions, loss of N$_2$ from both these to give both Ar$^+$ ions, and loss of N$_2$ with a skeletal rearrangement, but none of these fragmentations would be diagnostic for the regiochemistry of my compounds. Furthermore it was even noted that isomeric *ortho* and *para* substituted compounds tended to give very similar spectra; the OH substituent was considered noteworthy because it was sometimes lost as CO rather than as OH but again *ortho* and *para* isomers were not distinguishable. The mass spectra of regioisomers **19** and **20** were recorded but there were no significant peaks that were unambiguously diagnostic for regiochemistry.

The regiochemistry problem was ultimately solved by synthesizing by an unambiguous route an analogue with the exact substitution pattern of one product regioisomer. There is a family of aromatic azoxy compound rearrangements called Wallach rearrangements; the photochemical version has been shown to be an *intramolecular* migration of oxygen from N to the *ortho* position of the distal aromatic ring[79] and a crude bridging mechanism was proposed[80].

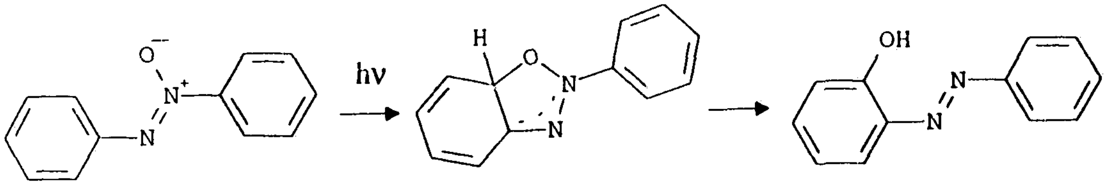

Figure 27. Proposed mechanism for Wallach rearrangement.

A substrate was therefore prepared as shown in Scheme **8** and photochemical rearrangement yields compound **28** which has the same substitution pattern on the trisubstituted ring as the product of diazonium attack *ortho* to the O⁻ group. In the ^{13}C NMR spectrum of **28** the disubstituted ring carbon signals are easily assigned by comparison with intermediates in the route shown but all assignments were confirmed by a heteronuclear 2D NMR spectrum. The ^{13}C NMR spectrum of the trisubstituted ring of compound **28** is superimposable on the spectra of the fast-running minor regioisomers from both the model and target series, confirming that diazonium attack is indeed predominantly *para* to the primary directing group O^-.

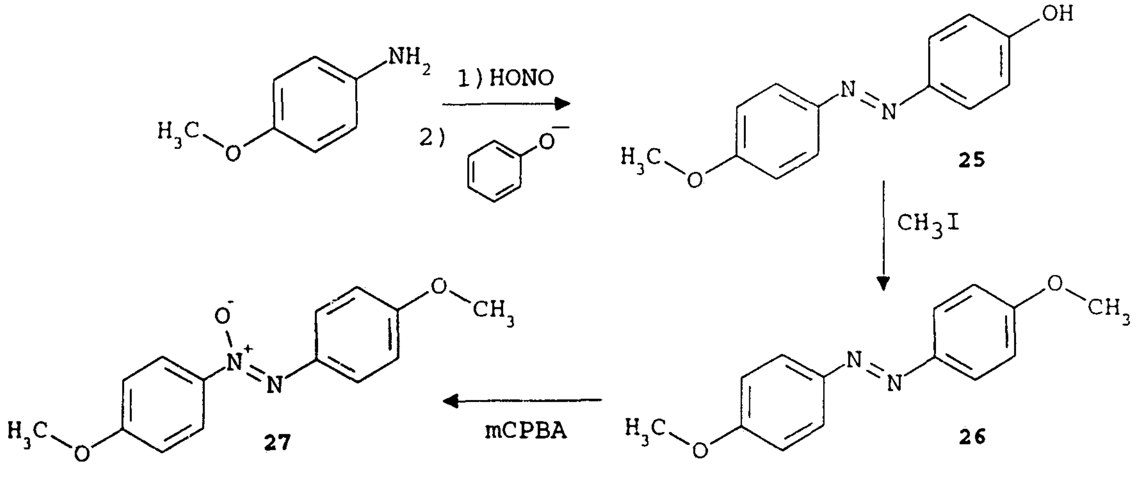
NH2
H3C
O
1) HONO
2)
O−
N
N
OH
25
CH3I
O
CH3
26
mCPBA
O−
N+
27

Scheme 8. Synthesis of substrate for Wallach rearrangement.

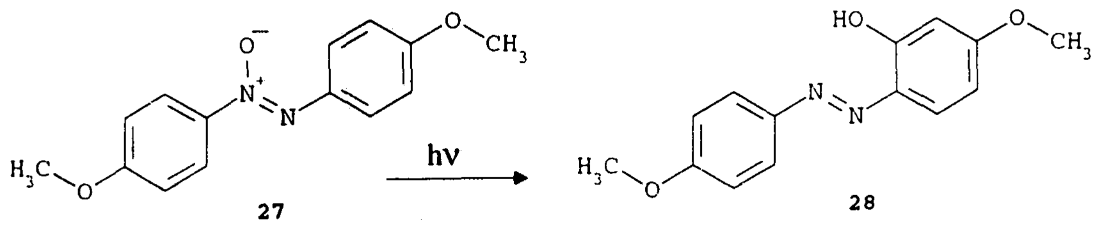
O−
N+
N
O
CH3
H3C
27
hν
HO
28

Scheme 9. Photochemical Wallach rearrangement.

At the same time the same result was obtained by the INADEQUATE NMR experiment. A comment should be made here with respect to the nOe (nuclear Overhauser effect) NMR experiment which might seem an obvious solution to this problem. The nOe experiment involves irradiating (saturating) one nucleus and observing intensity changes in the signal of another nucleus; it involves dipolar (through space) coupling and so normally depends on the distance between the irradiated and observed nuclei. In my case H6 is the one label positioned to distinguish the two isomers and it would be expected to show interaction with the side-chain O-C$\underline{H_2}$ protons of one regioisomer only, the one resulting from attack *ortho* to O^-. The nOe experiment, however, has its drawbacks. For one thing, the effect does not necessarily show up even when nuclei are close. Whether or not it is seen depends on the relaxation pathways available; if single quantum pathways dominate then the effect is not seen and competing multiple quantum pathways may influence the intensity in opposite directions so that the net effect is small. When more than two nuclei are involved the signal intensities come to depend on internuclear distances and angles in a complex way. For another thing, the nOe may show up even when nuclei are not close. Theoretically a nOe will occur at infinite distance if the observed nucleus is the only source of relaxation for the irradiated nucleus although this can hardly apply in most real cases. It can be seen however over relatively large distances if magnetization is transferred through another nucleus located in space between the irradiated and observed nuclei. In short, it is dangerous to interpret nOes in terms of internuclear distances without corroborating evidence.

INADEQUATE is an acronym for Incredible Natural Abundance DoublE QUAntum Transfer Experiment. As an illustration consider a ^{13}C two-spin system. The INADEQUATE pulse sequence distributes the spin population among all energy levels of the system creating quantum mechanically forbidden double quantum coherence in addition to normal allowed single quantum coherence. This pulse sequence is then followed by a "read" pulse to further shuffle the spin population so that some double quantum coherence is converted to single quantum coherence, which is observable by the detector. Sensitivity to phase changes in the pulse sequence varies as the order of the quantum coherence (i.e. double quantum coherences are twice as sensitive as single) so a co-ordinated cycle of pulse and receiver phases allows editing of the observed single quantum coherence signals on the basis of the order of the multiple quantum coherence through which they have passed (this technique may be familiar from the DEPT experiment in which heteronuclear multiple quantum coherences are edited to identify CH, CH_2, and CH_3 groups). Thus normal single quantum coherence signals are filtered out and only two-spin systems are observed; triple and higher order coherence could be filtered out in this way although this is unnecessary in a natural abundance ^{13}C experiment. A choice of a delay time during the pulse sequence selects for the value of the coupling constant for the two-spin system so by selecting a typical $^1J_{C\text{-}C}$ (for aromatics 55-58 Hz) the only signals observed are from directly bonded ^{13}C nuclei, and the result is a map of the carbon skeleton of the molecule. The drawback of course is that ^{13}C has a 1% natural abundance so without enrichment the probability of adjacent ^{13}C nuclei is 1 part in 10^4. Consequently my experiment required a sample that was so concentrated that it was a syrup (the ^{13}C NMR spectrum was identical to that recorded in much more dilute solution) and an entire weekend of accumulation time on the NMR instrument but the result was clear direct evidence for the regiochemistry of the compound. Figure 28 is the ^{13}C

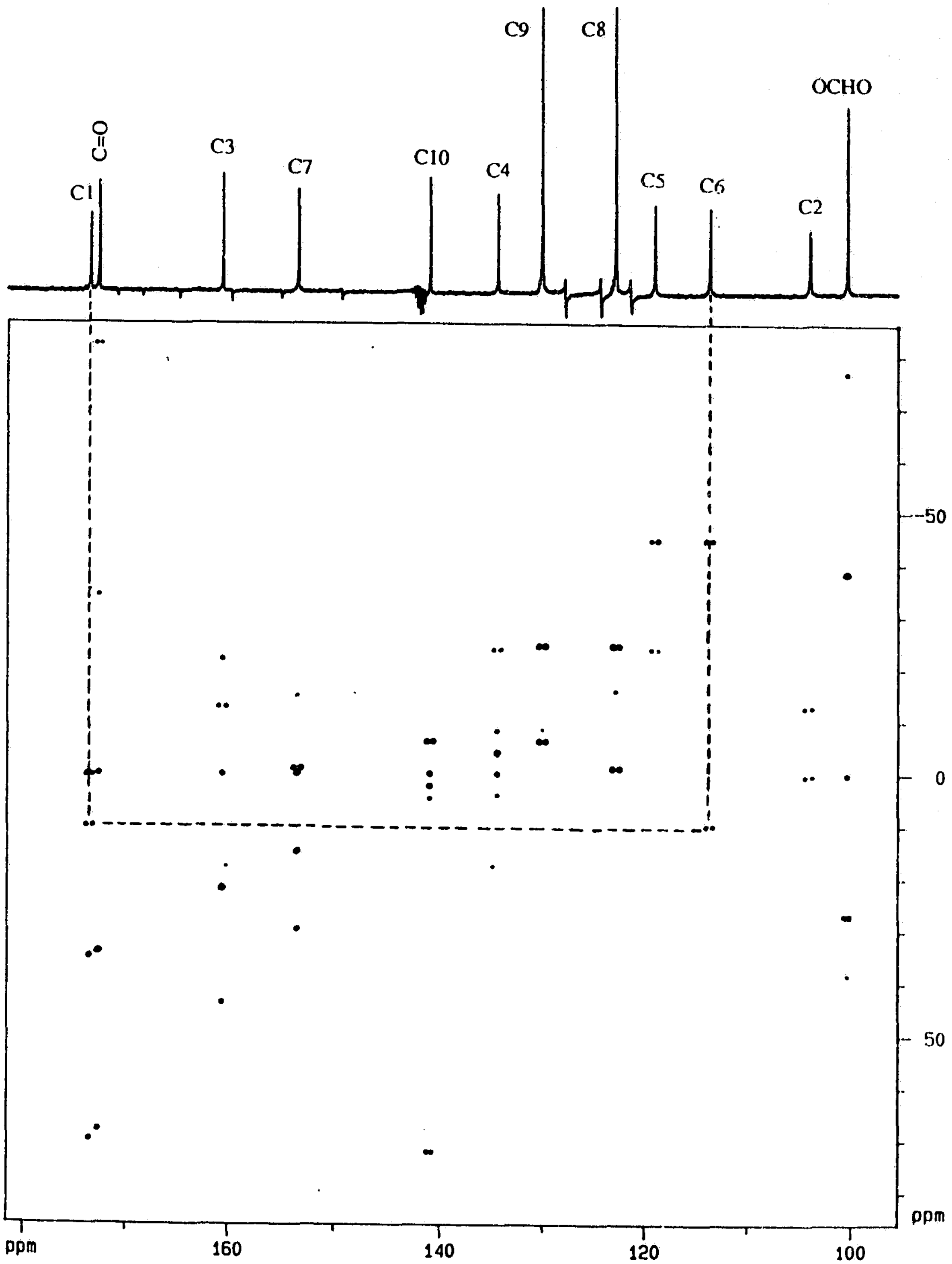

Figure 28. ^{13}C - ^{13}C INADEQUATE spectrum of compound **23** in CD_3OD/CD_3O^-.

INADEQUATE spectrum of the major isomer **23**. The appearance of the spectrum requires some explanation. During the time between the pulse sequence establishing the double quantum coherence and the read pulse what evolves are the double quantum frequencies, which are the sums of the chemical shifts of the paired nuclei; during the acquisition time following the read pulse what evolves are the frequencies of the single quantum coherences to which the magnetization was transferred by the read pulse. The result is a 2D frequency domain spectrum with AB (or AX) doublets at $(\nu_A,\nu_A+\nu_B)$ and $(\nu_B,\nu_A+\nu_B)$. Thus in Figure **28** the horizontal axis corresponds to chemical shift and the normal ^{13}C spectrum is printed above it; the vertical axis corresponds to the double quantum frequency (i.e. $\nu_A+\nu_B$) and is printed at twice the scale so that pairs of directly bonded carbons appear as doublets equidistant from the corner to corner diagonal. The strong correlation between C6 and the C-O$^-$ carbon (C1) indicated in Figure **28** means they are adjacent, so this regioisomer must be the result of *para* attack. All other predicted correlations show up except the other diagnostic one, between C3 and C4, which does actually appear but is even fainter than some spurious peaks, probably because both carbons involved are bonded to heteroatoms.

The uv spectra of the model regioisomers **19** and **20** show λ_{max} 368 nm (ε=22,500) and λ_{max} 378 nm (ε=24,500) respectively. These are comparable to literature values from Shinkai[63,64,66,67,68] for closely related azobenzenes. The n-π^* band noted for the parent azobenzene is not seen even as a shoulder; certainly because the π-π^* transition is at higher wavelength than in the parent, and the n-π^* may also be shifted to lower wavelength. The spectra were unchanged after a week in the dark.

Now that the regiochemistry of the azo compounds was established the second arm was added to **19** and **20** as shown giving **29** and **30** respectively. In the uv spectra

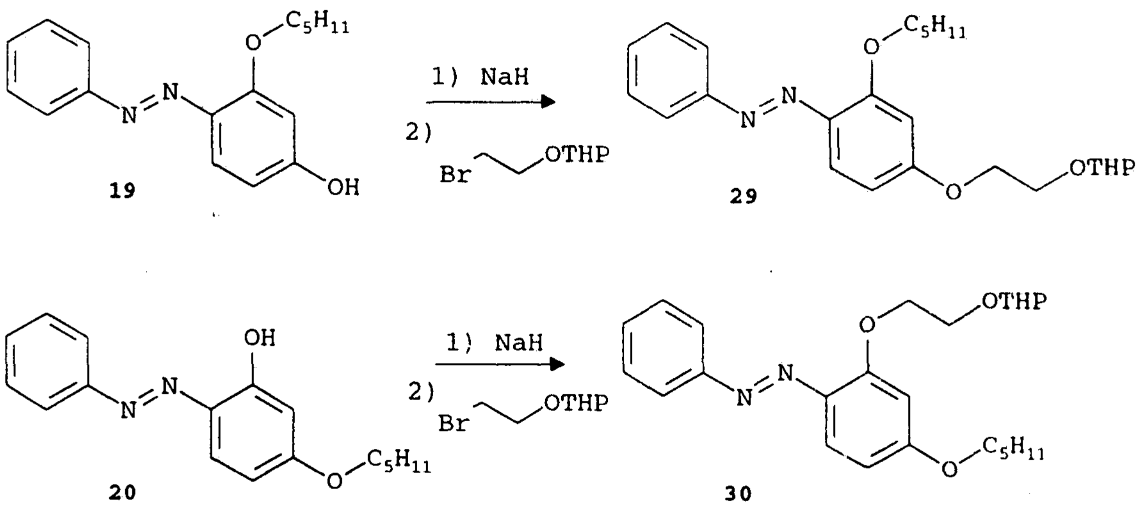

Scheme 10. Addition of second arm in model series.

of these compounds both the π-π^* and n-π^* bands could be seen; maxima for **29** were 366 nm (ε=17,820) and 443 nm (ε=2070), maxima for **30** were 366 nm (ε=17,680) and 442 nm (ε=1750). The position of photochemical equilibrium (photostationary state) for the *cis-trans* isomerisation and the rate of the thermal *cis* → *trans* back reaction were measured by irradiating these compounds in a standard photochemical reactor with a 300 nm cutoff, and following the absorption at 366 nm. As expected, irradiation caused the A_{366} to decrease and A_{442} to increase as more *cis* was formed. The photostationary state was reached within 90 seconds. To determine the exact position of the photostationary state requires a value of A_{366} for the pure *cis* isomer which is not known but using a reasonable value[52,81] of ε=500 the photostationary mixtures from **29** and **30** were 56% *cis* and 59% *cis* respectively. The rate of the back reaction was monitored; over the first day a plot of ln A_{366} against time gives the straight line characteristic of exponential decay of *cis*, with half life values of the decay for **29** and **30** being 39 and 42 hours respectively (again using ε_{cis}=500 at 366 nm). At longer times the decay rate falls off (see **Figure 43**). These values are comparable to the longer ones measured by Shinkai. Thus the compounds show rapid photochemical *trans* → *cis* isomerisation and a slow thermal back reaction and as expected are suitable for the purposes of this study.

2.1.3 Blocking Group Manipulation

The focus now turns to consideration of the synthesis of the photogate proper. As discussed the choices for aliphatic amine blocking group were severely limited and I settled reluctantly on the acetyl group. It will certainly withstand all the reaction and workup conditions through the synthesis; the problem is that amides do not hydrolyse readily. There are, however, a couple of promising new procedures to hydrolyse amides under mild conditions, and even if harsh conditions are necessary the rest of the molecule is relatively stable.

The second arm was prepared according to Scheme **11** and then coupled to the correct regioisomer as shown in Scheme **12**. In the event that acid hydrolysis of the acetyl group is necessary the isopropylidene and THP protecting groups would of course be completely hydrolysed as well; but after this point no more acidic conditions will be encountered so the amine can be selectively protected with the acid labile tBOC (*tert-*

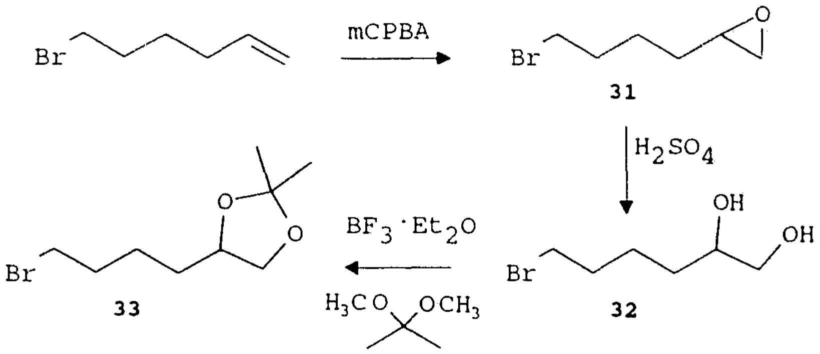
Br
mCPBA
Br
O
31
H2SO4
OH
OH
Br
32
BF3·Et2O
H3CO OCH3
O
O
Br
33

Scheme 11. Synthesis of the six-carbon wall / head unit.

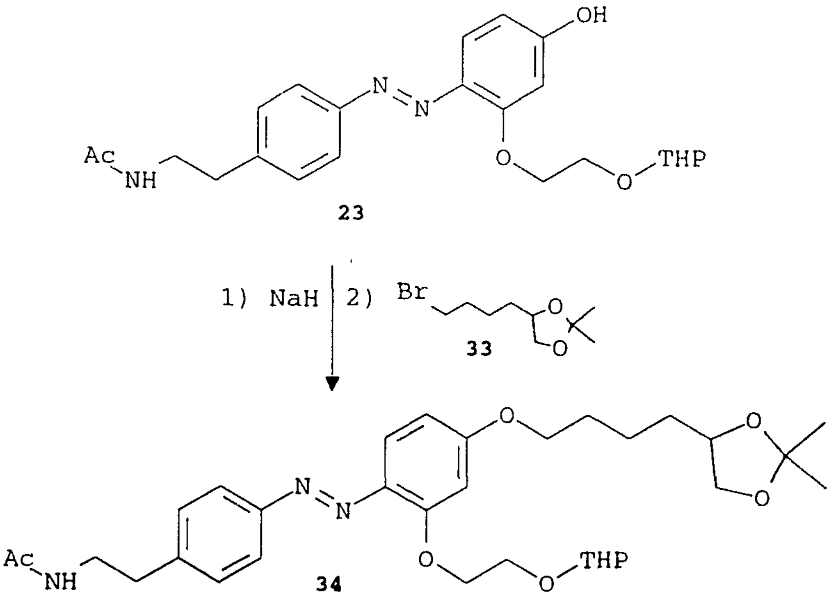
OH
N
N
Ac
NH
O
O
THP
23
1) NaH
2) Br
O
O
33
O
O
O
N
N
Ac
NH
34
O
O
THP

Scheme 12. Synthesis of the fully protected photogate.

butyloxycarbonyl)group and the terminal glycol then selectively protected in the presence of the primary alcohol, once again as isopropylidene, to give the completely assembled photogate suitably blocked for linking to the crown, as shown in Scheme 13. This seems like a lot of manoeuvering but given the restrictions on the amine blocking group there were few choices and the blocking reactions should give very high yields.

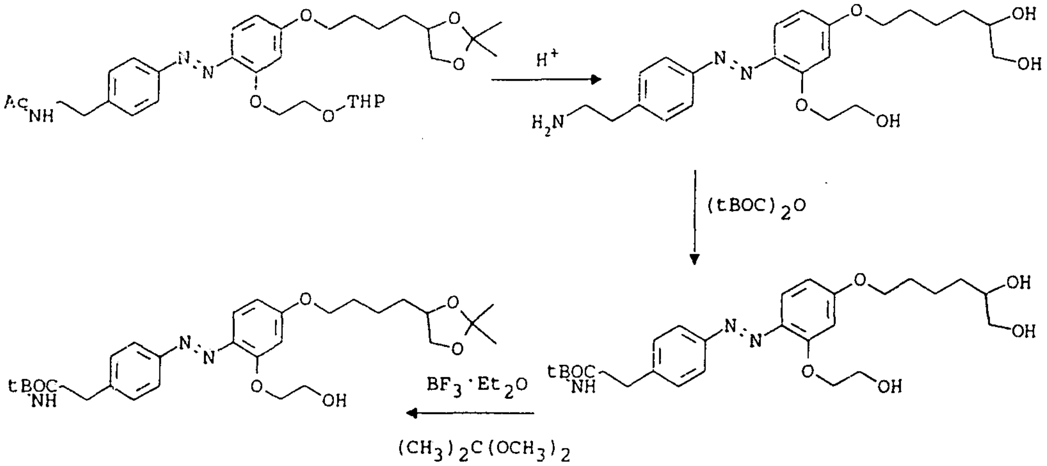

Scheme 13. Proposed selective blocking route.

The fully blocked photogate **34** was prepared as planned and it was shown that as expected mild acid hydrolysis would cleave the isopropylidene and THP groups and that the former could be re-introduced by treatment with acetone dimethylacetal and BF_3 etherate while leaving the primary alcohol free (see Scheme 13). Attempted hydrolysis of the acetyl group, however, was a serious problem. As expected, basic hydrolysis failed; by the time there was appreciable disappearance of the acetyl group there was significant decomposition to unidentified brown material. The anticipated acid hydrolysis, however, was similarly unsuccessful. It was evident from the NMR spectra of the product that the six-carbon arm had been lost and Figure **29** shows the probable mechanism.

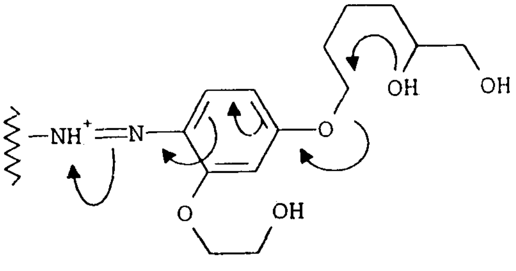

Figure 29. Mechanism proposed for loss of six-carbon arm.

The protonated structure shown is resonance stabilized and so should form readily but should also be relatively unreactive. Loss of the ethylene glycol arm by the analogous mechanism involves a three membered rather than six membered cyclic transiton state and so should be much slower. Therefore it might be possible to remove the acetyl group before the six-carbon arm is added, but attempted hydrolysis of the initial azo coupling product **23** under acidic conditions cleaved the ethylene glycol arm before significant cleavage of the acetyl group.

It has been reported that *cis* $[Co(trpn)(H_2O)_2]^{3+}$ and some related complexes (trpn is tris(3-aminopropyl)amine) will catalyse the hydrolysis of esters, amides, nitriles, and phosphodiesters between pH 5 and pH 8. Specifically the amides were simple formamides[82]. It was proposed that in this pH range one Co ligand is H_2O which is easily substituted by the substrate while another Co ligand is the active OH^- which is in position to attack the bound substrate as shown in Figure **30**.

The complex $[Co(trpn)Cl_2]Cl$ was prepared by literature procedures[83] and hydrolysis of the fully blocked photogate **34** attempted under the same conditions as reported[82]

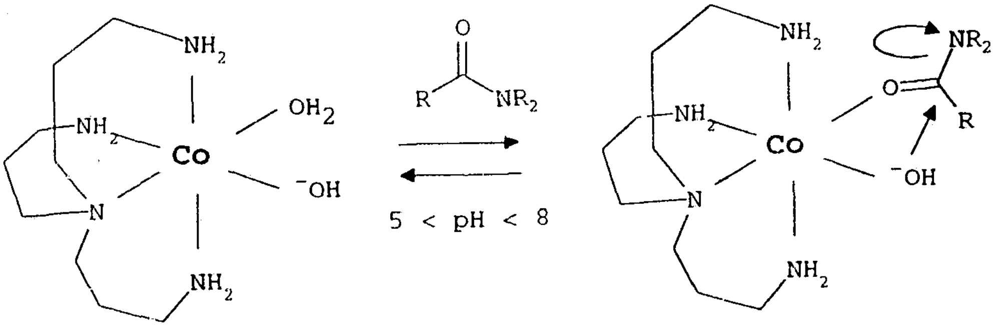

Figure 30. Amide hydrolysis by *cis* [Co(trpn)(H_2O)$_2$].

except that water was replaced with 20% n-propanol in water in order to dissolve the photogate compound. In my hands the reaction was completely unsuccessful giving back starting blocked amide even after a week at 100°C. Because of the required pH range the pH was monitored and was seen to rise from pH 5 to pH 7 within the first half hour of the reaction; the most likely explanation is free amine released by decomposition of the catalyst. This behavior has been noted in the literature[84].

There have also been preliminary reports of amide hydrolysis catalysed by phosphate buffer solutions at pH 7.8, although these results were obtained with formamides only[85]. Again my fully blocked photogate was inert, with starting amide the only material recovered after 1 week at 100°C.

The group of choice to ultimately protect the amine was tBOC but the acetyl group was used because of the acidic conditions in the first step of the synthesis. On reconsideration, however, it was noted that the diazotization reaction is complete within a few minutes at 0°C and the tBOC group may be able to stand these conditions. Further experiments established that the diazotization reaction is in fact complete within 1 minute at 0°C and that the tBOC group did withstand this reaction, so the problem of an amine protecting group was easily resolved. This result also raised the possibility that the tBOC group was more stable to acid than the THP ketal group blocking the short linkage arm.

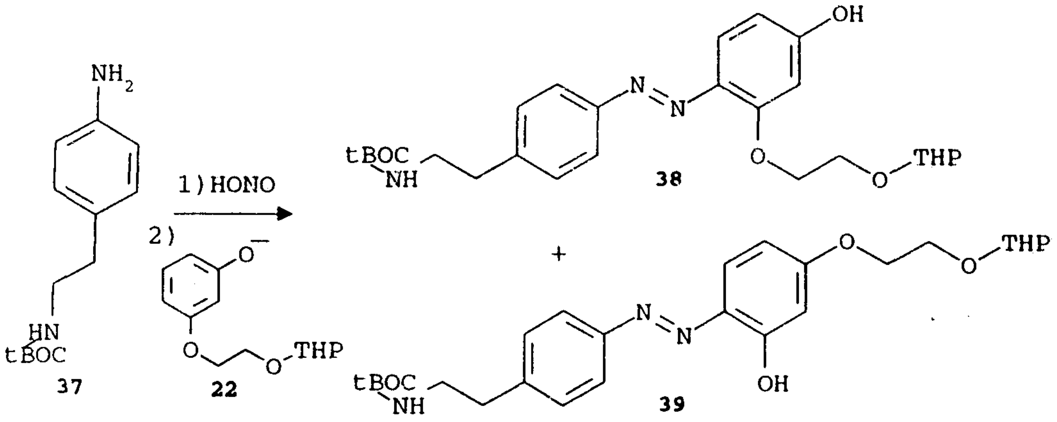

Scheme 14. Azo coupling with tBOC-protected amine.

The azo coupling reaction was carried out using tBOC blocked amine as shown in Scheme **14** and the desired major product **38** was subjected to careful acid hydrolysis in 0.4 M HCl in 60% methanol / water starting at 0°C then warming to room temperature. Selective hydrolysis was in fact achieved; cleavage of THP was complete after 15 minutes at room temperature while loss of tBOC was observed only after 2 hours at room temperature.

These results then lead to a far more efficient route to the desired selectively protected photogate **13**, shown as Scheme **15**. The azo coupling reaction proceeded as before giving a fast-running minor product and a slow-running major product. The former was seen by ^{13}C NMR to consist of two compounds, the *ortho* attack product seen in the earlier series and another which is probably the product of the other *ortho* attack, between the two oxygen substituents, but whose identity was not proved. The latter was the expected *para* attack product; the relevant peaks in its ^{13}C NMR spectrum were superimposable on the spectra of the major products of the model and acetyl-blocked series.

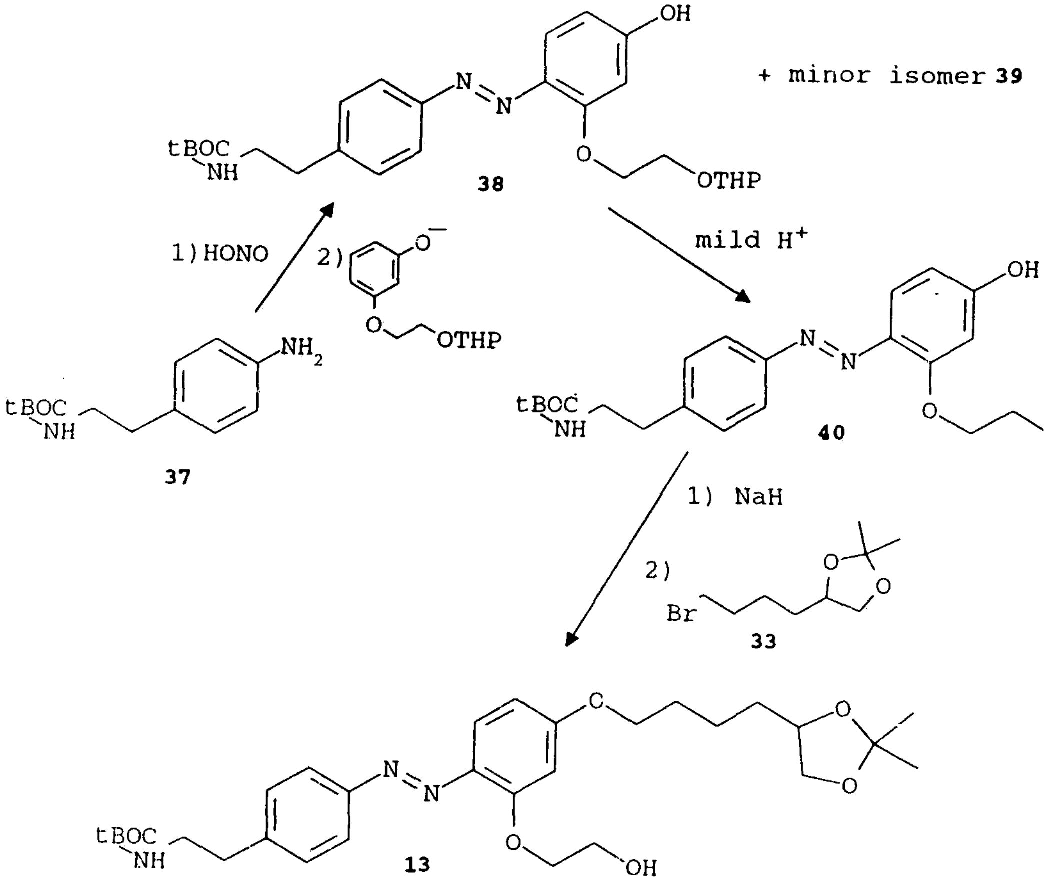

OH
+ minor isomer 39
N
N
tBOC
NH
38
O
OTHP
1) HONO
2)
O⁻
O
OTHP
mild H⁺
OH
NH2
N
N
tBOC
NH
tBOC
NH
37
40
O
OH
1) NaH
2)
O
O
Br
33
O
O
O
N
N
tBOC
NH
13
O
OH

Scheme 15. Complete synthesis of photogate target.

It was noted earlier that the analogous compound from the acetyl-blocked series showed broadened lines in the ^{13}C NMR spectrum in $CDCl_3$ but not in CD_3OD / CD_3O^-, and this was attributed to small aggregates. Compound **38** shows the same behavior in $CDCl_3$; again if there are aggregates they must be small since the sample solution was perfectly clear. In CD_3OD or CD_3OD / CD_3O^- the ^{13}C spectrum of **38** appeared normal and is shown as Figure **31**. The ^1H NMR spectrum of exactly the same solution showed broadening of all peaks; chemical shifts and integration could still be read from the spectrum but there was no resolution of multiplets. Probably as a result of this phenomenon 2D NMR and INADEQUATE spectra could not be recorded successfully, but in light of the NMR evidence the structure of **38** is adequately proved. In addition the +FAB mass spectrum had m/e 486 (corresponding to M+1) as the highest molecular weight peak, accompanied by large peaks corresponding to loss of THP and to loss of THP with subsequent loss of t-butyl. Spectra of the samples recovered from the attempted 2D and INADEQUATE experiments were re-recorded and even in CD_3OD or CD_3OD / CD_3O^- showed broadening or, more usually, apparent doubling of many peaks, particularly aromatic and O-$\underline{C}H_2$ peaks. It was not always exactly the same peaks that were doubled so the aggregation appears to be unspecific and somewhat irreversible depending on the exact history of the sample. The selective deblocking of THP and coupling of the second arm went smoothly as anticipated to give **13**, the complete photogate ready for the link to the crown. The yields for the azo coupling and side arm coupling reactions are mediocre (40% and 60% chromatographed yields respectively, the selective deblocking of THP is quantitative) but they were not optimized and the emphasis in the workup and chromatography was always on quality over quantity. In any case the route is short, using readily available materials, so the yields are acceptable.

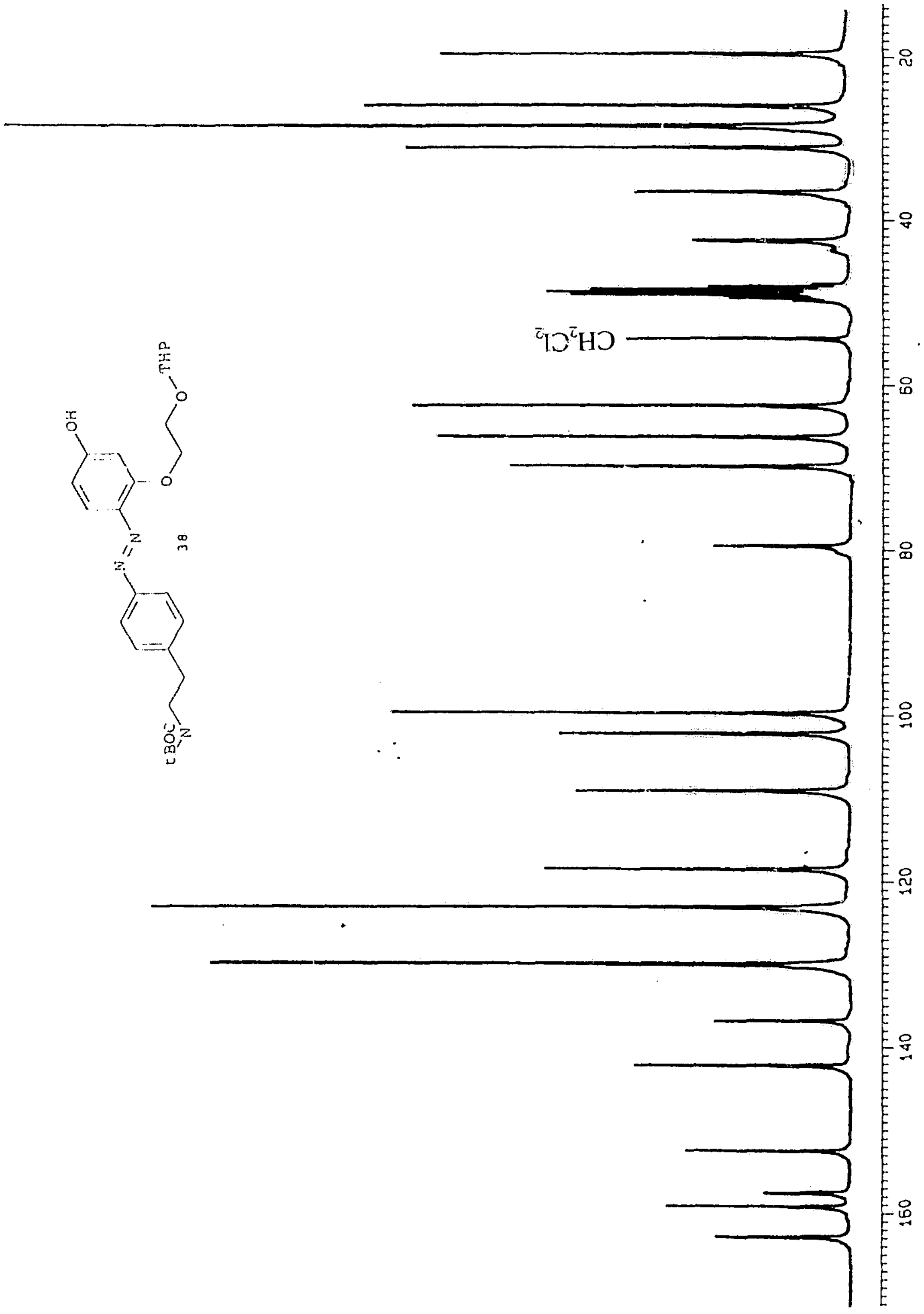

Figure 31. ^{13}C NMR spectrum of compound 38 in CD_3OD.

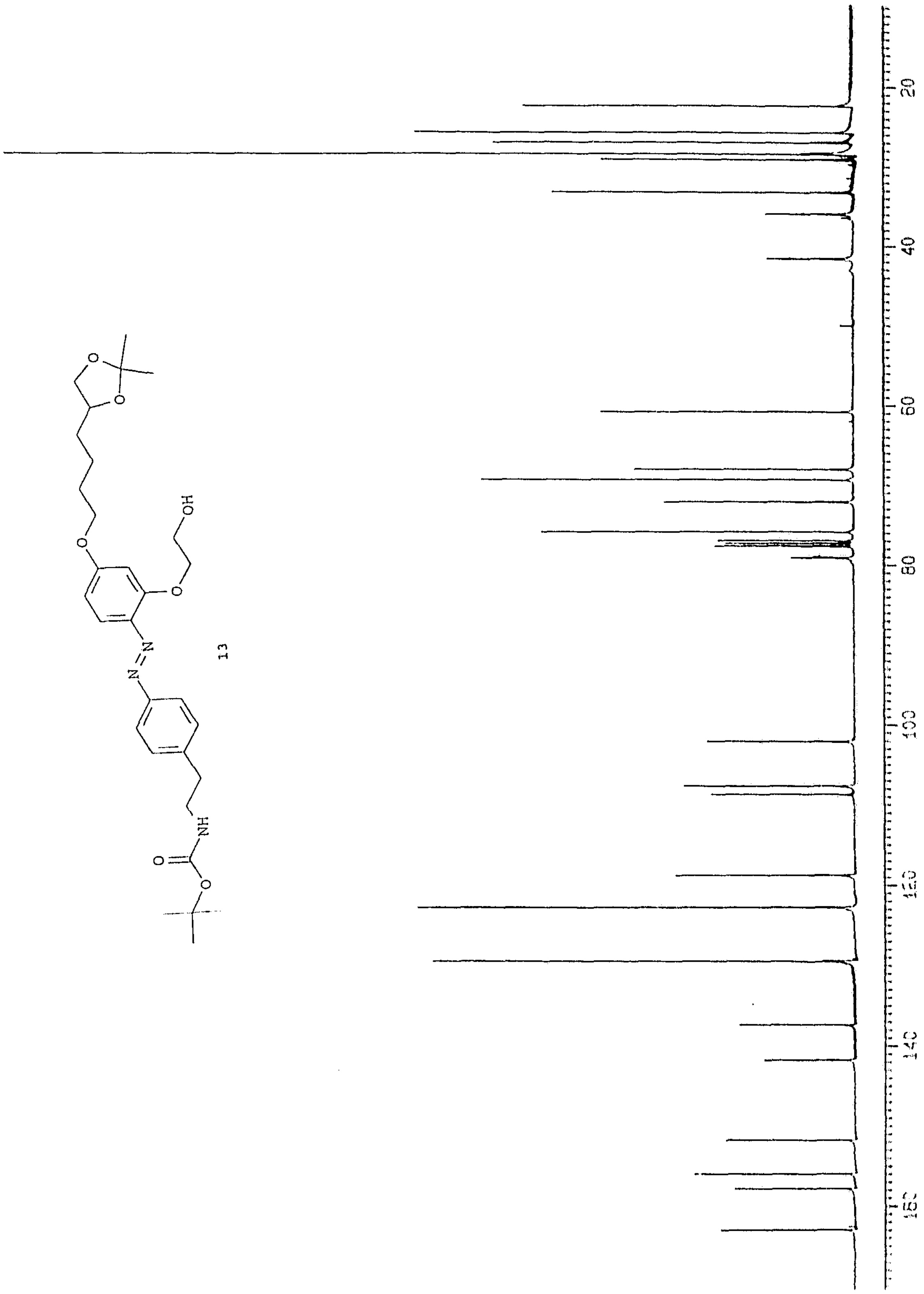

13

Figure 32. ^{13}C NMR spectrum of photogate target **13** in $CDCl_3$.

2.2 Monofunctionalized Crown Ether

2.2.1 Capping Reaction

As discussed in the introduction the proposal to achieve functionalization of one of four identical carboxylate groups is to cap a crown dianhydride with an aromatic alcohol / amine and then selectively hydrolyse the ester of the resulting ester / amide. This is illustrated in Scheme **3**. The capping reaction must be carried out under high dilution conditions. The high dilution principle, first set out by Ziegler[86], holds that in very dilute solution when *intra*molecular reaction is possible it is favored over *inter*molecular reaction since a reactive group on a molecule is more likely to run into the other reactive group on its own end before it runs into another molecule. In a bimolecular reaction such as the crown capping both components must be added at exactly equal rates so that one component is never in excess. High dilution is achieved either by using a very large solvent volume or by very slow addition so that intramolecular reaction is faster than the rate of addition of fresh reagents and effectively there is high dilution in a small volume. A high stirring rate is also necessary to preclude high local concentrations as reagents are added. In the case of crown capping the reaction of amine with the first anhydride should be very rapid but the critical intramolecular reaction of the alcohol with the second anhydride is relatively slow so both a large solvent volume and very slow addition were used to ensure intramolecular reaction.

In a typical procedure the dianhydride **4** was freshly made by refluxing the crown tetraacid in acetyl chloride[35a,49], then prolonged evaporation gave the dianhydride as a powder which can be stored in a desiccator for several days; the dianhydride was checked by NMR before each experiment. Two solutions, one the dianhydride in THF (0.5 to 1.5 mmoles in 60 ml) and the other an equimolar amount of the alcohol / amine (e.g. compound **8**) with about 100 equivalents of Et_3N in 60 ml THF were added from identical syringes at exactly the same rate, by driving both syringes with a single metal plate driven by a variable speed electric motor, into about 1.5 L THF. The reaction solution was kept under dry nitrogen and vigorously stirred at all times. The addition rate was about 1 ml/hr from each syringe so addition took 2 - 3 days. The result from either *meta* or *para* alcohol / amines was the same; any extraction or chromatography fraction when examined by ^{13}C NMR had the peaks at generally the right chemical shifts but there were far too many peaks indicating a complex mixture of products. Figure **33** is a typical example of a ^{13}C spectrum after preliminary workup. A number of purification techniques were applied to separate the various mixtures, including: successive liquid - liquid extractions into organic solvents of increasing polarity; gel permeation chromatography; partition chromatography on a silica gel plate mounted on a "chromatotron" which is essentially preparative tlc on a round plate with sample and solvent added at the centre and driven to the outside as the plate rotates; countercurrent chromatography, a combination of liquid - liquid chromatography and countercurrent distribution, in which sample is partitioned between immiscible solvents as it passes through a long coiled column rotating at high speed; and HPLC with an analytical gel permeation column. The latter column did give good separation of the components to reveal that there were a number of compounds in comparable amounts so if the desired product was there it was certainly not in good yield. In case there was some hydrolysis of the ester during workup the ester was deliberately

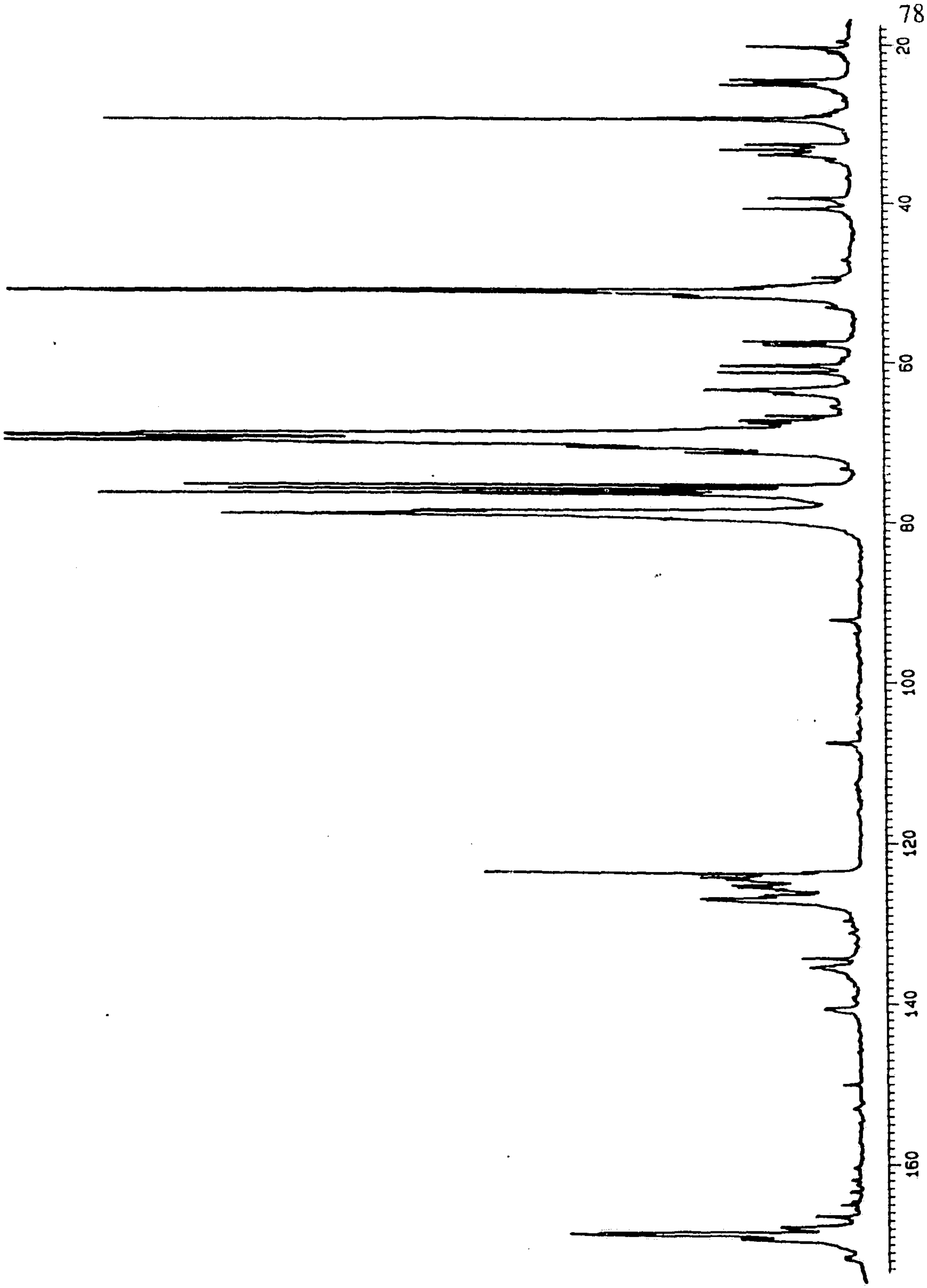

Figure 33. ^{13}C NMR spectrum of typical capping reaction product. This particular sample was from the *meta* amine / alcohol after hydrolysis, ion exchange chromatography and permethylation.

hydrolysed, then the resulting product, in theory now the amide / triacid, was permethylated with diazomethane so that as the amide / triester it would be soluble in organic solvents and readily amenable to chromatography. This procedure gave mixtures of products after chromatography, no less complex than before. The triethylamine base in the capping reaction was replaced with cesium carbonate but the results were similar. Eventually five different alcohol / amine substrates (shown in Figure 34) were used including a primary aromatic and primary aliphatic amine. These last two lead to a synthetic dead end because a tertiary amide is needed when the ion channel wall units are attached as esters but it was hoped that using these substrates might provide some insight with a successful capping reaction. The results were comparable to those obtained with any substrate; any fraction from any separation technique contained mixtures of related compounds so if the desired product was made it was in poor yield accompanied by a number of byproducts that are very difficult if not impossible to completely remove.

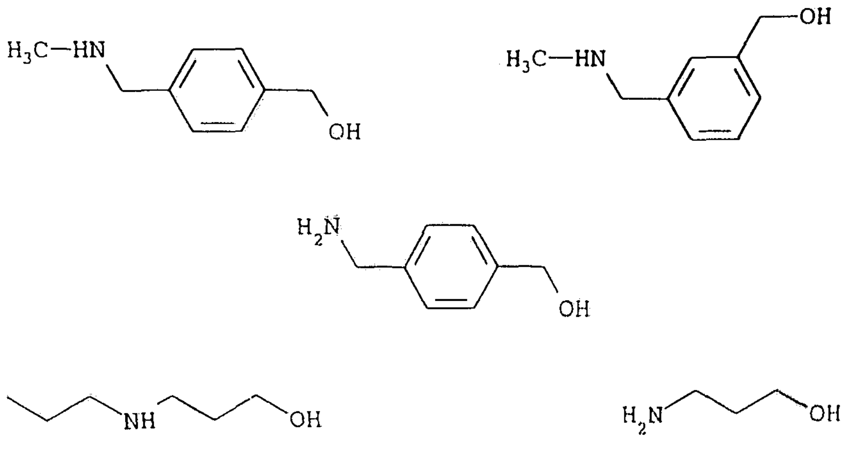

Figure 34. Alcohol / amine capping substrates.

2.2.2 Bulk Addition

Bulk addition means addition without high dilution, in other words the normal addition of all the reagent at once into a small reaction volume; and at this point bulk addition of the alcohol / amine to the dianhydride **4** followed by addition of water to give the monoamide / triacid without capping began to look like a viable option despite the limited yield (statistically 50% monoamide with 25% diamide and 25% tetraacid). The preliminary reaction shown in Scheme **16** gave two major products which might be either the *syn* and *anti* isomers with respect to the amide goup or else an amide and an ester if atttack by the alcohol is competitive with attack by the amine. The ^{13}C NMR spectrum of this product mixture was unchanged between ambient temperature and 100° so the mixture must be ester and amide; at this temperature *syn* and *anti* isomers should exchange rapidly and so their NMR signals should coalesce.

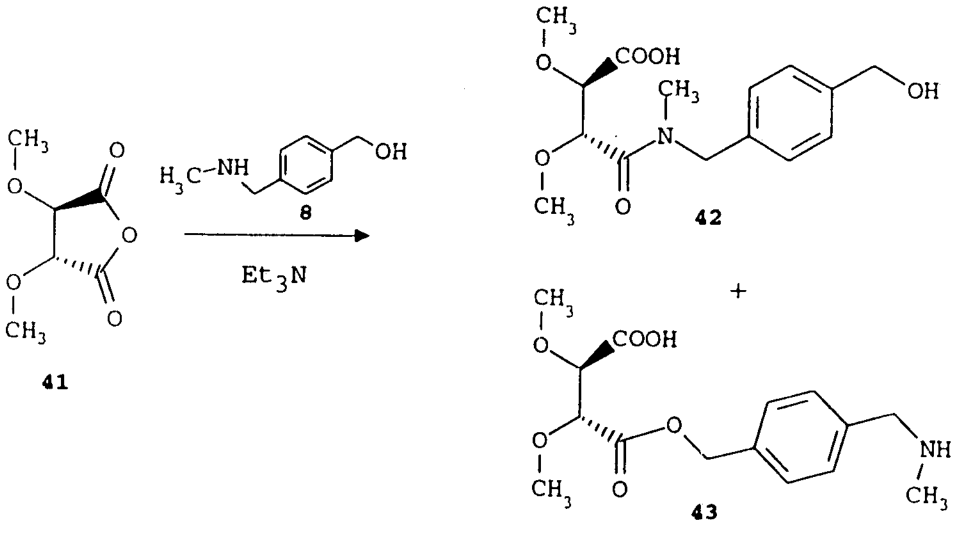

Scheme 16. Preliminary bulk addition reaction.

The reaction was therefore repeated with the THP-blocked derivative **44**. The crude product was partitioned between chloroform and dilute acid to remove the triethylammonium salt and this also served to remove the acid labile THP group. Although a lot of impurities were evident in the NMR spectra of the crude product a clean sample of the desired amide **42** was isolated from a silica gel column. Figure 35 is the ^{13}C NMR spectrum of this compound.

With this result in hand, **44** was then reacted with the dianhydride **4**, as shown in Scheme **17**. This should lead to the target **10**. The crude product was analysed by HPLC using a gel permeation column and appeared to consist of two major products and many minor ones. The two major fractions were isolated by HPLC; one turned out to be a mixture of several compounds according to its ^{13}C NMR spectrum and the other appeared to be a ≈ 2:1 mixture of *anti* and *syn* diamides **45** and **46**. Once again if the desired monoamide **10** is a product it is a minor component of an essentially inseparable mixture.

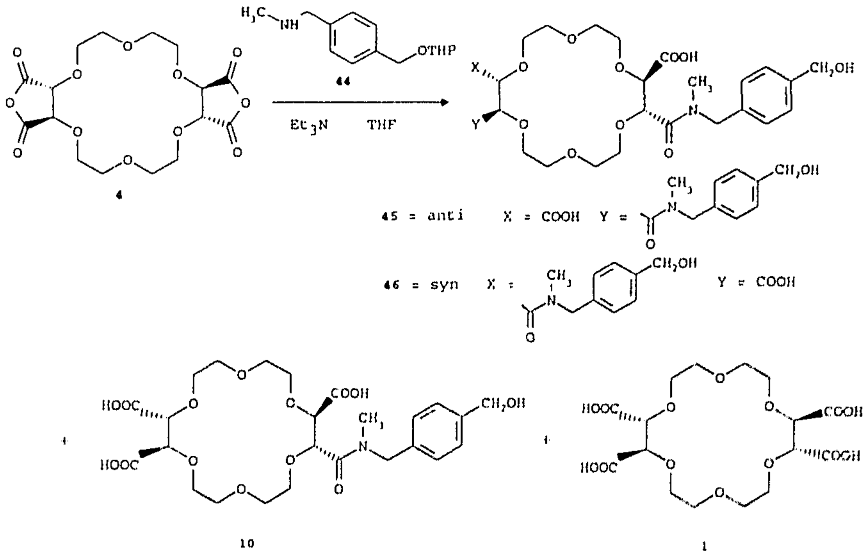

Scheme 17. Proposed bulk addition of amine **44**, aimed at target **10**.

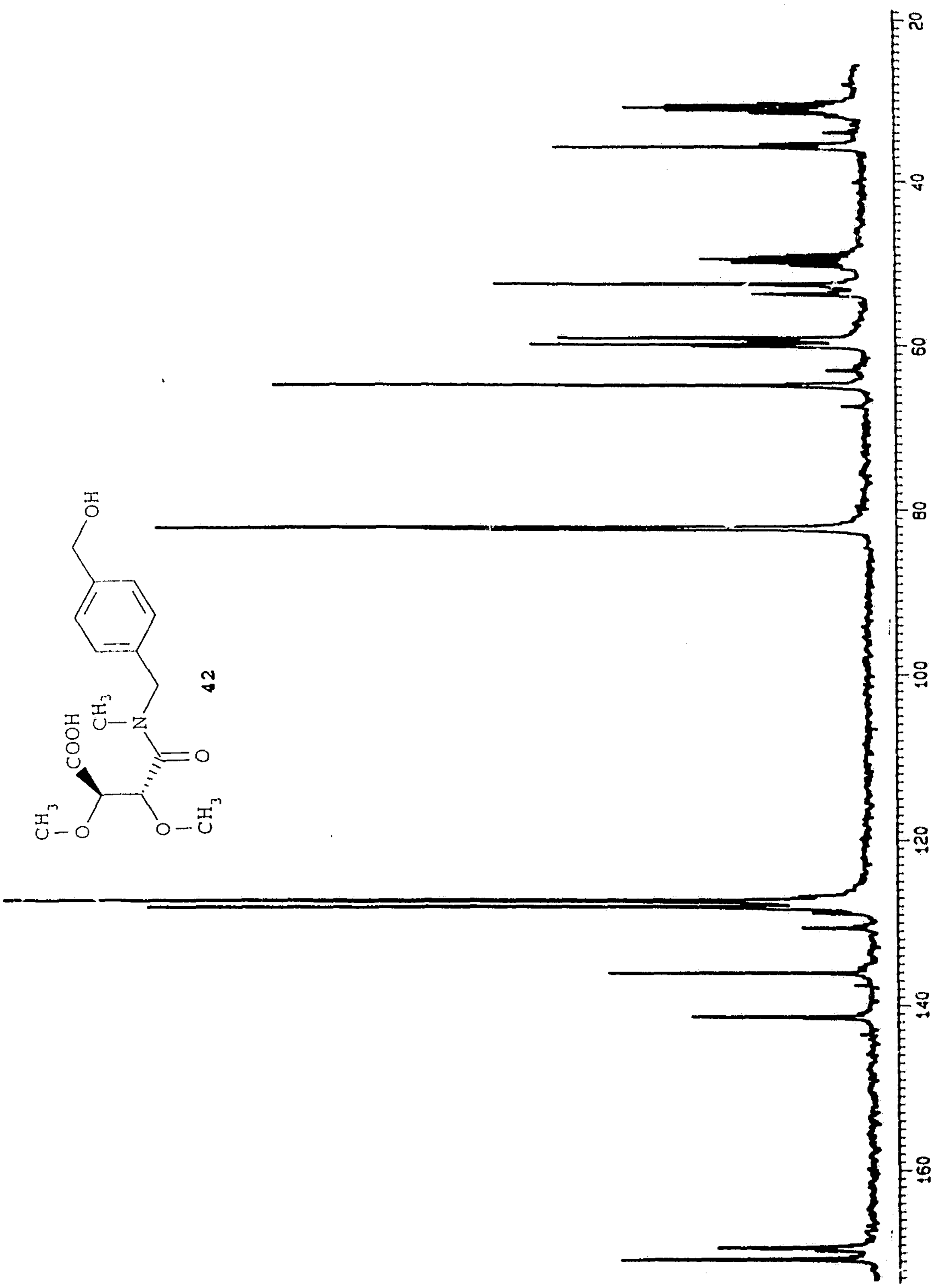

Figure 35. ^{13}C NMR spectrum of compound **42** in methanol-d_4 / acetone-d_6.

2.2.3 Reactions of Crown Ether Dianhydride with Simple Amines

In view of the result described above the reaction was explored at the most basic level; the dianhydride **4** was reacted with one equivalent of benzylamine under the same conditions (in THF solution with an excess of triethylamine). Surprisingly the reaction gave a quantitative yield of the *di*amide, and from the ^{1}H NMR spectrum it is the *anti* isomer **47** only. For whatever reason, the initial product monoamide / monoanhydride is much more reactive than the dianhydride **4** with benzylamine. It appeared as expected that the only other product is the tetraacid **1**, although in its ^{13}C spectrum the methine carbon signal, normally a sharp single peak, appears as several overlapped peaks; in the ^{1}H NMR spectrum the methine proton, again normally a sharp singlet, appears as the multiplet shown in Figure **36**. These spectral results suggest that the product is in fact the epimerized tetraacid **48**. Otherwise the NMR and mass spectra are consistent with this product being the tetraacid as expected.

The product distribution in the formation of diamides from **4** has an interesting history. Lehn and coworkers[87] found that in dichloromethane the reaction between the dianhydride **4** and *two* equivalents of aniline with excess triethylamine as base gave the *syn* diamide only, but that with excess aniline as the only amine an approximately equal mixture of *syn* and *anti* was obtained. The structures were assigned unambiguously from crystal structures of the products as metal complexes. It was found that the *syn* isomer had its two methine singlets separated by 0.02 ppm in the ^{1}H NMR spectrum while the *anti* isomer had the same two signals separated by 0.16 ppm; this was the criterion I used to make my assignment in the benzylamine case. A reasonable explanation was evident:

after initial attack by aniline the strongest base, here triethylamine, abstracts a proton and then serves as counterion for the newly formed carboxylate, thus blocking the face of the crown opposite to the newly formed amide. Attack of the second amine must be from the same side as the first and the *syn* isomer results. With aniline only, the aniline cation occupies the opposite face and with the assistance of another aniline to remove a proton can act as a nucleophile from the opposite face and give the *anti* isomer; attack to give the *syn* isomer is of course still possible and from the product distribution the rates of the two reactions must be about the same. Similarly Dugas and Ptak[35b,35c] reacted the crown

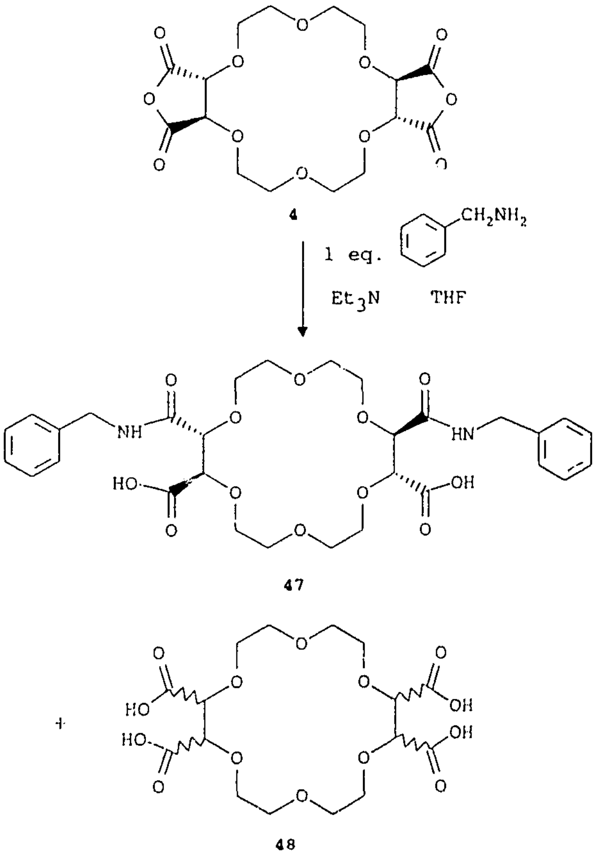

Scheme 18. Bulk addition of benzylamine.

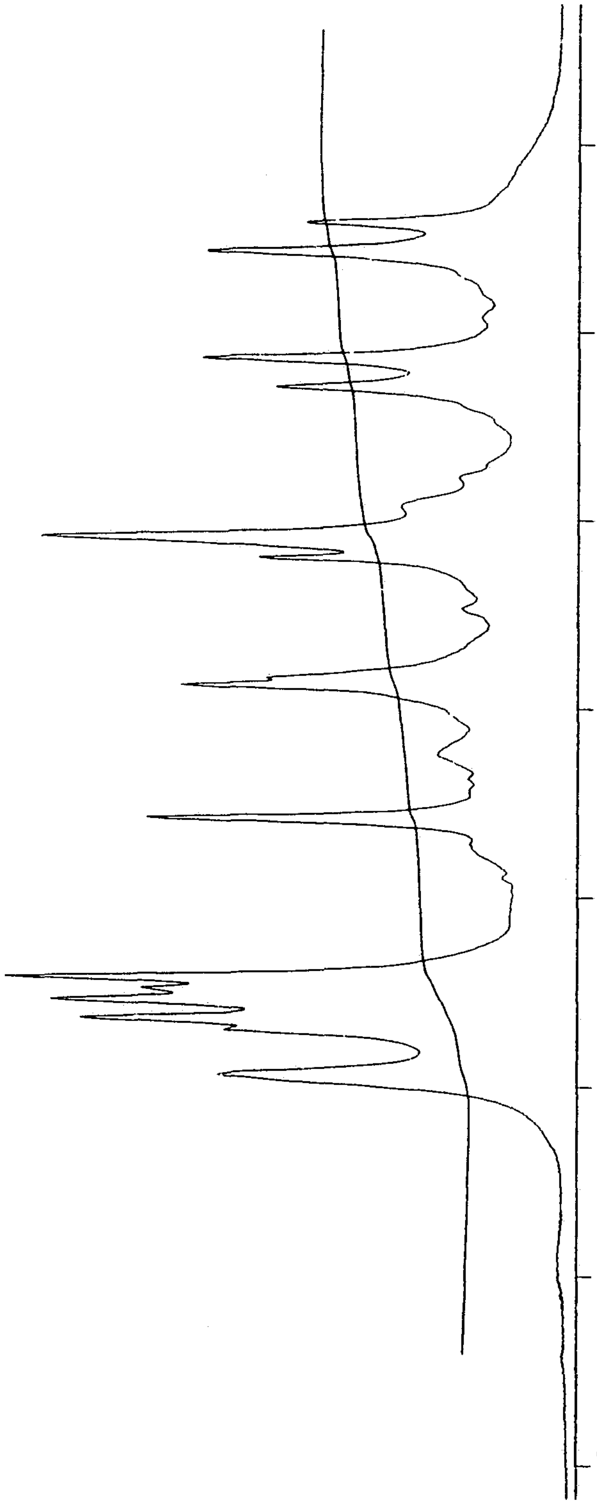

Figure 36. Expanded methine region of the ^1H NMR spectrum of epimerized tetraacid **48** in CD_3OD.

dianhydride **4** in dichloromethane with a primary amine bearing a six membered ring nitroxide and found the same result; with two equivalents of amine plus triethylamine the product was *syn* diamide only, while with excess amine a 1:1 mix of *syn* and *anti* was obtained. The nitroxide allowed unambiguous assignment of products based on the ESR spectra. The explanation is the same; although this primary amine is a much stronger base than aniline, in dichloromethane the triethylamine is still the stronger base (see discussion below). In contrast Whitfield[88] reacted the dianhydride **4** in dichloromethane with two equivalents of n-octylamine and found that under either set of conditions the product was a 1:1 mixture of *syn* and *anti* isomers. Whitfield reasonably justified this result on the grounds that although triethylamine was still the stronger base the lower steric demands of the linear alkylamine allowed attack from the face occupied by the counterion. In previous work I similarly found that the dianhydride **4** reacted with histamine in the presence of excess triethylamine to give a roughly 1:1 mix of the two isomers[89]; this result is amenable to the same steric explanation. The preceding analysis would then suggest that in my reaction, in THF, benzylamine is a stronger base than triethylamine, although in water benzylamine has $pK_a = 9.33$ and triethylamine has $pK_a = 10.72$. Relative amine basicities in organic solvents must then be briefly considered.

In the gas phase amine basicities follow the inductive order $NH_3 < 1^\circ < 2^\circ < 3^\circ$, but in solution solvation effects become important. In water (the medium for virtually all cited pK_a values) and other H-bonding solvents these effects would give the order $1^\circ > 2^\circ > 3^\circ$ reflecting the possible number of H-bonds. The following, however, must be borne in mind: i) solvation and inductive effects generally go in opposite directions and may be largely compensatory ii) enthalpy and entropy terms of the solvation energy generally influence in opposite directions and so solvation energy may end up being very small iii) with large amine substituents steric effects may become dominant iv) particularly with solvents of low dielectric constant and / or no H-bonding ability ion pairing may become a significant effect. In short, the order of basicities is variable. In dichloromethane the order is normally the inductive order[90]; there appears to be little data on basicities in THF although as a potential H-bond acceptor it could reasonably stabilize the benzylammonium cation to the extent that it would be a stronger base than triethylamine. The equilibrium constants for the acid-base reaction of amines with acetic acid were measured[91] in diethyl ether; for triethylamine K = 12 and for n-butylamine K = 72. In the case of my benzylamine reaction therefore the proposal that benzylamine is a stronger base than triethylamine is reasonable but not proven. Crown ring conformational effects and association between the crown and the amines and / or their cations may be significant as well, making any explanation somewhat speculative.

The experiment was repeated using a secondary amine (Scheme **19**). Thus dianhydride **4** was reacted with one equivalent of di-n-butylamine with excess triethylamine in THF. The products were the diamide, the monoamide and the tetraacid. The compounds were not completely separated but two problems were evident. From the integration of the ^{1}H NMR spectra it could be seen that again diamide (**49** and / or **50**) was the predominant product and it was also clear that the methine regions of both ^{13}C and ^{1}H NMR spectra were unexpectedly complex, not only in the spectra of the tetraacid as before but in the spectra of the amides as well. These phenomena are considered in the next section.

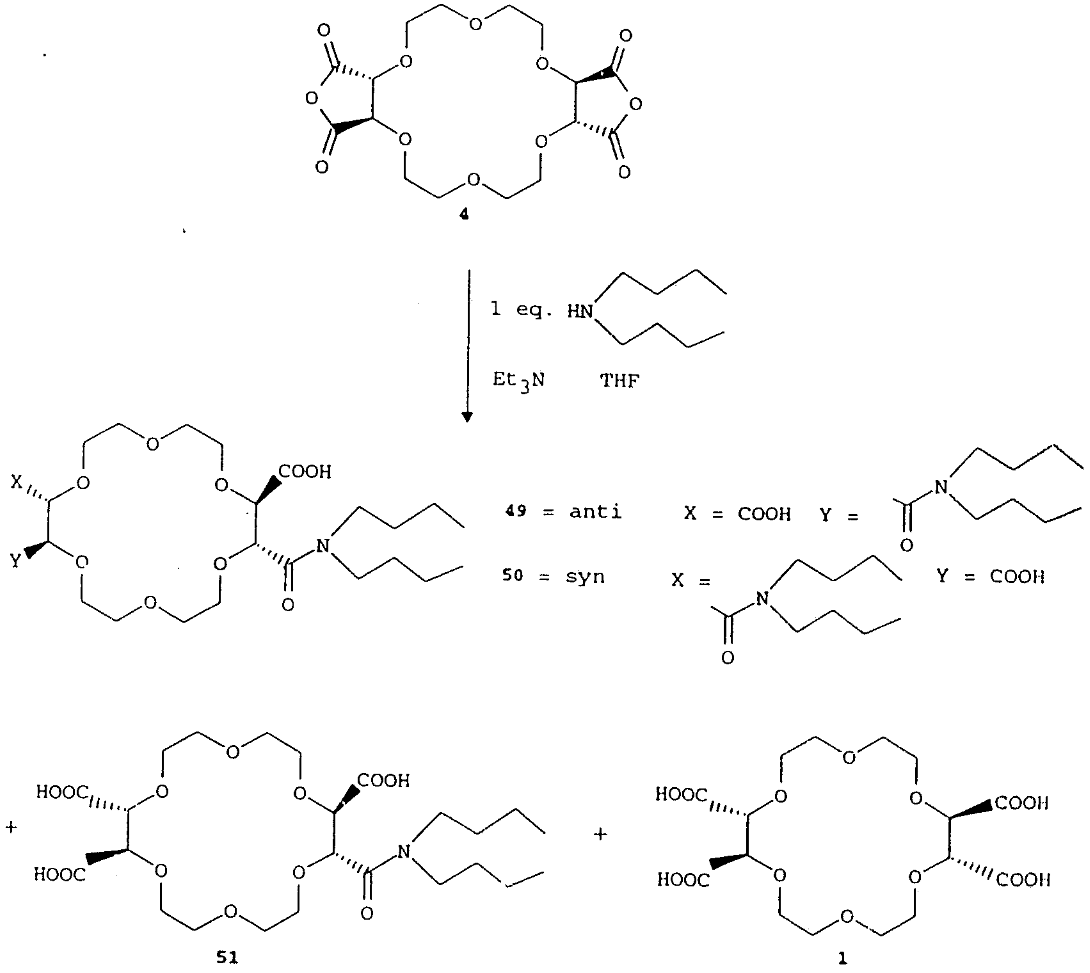
4
1 eq. HN
Et3N THF
COOH
X
Y
N
O
49 = anti X = COOH Y =
50 = syn X = Y = COOH
HOOC
51
1

Scheme 19. Proposed bulk addition of di-n-butylamine.

2.2.4 Bulk Addition Preceded by Water

i) Benzylamine Bulk addition gave predominantly diamide with very little of the desired monoamide despite the fact that statistically the latter is expected to be the major product. This problem was resolved by first reacting the dianhydride **4** with one equivalent of water, which should be free of the effects possible with amines and give the statistical product distribution, then reacting this solution with the one equivalent of the amine. The first procedure was with benzylamine as shown in Scheme **20**.

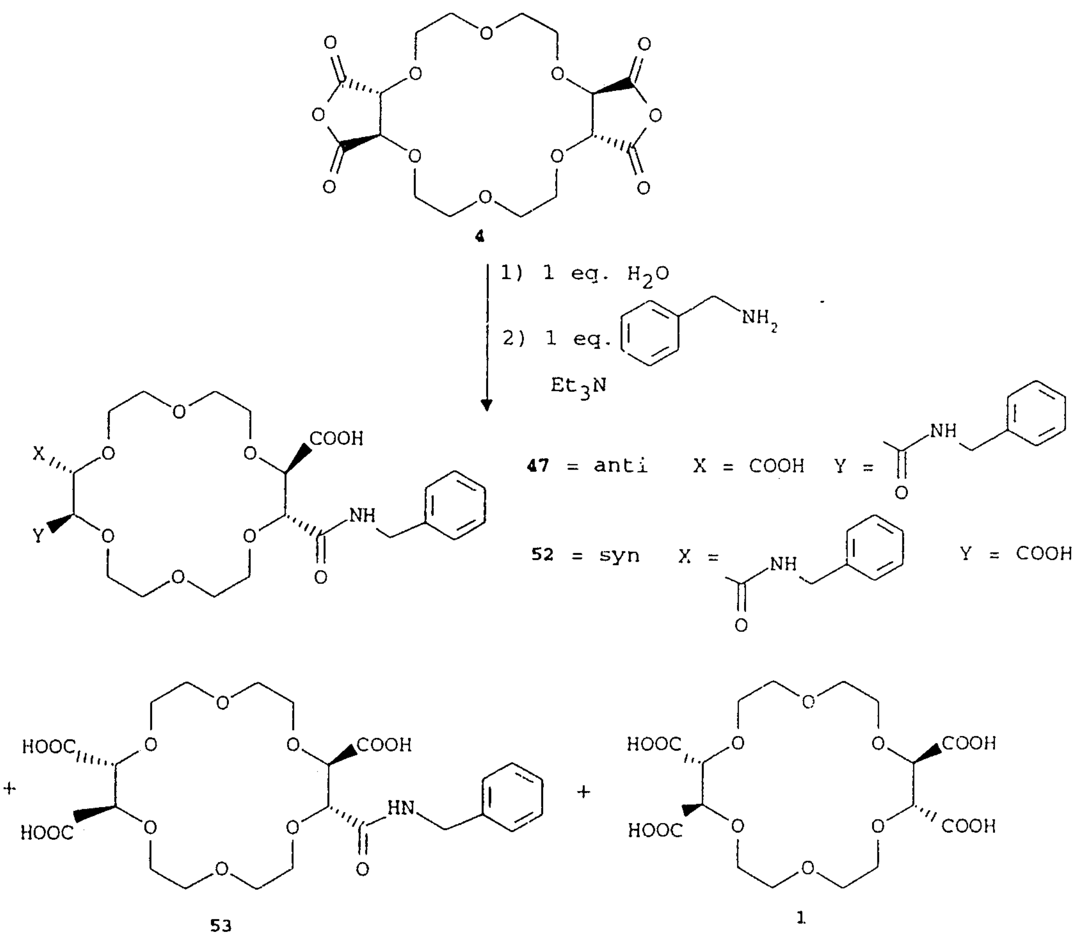
4
1) 1 eq. H2O
2) 1 eq. NH2
Et3N
COOH
NH
X
Y
O
47 = anti X = COOH Y =
52 = syn X = Y = COOH
HOOC
COOH
HN
+
53
1

Scheme 20. Bulk addition preceded by water to give monoamide **53**.

To a solution of the dianhydride **4** in dry THF one equivalent of water was added then this solution stirred for two days to ensure that reaction was complete. One equivalent of benzylamine and a slight excess of triethylamine were then added and this solution stirred for a couple of hours which again should ensure complete reaction. The crude reaction product was partitioned between dilute acid and chloroform and the organic layer was found to be a clean sample of both *anti* and *syn* isomers of the diamide (**47** and **52** respectively). Continuous chloroform extraction of the aqueous layer yielded a very clean sample of the desired monoamide **53** in slightly better than the expected statistical yield of 50%. Figures **37** through **40** are the ^{13}C and ^{1}H nmr spectra of **53** including expansions of the diagnostic areas. The remaining aqueous layer contained the tetraacid with methine group signals in both ^{13}C and ^{1}H NMR spectra as sharp single peaks, so the tetraacid had formed with intact stereochemistry.

ii) Di-*n*-butylamine The reaction was repeated with a simple secondary amine. Thus dianhydride **4** was reacted first with one equivalent of water then with one equivalent of di-*n*-butylamine and excess triethylamine in THF. The results were comparable to the benzylamine case although the reaction was not as clean. The single organic extract contained most of the monoamide **51** as well as one of the *syn* and *anti* diamides **49** and **50**. Although the NMR spectra were fairly clean they showed small peaks particularly in the methine region which are suggestive of epimerization. The continuous organic extract contained only a very small amount of material whose ^{1}H NMR spectrum integrated for the monoamide and again was fairly clean but showed small extra peaks. The aqueous extract contained tetraacid only and with the methine peaks in both ^{13}C and ^{1}H NMR

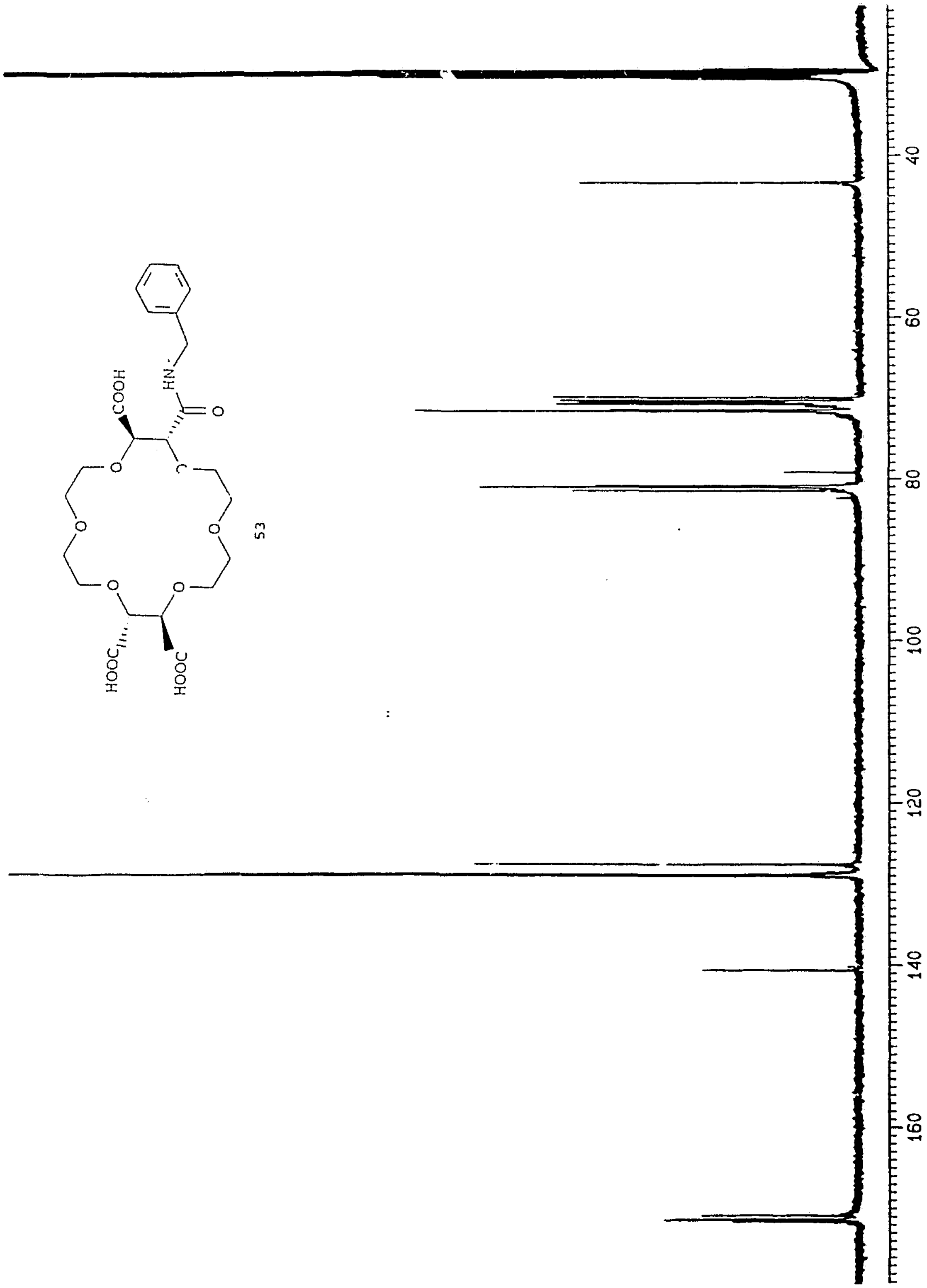

53

Figure 37. ^{13}C NMR spectrum of monoamide **53** in acetone-d_6.

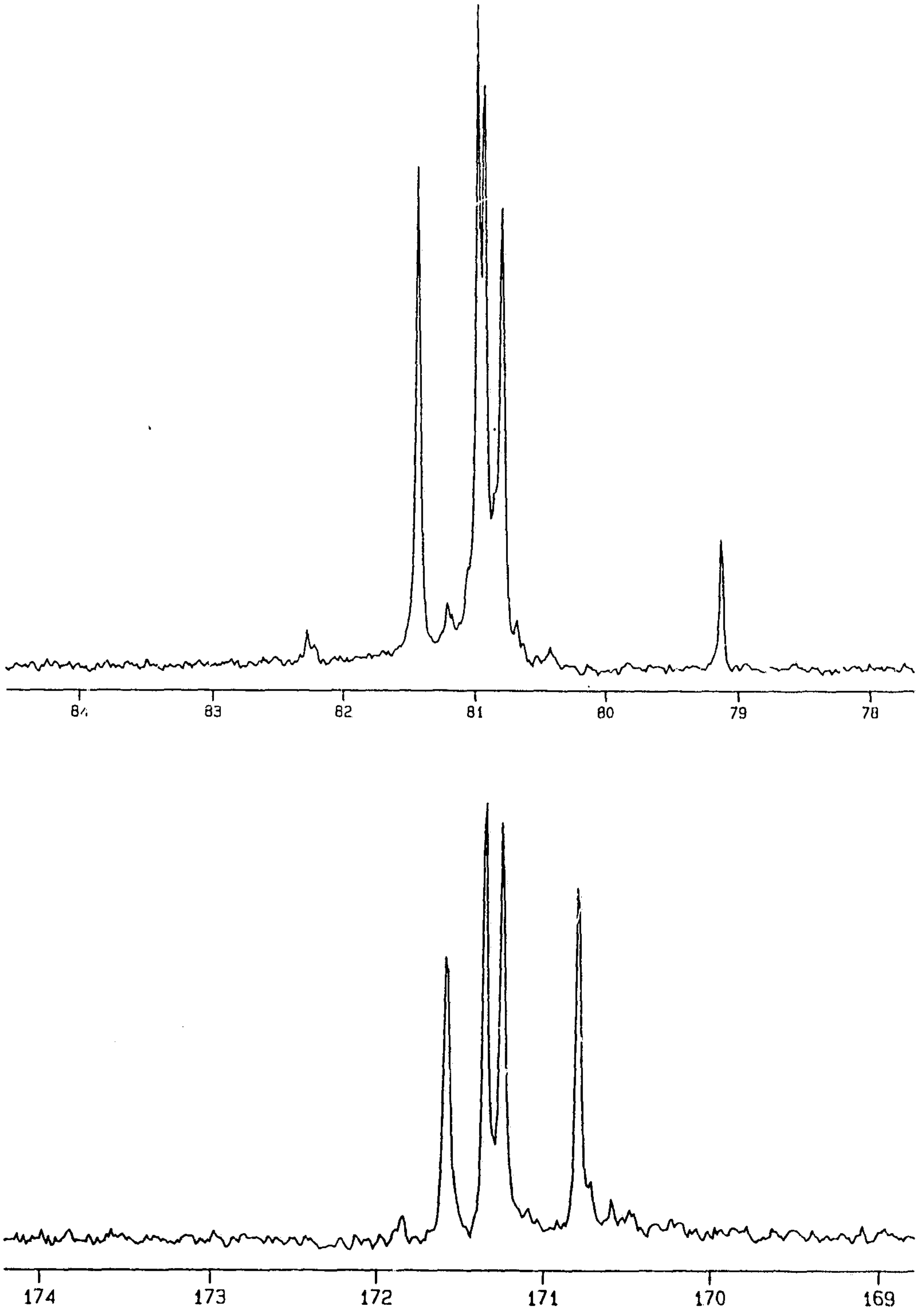

Figure 38. ^{13}C NMR of monoamide **53** in acetone-d_6. Top: expanded methine region. Bottom: expanded carbonyl region.

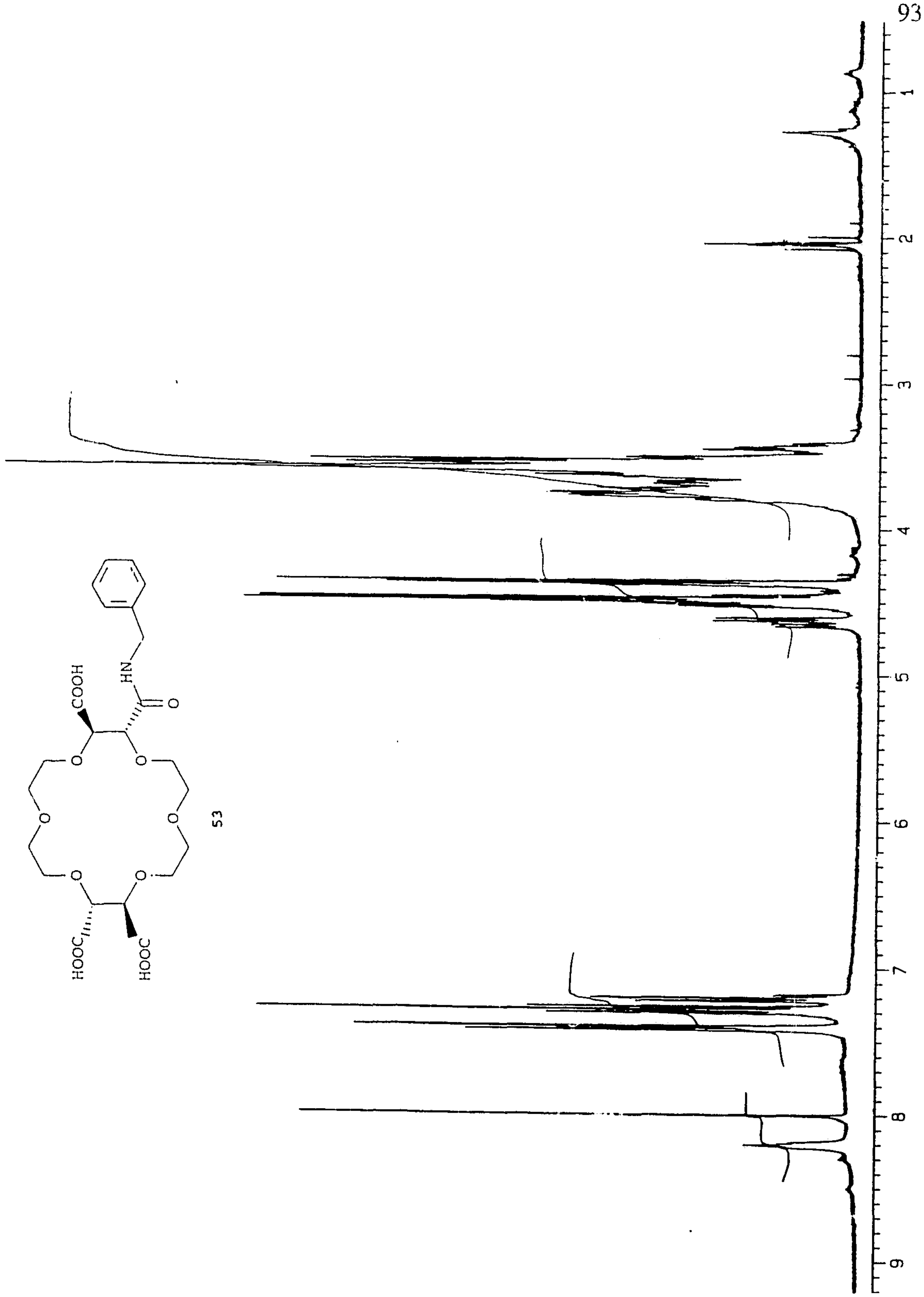

Figure 39. ${}^{1}H$ NMR spectrum of monoamide **53** in acetone-d_6.

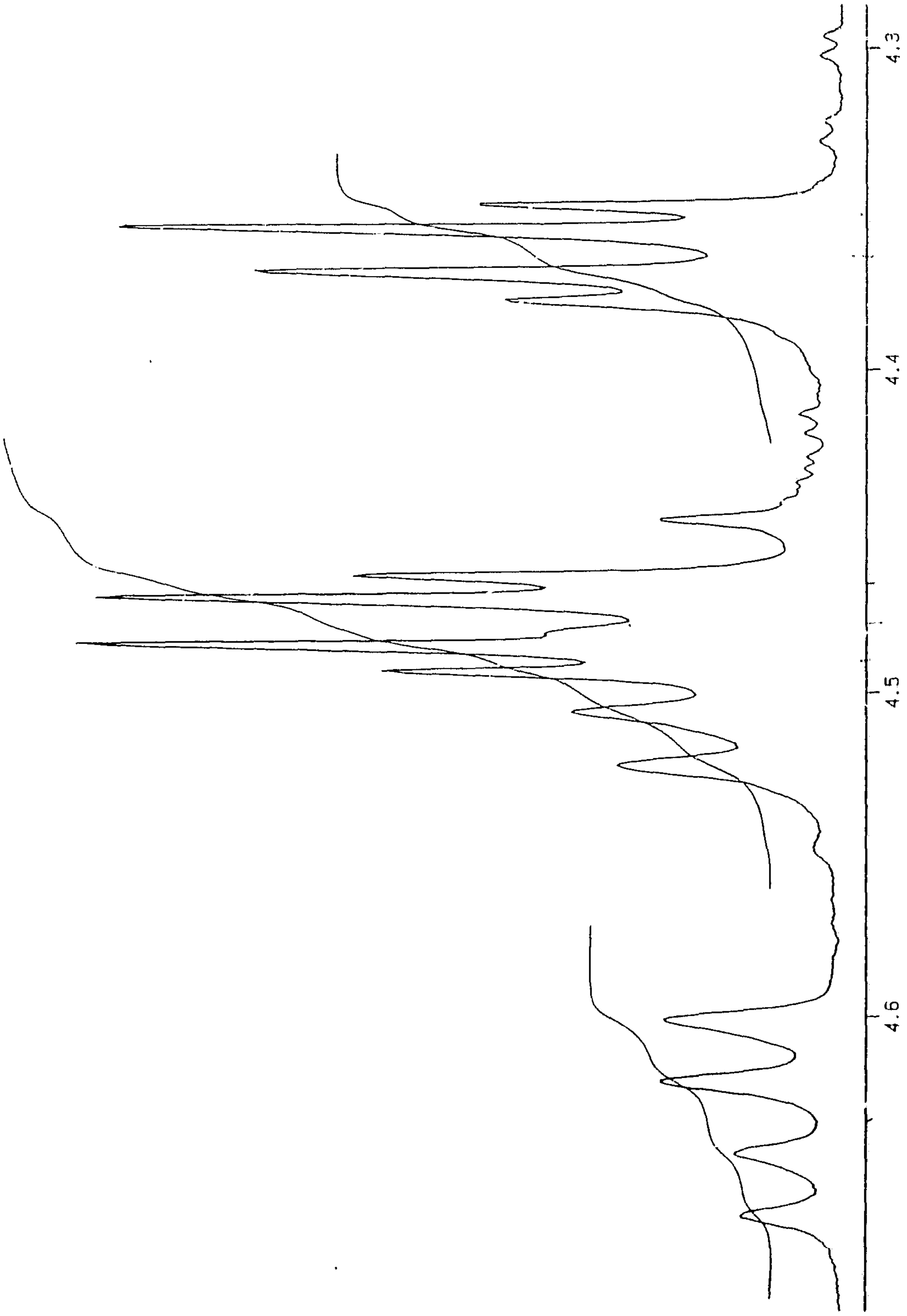

Figure 40. ^1H NMR spectrum of monoamide **53** in acetone-d_6. Expanded methine region.

spectra being the sharp singlets indicative of intact original stereochemistry. This reaction is shown in Scheme **21**.

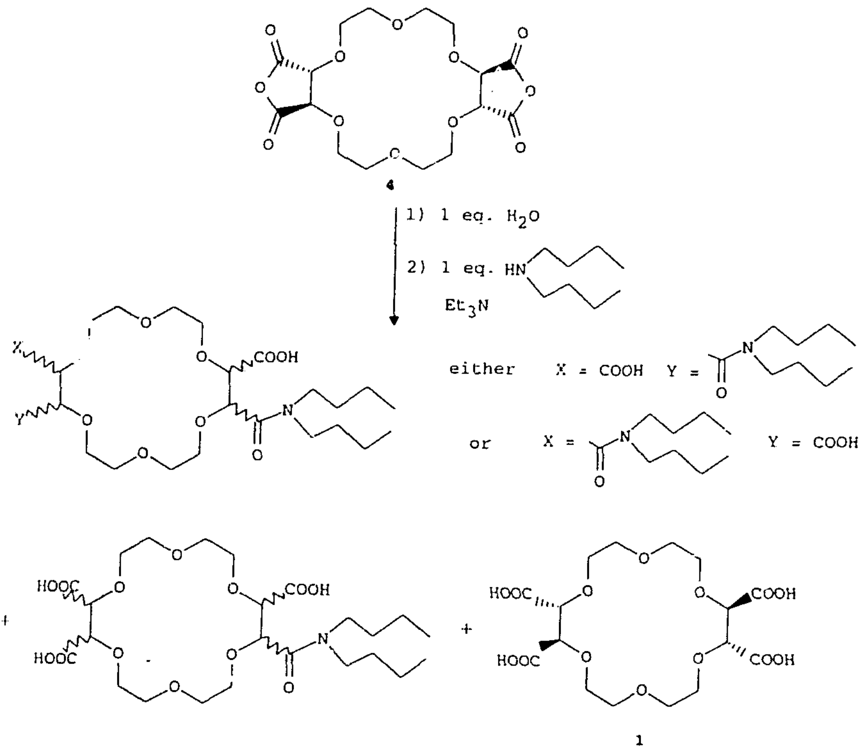

Scheme 21. Bulk addition of di-n-butylamine preceded by water.

iii) Target Amine 44 The reaction was now repeated using the amine **44** which leads to the monoamide **10**, which then leads to the ultimate target **12**. Once again workup involves partitioning between chloroform and dilute acid to remove triethylammonium salt and this also cleaves the THP group. The single organic extract appeared from the integration of the ^{1}H NMR spectrum to contain both monoamide and diamide although it was now impossible because of additional peaks in the methine region (from Ar-C$\underline{H_2}$N and Ar-C$\underline{H_2}$O protons) to determine if the diamide was *anti* or *syn* or both. There were the additional small peaks in the methine regions of the ^{13}C and ^{1}H NMR spectra suggestive of epimerization. The continuous organic extract gave integration of the ^1H NMR spectrum consistent with it being the monoamide but the spectrum was far too complex. The methine region of the ^{13}C NMR spectrum is shown as Figure **41**. The aqueous extract contained a clean sample of epimerized tetraacid **48**. This last result is surprising since the tetraacid should have been formed with intact stereochemistry before the amine was added and should not itself be subject to epimerization.

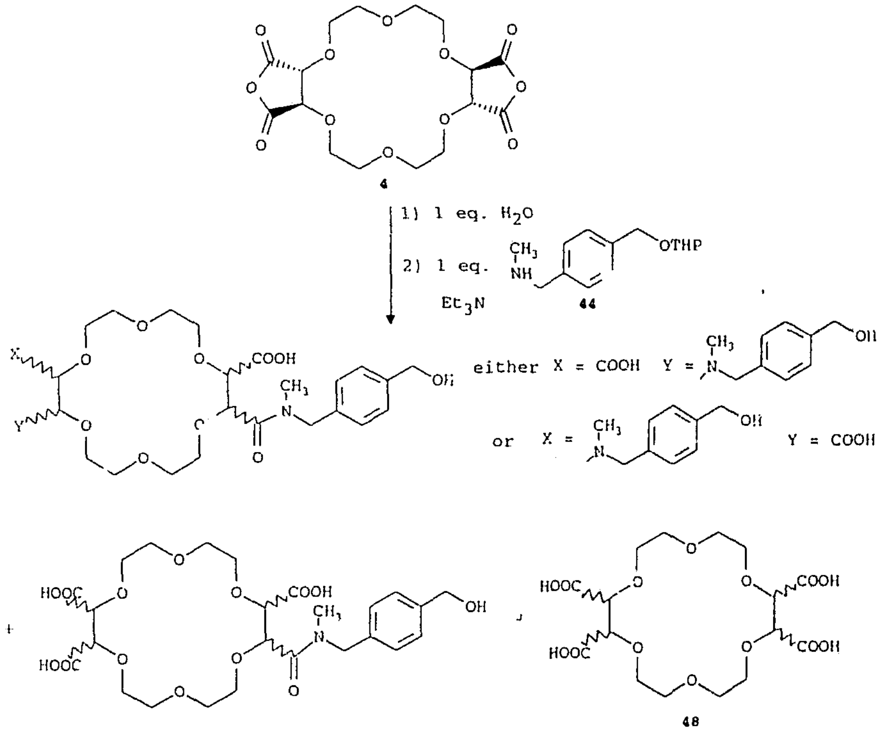
4
1) 1 eq. H2O
2) 1 eq.
CH3
NH
OTHP
44
Et3N
COOH
CH3
N
OH
either X = COOH Y = N CH3 OH
or X = CH3 N OH Y = COOH
HOOC
COOH
CH3
N
OH
+
HOOC
COOH
48

Scheme 22. Bulk addition of amine **44** preceded by water.

Much of the spectral evidence to this point indicates varying degrees of epimerizaton at the methine carbon. The methine proton is the most acidic in the crown ether molecule and in the presence of base could epimerize either by reversible formation of the anhydride enolate anion or by formation of a ketene which is open to attack by

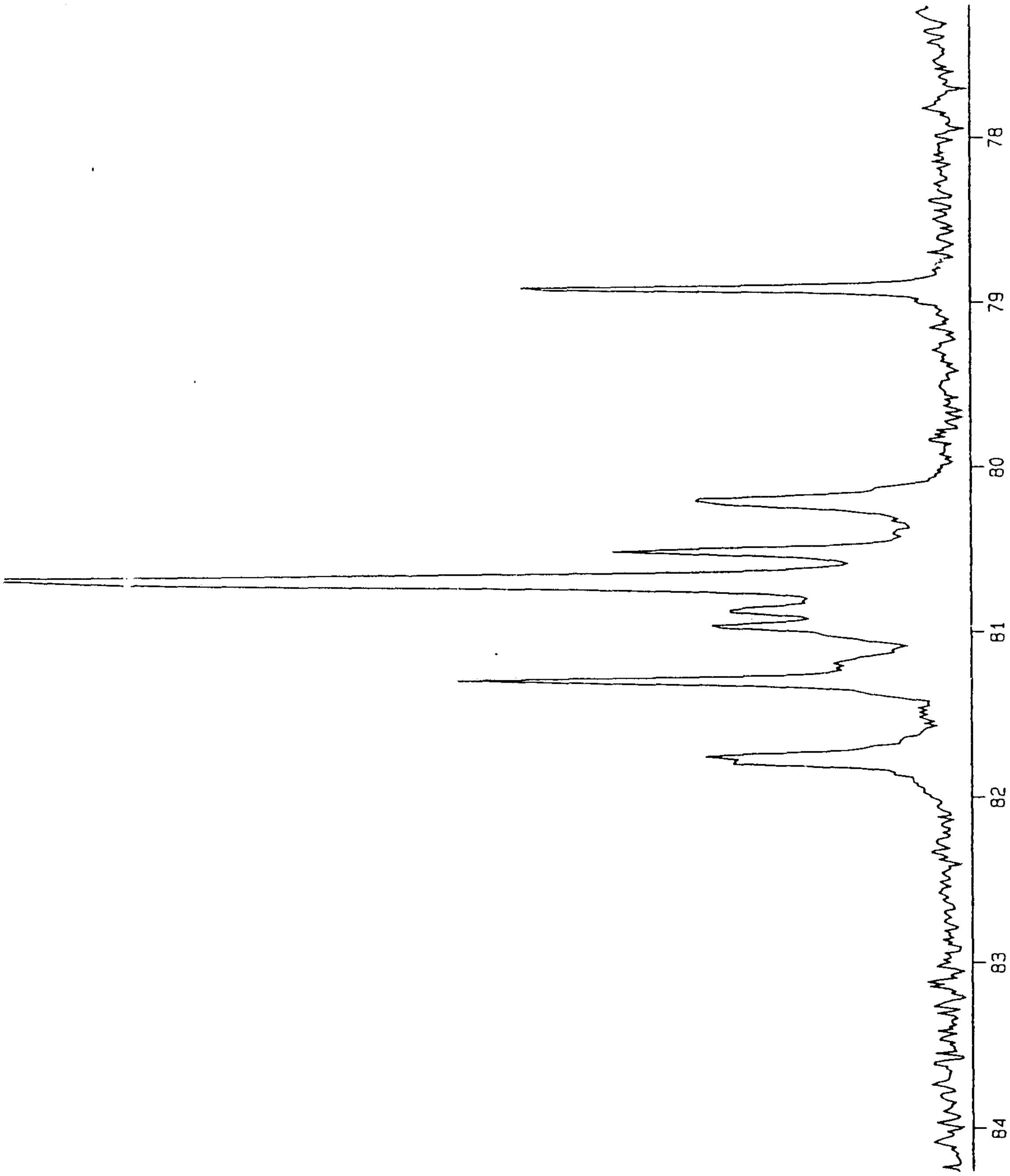

Figure 41. ^{13}C NMR spectrum of purported monoamide **10** in acetone-d_6. Expanded methine region.

amine from either face to give epimeric amides. Table **2** shows optical rotation values measured in methanol for various recovered tetraacid samples. The literature value, measured in water[35a], is $[\alpha]_D^{20} = +67.0°$. I measured a value for a standard sample of tetraacid in methanol and found it to be $[\alpha]_D^{20} = +59.4°$. The values in Table **2** are consistent with incomplete epimerization at the methine position. Table **3** gives optical rotation values for the products isolated from the organic extracts of the various monofunctionalization reactions. None of the entries have a reference value to which they can be compared but the values are all positive so that if epimerization is occurring then it is not complete. In Dutton's ion channel preparation[22] esterification via the hexaacid chloride resulted in some epimerization; hence the subsequent use of the carboxylate nucleophile method by James[28] (see the introduction). James attributed this to ketene formation which is likely since treating an acid chloride bearing an α-hydrogen with an amine is a literature procedure to generate ketenes[92]. In my anhydride case COO^- is not nearly as good a leaving group as Cl^- so ketene formation may not take place although it is not precluded either. If a ketene were formed it could react readily with a primary or secondary amine to give an amide[93].

An attempt was made to trap a ketene intermediate by adding a large excess of ethyl vinyl ether to the reaction mixture before adding di-n-butylamine and triethylamine but there was nothing in the complex NMR spectra of the product mixture to suggest a cyclobutanone trapping product. There would probably be one regioisomer and four stereoisomers but the chemical shifts should be diagnostic for cyclobutanone. Similarly an attempt was made to trap an enolate anion, if this was in fact the epimerization

Amine	Procedure	Extract / Product	^{1}H NMR - methine region	$[\alpha]_D^{20}$
benzylamine (Et$_3$N)	bulk addition	aqueous - tetraacid	complex	+ 7.3°
di-n-butylamine (Et$_3$N)	"	"	complex	+ 14.4°
benzylamine (Et$_3$N)	1) 1 eq. H$_2$O 2) amine	"	singlet	+ 58.7°
di-n-butylamine (Et$_3$N)	"	"	singlet	+ 54.6°
amine **44** (Et$_3$N)	"	"	complex	+ 49.0°

Table 2 Optical rotation values for recovered tetraacid.

Amine	Procedure	Extract / product	^{1}H NMR - methine region	$[\alpha]_D^{20}$
di-n-butylamine (Et$_3$N)	bulk addition	single organic	complex	+ 32.5°
benzylamine (Et$_3$N)	1) 1 eq. H$_2$O 2) amine	single organic - **47** and **52**	simple multiplet	+ 64.8°
"	"	continuous organic - **53**	simple multiplet	+ 56.5°
di-n-butylamine (Et$_3$N)	"	single organic	complex	+ 39.9°
"	"	continuous organic	complex	+ 37.2°
amine **44** (Et$_3$N)	"	single organic	complex	+ 36.2°
"	"	continuous organic	complex	+ 51.5°

Table 3. Optical rotation values for products of the monofunctionalization reactions.

intermediate, by adding a large excess of methyl iodide to the reaction mixture before adding di-*n*-butylamine and triethylamine but again there was nothing in the complex spectra of the product to suggest a methyl group substituted at the methine position. The mono-*n*-butyl imide made from the 18-crown-6 *di*acid will react with hydroxide to open the imide ring to the amide / acid with stereochemistry intact which would lead to the conclusion that enolate formation is not facile in this system but this result is not directly comparable since the monoanhydride from this diacid can be reacted with a secondary amine and excess triethylamine to give the amide / acid without any significant epimerization[88,89].

If there is indeed epimerization, then an explanation for all the results is evident. When benzylamine is added first, the nucleophilic attack on anhydride is much faster than the proton abstraction. Once nucleophilic attack has taken place epimerization of the amide / acid cannot occur so the diamide product has intact stereochemistry. The remaining anhydride groups, however, can then epimerize in the presence of the basic triethylamine, so subsequent addition of water gives the epimerized tetraacid, as illustrated in Scheme **18**. The secondary di-*n*-butylamine is of comparable basicity (see discussion above) but a weaker nucleophile so that by the time nucleophilic amine attack occurs proton abstraction has already resulted in significant epimerization, by whatever mechanism, which shows up in all products. When one equivalent of water is added first the tetraacid is already formed with stereochemistry intact before the amine is even added; then when benzylamine is added nucleophilic attack on all remaining anhydride moeities is rapid so that the methine stereochemistry is maintained in amide products as well (see

Scheme **20**). When di-*n*-butylamine is added after water the stereochemically intact tetraacid is already formed but all remaining anhydride moieties are subject to epimerization before the slower nucleophilic attack by the secondary amine (see Scheme **21**). This argument requires that the basicities of primary and secondary amines be roughly equal in THF which in view of the discussion above is reasonable; it also requires that primary amines be better nucleophiles than secondary in this solvent so the relative nucleophilicities of amines in organic solvents must be considered.

This discussion refers to nucleophilicity with respect to a carbonyl group which is much different from the more commonly considered nucleophilicity towards an sp^3 carbon such as methyl iodide, which a much "softer" electrophile. Nucleophilicity of amines towards carbonyl carbon is often covered by the blanket statement that it parallels basicity[94]. This is intuitively sensible since it compares reactivity towards the relatively "hard" nucleophiles C=O and H^+. Even neglecting steric factors what is really being compared by relative rates is the relative strengths of C-N, C-O, and H-N bonds in the relevant transition states, so the parallel will not always hold. Most of the work on relative nucleophilicity of amines concerns rates of ester aminolysis in water or alcohol solution where a variety of kinetic regimes are encountered depending on the pH; catalysis varies from specific acid to general acid to general base to specific base as the pH varies from very low to very high[95]. There is often a pH range where uncatalysed nucleophilic attack is observed, usually when the alkoxide is a very good leaving group[96]. The blanket statement that nucleophilicity parallels basicity sometimes reflects the fact that the bulk of the work was ultimately directed towards synthesizing artificial esterases and therefore was primarily in the physiological pH range where general base catalysis dominates. Many workers, however, manipulated their data to extract separate general base catalysis and uncatalysed nucleophilic attack terms, and the nucleophilic reaction rates still followed basicity[97]. The work on relative nucleophilicities in non-hydroxylic solvents usually concerns solvents such as acetonitrile, THF, ether, and chloroform because in less polar solvents ion aggregates dominate the behavior. Aminolysis of esters in non-hydroxylic solvents is generally described by the expression[91]:

$$\text{rate} = k_{obs}[\text{ester}] = (k_1[\text{amine}] + k_2[\text{amine}]^2)\ [\text{ester}]$$

Apparently the transition state for the mechanism described by the k_1[amine] term is the more polar since in acetonitrile (ε=38) this term dominates, in diethyl ether (ε=4.3) both terms are important , and in substituted benzenes which have no H-bonding capability the k_2[amine]^2 term dominates[98]. The transition state in the latter case must involve two amine molecules, probably with one as nucleophile and the other as general base catalyst, and in these solvents much more amine will already be dimerized because there is no significant H-bonding to solvent. It has been noted[99] that diethyl ether (ε=4.3) and chloroform (ε=4.8) despite similar values for dielectric constant have much different kinetic solvent effects because the former is a Lewis base. The consensus is that in the absence of significant electronic effects, such as a directly adjacent heteroatom, steric effects are by far the most important factor in determining amine nucleophilicity. Satchell and Secemski[98] found the order of reactivity in ether to be n-BuNH$_2$ $>$ Et$_2$NH $>$ t-BuNH$_2$ and deTar and Delahunty[100] actually propose ester aminolysis as a standard probe for steric hindrance. They found a reactivity order among primary amines to be n-BuNH$_2$ $>$

$iPrNH_2$ > $secBuNH_2$ ≫ $tBuNH_2$ in acetonitrile. This solvent was chosen deliberately to eliminate the second order $k_2[\text{amine}]^2$ term. This term did arise anyway as a minor factor but its behavior was similar to the first order $k_1[\text{amine}]$ term, presumably reflecting the fact that the second amine is not subject to significant steric hindrance. I could not find any data on relative rate of aminolysis by benzylamine; it does have a large phenyl component but it is one CH_2 unit removed from the amine and it is entirely possible that benzylamine is a much better nucleophile in THF than di-n-butylamine.

iv) Excess Benzylamine To this point the results can be explained even if they have been synthetically unproductive. Unfortunately further exploration produced further difficulties and inconsistencies. It has already been noted that the reaction shown in Scheme **20** gave both *syn* and *anti* diamides while the one shown in Scheme **18** gave *anti* only. It has also been noted already that the reaction of dianhydride **4** with one equivalent of water then the amine **44** unexpectedly gave epimerized tetraacid (see Scheme **22**). The dianhydride **4** was now reacted with one equivalent of water followed by an excess of benzylamine as the only amine. There was formed almost immediately a precipitate and the NMR spectra of any isolated fraction showed unexpected complexity. This included the tetraacid isolated from the aqueous extract despite the fact that it should have been formed and held safe from epimerization before any amine was added to the reaction. The methine region of the ^1H NMR spectrum of this tetraacid fraction is shown in Figure **42**. It appears to be substantially different from the same spectral region for what is supposedly the same compound shown in Figure **36** and indeed none of the spectra of the tetraacid fractions are identical in this spectral region. This is not necessarily significant

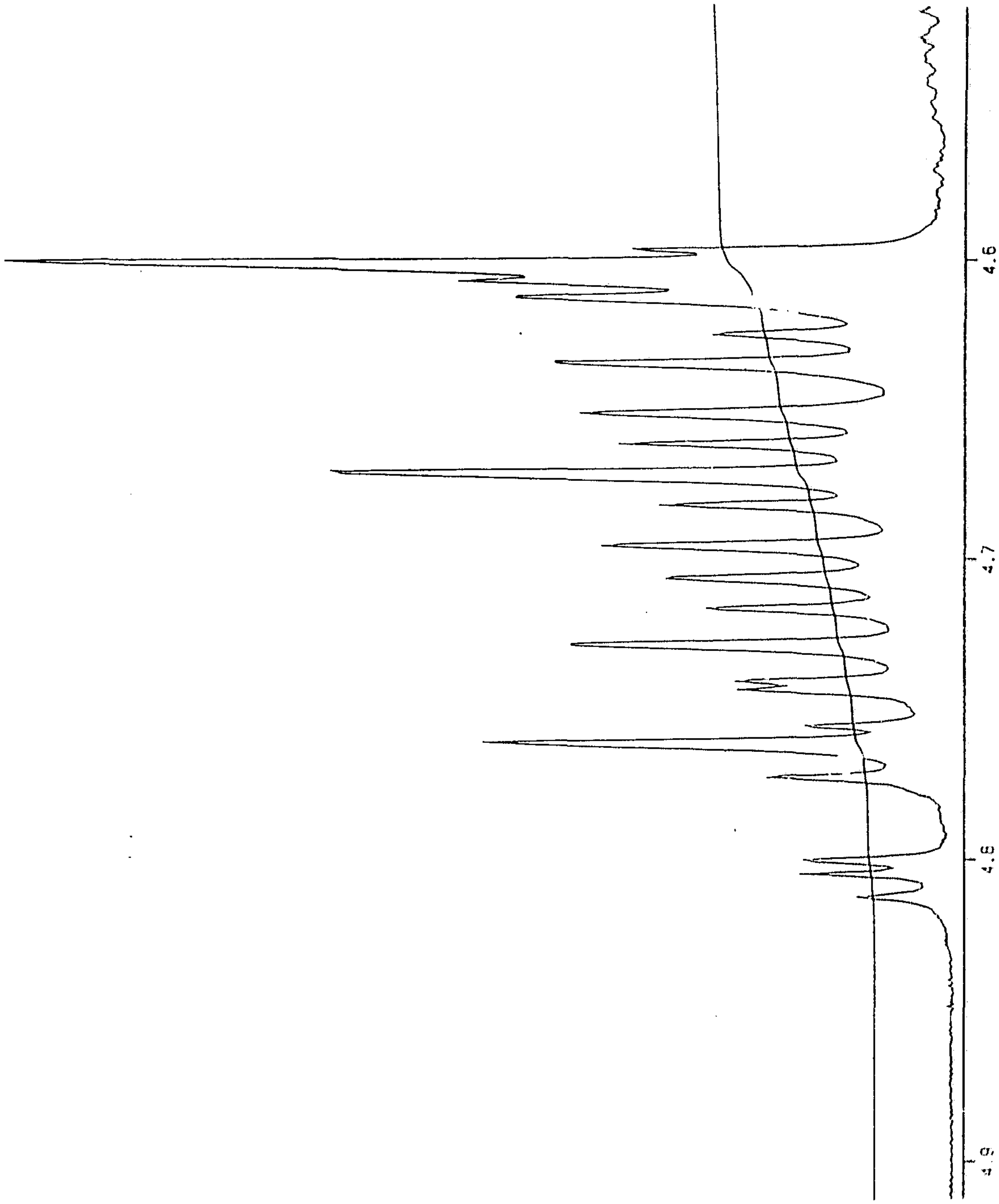

Figure 42. ^{1}H NMR spectrum of tetraacid isolated from reaction of dianhydride **4** with excess benzylamine only. Expanded methine region.

as the various fractions would be epimerized to different extents and this might alter the profile of the complex multiplet.

v) Other Primary Amines Anomalous behavior was also seen in the same procedure applied to the primary amines **54** and **55**. Since they are primary they lead to a synthetic dead end, since in the ultimate target **12** they are vicinal to an ester and there is the danger of cyclic imide formation. If either desired monoamide product were isolated, however, it could be coupled to the photogate and the resulting compound, analogous to **11**, used to compare ion binding constants of its *trans* and *cis* isomers (i.e. before and after uv irradiation). This would then serve to evaluate the overall design of the target.

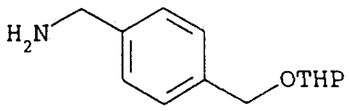

54

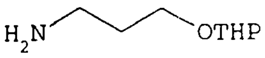

55

In both reactions there was rapid formation of a gummy precipitate, and any purification fraction either from precipitate or supernatant gave very complex NMR spectra. This was true even for the aqueous fraction which should contain predominantly stereochemically intact tetraacid **1**. This result is surprising since **54** differs from benzylamine only at a position remote from the amine.

2.2.5 Reaction Using DCC

There are other strategies besides reaction of dianhydride **4** to make a monoamide crown, as long as the statistical yield is deemed acceptable. For instance, a number of reagents have been developed for peptide syntheses. I carried out a reaction in which the tetraacid **1** was activated with DCC (1,3-dicyclohexylcarbodiimide), a reagent which is widely used in peptide synthesis, with one of the reasons being that it activates a carboxylate group without inducing epimerization at the α carbon. The DCC activates all four carboxylates so the anticipated statistical yield of monoamide is about 42%. Tri- and tetraamide byproducts are now expected although they could probably be separated, along with the diamides, from the monoamide by the single organic / continuous organic extraction sequence used previously. The reaction was carried out with benzylamine and results were mediocre. The yield was approximately statistical, and tetraacid was recovered from the aqueous extract with no sign of epimerization. The continuous organic extract could be seen from comparison of its NMR spectra with those from the reaction described in section **2.2.4 i)** to be predominantly stereochemically intact monoamide **53** but the reaction was not nearly as clean, even using this simple primary amine.

2.3 Summary and Prospects.

The synthesis of the photogate was very successful, with the final route being short and simple. The azo coupling reaction can be accomplished quickly in good yield with unequivocally established regiochemistry, and the products are chemically robust, with the expected photochemical properties. The route is very general with virtually any reasonable substituent possible at either position of the resorcinol ring. Similarly a wide variety of substituents is also possible on the aniline ring portion of the molecule. Here the synthesis was achieved with a substituent bearing a primary amine, a functional group which is likely from the perspective of a useful target.

In contrast, the proposed route to monofunctionalized 18-crown-6 tetracarboxylate exhibits complex behavior which defies a comprehensive explanation. This not only constitutes a dead end to this individual synthesis, but calls into question the overall suitability of the tetracarboxylate as a molecular framework. Its conformational and binding properties must be part of the problem since results from comparable reactions of the 18-crown-6 monoanhydride are far more straightforward[88,89,101]. Indeed, this was the rationale behind the synthetic strategy in the first place. The four carboxylates, however, are an essential component of the design, specifically because they direct the substituents perpendicular to the ring plane.

Epimerization at the α-carbon positions is an inherent flaw in this system which has been noted before as a peripheral problem[28]. Here it became a serious one, all the more so because the architecture of the target demands intact stereochemistry, and because purification of the correct epimer would probably be extremely tedious. In the present case the epimerization problem is further compounded by the need for a secondary amine. In addition to epimerization, other inconsistencies have been noted in the discussion above, most significantly the result that reaction using the primary benzylamine derivative **54** was unsuccessful even though the additional substituent was at a position remote from the amine group. The 18-crown-6 tetracarboxylate has been a widely used framework with an impressive history. Lehn[23,35a,71,102], Dugas[35b,35c,103], Fyles[22,29,31,104], and others[105] have all reported successful syntheses based on this system, but the routes all involved symmetrical multiple substitutions to the tetracarboxylate. For our present purposes and for general utility a framework must be amenable to monofunctionalization. In this case the monofunctionalization reaction was extensively explored, and the crown tetracarboxylate was found to be inherently unsuitable. The strategy did afford monoamide **53** by a convenient procedure in good yield and conditions could be found to make other targets on an individual basis. The bottom line, however, is that without a convenient, generally applicable monosubstitution methodology the continuing prospects for 18-crown-6 as a molecular framework are seriously limited. At our present level of understanding it is simply too unreliable. The target monoamides **11** and **12** could be made, but not within the original design criteria.

This is a property directed synthesis, so we are free to consider any other framework as an alternative. The most prominent in current use are cyclodextrins, calixarenes and cyclophanes. All bear multiple identical functional groups so again the problem of monosubstitution must be addressed. I am not aware of any literature reports of monofunctionalized cyclophanes[106]. There has been a report in which the reaction of a calixarene bearing four identical functional groups yielded monosubstituted product but this was an unexpected byproduct of a tetrasubstitution procedure. Another reaction with the same calixarene gave a trisubstituted product, which essentially accomplished a monosubstitution, but once again this was an unintended byproduct[107]. The few deliberate syntheses of monofunctionalized calixarenes reported to date have been via tedious, low yield stepwise routes[108]. On the other hand, a number of monofunctionalized cyclodextrins have been reported in the literature[109]. What has yet to be established, however, is a suitable architecture for a functional cyclodextrin based ion channel. Both Tabushi[18] and Lehn[23] have reported cyclodextrin based channels which can be classified as functional, but the transport rates were unacceptably low.

The goal of a functioning artificial photogated ion channel remains elusive. Most importantly it requires a molecular framework that is suitable both in terms of a facile general monofunctionalization and in terms of the overall molecular architecture. This is a goal that can be achieved, but at this point we still have a long way to go.

CHAPTER 3 EXPERIMENTAL

General Procedures

Proton NMR spectra were recorded with a Bruker WM 250 (250 MHz, FT) or Bruker AMX 360 (360 MHz, FT) spectrometer in $CDCl_3$, CD_3OD, or acetone-d_6 as indicated for each spectrum. Spectra were referenced to the central solvent line as standard (δ 7.24 ppm for $CDCl_3$, δ 3.30 ppm for CD_3OD, and δ 2.04 for acetone-d_6, all relative to Me_4Si). Carbon NMR spectra were recorded on a Bruker WM 250 (62.89 MHz) or Bruker AMX 360 (90.57 MHz) instrument with central solvent line as standard (77.0 ppm for $CDCl_3$, 49.0 ppm for CD_3OD, and 29.8 ppm for acetone-d_6, all relative to Me_4Si). Heteronuclear 2D NMR and INADEQUATE NMR experiments were recorded on the Bruker AMX 360 instrument. Electron impact (EI) and methane chemical ionization (CI) mass spectra were recorded with a Finnegan 3300 GC-MS instrument. High resolution mass spectra were recorded with a Kratos Concept-H instrument with perfluorokerosene as standard. Fast atom bombardment (FAB) mass spectra were recorded with a Kratos Concept-H instrument with either glycerol or *meta*-nitrobenzyl alcohol as matrix as indicated for each compound. Ultraviolet spectra were recorded with a Phillips PU8740 uv/vis instrument using a 1 cm pathlength with spectral grade methanol as solvent. Infrared spectra were recorded with a Perkin-Elmer 1600 FTIR instrument. Optical rotation measurements were recorded with a Russel Research Autopol III polarimeter using a low volume (1.5 mL) cell with a 10 cm pathlength and using spectral grade methanol as solvent. Melting points were determined using a Büchi SMP 20 instrument. Unless specified otherwise solvents were reagent grade. Dichloromethane was distilled before use. THF was dried by refluxing over then distilling from K metal under a dry N_2 atmosphere, and was freshly dried for each procedure. DMA was dried by refluxing over then distilling under vacuum from CaH and storing over 4Å molecular seives. Solutions in organic solvents were dried using anhydrous $MgSO_4$. Thin layer chromatography was carried out using Eastman Kodak silica gel on polyester sheets with fluorescent indicator.

(2,4-dihydroxyphenyl)phenyldiazene (17)

To a stirred solution of aniline•HCl (1.3 g, 10 mmol) and HCl (20 mmol) in ice / water (50 mL) was added dropwise a solution of $NaNO_2$ (0.76 g, 11 mmol) in ice / water (50 mL). After addition was complete the solution was stirred 1/2 hour at 0°C. This solution was then added dropwise to a solution of resorcinol mono-O-acetate (1.52 g, 10 mmol) in 100 mL Na_2CO_3 / $NaHCO_3$ buffer (pH = 9.9). A deep orange colour was seen immediately. After addition was complete the mixture was acidified to pH < 7 then extracted with 3x100 mL CH_2Cl_2. The combined organic layers were dried and evaporated. The ^{13}C NMR spectrum in $CDCl_3$ was not completely assigned but the presence of two acetate $\underline{C}{=}O$ peaks (170.4 and 170.6 ppm) and two acetate $\underline{C}H_3$ peaks (20.7 and 21.1 ppm) indicated two acetylated products, identified tentatively as **15** and **16**. The ^{13}C NMR spectrum of this crude product was re-recorded after 24 hours in the dark and was identical. The crude product was heated at reflux in 1 M aq. NaOH for 2 hours then this mixture was acidified and extracted with CH_2Cl_2. The ^{13}C NMR spectrum in $CDCl_3$ of the dried and evaporated organic layer was not completely assigned but there were no longer any acetate signals and the number of aromatic peaks was approximately halved so the product was tentatively identified as **17**. There were peaks in the spectrum corresponding to all the peaks in a ^{13}C NMR spectrum of a genuine sample: ^{13}C NMR (δ, acetone-d_6 / CD_3OD) 103.8($\underline{C}$2), 109.9($\underline{C}$6), 122.2($\underline{C}$8), 130.1($\underline{C}$9), 130.8($\underline{C}$5), 133.3($\underline{C}$4), 135.3($\underline{C}$10), 151.5($\underline{C}$3), 157.0($\underline{C}$7), 164.0($\underline{C}$1); mp 165-166° with decomposition, literature mp[110] 166-166.5°. This experiment established the approximate time and temperature conditions for subsequent azo coupling reactions.

Mono-O-*tert*-butyldimethylsilyl resorcinol and its azo coupling reaction

A solution of *tert*-butyldimethylsilyl chloride (2.08 g, 13.8 mmol) in dry THF (100 mL) at 0°C was added dropwise to a solution of resorcinol (7.70 g, 70 mmol) and imidazole (2.82 g, 40 mmol) in dry THF (500 mL) at 0°C and the resulting solution was stirred 1 hour. The solution was evaporated and partitioned between dilute aqueous acid and CH_2Cl_2. The product from the organic extract was chromatographed on 200 g of silica gel, eluting with CH_2Cl_2. The first major product eluted was the di-silylated material; the second major product was the desired mono-O-*tert*-butyldimethylsilyl resorcinol: ^{13}C NMR ($CDCl_3$) 2.0($Si\underline{C}H_3$), 18.1($Si\underline{C}(CH_3)_3$), 25.6($SiC(\underline{C}H_3)_3$), 107.7, 108.8, 112.7, 130.0(aromatic $\underline{C}H$), 156.4, 156.8(aromatic $\underline{C}O$); high resolution MS calculated for $C_{12}H_{20}O_2Si$ m/e 224.12330, found m/e 224.12351 (intensity 21%). The ^{13}C NMR spectrum is shown as Figure **44**. For the azo coupling reaction, the diazonium salt of aniline was prepared as described above and added to a solution of TBDMS-resorcinol in CH_3O^- /

CH_3OH solution (slight excess of base only), stirred 1/2 hour, acidified to pH ≤ 7, then extracted into CH_2Cl_2. The evaporated organic extract was chromatographed on silica gel. The ^{13}C NMR spectrum of the major product showed no TBDMS group peaks, and on the basis of this spectrum it was identified as the deblocked compound (2,4-dihydroxyphenyl)phenyl diazene (**17**, see spectrum above): ^{13}C NMR (acetone-d_6) 104.0($\underline{C}$2), 109.8($\underline{C}$6), 122.3($\underline{C}$8), 130.2($\underline{C}$9), 130.3($\underline{C}$5), 130.9($\underline{C}$4), 135.5($\underline{C}$10), 151.4($\underline{C}$3), 157.0($\underline{C}$7), 163.5($\underline{C}$1).

O-n-pentylresorcinol (18)

Sodium hydride (2.04 g, 53% in mineral oil, 45 mmol) was washed several times with light petroleum ether, then the resulting grey powder was stirred in dry DMA (20 mL) until a homogeneous slurry was obtained. This slurry was added in small portions to a stirred solution of resorcinol (4.50 g, 41 mmol) in dry DMA (200 mL). To the resulting mixture was added 1-iodopentane (8.10 g, 41 mmol) and this mixture was stirred overnight at 60°C under inert atmosphere. The reaction mixture was evaporated to a gum which was partitoned between dilute aqueous acid and CH_2Cl_2. The organic layer was dried, evaporated, and chromatographed on 110 g of silica gel, eluting with CH_2Cl_2. The middle of the three bands to elute ($R_f \approx 0.4$ on silica TLC eluting with CH_2Cl_2)) was the desired monoalkylated product **18** (2.60 g, 14 mmol, 35%): ^1H NMR (δ, $CDCl_3$) 0.90(t, 3H, $C\underline{H}_3$), 1.36(m 4H, $C\underline{H}_2C\underline{H}_2CH_3$), 1.70(~t, 2H, $OCH_2C\underline{H}_2$), 3.85(t, 2H, $OC\underline{H}_2$), 6.40(m, 3H, aromatic $\underline{H}$4, $\underline{H}$5, $\underline{H}$6), 7.08(~t, 1H, aromatic $\underline{H}$2); ^{13}C NMR ($CDCl_3$) 13.9($\underline{C}H_3$), 22.4, 28.1, 28.8($\underline{C}H_2\underline{C}H_2\underline{C}H_2$), 68.1($O\underline{C}H_2$), 102.1, 107.2, 107.7 ($\underline{C}$2, $\underline{C}$4, $\underline{C}$6), 130.1($\underline{C}$5), 156.6($\underline{C}$3), 160.4($\underline{C}$1); high resolution MS calculated for $C_{11}H_{16}O_2$ m/e 180.11508, found m/e 180.11392 (intensity 26%). The ^{13}C NMR spectrum is shown as Figure **45**.

(4-hydroxy-2-(1-oxa-n-pentyl)phenyl)phenyldiazene (19) and (2-hydroxy-4-(1-oxa-n-pentyl)phenyl)phenyldiazene (20)

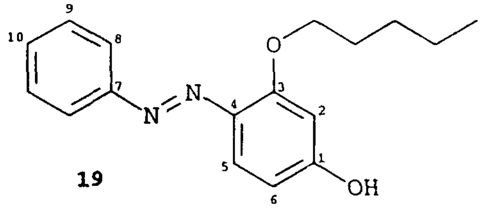

19

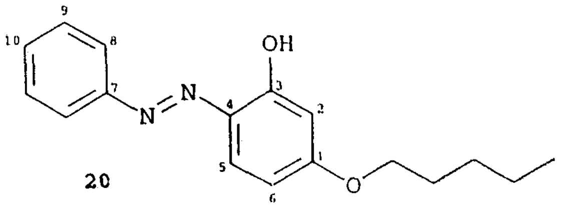

20

To a solution of aniline•HCl (511 mg, 3.9 mmol) and HCl (12 mmol) in water (10 mL) at 0°C was added $NaNO_2$ (300 mg, 4.3 mmol) in water (5 mL) at 0°C and the resulting solution stirred at 0°C for 5 minutes. This solution was then added 1 mL at a time to a solution of **18** (710 mg, 3.9 mmol) in a mixture of Na_2CO_3 / $NaHCO_3$ buffer and methanol (1:1 (v/v), pH 11, 50 mL). Each 1 mL addition was followed by the addition of 1 mL CH_3O^-/CH_3OH solution at the same concentration ($\approx$ 1 M) of base as the excess HCl in the diazonium salt solution, so the pH remained fairly constant throughout the addition. An intense orange colour was seen immediately. The resulting mixture was stirred for 1/2 hour, acidified to pH < 7, then extracted with 2x100 mL CH_2Cl_2. The dried, evaporated organic layer was chromatographed on 100 g of silica gel. Elution with 600 mL of 1:1 hexane / benzene yielded one significant mobile orange band which on evaporation gave **20** (180 mg, 0.63 mmol, 16%): ^1H NMR (δ, CD_3OD / CD_3O^-) 0.97(t, J = 7 Hz, 3H, $C\underline{H}_3$), 1.45(m, 4H, $C\underline{H}_2C\underline{H}_2CH_3$), 1.82(m, 2H, $OCH_2C\underline{H}_2$), 3.98(t, J = 7 Hz, 2H, $OC\underline{H}_2$), 6.06(dd, J = 9 Hz, J = 2 Hz, 1H, $\underline{H}$6), 6.33(d, J = 2 Hz, 1H, $\underline{H}$2), 7.33(br t, J = 8 Hz, 1H, H10), 7.44(br t, J = 8 Hz, 2H, H9), 7.60(d, J = 9 Hz, 1H, H5), 7.86(br d, J = 8 Hz, 2H, H8); ^{13}C NMR (CD_3OD/CD_3O^-) 14.5($\underline{C}H_3$), 23.6, 29.5, 30.1($\underline{C}H_2\underline{C}H_2\underline{C}H_2$), 68.6($O\underline{C}H_2$), 104.7(C6), 106.4(C2), 118.7(C5), 123.1(C8), 129.0(C10), 129.8(C9), 140.3(C4), 155.6(C7), 166.0(C1), 172.5(C3); the ^{13}C NMR spectrum is shown as Figure **46**; all assignments are consistent with the heteronuclear 2D NMR spectra selecting for correlations with J = 130 Hz, J = 7 Hz, and J = 2 Hz; the aromatic region of the heteronuclear 2D NMR spectrum (J = 130 Hz) is shown as Figure **24**; high resolution MS calculated for $C_{17}H_{20}N_2O_2$ m/e 284.15246, found m/e 284.15127 (intensity 100%); uv (CH_3OH) λ_{max} 378 nm (ε = 24,500); uv (CH_3OH/CH_3O^-) λ_{max} 424 nm (ε = 12,900), 460 nm (ε = 12,000). The chromatography solvent was changed to benzene then to CH_2Cl_2 without any significant amount of material being eluted, although some orange bands spread on the column. The solvent was changed to 2% CH_3OH / CH_2Cl_2 and the bands were refocussed and eluted; the one large orange band contained **19** (940 mg, 3.31 mmol, 76%): ^{1}H NMR (δ, CD_3OD / CD_3O^-) 0.94(t, J = 7 Hz, 3H, $C\underline{H}_3$), 1.43(m, 2H, $C\underline{H}_2CH_3$), 1.51(m, 2H, $CH_2C\underline{H}_2CH_2$), 1.85(m, 2H, $OCH_2C\underline{H}_2$), 4.09(t, J = 7 Hz, 2H, $OC\underline{H}_2$), 6.24(dd, J = 9 Hz, J = 2.4 Hz, 1H, H6), 6.28(d, J = 2.4 Hz, 1H, H2), 7.26(m, 1H, H10), 7.38(m, 2H, H9), 7.63(d, J = 9 Hz, 1H, H5), 7.72(m, 2H, H8); ^{13}C NMR (CD_3OD/CD_3O^-) 14.5($\underline{C}H_3$), 23.5, 29.5, 30.0($\underline{C}H_2$), 70.0($O\underline{C}H_2$), 104.4(C2), 114.8(C6), 118.9(C5), 122.7(C8), 129.0(C10), 129.8(C9), 133.8(C4), 155.3(C7), 161.6(C3), 177.4(C1); the ^{13}C NMR spectrum is shown as Figure **47**; all assignments are consistent with the heteronuclear 2D NMR spectra selecting for correlations with J = 130 Hz, J = 7 Hz, and J = 2 Hz; the aromatic region of the heteronuclear 2D NMR spectrum (J = 130

Hz) is shown as Figure **25**, and the aromatic region of the heteronuclear 2D spectrum (J = 7 Hz) is shown as Figure **26**; high resolution MS calculated for $C_{17}H_{20}N_2O_2$ m/e 284.15246, found m/e 284.15459 (intensity 67%); uv (CH_3OH) λ_{max} 368 nm (ε = 22,500); uv (CH_3OH/CH_3O^-) λ_{max} 410 nm (ε = 26,600).

4-(2-acetamidoethyl)aniline (21)

To a stirred solution of 4-(2-aminoethyl)aniline (3.0 g, 22 mmol) and triethylamine (30 mL, 22 g, 215 mmol) in dry THF (100 mL) at 0°C was added dropwise a solution of acetyl chloride (1.90 g, 24 mmol) in dry THF (50 mL) at 0°C. This solution was stirred overnight while warming to room temperature. The solution was evaporated to a gum which was partitioned between water and CH_2Cl_2. The organic layer was dried and evaporated to a gum which was chromatographed on 150 g silica gel, eluting with 6% CH_3OH / CH_2Cl_2. In this system the monoacetylated material elutes faster ($R_f \approx .45$ on silica TLC eluting with 6% CH_3OH / CH_2Cl_2) than the major impurity, the diacetylated material ($R_f \approx .26$ using the same system). The appropriate fractions were pooled and evaporated to give **21** (1.77 g, 10 mmol, 45%): ^1H NMR (δ, $CDCl_3$) 1.85(s, 3H, $\underline{C}H_3$), 2.63(~q, 2H, $ArC\underline{H_2}$), 3.29(~t, 2H, $NHC\underline{H_2}$), 6.56(d, J = 8 Hz, 2H, aromatic), 6.88(d, J = 8 Hz, 2H, aromatic); ^{13}C NMR ($CDCl_3$) 22.8($\underline{C}H_3$), 34.4($Ar\underline{C}H_2$), 40.7($NH\underline{C}H_2$), 115.0($\underline{C}2$), 128.3($\underline{C}4$), 129.2($\underline{C}3$), 144.7($\underline{C}1$), 170.0($\underline{C}$=O); the ^{13}C NMR spectrum is shown as Figure **48**; high resolution MS calculated for $C_{10}H_{14}N_2O$ m/e 178.11072, found m/e 178.11038 (intensity 29%).

O-(O-(2-tetrahydropyranyl)-3-oxapropyl)resorcinol (22)

Sodium hydride (2.04 g, 53% in mineral oil, 45 mmol) was washed twice with light petroleum ether, then stirred in dry DMA (20 mL) until a homogeneous slurry was obtained. The slurry was added in small portions to a stirred solution of resorcinol (4.50 g, 41 mmol) in dry DMA (200 mL). The mixture goes from grey to brown to almost black. To this mixture was added O-2-tetrahydropyranyl-2-bromoethanol[34] (8.57 g, 41 mmol) and the resulting mixture was stirred at 60°C overnight. The mixture was evaporated to an oil which was partitioned between water and CH_2Cl_2, with the pH of the water layer was adjusted to ~7. The organic layer was dried and evaporated to an oil which was chromatographed on 300 g of silica gel eluting with 1% CH_3OH / CH_2Cl_2. The two significant bands were the dialkylated material ($R_f \approx .67$) and monoalkylated **22** ($R_f \approx .33$ on silica TLC eluting with 1% CH_3OH / CH_2Cl_2). Fractions containing both products were re-chromatographed on 100 g of silica gel. All appropriate fractions from both columns were combined and evaporated to give **22** as a colourless oil (5.18 g, 22 mmol, 53%): ^{1}H NMR (δ, $CDCl_3$) 1.4-1.9(m, 6H, $C\underline{H}_2C\underline{H}_2C\underline{H}_2$), 3.3-4.2(m, 6H, 3x$OC\underline{H}_2$), 4.70(m, 1H, $OC\underline{H}O$), 6.3-6.6(m, 3H), 6.8(br s, 1H), 7.06(t, 1H); ^{13}C NMR ($CDCl_3$) 19.1, 25.2, 30.4($\underline{C}H_2\underline{C}H_2\underline{C}H_2$), 62.2, 65.9, 67.2(3x$O\underline{C}H_2$), 99.0($O\underline{C}HO$), 102.3, 106.6, 108.1, 129.9(aromatic $\underline{C}H$), 157.1, 160.0(aromatic $\underline{C}O$); the ^{13}C NMR spectrum is shown as Figure **49**; high resolution MS calculated for $C_{13}H_{18}O$ m/e 238.1205, found m/e 238.1218 (intensity 74%).

[4-(2-acetamidoethyl)phenyl][4-hydroxy-2-(3-(2-tetrahydropyranyloxy)-1-oxapropyl)phenyl]diazene (23) and [4-(2-acetamidoethyl)phenyl][2-hydroxy-4-(3-(2-tetrahydropyranyloxy)-1-oxapropyl)phenyl]diazene (24)

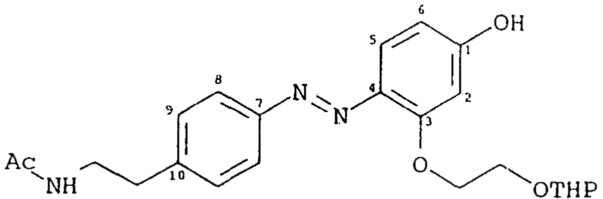

23

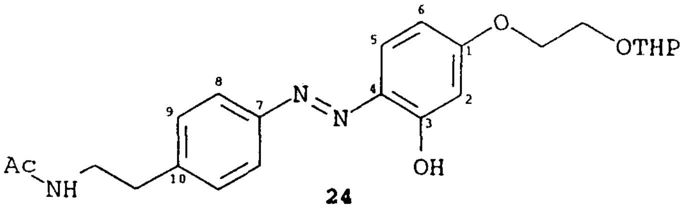

24

To a stirred solution of **21** (712 mg, 4.0 mmol) plus conc HCl (1.33 mL, 16 mmol) in water (10mL) at 0°C was added a solution of $NaNO_2$ (304 mg, 4.4 mmol) in water (5 mL) at 0°C and the resulting solution stirred at 0°C for 5 minutes. This solution was then added in 1 mL portions to a stirred solution of **22** (952 mg, 4.0 mmol) in a mixture of Na_2CO_3 / $NaHCO_3$ buffer and CH_3OH (1:1 (v/v), pH 11, 160 mL). After each 1 mL addition another 1 mL of CH_3O^- / CH_3OH solution was added; this base solution was made to be the same concentration as the concentration of excess acid in the diazonium salt solution (≈ 0.5 M) so the pH of the reaction mixture remained fairly constant. An intense orange colour was seen immediately. After addition was complete the mixture was stirred another 1/2 hour. The reaction solution was then mixed with an equal volume of

CH_2Cl_2 and stirred while 1 M HCl was added carefully to a pH of ≈ 8, at which point all the orange colour went to the organic layer. The layers were separated and the organic layer was dried and evaporated to a dark orange oil. This material was chromatographed on 100 g of silica gel, eluting with 6% CH_3OH / CH_2Cl_2. The faster moving of the two major bands ($R_f \approx .62$ on silica TLC eluting with 6% CH_3OH / CH_2Cl_2) was evaporated to give **24** as an orange gum (220 mg, 0.52 mmol, 13%): ^{1}H NMR (δ, CD_3OD / CD_3O^-) 1.40-1.55(m, 4H, 4xTHP $C\underline{H}_2$), 1.66(m, 1H, THP $C\underline{H}_2$), 1.79(m, 1H, THP $C\underline{H}_2$), 1.89(s, 3H, $C\underline{H}_3$), 2.78(t, J = 7 Hz, 2H, $ArC\underline{H}_2$), 3.37(t, J = 7 Hz, 2H, $NHC\underline{H}_2$), 3.49(m, 1H, $OC\underline{H}_2$), 3.75(m, 1H, $OC\underline{H}_2$), 3.86(m, 1H, $OC\underline{H}_2$), 3.98(m, 1H, $OC\underline{H}_2$), 4.08(~t, J ≈ 4.7 Hz, 2H, $OC\underline{H}_2$), 4.66(dd, J ≈ 4 Hz, J ≈ 3 Hz, 1H, $OC\underline{H}O$), 6.06(dd, J = 9.1 Hz, J = 2.7 Hz, 1H, $\underline{H}6$), 6.32(d, J = 2.7 Hz, 1H, $\underline{H}2$), 7.24(d, J = 8.4 Hz, 2H, $\underline{H}9$), 7.56(d, J = 9.1 Hz, 1H, $\underline{H}5$), 7.78(d, J = 8.4 Hz, 2H, $\underline{H}8$); ^{13}C NMR (CD_3OD/CD_3O^-) 22.7($\underline{C}H_3$), 20.4, 22.7, 26.5($\underline{C}H_2\underline{C}H_2\underline{C}H_2$), 36.2($Ar\underline{C}H_2$), 41.9($NH\underline{C}H_2$), 63.2, 67.1, 68.1(3x$O\underline{C}H_2$), 100.3($O\underline{C}HO$), 104.2($\underline{C}6$), 106.6($\underline{C}2$), 118.8($\underline{C}5$), 123.1($\underline{C}8$), 130.1($\underline{C}9$), 140.5($\underline{C}10$), 140.5($\underline{C}4$), 154.1($\underline{C}7$), 165.4($\underline{C}1$), 172.3($\underline{C}3$), 173.0($\underline{C}$=O); the ^{13}C NMR spectrum is shown as Figure **50**; all assignments are consistent with the heteronuclear 2D NMR spectra selecting for correlations with J = 130 Hz, J = 7 Hz, and J = 2 Hz; high resolution MS calculated for $C_{23}H_{29}N_3O_5$ m/e 427.21087, found m/e 427.20791 (intensity 12%). The slower moving of the two major bands ($R_f \approx .38$) was evaporated to give **23** as an orange gum (1.28 g, 3.0 mmol, 75%): ^{1}H NMR (δ, CD_3OD/CD_3O^-) 1.4-1.6(m, 4H, 4xTHP $C\underline{H}_2$), 1.67(m,1H, THP $C\underline{H}_2$), 1.79(m, 1H, THP $C\underline{H}_2$), 1.90(s, 3H, $C\underline{H}_3$), 2.79(t, J = 7.5 Hz, 2H, $ArC\underline{H}_2$), 3.38(t, J = 7.4 Hz, 2H, $NHC\underline{H}_2$), 3.48(m, 1H, $OC\underline{H}_2$), 3.90(m, 1H, $OC\underline{H}_2$), 4.05(m, 1H, $OC\underline{H}_2$), 4.25(m, 1H, OCH_2), 4.78(dd, J = 4.2 Hz, J = 3.1 Hz, OCHO), 6.23(dd, J = 9.0 Hz, J = 2.3 Hz, 1H, H6), 6.27(d, J = 2.3 Hz, 1H, H2), 7.24(d, J = 8.4 Hz, 2H, H9), 7.60(d, J = 9.0 Hz, 1H, H5), 7.64(d, J = 8.4 Hz, 2H, H8); ^{13}C NMR (CD_3OD/CD_3O') 22.7(CH_3), 20.4, 26.5, 31.6($CH_2CH_2CH_2$), 36.3($ArCH_2$), 42.0($NHCH_2$), 63.3, 67.0, 69.8(3xOCH_2), 100.5(OCHO), 104.5(C2), 115.1(C6), 119.0(C5), 122.8(C8), 130.3(C9), 133.8(C4), 140.8(C10), 154.0(C7), 161.3(C3), 173.0(C=O), 177.4(C1); the ^{13}C NMR spectrum is shown as Figure **51**; all assignments are consistent with the heteronuclear 2D NMR spectra selecting for correlations with J = 130 Hz, J = 7 Hz, and J = 2 Hz; high resolution MS calculated for $C_{23}H_{29}N_3O_5$ m/e 427.21087, found m/e 427.21168 (intensity 14%).

[2-(1-oxa-n-hexyl)-4-(3-(2-tetrahydropyranyloxy)-1-oxapropyl)phenyl]phenyldiazene (29)

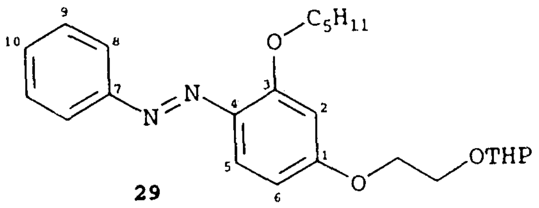

29

Sodium hydride (290 mg, 53% in mineral oil, 6.4 mmol) was washed twice with light petroleum ether, then stirred in dry DMA (5 mL) until a homogeneous slurry was obtained. This slurry was added in small portions to a solution of **19** (1.66 g, 5.85 mmol) in dry DMA (75 mL) at 0°C. O-(2-tetrahydropyranyl)-2-bromothanol[34] (1.22g, 5.85 mmol) was added and the resulting mixture stirred at 60°C overnight. The mixture was evaporated to an oil which was partitioned between water and CH_2Cl_2. The organic layer was dried and evaporated to an orange oil. This was chromatographed on 100 g of silica gel, eluting with 1% CH_3OH / CH_2Cl_2. The large orange band was evaporated to give **29** (1.50 g, 3.6 mmol, 62%): ^1H NMR (δ, $CDCl_3$) 0.92 (overlapped with TMS sideband, C$\underline{H}_3$), 1.30-2.00(m, 12H, C$\underline{H}_2$), 3.30-4.20(m, 8H, OC$\underline{H}_2$), 4.65(m, 1H, OC$\underline{H}$O), 6.55(m, 2H, aromatic), 7.40(m, 3H, aromatic), 7.80(m, 3H, aromatic); ^{13}C NMR ($CDCl_3$) 13.9($\underline{C}H_3$), 19.2, 22.3, 25.2, 28.0, 28.7, 30.3(2x$\underline{C}H_2\underline{C}H_2\underline{C}H_2$), 62.0, 65.5, 67.5, 69.6(4xO$\underline{C}H_2$), 98.3(O$\underline{C}$HO), 101.0($\underline{C}$2), 106.4($\underline{C}$6), 117.7($\underline{C}$5), 122.5($\underline{C}$8), 128.7($\underline{C}$10), 129.7($\underline{C}$9), 137.0($\underline{C}$4), 153.1($\underline{C}$7), 158.3, 162.7($\underline{C}$1 and $\underline{C}$3); the ^{13}C NMR spectrum is shown as Figure **52**; high resolution MS calculated for $C_{24}H_{32}N_2O_4$ m/e 412.23636, found m/e 412.23692 (intensity 31%); uv (CH_3OH) λ_{max} 366 nm (ε = 17,825), 442 nm (ε = 2070).

[4-(1-oxa-n-hexyl)-2-(3-(2-tetrahydropyranyloxy)-1-oxapropyl)phenyl]phenyl diazene (30)

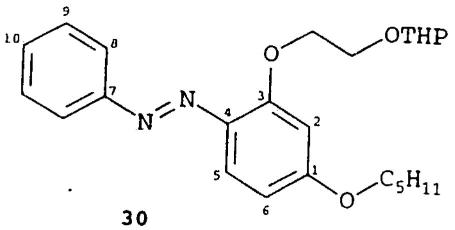

30

The procedure was identical to that described above for the conversion of **19** to **29**, starting with 1.65 mmol of compound **20**. Chromatography yielded **30** as an orange oil (300 mg, 0.73 mmol, 44%): ^1H NMR (δ, $CDCl_3$) 0.94(overlapped with TMS sideband, C$\underline{H}_3$), 1.10-1.90(m, 12H, C$\underline{H}_2$), 3.30-4.40(m, 8H, OC$\underline{H}_2$), 4.77(m, 1H, OC$\underline{H}$O), 6.50(m, 2H, aromatic), 7.40(m, 3H, aromatic), 7.80(m, 3H, aromatic); ^{13}C NMR ($CDCl_3$) 14.0($\underline{C}H_3$), 19.2, 22.4, 25.4, 28.1, 28.8, 30.5(2x $\underline{C}H_2\underline{C}H_2\underline{C}H_2$), 62.0, 65.7, 68.3, 69.6(4x

OCH$_2$), 99.0(OCHO), 101.5(C2), 107.2(C6), 117.9(C5), 122.6(C8), 128.8(C10), 129.9(C9), 137.1(C4), 153.3(C7), 158.4, 163.1(C1, C3); the ^{13}C NMR spectrum is shown as Figure **53**; high resolution MS calculated for $C_{24}H_{32}N_2O_4$ m/e 412.23636, found m/e 412.23588 (intensity 26%); uv (CH_3OH) λ_{max} 366 nm (ε = 17,680), 442 nm (ε = 1750).

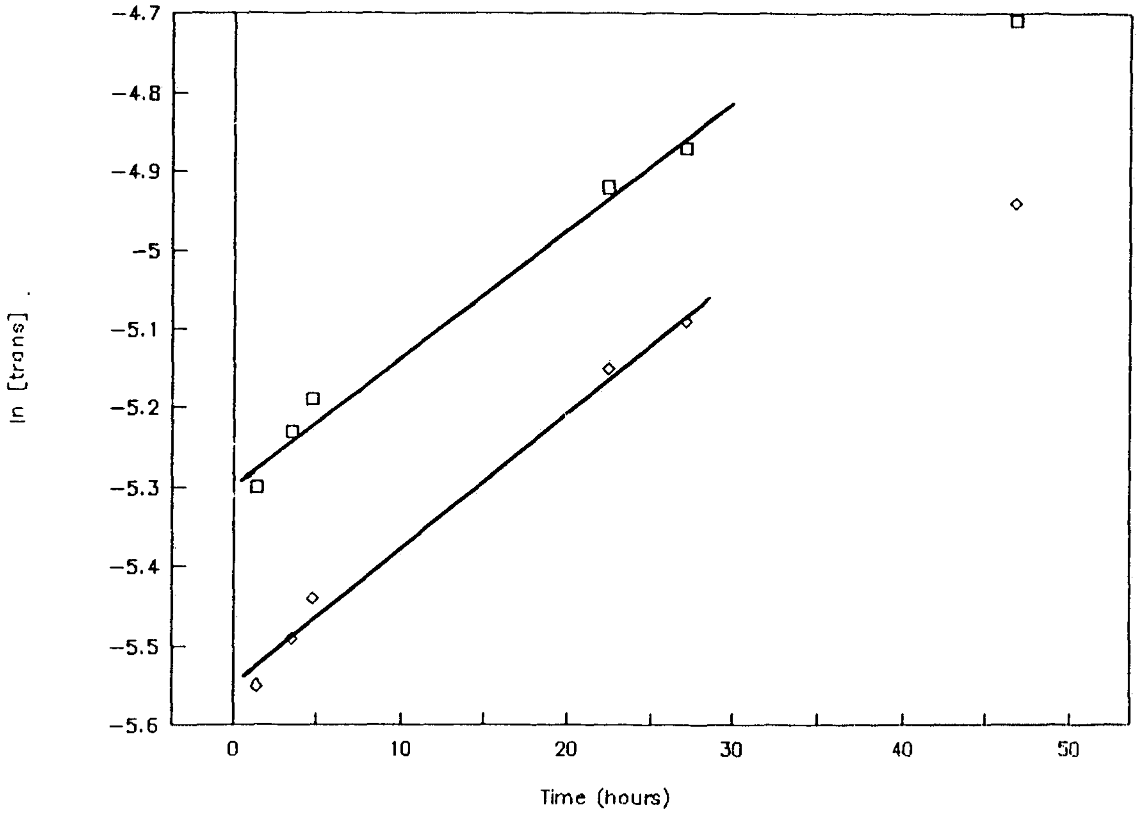

Figure 43. Rate of thermal back reaction from *cis* to *trans* isomer. Squares are compound **19**, giving $t_{1/2}$= 39 hr (r= 0.954); diamonds are for compound **20**, giving $t_{1/2}$= 42 hr (r= 0.952).

Di-4-methoxyphenyl diazene-1-oxide (27)

To a stirred solution of anisidine (1.23 g, 10 mmol) and HCl (40 mmol) in water (20 mL) at 0° was added $NaNO_2$ (760 mg, 11 mmol) in water (10 mL) at 0° and the resulting solution stirred for 10 minutes. The solution was then added to a solution of phenol 940 mg, 10 mmol) in a mixture of Na_2CO_3 / $NaHCO_3$ buffer and methanol (1:1 (v/v), pH 11, 200 mL) while simultaneously adding a solution of NaOMe (20 mmol) in methanol (30 mL). The resulting solution was stirred while warming to room temperature. The solution was mixed with an equal volume of CH_2Cl_2 and stirred while 1 M HCl was added until the orange colour went into the organic layer. The organic layer was dried and evaporated to an orange solid. This was chromatographed on silica gel (150 g), eluting with 2% CH_3OH / CH_2Cl_2. The one large orange band (1.45 g, 6.36 mmol assuming compound **25**) was used without characterization in the next step.

Sodium hydride 336 mg, 50% in mineral oil, 7.0 mmol) was washed twice with light petroleum ether, then stirred in dry DMF (5 mL) until a homogeneous slurry was obtained. This slurry was added dropwise to a solution of the product of the last step (1.45 g) in dry THF. To the resulting solution was added CH_3I until the reaction was complete by TLC (silica gel, eluting with 1% CH_3OH / CH_2Cl_2, starting material had $R_f \approx 0.3$, product had $R_f \approx 0.8$), total volume $CH_3I \approx 4$ mL. This solution was evaporated to an orange solid which was filtered through a pad of silica gel as a solution in 1% CH_3OH / CH_2Cl_2, then evaporated to an orange solid (1.50 g, 6.19 mmol assuming compound **26**) which was used without characterization in the next step.

The product of the last step (1.50 g) and *meta*-chloroperbenzoic acid (10.7 g, 50%

mixture with *meta*-chlorobenzoic acid, 30 mmol) were dissolved in CH_2Cl_2 (200 mL) and stirred overnight at room temperature. The solution was evaporated to a yellow solid which was chromatographed on silica gel (100 g) eluting with CH_2Cl_2. The one large coloured band ($R_f \approx 0.5$) was evaporated to give **27** as a yellow powder (1.50 g, 5.8 mmol): ^1H NMR (δ, $CDCl_3$) 3.81(s, 6H, 2xC$\underline{H}_3$), 6.93(d, J = 9.0 Hz, 2H, C$\underline{H}$3), 6.95(d, J = 9.0 Hz, 2H, C$\underline{H}$3'), 8.22(d, J = 9.0 Hz, 2H, C$\underline{H}$2), 8.25(d, J = 9.0 Hz, 2H, C$\underline{H}$2'); ^{13}C NMR ($CDCl_3$) 55.3, 55.5(2xO$\underline{C}H_3$), 113.4, 113.6($\underline{C}$2 and $\underline{C}$2'), 123.6, 127.7($\underline{C}$3 and $\underline{C}$3'), 137.9, 141.6($\underline{C}$4 and $\underline{C}$4'), 160.1, 161.7($\underline{C}$1 and$\underline{C}$1'); high resolution MS calculated for $C_{14}H_{14}N_2O_3$ m/e 258.1005, found m/e 258.1027 (intensity 100%); mp 113.5-114°, 127.5-128°; literature mp[111] 116.5-118.5°, 134.5-135.5°

Wallach rearrangement of 27 to (2-hydroxy-4-methoxyphenyl)-4-methoxyphenyl diazene (28)

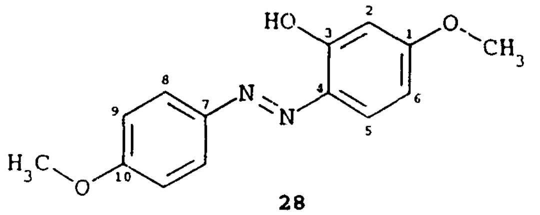

28

A solution of **27** (400 mg, 1.55 mmol) in 95% ethanol (200 mL) was placed in a standard Rayonet photoreactor with a 300 nm cutoff under continuous irradiation with argon bubbling for 12 hours. The solution was evaporated and the crude product was dissolved in ether. The ether solution was extracted with several portions of 0.1 M aqueous NaOH until there was no more colour in the aqueous layer. The combined aqueous layers were stirred vigorously with an equal volume of ether and 1 M HCl was added dropwise until the yellow colour was all in the ether layer. This organic layer was dried and evaporated to give **28** as an orange solid (50 mg, 19 mmol, 13%): ^{1}H NMR (δ, CD_3OD / CD_3O^-) 3.74(s, 3H, OC$\underline{H}_3$), 3.80(s, 3H, OC$\underline{H}_3$), 6.02(dd, J = 9.0 Hz, J = 3.0 Hz, $\underline{H}$6), 6.31(d, J = 3.0 Hz, 1H, $\underline{H}$2), 6.95(d, J = 9.0 Hz, 2H, $\underline{H}$9), 7.40(d, J = 9.0 Hz, 1H, $\underline{H}$5), 7.80(d, J = 9.0 Hz, 2H, $\underline{H}$8); ^{13}C NMR (CD_3OD / CD_3O^-) 55.4(O$\underline{C}H_3$), 56.0(O$\underline{C}H_3$), 103.7($\underline{C}$6), 105.9($\underline{C}$2), 115.0($\underline{C}$9), 118.7($\underline{C}$5), 124.5($\underline{C}$8), 140.4($\underline{C}$4), 149.8($\underline{C}$7), 161.4($\underline{C}$10), 165.9($\underline{C}$1), 171.8($\underline{C}$3); the ^{13}C NMR spectrum is shown as Figure **54**; all assignments are consistent with the heteronuclear 2D NMR spectra selecting for correlations with J = 130 Hz, J = 7 Hz, and J = 2 Hz; high resolution MS calculated for $C_{14}H_{14}N_2O_3$ m/e 258.10052, found m/e 258.10055 (intensity 100%).

5,6-di-O-isopropylidene-1-bromohexane (33)

6-Bromo-1-hexene (25 g, 150 mmol) and *meta* chloroperbenzoic acid (52 g, 50% mixture with *meta*-chlorobenzoic acid, 150 mmol) in CH_2Cl_2 (1 L) was stirred overnight at room temperature. The solution was washed several times with saturated bicarbonate solution then dried and evaporated to give **31** as a colourless oil (20 g, 120 mmol): ^{1}H NMR (δ, $CDCl_3$) 1.70(m, 4H, BrCH$_2$C$\underline{H}_2$C$\underline{H}_2$), 2.00(m, 2H, C$\underline{H}_2$ adjacent to epoxide ring), 2.47(m, 1H, epoxide ring), 2.74(m, 1H, epoxide ring), 2.91(m, 1H, epoxide ring), 3.42(t, J = 7 Hz, 2H, BrC$\underline{H}_2$); literature ^{1}H NMR[112] (δ, $CDCl_3$) 1.61(m, 4H), 1.88(m, 2H), 2.48(m, 1H), 2.76(m, 1H), 2.90(m, 1H), 3.44(t, J = 7 Hz, 2H).

This material was stirred in a mixture of THF (400 mL) and 1 M H_2SO_4 (50 mL) at room temperature for 2 days. An equal volume of saturated $NaHCO_3$ solution was added (carefully) then this solution extracted with an equal volume of CH_2Cl_2. The organic layer was dried and evaporated. The resulting material was dissolved in 2,2-dimethoxypropane (200 mL) then BF_3 etherate (200 μL) added and the resulting solution stirred 2 days at room temperature. The solution was then filtered through a silica gel pad and the pad washed with CH_2Cl_2. The filtrate was dried over $MgSO_4$ and evaporated to give **33** as a pale yellow oil (15.9 g, 67 mmol): ^1H NMR (δ, $CDCl_3$) 1.31(s, 3H, $C\underline{H}_3$), 1.39(s, 3H, $C\underline{H}_3$), 1.57(m, 4H, $C\underline{H}_2$), 1.88(m, 2H, $C\underline{H}_2$), 3.39(t, J = 7 Hz, 2H, $BrC\underline{H}_2$), 3.47(m, 2H, $C\underline{H}_2O$), 4.00(m, 1H, $C\underline{H}O$); ^{13}C NMR ($CDCl_3$) 24.4, 25.7($\underline{C}H_3$), 26.9, 32.6, 32.7, 33.3($Br\underline{C}H_2\underline{C}H_2\underline{C}H_2\underline{C}H_2$), 69.4($\underline{C}H_2O$), 75.8($\underline{C}HO$), 108.8($O\underline{C}O$); the ^{13}C NMR spectrum is shown as Figure **55**; methane CI MS 239,237 (20%, M+1), 181, 179, 163, 161, 99, 82.

[4-(2-acetamidoethyl)phenyl][2-(3-(2-tetrahydropyranyloxy)-1-oxapropyl)-4-(6,7-(di-O-isopropylidene)-1-oxaheptyl)phenyl] diazene (34)

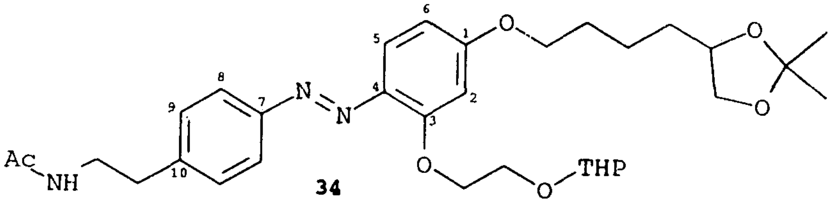

34

Sodium hydride (297 mg, 50% in mineral oil, 6.18 mmol) was washed twice with light petroleum ether, then stirred with dry DMA (5 mL) until a homogeneous slurry was obtained. The slurry was added in small portions to a solution of **23** (2.40 g, 5.62 mmol) in dry DMA (175 mL) at 0°C. When no more gas was being evolved a solution of **33**

(1.33 g, 5.62 mmol) in a few mL dry DMA was added and the resulting mixture was stirred at 60°C overnight. The reaction mixture was evaporated to an oil which was partitioned between water and CH_2Cl_2, with salting of the aqueous layer and the addition of a little CH_3OH necessary to break up the emulsion and separate the layers. The organic layer was dried and evaporated to an orange gum which was chromatographed on 400 g silica gel, eluting with 5% CH_3OH / CH_2Cl_2. The first major coloured band was evaporated to give **34** as an orange gum (2.54 g, 4.36 mmol, 78%): ^1H NMR (δ, $CDCl_3$) 1.26(s, 3H, $C(C\underline{H}_3)_2$), 1.32(s, 3H, $C(C\underline{H}_3)_2$), 1.45 - 1.85(m, 12H, 2 x $C\underline{H}_2C\underline{H}_2C\underline{H}_2$), 1.86(s, 3H, $C\underline{H}_3C{=}O$), 2.77(t, J = 7 Hz, 2H, $ArC\underline{H}_2$), 3.42(m, 4H, $NHC\underline{H}_2$ and $OC\underline{H}_2$), 3.80 - 4.08(m, 7H, 3 x $OC\underline{H}_2$, $OC\underline{H}$), 4.28(t, J = 6 Hz, 2H, $OC\underline{H}_2$), 4.69(m, 1H, $OC\underline{H}O$), 6.05(br t, J = 5 Hz, 1H, $N\underline{H}$), 6.45(dd, J = 8 Hz, J = 2 Hz, 1H, $\underline{H}2$), 7.19(d, J = 7 Hz, 2H, $\underline{H}9$), 7.63(d, J = 8 Hz, 1H, $\underline{H}5$), 7.72(d, J = 7 Hz, 2H, $\underline{H}8$); ^{13}C NMR ($CDCl_3$) 19.1, 22.2, 23.0($C(\underline{C}H_3)_2,C{=}O(\underline{C}H_3)$), 25.3, 25.6, 26.8, 29.0, 30.4, 33.1(2x$\underline{C}H_2\underline{C}H_2\underline{C}H_2$), 35.3($Ar\underline{C}H_2$), 40.4($NH\underline{C}H_2$), 61.9, 65.6, 67.9, 69.2, 69.5(5x$O\underline{C}H_2$), 75.7($O\underline{C}H$), 98.8($O\underline{C}HO$), 101.4($\underline{C}(CH_3)_2$), 107.0($\underline{C}2$), 108.6($\underline{C}6$), 117.8($\underline{C}5$), 122.7($\underline{C}8$), 129.1($\underline{C}9$), 138.0($\underline{C}10$), 141.1($\underline{C}4$), 151.9($\underline{C}7$), 158.2, 162.8($\underline{C}1$, $\underline{C}3$), 170.0($\underline{C}{=}O$); the ^{13}C NMR spectrum is shown as Figure **56**; high resolution +FAB MS (*meta* nitrobenzyl alcohol matrix) calculated for M+1, $C_{32}H_{46}N_3O_7$, m/e 584.3338, found m/e 584.3340 (intensity 59%).

4-(N-*tert*-butyloxycarbonyl-2-aminoethyl)aniline (37)

To a stirred soluton of 4-(2-aminoethyl)aniline (10.0 g, 73 mmol) in dry THF (500 mL) at room temperature was added dropwise a solution of di-*tert*-butyldicarbonate (15.0

g, 69 mmol) in dry THF (100 mL). The resulting solution was stirred for 1 hour at room temperature. The solution was evaporated to give **37** as a pale yellow solid (16.5 g, 70 mmol, 100 %): ^{1}H NMR (δ, CDCl$_3$) 14.2(s, 9H, $C(C\underline{H}_3)_3$), 2.65(br t, 2H, Ar-$C\underline{H}_2$), 3.29(br q, 2H, $NHC\underline{H}_2$), 3.58(br s, 2H, N$\underline{H}$, N$\underline{H}_2$), 6.61(br d, J = 8 Hz, $\underline{H}$2), 6.95(d, J = 8 Hz, $\underline{H}$3); ^{13}C NMR (CDCl$_3$) 28.3($C(\underline{C}H_3)_3$), 35.2($Ar\underline{C}H_2$), 41.9($NH\underline{C}H_2$), 79.0($\underline{C}(CH_3)_3$), 115.2($\underline{C}$2), 128.7($\underline{C}$4), 129.5($\underline{C}$3), 144.8($\underline{C}$1), 155.8($\underline{C}$=O); the ^{13}C NMR spectrum is shown as Figure **57**; high resolution MS calculated for $C_{13}H_{20}N_2O_2$ m/e 236.1526, found m/e 236.1533 (intensity 46%).

[4-(N-(*tert*-butyloxycarbonyl)-2-aminoethyl)phenyl][4-hydroxy-2-(3-(2-tetrahydropyranyloxy)-1-oxapropyl)phenyl] diazene (38)

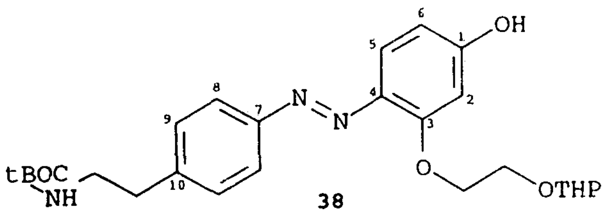

38

To a stirred suspension of **37** (3.00 g, 12.6 mmol) in water / CH$_3$OH (2:1, 50 mL) at 0°C was added 4 M HCl (12 mL, 48 mmol) at 0°C then *immediately* a solution of NaNO$_2$ (870 mg, 12.6 mmol) in water (12 mL) at 0°C was added. The resulting suspension was stirred for *1 minute only* then added to a solution of **22** (3.00 g, 12.6 mmol) in a mixture of CH$_3$OH and Na$_2$CO$_3$ / NaHCO$_3$ buffer (1:1 (v/v), pH 11, 300 mL) at 0°C. The addition was accompanied by simultaneous addition of a CH$_3$O$^-$ / CH$_3$OH solution at 0°C, made at the same concentration of base as the diazonium salt solution had of excess acid so that the pH remained fairly constant through the few seconds required for the addition. An intense orange colour was seen immediately. The reaction mixture was allowed to warm to room temperature. A 300 mL portion of CH_2Cl_2 was added and the mixture stirred vigorously while 1 M HCl was added until the orange colour all went to the organic layer (pH ≈ 7). The organic layer was dried and evaporated to an oil. The crude product was divided in half and each half chromatographed on 375 g of silica gel, eluting with 2% CH_3OH / CH_2Cl_2. The largest orange band from each column ($R_f \approx .25$ on silica TLC eluting with 2% CH_3OH / CH_2Cl_2) was evaporated to **38** as an orange gum (combined yield 2.37 g, 4.89 mmol, 39%): ^1H NMR (δ, CD_3OD / CD_3O^-) 1.21(s, 9H, $C(C\underline{H}_3)_3$), 1.20 - 1.70(m, 6H, $C\underline{H}_2C\underline{H}_2C\underline{H}_2$), 2.57(t, J = 8 Hz, 2H, $ArC\underline{H}_2$), 3.05(t, J = 8 Hz, 2H, $NHC\underline{H}_2$), 3.28(m, 1H, ring $OC\underline{H}_2$), 3.71(m, 2H, $OC\underline{H}_2$), 3.86(m, 1H, ring $OC\underline{H}_2$), 4.05(t, J = 7 Hz, 2H, $OC\underline{H}_2$), 4.59(m, 1H, $OC\underline{H}O$), 6.04(dd, J = 8 Hz, J = 2 Hz, 1H, $\underline{H}6$), 6.07(d, J = 2 Hz, 1H, $\underline{H}2$), 7.04(d, J = 7 Hz, 2H, $\underline{H}9$), 7.41(d, J = 8 Hz, 1H, $\underline{H}5$), 7.44(d, J = 7 Hz, 2H, $\underline{H}8$); ^{13}C NMR (CD_3OD / CD_3O^-) 20.4, 26.5, 31.6($\underline{C}H_2\underline{C}H_2\underline{C}H_2$), 28.9($C(\underline{C}H_3)_3$), 36.9($Ar\underline{C}H_2$), 43.0($NH\underline{C}H_2$), 63.5, 67.1, 69.9($O\underline{C}H_2$), 80.0($\underline{C}(CH_3)_3$), 100.6($O\underline{C}HO$), 104.7($\underline{C}2$), 115.2($\underline{C}6$), 119.1($\underline{C}5$), 122.8($\underline{C}8$), 130.4($\underline{C}9$), 133.8($\underline{C}4$), 140.9($\underline{C}10$), 153.9($\underline{C}7$), 158.4($\underline{C}=O$), 161.1($\underline{C}3$), 177.5($\underline{C}1$); the ^{13}C NMR spectrum is shown as Figure 31; high resolution +FAB MS (glycerol matrix) calculated for M+1, $C_{26}H_{36}N_3O_6$, m/e 486.2606, found m/e 486.2579 (intensity 84%).

[4-(N-(*tert*-butyloxycarbonyl)-2-aminoethyl)phenyl][2-(1,4-dioxabutyl)-4-hydroxyphenyl]diazene (40)

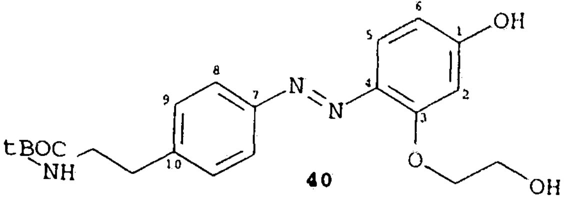

40

To a stirred solution of **38** (2.37 g, 4.90 mmol) in CH_3OH (100 mL) was added 1 M HCl (50 mL) and the resulting solution stirred at room temperature for 1 hour then neutralized with 1 M NaOH soluton to pH ≈ 7. The soluton was evaporated to an orange solid which was partitoned between water and CH_2Cl_2. The water layer was washed once more with CH_2Cl_2 and the combined organic layers dried and evaporated to give **40** as an orange glass (1.90 g, 4.74 mmol, 97%): ^{1}H NMR (δ, CD_3OD) 1.40(s, 9H, $C(C\underline{H}_3)_3$), 2.76(br t, J = 7 Hz, $ArC\underline{H}_2$), 3.26(br t, J = 7 Hz, $NHC\underline{H}_2$), 3.90(m, 2H, $OC\underline{H}_2$), 4.18(m, 2H, $OC\underline{H}_2$), 6.45(m, 2H, $\underline{H}2$,$\underline{H}5$, $\underline{H}6$), 7.27(d, J = 8 Hz, 2H, $\underline{H}8$), 7.65(d, J = 8 Hz, 2H, $\underline{H}9$); ^{13}C NMR (CD_3OD) 28.8($C(\underline{C}H_3)_3$), 36.8($Ar\underline{C}H_2$), 42.7($NH\underline{C}H_2$), 61.5, 71.9($2xO\underline{C}H_2$), 79.9($\underline{C}(CH_3)_3$), 103.0($\underline{C}2$), 111.8($\underline{C}6$), 119.7($\underline{C}5$), 123.0($\underline{C}8$), 130.4($\underline{C}9$), 135.9($\underline{C}10$), 142.2($\underline{C}4$), 153.3($\underline{C}7$), 158.2($\underline{C}$=O), 160.0($\underline{C}1$), 168.7($\underline{C}3$); the ^{13}C NMR spectrum is shown as Figure **58**; high resolution +FAB MS (glycerol matrix) calculated for M+1, $C_{21}H_{28}N_3O_5$, m/e 402.2030, found m/e 402.2019 (intensity 17%).

[4-(N-(*tert*-butyloxycarbonyl)-2-aminoethyl)phenyl][2-(1,4-dioxabutyl)-4-(6,7-(di-O-isopropylidene)-1-oxaheptyl)phenyl]diazene (13)

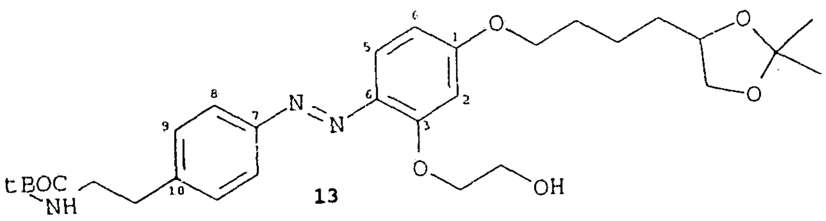

13

To a stirred solution of **40** (330 mg, 0.82 mmol) in dry DMA (25 mL) was added Cs_2CO_3 (400 mg, 1.2 mmol) which did not all dissolve even on warming. To this mixture was added **33** (200 mg, 0.85 mmol) and the resulting mixture was stirred at 60°C overnight. The reaction mixture was evaporated to an oil which was partitioned between water and CH_2Cl_2, with salting being necessary to separate the layers. The organic layer was dried and evaporated to an orange oil which was chromatographed on 40 g of silica gel, eluting with 2% CH_3OH/CH_2Cl_2. The largest orange band ($R_f \approx .15$ on silica TLC eluting with 2% CH_3OH / CH_2Cl_2) was evaporated to **13** as an orange gum (280 mg, 50 mmol, 61%): ^1H NMR (δ, $CDCl_3$) 1.25(s, 3H, $C(C\underline{H}_3)_2$), 1.35(s, 3H, $C(C\underline{H}_3)_2$), 1.37(s, 9H, $C(C\underline{H}_3)_3$), 1.40 - 1.80(m, 6H, $C\underline{H}_2C\underline{H}_2C\underline{H}_2$), 2.71(br s, 2H, $ArC\underline{H}_2$), 3.26(br s, 2H, $NHC\underline{H}_2$), 3.43(m, 1H, $OC\underline{H}$), 3.80 - 4.20(m, 8H, 4 x $OC\underline{H}_2$), 4.86(br s, 1H, $N\underline{H}$), 6.45(m, 2H, $\underline{H}2$ and $\underline{H}6$), 7.15(br d, J = 8 Hz, 2H, $\underline{H}9$), 7.58 - 7.68(m, 3H, $\underline{H}5$ and $\underline{H}8$); ^{13}C NMR ($CDCl_3$) 22.2, 25.6, 26.8, 29.0, 33.1($\underline{C}H_2\underline{C}H_2\underline{C}H_2$ and $2xC(\underline{C}H_3)_2$), 28.3($C(\underline{C}H_3)_3$), 35.8($Ar\underline{C}H_2$), 41.5($NH\underline{C}H_2$), 60.7, 67.9, 69.2, 72.0($4xO\underline{C}H_2$), 75.7($O\underline{C}H$), 78.9($\underline{C}(CH_3)_3$), 101.9($O\underline{C}O$), 107.5($\underline{C}2$), 108.5($\underline{C}6$), 118.6($\underline{C}5$), 122.6($\underline{C}8$), 129.3($\underline{C}9$), 137.2($\underline{C}10$), 141.6($\underline{C}4$), 151.6($\underline{C}7$), 155.8($\underline{C}$=O), 157.7($\underline{C}1$), 162.8($\underline{C}3$); the complete ^{13}C NMR spectrum is shown as Figure **32**; high resolution +FAB MS (glycerol matrix) calculated for M+1, $C_{30}H_{44}N_3O_7$, m/e 558.3181, found m/e 558.3201 (intensity 76%).

[Co(trpn)Cl_2]Cl and attempted hydrolysis

Tris(3-aminopropyl)amine (trpn)[82] was prepared from tris(2-cyanoethyl)amine by refluxing in BH_3.THF solution (15X excess BH_3) for 5 hours then stirring at room temperature overnight. The mixture was cooled to 0°C and excess BH_3 was destroyed by careful dropwise addition of methanol. The mixture was evaporated to dryness and the residue refluxed in conc. HCl / water / CH_3OH (2:3:10) for 5 hours. The volume was reduced, the solution was made basic with NaOH solution (pH 13), and this solution continuously extracted overnight with $CHCl_3$ to give trpn (2.00 g, 10.6 mmol, 75%) as a light brown oil. The cobalt complex [Co(trpn)Cl_2]Cl was prepared by a literature procedure[86]. For the attempted hydrolysis, [Co(trpn)Cl_2]Cl (100 mg, 0.30 mmol) was dissolved in water (15 mL, pH of this solution was measured at 5.0) and the fully blocked azo compound **34** (173 mg, 0.30 mmol) added as a solution in n-propanol / water (1:1, 10 mL). This solution was stirred at 100°C. The pH was checked after 2 hours and had risen to 8, possibly as a result of breakdown of the amine complex (this behavior has been noted in the literature[87]). The solution was stirred at 100°C for 5 days. The solution was extracted with CH_2Cl_2 and almost all orange colour went to the organic layer. The ^{13}C NMR spectrum of the evaporated organic layer showed that the isopropylidene and THP groups had been removed but there had been little, if any, hydrolysis of the acetyl group.

Attempted phosphate catalysed hydrolysis

To Na_2HPO_4 solution (200 mM, 50 mL) was added NaH_2PO_4 solution (200 mM) until the pH was 7.8 (about 2 - 3 mL). To this solution was added a solution of fully blocked azo compound **34** (175 mg) as a solution in n-propanol / water (1:1, 10 mL). The resulting solution was stirred at 100°C for 5 days. The solution was extracted with CH_2Cl_2 and all orange colour went to the organic layer. The ^{13}C NMR spectrum of the evaporated organic layer showed it to be the fully blocked starting material **34**.

Typical high dilution capping reaction procedure

Tetraacid **1** and dianhydride **4** were prepared according to literature procedures[35a, 49] and found to be identical to previosly prepared samples. A solution of triethylamine (23 mL, 16.8 g, 166 mmol, 50X excess) in dry THF (900 mL) was stirred at maximum speed with a large magnetic stirring bar in a flask with indented walls, at room temperature under an atmosphere of dry N_2. To this was added simultaneously a solution of the appropriate alcohol / amine (1.66 mmol) in dry THF (60 mL) and a solution of dianhydride **4** in dry THF (60 mL). The latter two solutions were dispensed from identical syringes, with a variable speed stepper motor driving a dual syringe pump. The solutions were added at about 1 mL per hour so the total addition took 2 - 3 days. Once addition was complete the reaction was stirred for another day, then the reaction mixture was evaporated. The product was passed through a strong acid ($-SO_3^-H^+$) cation exchange resin, eluting with 90% CH_3OH / water. This product was hydrolysed by refluxing for 2 hours in $(CH_3)_4N^+OH^-$ in CH_3OH (2 M, 25 mL), and the ammonium salt was removed with another strong acid cation exchange column, eluting with water. Permethylation was accomplished by treating a THF solution of the product with a solution of diazomethane in THF until the yellow colour of the diazomethane persisted. A brief description of further purification techniques is included in the discussion. None gave material that was suitable for further use. The ^{13}C NMR spectrum of a typical product is shown as Figure 33.

2R,3R-N-(4-hydroxymethylbenzyl)-N-methyl-4-carboxamido-2,3-dimethoxypropanoic acid (42) and 2R,3R-O-(4-(N-methyl-aminomethyl)benzyl)-2,3-di-O-methyltartarate monoester (43)

2R,3R-di-*O*-Methyl tartaric acid was prepared according to literature procedures[113] and found to be identical to a previously prepared sample. 2R,3R-2,3-di-*O*-Methyl tartaric anhydride (**41**) was prepared by refluxing this diacid (500 mg, 2.8 mmol) in acetyl chloride (40 ml) overnight then evaporating to give **41** as a white solid: ^{1}H NMR (δ, $CDCl_3$) 3.65(s, 6H, $OC\underline{H}_3$), 4.42(s, 2H, $C\underline{H}$); ^{13}C NMR (δ, $CDCl_3$) 59.8($\underline{C}H_3O$), 80.8($\underline{C}H$), 166.1($\underline{C}$=O); the ^{13}C NMR spectrum is shown as Figure **59**; high resolution MS calculated for $C_6H_8O_5$ m/e 160.0371, found m/e 160.0375 (intensity 2%).

A solution of **41** (450 mg, 2.8 mmol) in dry THF (20 mL) was added to a mixture of alcohol / amine **8** (424 mg, 2.8 mmol) and Cs_2CO_3 (7.0 g, large excess) in dry THF (75 mL) and the resulting mixture was stirred at room temperature overnight. The THF was evaporated and the residue was dissolved in water which was then adjusted to pH $\leq$ 2 with 1 M HCl and the solution was evaporated to a solid. The solid was stirred in acetone overnight and then filtered to remove the salts. The filtrate was evaporated to a pale brown gum, which was dissolved in a small volume of water and run through a small column of strong acid ($-SO_3^-H^+$) cation exchange resin, eluting with water. The eluate was evaporated to a pale brown gum (710 mg, 81%). The ^{13}C NMR spectrum was not completely assigned but it was clear from the number of peaks that there were either two compounds or two conformers of a single compound. The ^{13}C NMR spectrum at 100°C was identical to that recorded at room temperature so the compounds were tentatively identified as **42** and **43**. Compound **42** free of its isomer was prepared from an O-protected derivative. Thus to a stirred solution of anhydride **41** (500 mg, 2.8 mmol) and Cs_2CO_3 (6.0 g, large excess) in dry THF (50 mL) was added a solution of the THP-blocked alcohol / amine **44** (650 mg, 2.78 mmol) and the resulting soluton was stirred for 1/2 hour at room temperature. The reaction mixture was evaporated to a solid which was dissolved in methanol / water which had been adjusted to pH ≤ 2 with HCl. This solution was stirred at room temperature for 1/2 hour to deblock the THP group then evaporated to a solid. This material was stirred with acetone overnight then filtered to remove the insoluble salts. The filtrate was evaporated to a light brown glass, which was then chromatographed on 15 g of silica gel, eluting initially with 5% CH_3OH / CH_2Cl_2 then with 10% and finally 20% CH_3OH / CH_2Cl_2. The later fractions gave **42** as a colourless glass (590 mg, 1.90 mmol, 68%): ^{13}C NMR 34.7($N\underline{C}H_3$), 51.8($N\underline{C}H_2Ar$), 58.4, 59.2($2xO\underline{C}H_3$), 64.2($\underline{C}H_2OH$), 81.7, 81.8($\underline{C}H$), 127.7, 128.4(aromatic $\underline{C}H$), 136.5, 141.9(aromatic $\underline{C}C$), 170.1, 171.5($2x\underline{C}=O$); The ^{13}C NMR spectrum of **42** is shown as Figure **35**; methane CI MS m/e 312(M+1), 340(M+29), 352(M+41).

4-(N-methyl-aminomethyl)-O-(2-tetrahydropyranyl)benzyl alcohol (44)

To the methyl ester of 4-bromobenzoic acid (9.4 g, 45 mmol) in dry THF at -35° in a high pressure glass bomb was added liquid methylamine (about 45 g, about 30x excess) at -35°. The bomb was stoppered and held in a metal cage while the solution was stirred at 50° for 36 hours. The bomb was cooled to -35° before opening. The solution was evaporated to give N-methyl-4-bromobenzamide as a light brown solid: ^{1}H NMR (δ, CD_3OD) 2.88(s, 3H, NC$\underline{H}_3$), 7.58(d, J = 8Hz, 2H, aromatic C$\underline{H}$), 7.64(d, J = 8 Hz, aromatic C$\underline{H}$); literature ^{1}H NMR[114] (δ, $CDCl_3$) 2.29(s, 3H), 7.55(d, J = 8.7 Hz, 2H), 7.65(d, J = 8.7 Hz, 2H).

To a stirred solution of N-methyl-4-bromobenzamide (10 g, 47 mmol) in THF (500 mL) at -70° under dry N_2 was added dropwise n-butyllithium (58.4 mL, 1.6 M in hexane, 94 mmol) resulting in a white precipitate. This mixture was stirred at -70° while bubbling CO_2 gas for 1/2 hour. The mixture was then warmed to room temperature, acidified with 1 M HCl to pH $<$ 2, then evaporated to a solid which was partitioned between water and ethyl acetate. The organic layer was dried over $MgSO_4$ and evaporated to a solid which was recrystallized from methanol / acetone to give 4-[(methylamino)carbonyl]benzoic acid (3.25g, 18 mmol): mp 257 - 259°; literature mp[115] 260 - 262°. This acid was esterified by refluxing in methanol (200 mL) saturated with HCl gas for 2 hours. This ester was used without purification or characterization.

A solution of the ester (5.37 g, 27.7 mmol) in dry THF (100 mL) was added dropwise to a suspension of $LiAlH_4$ (4.21 g, 110 mmol) in dry THF (400 mL) and the resulting mixture was refluxed under dry N_2 for 4 hours. The mixture was cooled to 0° then water added (carefully) until there was no more bubbling and the solid was white. The mixture was filtered and the filtrate evaporated to give 4-(N-methylaminomethyl)benzyl alcohol (**8**) as a colourless oil (3.30 g, 21.9 mmol): ^1H NMR (δ, CD_3OD) 2.33(s, 3H, $NC\underline{H}_3$), 3.65(s, 2H, $ArC\underline{H}_2N$), 4.58(s, 2H, $ArC\underline{H}_2O$), 4.88(br s, 2H, $N\underline{H}$ and $O\underline{H}$), 7.27 - 7.34 (m, 4H, aromatic $C\underline{H}$); ^{13}C NMR (δ, CD_3OD) 35.4($N\underline{C}H_3$), 56.0($Ar\underline{C}H_2N$), 64.8($Ar\underline{C}H_2O$), 128.0 and 129.4(aromatic $\underline{C}H$), 139.1 and 141.4(aromatic $\underline{C}CH_2$); the ^{13}C NMR spectrum is shown as Figure **60**; high resolution MS calculated for $C_9H_{13}NO$ m/e 151.09979, found m/e 151.10015 (intensity 49%). Compound **8** has been reported[116] but no preparation or characterization was provided.

To a solution of **8** as its HCl salt (520 mg, 2.78 mmol) in DMF (10 mL) was added dihydropyran (2 mL, 22 mmol) and conc HCl (1 drop) and the resulting solution stirred at room temperature overnight. The solution was evaporated to give a light brown solid. This material was dissolved in methanol (5 mL), added to a suspension of basic anion exchange resin ($-NR_3^+CH_3O^-$, 50 mL) in methanol (100 mL) and stirred overnight. The mixture was filtered and the filtrate evaporated to give **44** as a colourless oil (400 mg, 1.70 mmol): ^1H NMR (δ, $CDCl_3$) 1.4-1.9(m, 6H, $C\underline{H}_2C\underline{H}_2C\underline{H}_2$), 2.34(s, 3H, $NC\underline{H}_3$), 3.46(m, 1H, $OC\underline{H}_2$), 3.65(s, 2H, $ArC\underline{H}_2NH$), 3.83(m, 1H, $OC\underline{H}_2$), 4.40(d, J = 12 Hz, 1H, $ArC\underline{H}_2O$), 4.63(m, 1H, $OC\underline{H}O$), 4.68(d, J = 12 Hz, 1H, $ArC\underline{H}_2O$), 7.24(m, 4H, $Ar\underline{H}$); ^{13}C NMR ($CDCl_3$) 19.2, 25.3, 30.4($\underline{C}H_2\underline{C}H_2\underline{C}H_2$), 35.6($N\underline{C}H_3$), 55.5($Ar\underline{C}H_2NH$), 61.9($O\underline{C}H_2CH_2$), 68.4($O\underline{C}H_2Ar$), 97.5($O\underline{C}HO$), 127.8, 128.1(aromatic $\underline{C}H$), 139.0, 140.6(aromatic $\underline{C}C$); the ^{13}C NMR spectrum is shown as Figure **61**; high resolution +ve

FAB MS (*meta*-nitrobenzyl alcohol matrix) calculated for M+1, $C_{14}H_{22}NO_2$, m/e 236.1652, found m/e 236.1683 (100%); compound **44** has been reported[116] but no preparation or characterization was provided.

Reaction of dianhydride 4 with amine 44

To a stirred solution of the dianhydride **4** (605 mg, 1.5 mmol) in dry THF (100 mL) was added dropwise a solution of THP-protected alcohol / amine **44** (300 mg, 1.28 mmol) and triethylamine (1.0 g, 10 mmol) in dry THF (50 mL), then the resulting solution was stirred overnight. The reaction mixture was evaporated and the residue was partitioned between dilute aqueous acid and $CHCl_3$. The NMR spectra of the organic extract had far too many peaks and from the relative sizes of the aromatic and crown ether peaks it was clear that if there were any amide it was the diamide. The aqueous extract was continuously extracted with $CHCl_3$ overnight. The continuous organic extract was analysed by HPLC using a gel permeation column (Alltech 500 Å - 5 µm column, 25 cm x 1 cm ID, elution with CH_3OH at ~30 atm, uv detection at 254 nm) and two large peaks were seen along with many smaller ones. Samples of the two major fractions were isolated by pooling the products from repeated injections onto this column. One fraction contained very little material and was composed of several compounds according to the ^{13}C NMR spectrum. The other fraction was identified as a single diamide (**45** or **46**): ^1H NMR (acetone-d_6) showed the relative integrated areas for the crown ether $OC\underline{H}_2$ peaks (16 H) and the aromatic $\underline{H}$ peaks (4H per ring) to be 2:1, so there must be two aromatic rings per crown ether; ^{13}C NMR (acetone-d_6) 33.4, 35.0($N\underline{C}H_3$), 51.1, 53.0($N\underline{C}H_2Ar$), 64.3($\underline{C}H_2OH$), 70.5 - 71.4(recorded as 7 peaks, $O\underline{C}H_2$), 78.9, 79.1, 81.6, 81.7($\underline{C}H$), 127.5, 127.6, 127.8, 128.5(aromatic $\underline{C}H$), 136.5, 136.8, 142.3, 142.6(aromatic $\underline{C}C$) 169.5, 170.6($\underline{C}$=O).

Reaction of dianhydride 4 with benzylamine

To a stirred solution of the dianhydride **4** (500 mg, 1.23 mmol) in dry THF (50 mL) was added dropwise a solution of benzylamine (132 mg, 1.23 mmol) and triethylamine (1 mL, 7 mmol) in dry THF (25 mL), and the resulting solution was stirred overnight. Water (25 mL) was then added and this solution was stirred for 1/2 hour. The reaction mixture was evaporated then partitioned between dilute aqueous acid and $CHCl_3$. The organic layer was dried and evaporated to give the *anti* diamide **47** (400 mg, 0.65 mmol, 100%) as a colourless glass: ^{1}H NMR (δ, $CDCl_3$) 3.2 - 3.8(m, 16H, $OC\underline{H}_2$), 4.19(s, 2H, $C\underline{H}$), 4.35(s, 2H, $C\underline{H}$), 4.37(m, 2H, $NHC\underline{H}_2$), 4.48(m, 2H, $NHC\underline{H}_2$), 7.10 - 7.40(m, 10H, aromatic $\underline{H}$); ^{13}C NMR ($CDCl_3$) 43.1($NH\underline{C}H_2Ar$), 69.2, 70.2, 70.3, 70.8(4x$O\underline{C}H_2$), 79.9, 80.1($\underline{C}H$), 127.3, 127.8, 128.5(aromatic $\underline{C}H$), 138.8(aromatic $\underline{C}C$), 170.3, 171.3(2x$\underline{C}$=O); the ^{13}C NMR spectrum is shown as Figure **62**; high resolution -ve FAB MS (*meta*-nitrobenzyl alcohol matrix) calculated for M-1, $C_{30}H_{37}N_2O_{12}$, m/e 617.2347, found m/e 617.2336 (intensity 100%). The aqueous extract was reduced to a small volume and passed through a strong acid ($-SO_3^-H^+$) cation exchange resin eluting with water. The eluate was evaporated to a colourless glass which was identified as epimerized tetraacid **48** (290 mg, .66 mmol, 100%): ^{1}H NMR (δ, CD_3OD) 3.1 - 3.9(m, 16H, $OC\underline{H}_2$), 4.2 - 4.6(m, 4H, $C\underline{H}$); the expanded methine region of the ^{1}H NMR spectrum of **48** is shown as Figure **36**; ^{13}C NMR 71 - 76 (several peaks, O$\underline{C}$H$_2$), 80.8 - 81.8(several peaks, $\underline{C}$H), 171 - 173(several peaks, $\underline{C}$=O); negative FAB MS (*meta* nitrobenzyl alcohol matrix) was recorded using a recovered NMR sample which had been standing in CD_3OD / CH_3OH solution for some time and was extensively esterified. There was a (M-1$^-$) peak for the tetraacid at m/e 439, but peaks corresponding to its diester, and in particular its triester, were larger. Since the ester peaks came in clusters corresponding to mixed OCH_3 and OCD_3 esters it was clear that the sample had originally been tetraacid and had esterified on standing in the mixed alcohol solvent.

Reaction of dianhydride 4 with di-n-butylamine

Reaction and workup were carried out by the procedures described above for benzylamine on the same scale, using 160 mg (1.23 mmol) di-n-butylamine. Comparing the integration of the methine region (δ 4.1 - 4.9) to the alkyl region (multiplets at δ 0.9, 1.3, and 1.5) of the ^{1}H NMR spectrum indicated a mix of mono- and diamides, predominantly the latter. The methine region appeared overly complex for a mixture of mono- and diamides, and the ^{13}C NMR spectrum also had multiple peaks in both the methine and carbonyl regions. The aqueous extract contained a small amount of amide but predominantly epimerized tetraacid **48**. NMR and mass spectra were comparable to the aqueous extract described above for the benzylamine reaction.

Reaction of dianhydride 4 with water then benzylamine - preparation of 2R,3R,11R,12R-2-N-benzylcarboxamido-1,4,7,10,13,16-hexaoxacyclooctadecane-3,11,12-tricarboxylic acid (53)

To a stirred solution of dianhydride **4** (200 mg, 0.5 mmol) in dry THF (1 mL) was added water (9 μL, 9 mg, 0.5 mmol) and the resulting solution was stirred at room temperature for two days. To this was added a solution of benzylamine (59 mg, 0.55 mmol) and triethylamine (220 mg, 2.2 mmol) in a few mL of dry THF. A precipitate formed initially but soon dissolved. The solution was stirred for 2 hours then evaporated to a white foam. This was dissolved in a small volume of water and passed through a small column of strong acid ($-SO_3^-H^+$) cation exchange resin, eluting with water. The product from this column was partitioned between water and $CHCl_3$. The organic extract contained a ~ 2:1 mixture of *anti* diamide **47** and *syn* diamide **52** (30 mg, .05 mmol, 10%): ^{1}H NMR (δ, $CDCl_3$) 3.2 - 3.8(m, 16H, OC$\underline{\mathrm{H}}_2$), 4.2 - 4.6(m, 8H, C$\underline{\mathrm{H}}$, ArC$\underline{\mathrm{H}}_2$NH), 7.1 - 7.3(m, 10H, aromatic); ^{13}C NMR ($CDCl_3$) [assignment of peaks as *anti* or *syn* is by comparison to spectrum of the *anti* isomer, whose preparation is described above] 42.9(Ar$\underline{\mathrm{C}}$H$_2$,*syn*), 43.2(Ar$\underline{\mathrm{C}}$H$_2$, *anti*), 68.6 - 71.0(7 peaks reported, O$\underline{\mathrm{C}}$H$_2$), 79.8($\underline{\mathrm{C}}$H, *syn*), 79.9($\underline{\mathrm{C}}$H, *anti*), 80.5($\underline{\mathrm{C}}$H, *anti*), 81.7($\underline{\mathrm{C}}$H, *syn*), 127.3, 127.8, 128.0, 128.3, 128.4, 128.5(6xaromatic $\underline{\mathrm{C}}$H), 138.3(aromatic $\underline{\mathrm{C}}$C, *anti*), 138.8(aromatic $\underline{\mathrm{C}}$C, *syn*), 169.8($\underline{\mathrm{C}}$=O, *syn*), 170.2($\underline{\mathrm{C}}$=O, *anti*), 171.6($\underline{\mathrm{C}}$=O, *anti*), 171.9($\underline{\mathrm{C}}$=O, *syn*). The aqueous extract was continuously extracted with $CHCl_3$ overnight. The continuous organic extract was dried and evaporated to give monoamide **53** as a white foam (150 mg, 0.28 mmol, 56%): ^{1}H NMR (δ, acetone-d$_6$) 3.40 - 3.85(m, 16H, OC$\underline{\mathrm{H}}_2$), 4.35(d, J = 3 Hz, 1H, C$\underline{\mathrm{H}}$), 4.38(d, J

= 3 Hz, 1H, C$\underline{H}$), 4.47(d, J = 3 Hz, 1H, C$\underline{H}$), 4.49(d, J = 3 Hz, 1H, C$\underline{H}$), 4.50(m, 1H, NHC$\underline{H}_2$), 4.64(m, 1H, NHC$\underline{H}_2$), 7.20 - 7.50(m, 5H, aromatic); the complete ^{1}H NMR spectrum of **53** is shown as Figure **39** and the expanded methine region as Figure **40**; ^{13}C NMR (acetone-d_6) 43.3(Ar$\underline{C}$H$_2$NH), 69.9 - 71.6(7 peaks reported, O$\underline{C}$H$_2$), 80.8, 80.9, 81.0, 81.4(4x$\underline{C}$H), 127.5, 128.8, 128.9(aromatic $\underline{C}$2, $\underline{C}$3, $\underline{C}$4), 140.5(aromatic $\underline{C}$1), 170.8, 171.2, 171.3, 171.6(4x$\underline{C}$=O); the complete ^{13}C NMR spectrum of **53** is shown as Figure **37**, and the expanded methine and carbonyl regions as Figure **38**; high reslution -ve FAB MS (*meta*-nitrobenzyl alcohol matrix) calculated for M-1, $C_{23}H_{30}NO_{13}$, m/e 528.1717, found m/e 528.1680 (intensity 1%). The remaining aqueous extract contained a little amide with predominantly tetraacid **1**: ^{1}H NMR (δ, acetone-d_6) 3.35 - 3.90(m, 16H, OC$\underline{H}_2$), 4.40(s, 4H, C$\underline{H}$); ^{13}C NMR (acetone-d_6) 70.2, 70.7(O$\underline{C}$H$_2$), 80.6($\underline{C}$H), 171.5($\underline{C}$=O); negative FAB MS (*meta* nitrobenzyl alcohol matrix) m/e 439 (M-1 for tetraacid **1**, 100%).

Reaction of dianhydride 4 with water then di-n-butylamine

The procedure is the same as described directly above for the reaction of **4** with water then benzylamine, using dianhydride **4** (250 mg, 0.62 mmol), water (11 μL, 11 mg, 0.62 mmol), di-n-butylamine (80 mg, 0.62 mmol), and triethylamine (250 mg, 2.48 mmol). The single organic extract contained 167 mg of a ~1:1 mixture of mono- and diamides according to the integration of the ^{1}H NMR spectrum, comparing the methine region (δ 4.3 - 4.9) with the alkyl region (multiplets at δ 0.90 and 1.2 - 1.8). The methine region was composed of 8 doublets as well as a number of smaller peaks; the most reasonable assignment is 4 doublets from the monoamide and 4 from one diamide.

Similarly the methine and carbonyl regions of the ^{13}C NMR spectrum each had 8 major peaks which can be explained in the same way. The continuous organic extract contained only 19 mg of monoamide **51**: ^{1}H NMR (δ, acetone-d_6) 0.90 (m, 6H, $C\underline{H}_3$), 1.25 - 1.90(m, 8H, $C\underline{H}_2C\underline{H}_2$), 3.33(m, 4H, $NC\underline{H}_2$), 3.50 - 3.95(m, 16H, $OC\underline{H}_2$), 4.28(br d, J = 3 Hz, 1H, $C\underline{H}$), 4.33(br d, J = 3 Hz, 1H, $C\underline{H}$), 4.52(d, J = 3 Hz, 1H, $C\underline{H}$), 4.54(d, J = 3 Hz, 1H, $C\underline{H}$); ^{13}C NMR 14.1($\underline{C}H_3$), 20.7, 32.3($\underline{C}H_2\underline{C}H_2$), 39.6($N\underline{C}H_2$), 70.2 - 71.9(6 peaks reported, $O\underline{C}H_2$), 80.9, 81.0, 81.1, 81.2(4x$\underline{C}$H), 170.4, 171.1, 171.2, 171.5(4x$\underline{C}$=O); negative FAB MS (*meta*-nitrobenzyl alcohol matrix) calculated for M-1, $C_{24}H_{40}NO_{13}$ m/e 550.2500, found m/e 550.2516 (intensity 22%). The aqueous extract contained 101 mg (0.23 mmol) of tetraacid **1**: ^{1}H NMR (δ, acetone-d_6) 3.62(m, 12H, $O\underline{C}H_2$), 3.81(m, 4H, $O\underline{C}H_2$), 4.43(s, 4H, $C\underline{H}$); ^{13}C NMR (acetone-d_6) 70.4, 71.0($O\underline{C}H_2$), 80.7($\underline{C}$H), 171.3($\underline{C}$=O); negative FAB MS m/e 439 (M-1 for **1**, 100%).

Reaction of dianhydride 4 with water then amine 44

Procedure was the same as described above, using dianhydride **4** (360 mg, 0.89 mmol), water (16 μL, 16 mg, 0.90 mmol), amine **44** (250 mg, 1.06 mmol), and triethylamine (450 μL, 327 mg, 3.2 mmol). The single organic extract gave material whose ^{1}H NMR spectrum integrated roughly as the monoamide **10** but the methine region of the spectrum was far too complex. Similarly the ^{13}C NMR spectrum had far too many peaks, most noticeably in the carbonyl and methine regions. The continuous organic extract similarly gave overly complex spectra and no unambiguous assignments were made. The aqueous extract contained epimerized tetraacid **48**. Its ^{13}C NMR spectrum showed only one peak in the methine region but there were at least three carbonyl peaks and the ^{1}H NMR spectrum of the same solution had a complex methine region; the expanded methine region of the ^{1}H NMR spectrum is shown as Figure **41**. The negative FAB MS (*meta* nitrobenzyl alcohol matrix) was recorded using a recovered NMR sample which had been sitting in CD_3OD for some time so that although there was a peak at m/e 439 (M-1 for **1**) the largest peaks were for the dimethyl-d_3 ester (m/e 473) and the trimethyl-d_3 ester (m/e 490).

Reaction of dianhydride 4 with water then excess benzylamine

To a stirred solution of dianhydride **4** (200 mg, 0.50 mmol) in dry THF (1.5 mL) was added water (9 µl, 9 mg, 0.50 mmol) and the resulting solution stirred for 2 days. A solution of benzylamine (270 µl, 268 mg, 2.50 mmol) in dry THF / dry DMF (1:1, 2 mL). A gummy white precipitate formed immediately. Some precipitate had been observed in previous reactions at this point but it always dissolved within a couple of minutes. In this case it did not dissolve on stirring even when more DMF was added. Workup was as described above. The single organic extraction product gave NMR spectra that were far too complex for diamide products. The ^{1}H NMR spectrum of the continuous organic extract product looked like a reasonable spectrum for the monoamide **53**, but the ^{13}C NMR spectrum of the same solution had extra peaks in the methine, aromatic and carbonyl regions. The aqueous extract contained the epimerized tetraacid **48**, identified by the ^{1}H NMR, ^{13}C NMR, and negative FAB mass spectra as described above.

Reaction of dianhydride 4 with primary amines 54 and 55

Primary amines **54** and **55** were reacted by the same procedure described above. The THP-blocked primary amine as a solution in dry THF with a slight excess of triethylamine was added to an equimolar amount of dianhydride **4** in dry THF. In both cases after few minutes a clear gum began to precipitate. In both cases there was no extraction fraction either from the precipitate or from the supernatant that could be determined to have a significant amount of the desired products.

Activation of tetraacid 1 with DCC and reaction with benzylamine

Water free tetraacid **1** was prepared by stirring dianhydride **4** in dry THF solution with 2 equivalents of water for 2 days. To a solution of this tetraacid (150 mg, 0.34 mmol) in 3 mL dry DMA was added a solution of DCC (70 mg, 0.34 mmol) in 1 mL dry DMA, then after a few minutes was added a solution of benzylamine (37 µl, 36 mg, 0.34 mmol) and triethylamine (156 µl, 113 mg, 1.12 mmol) in 1 mL dry DMA. The resulting solution was stirred overnight. Workup was as described above for all the reactions of dianhydride **4**. The single organic extract did not contain any recognizable product. The product from the continuous organic extract looked from its ^{13}C NMR spectrum to be a good sample of the desired monoamide **53**, but the ^{1}H NMR spectrum of the same sample showed many extra peaks. The aqueous extract was a clean sample of stereochemically intact tetraacid **1**.

APPENDIX

^{13}C NMR SPECTRA OF NEW COMPOUNDS

^{13}C NMR spectrum of compound **38** is Figure **31**

^{13}C NMR spectrum of compound **13** is Figure **32**

^{13}C NMR spectrum of compound **42** is Figure **35**

^{13}C NMR spectrum of compound **53** is Figure **37**

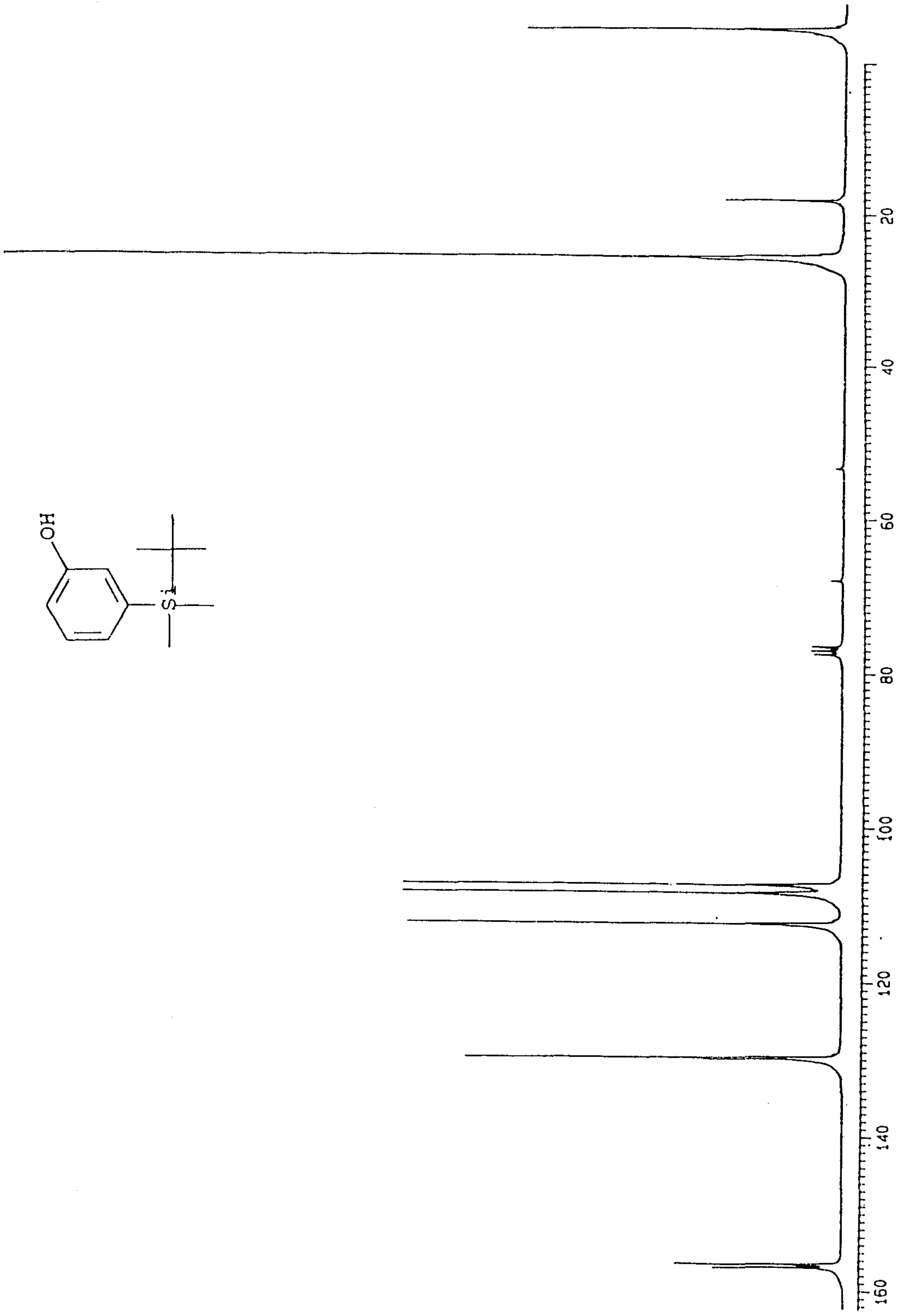

Figure 44. ^{13}C NMR spectrum of mono-*O*-*tert*-butyldimethylsilyl resorcinol in CDCl$_3$.

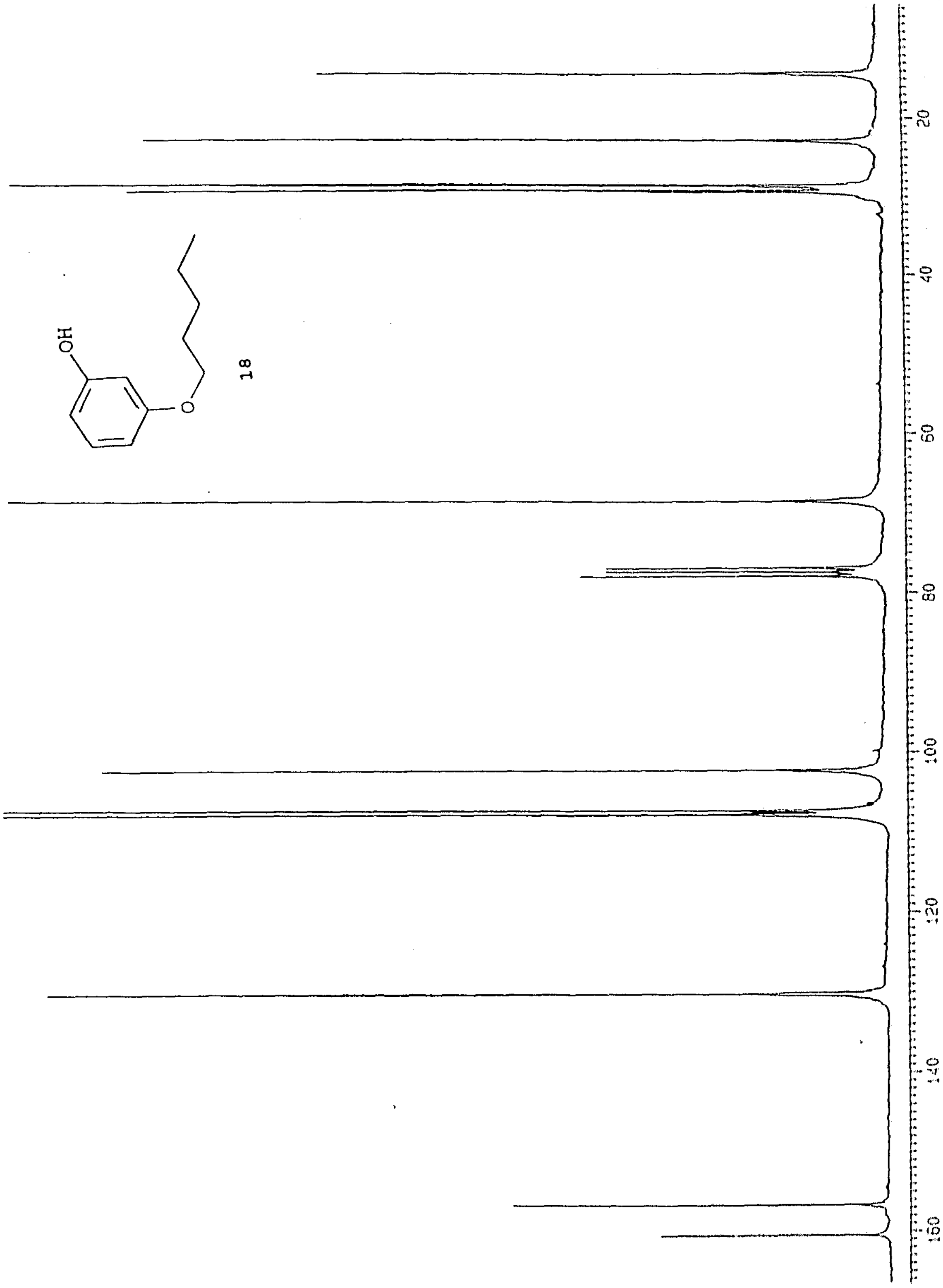

Figure 45. ^{13}C NMR spectrum of compound **18** in $CDCl_3$.

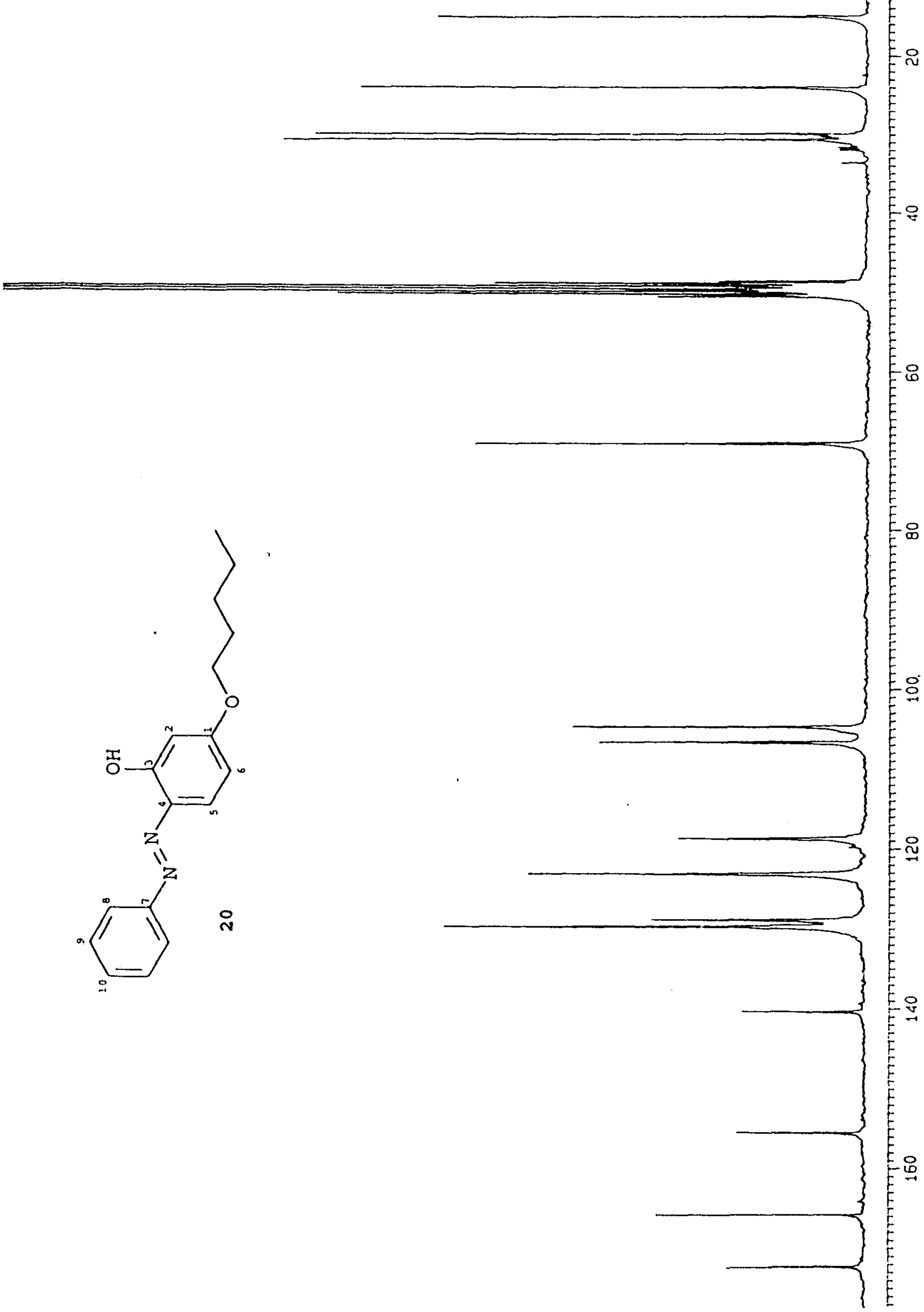

Figure 46. ^{13}C NMR spectrum of compound **20** in CD_3OD / CD_3O^-.

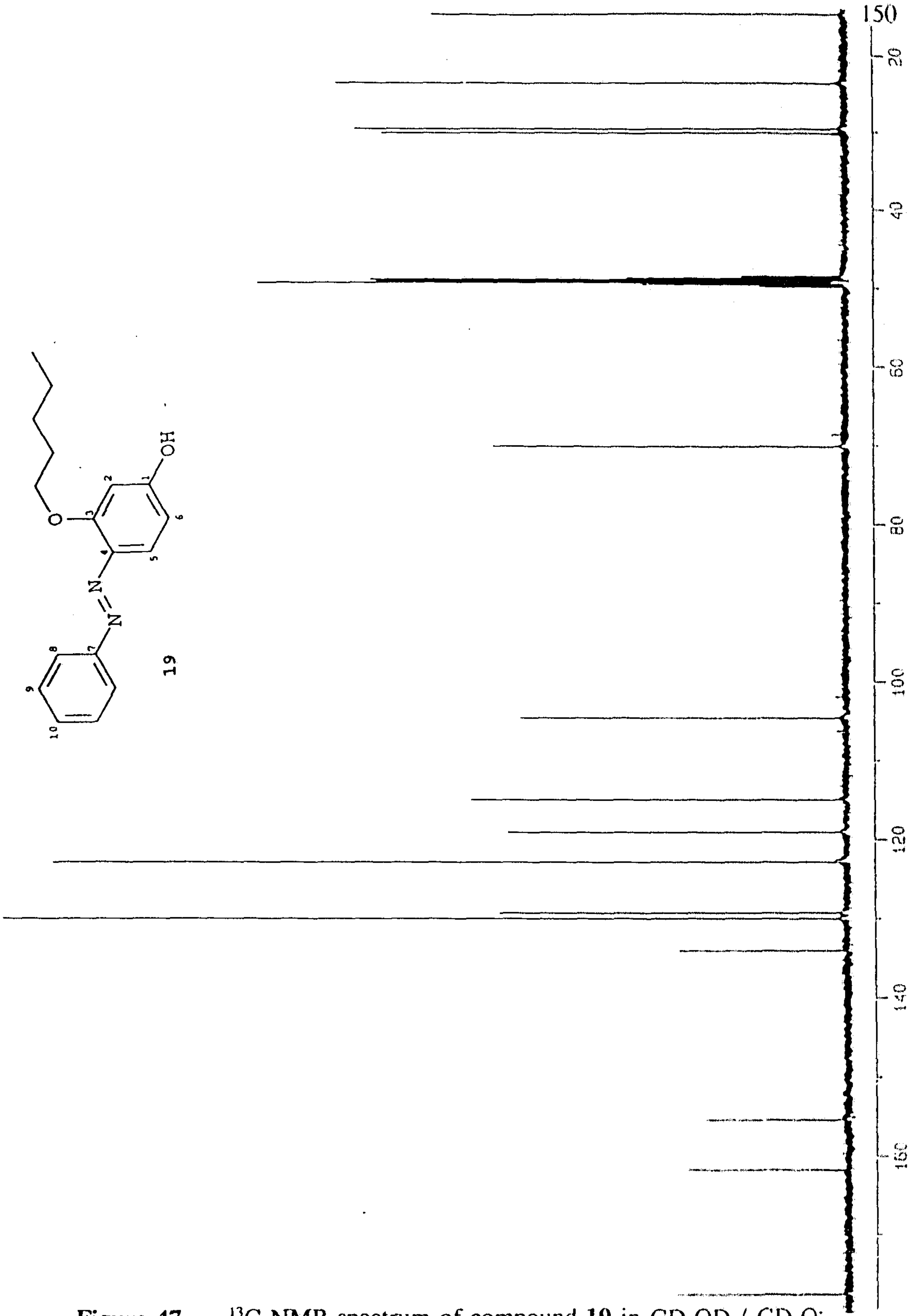

19

Figure 47. ^{13}C NMR spectrum of compound **19** in CD_3OD / CD_3O^-.

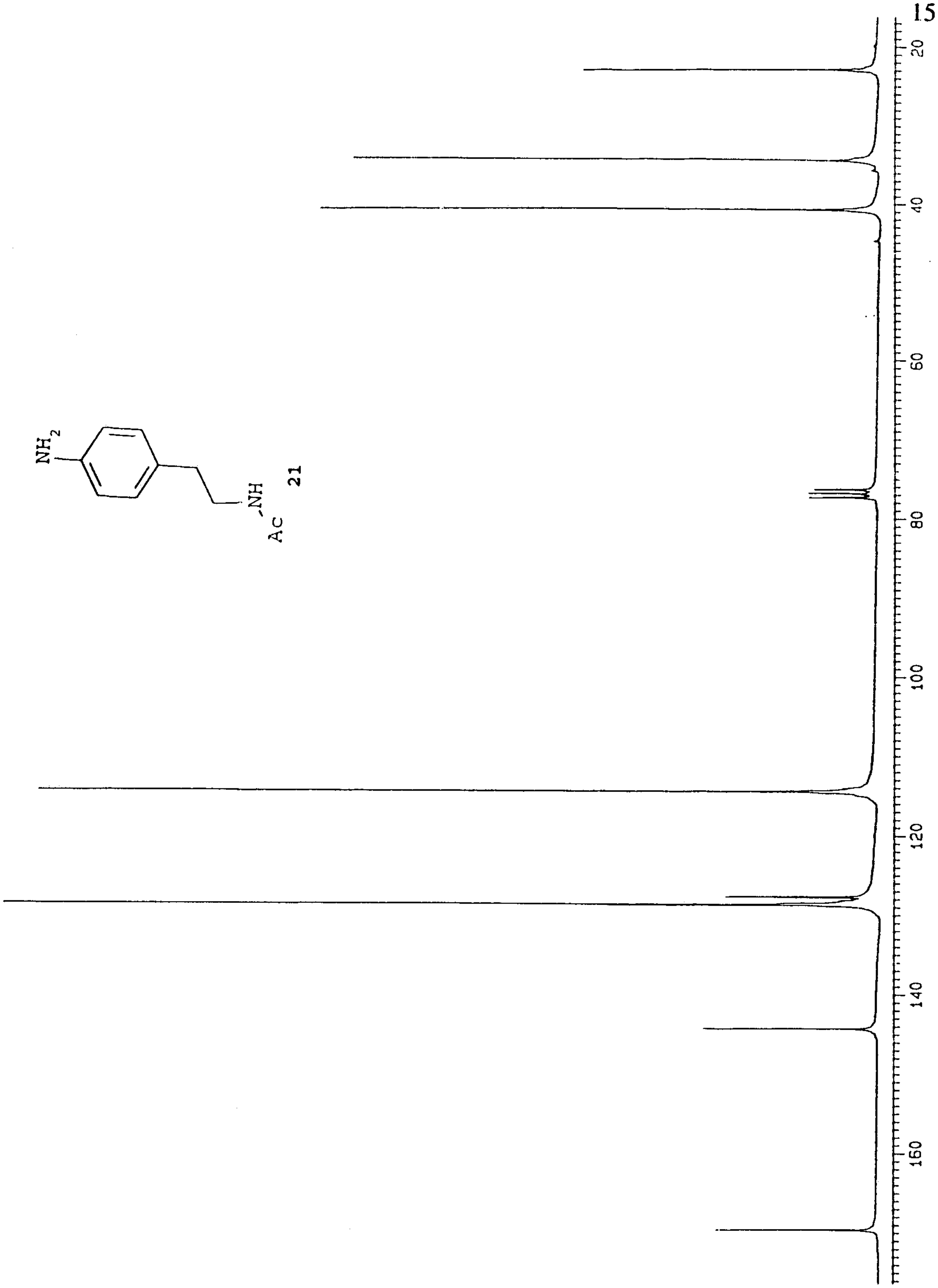

21

Figure 48. ^{13}C NMR spectrum of compound **21** in $CDCl_3$.

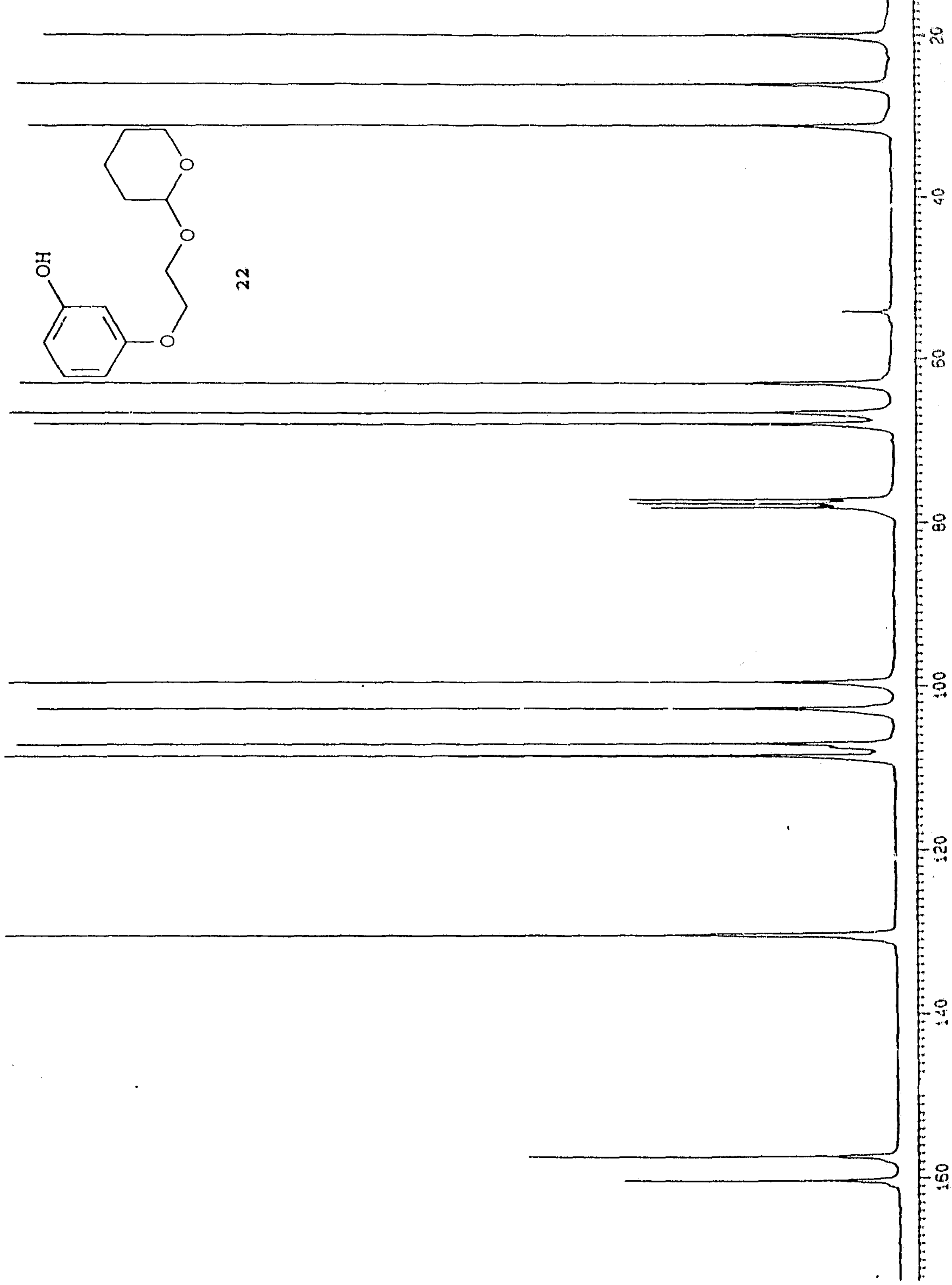

Figure 49. ^{13}C NMR spectrum of compound **22** in $CDCl_3$.

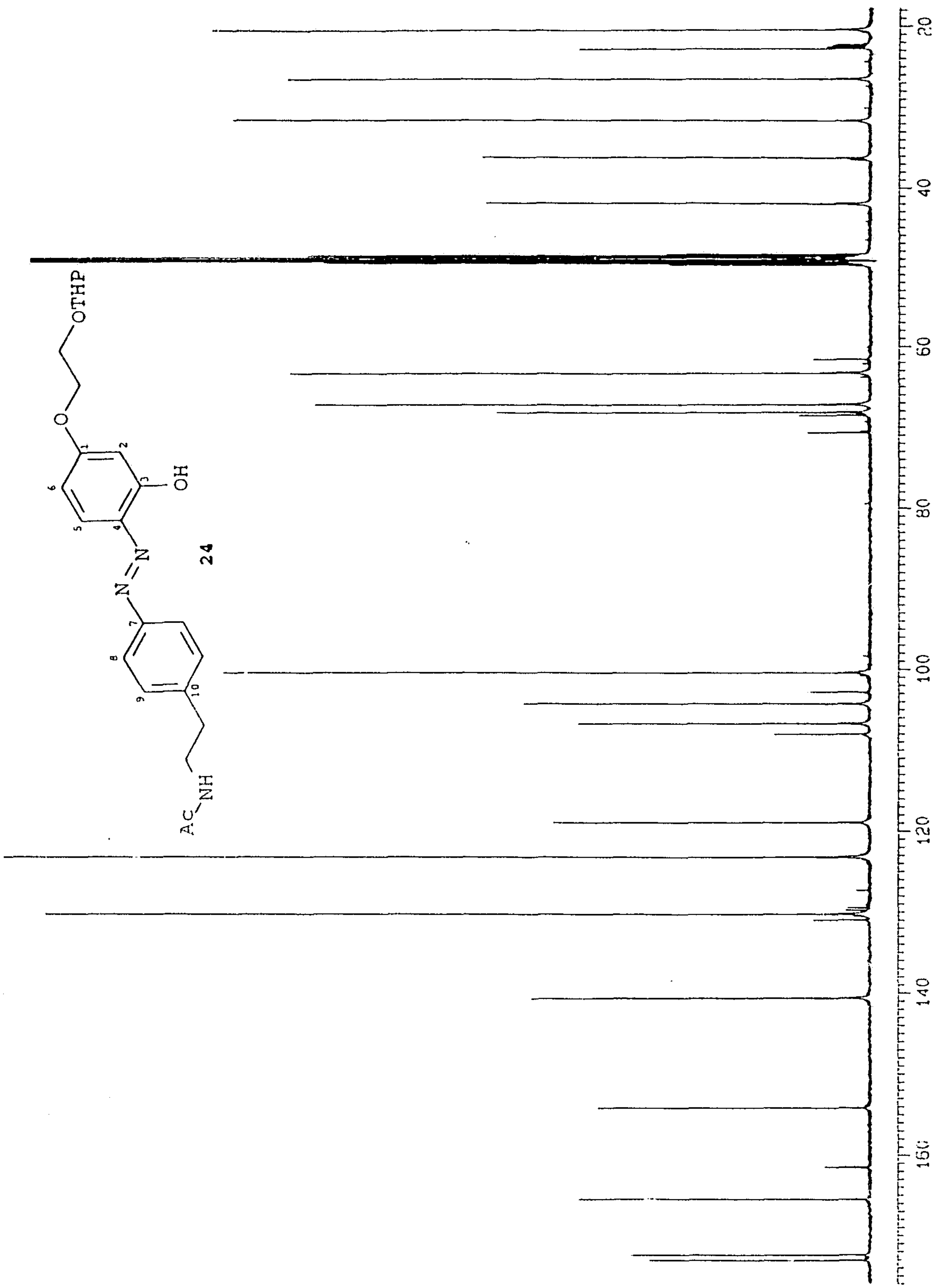

24

Figure 50. ^{13}C NMR spectrum of compound **24** in CD_3OD / CD_3O^-.

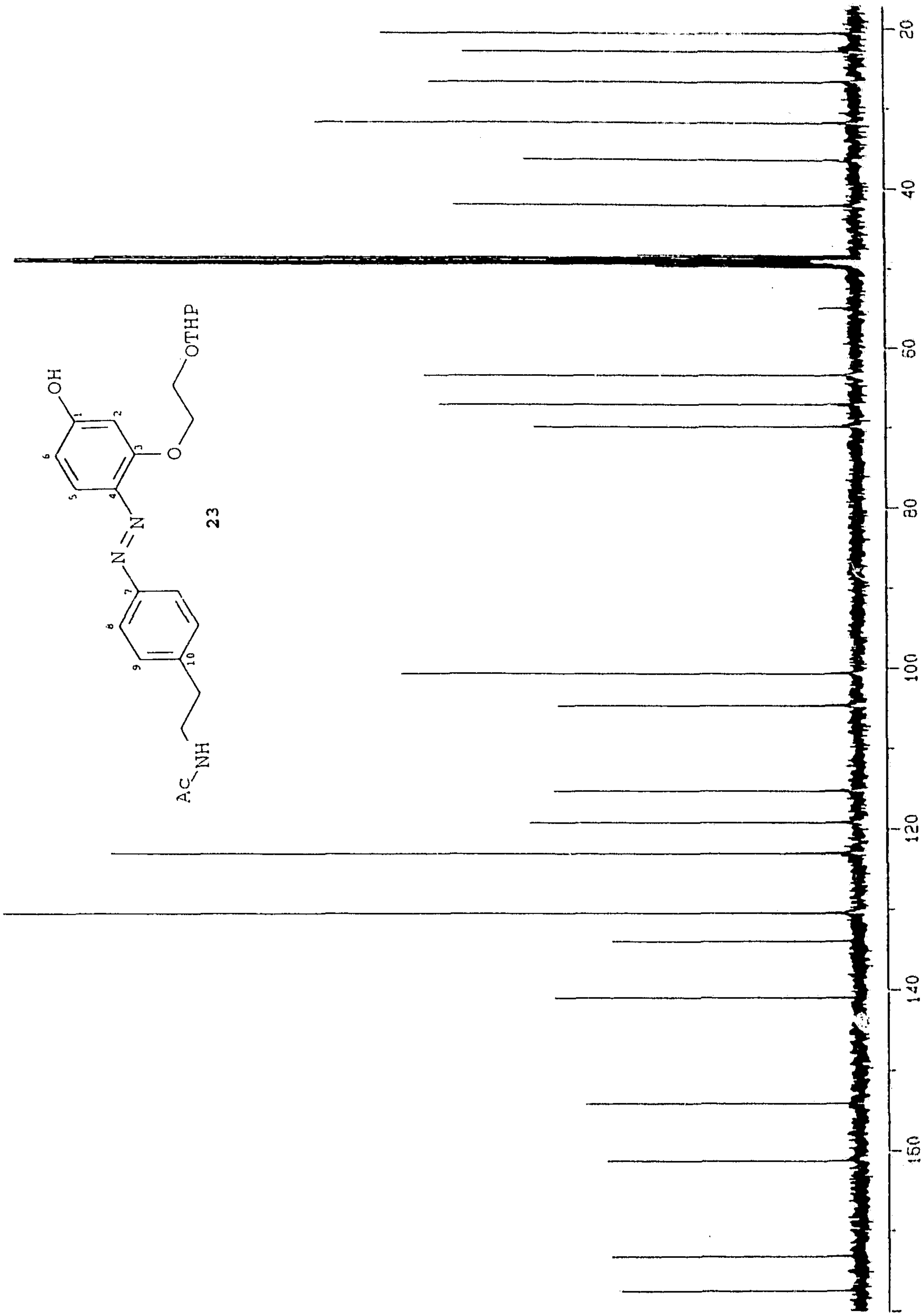

23

Figure 51. ^{13}C NMR spectrum of compound **23** in CD_3OD / CD_3O^-.

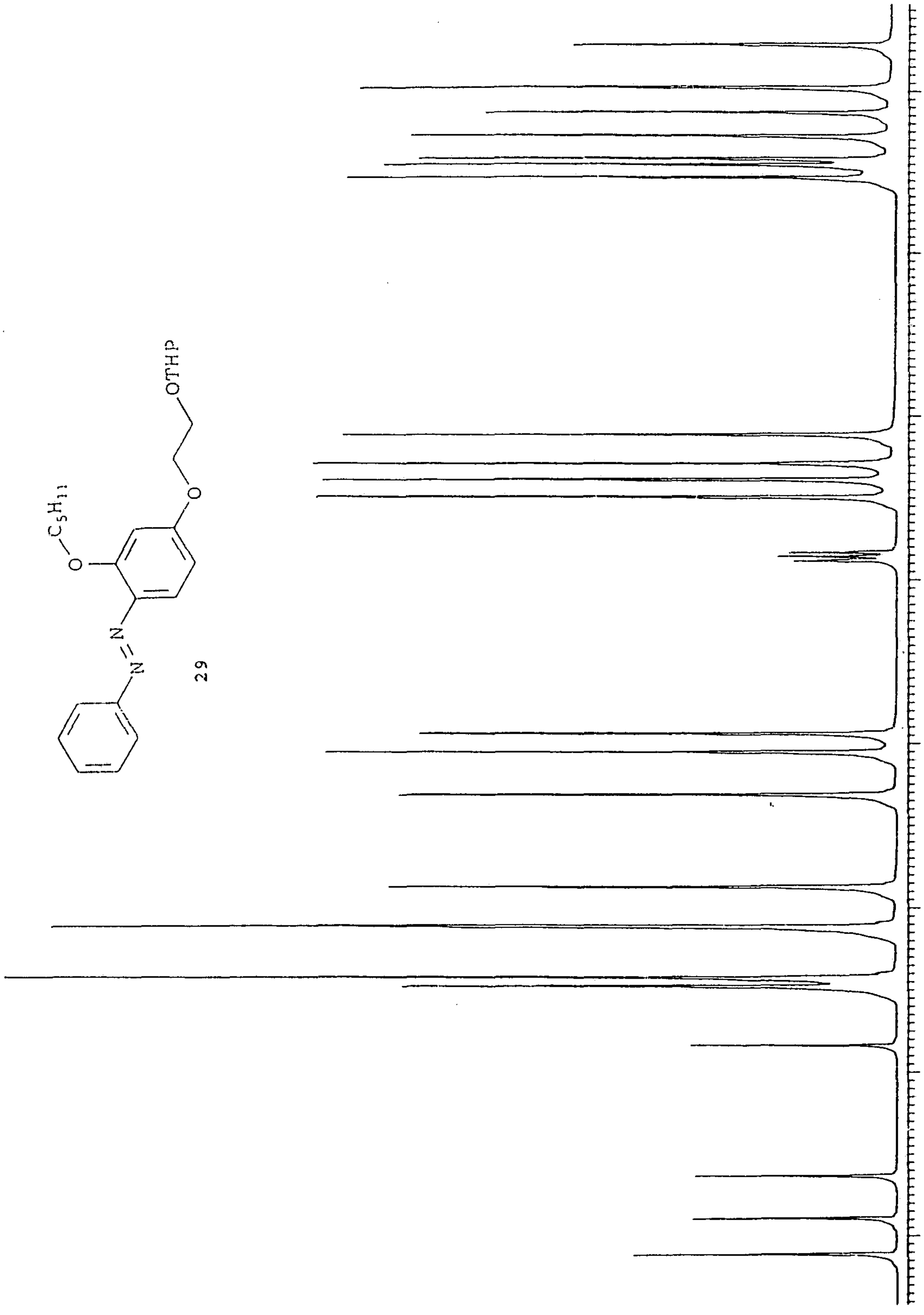

Figure 52. ^{13}C NMR spectrum of compound **29** in $CDCl_3$.

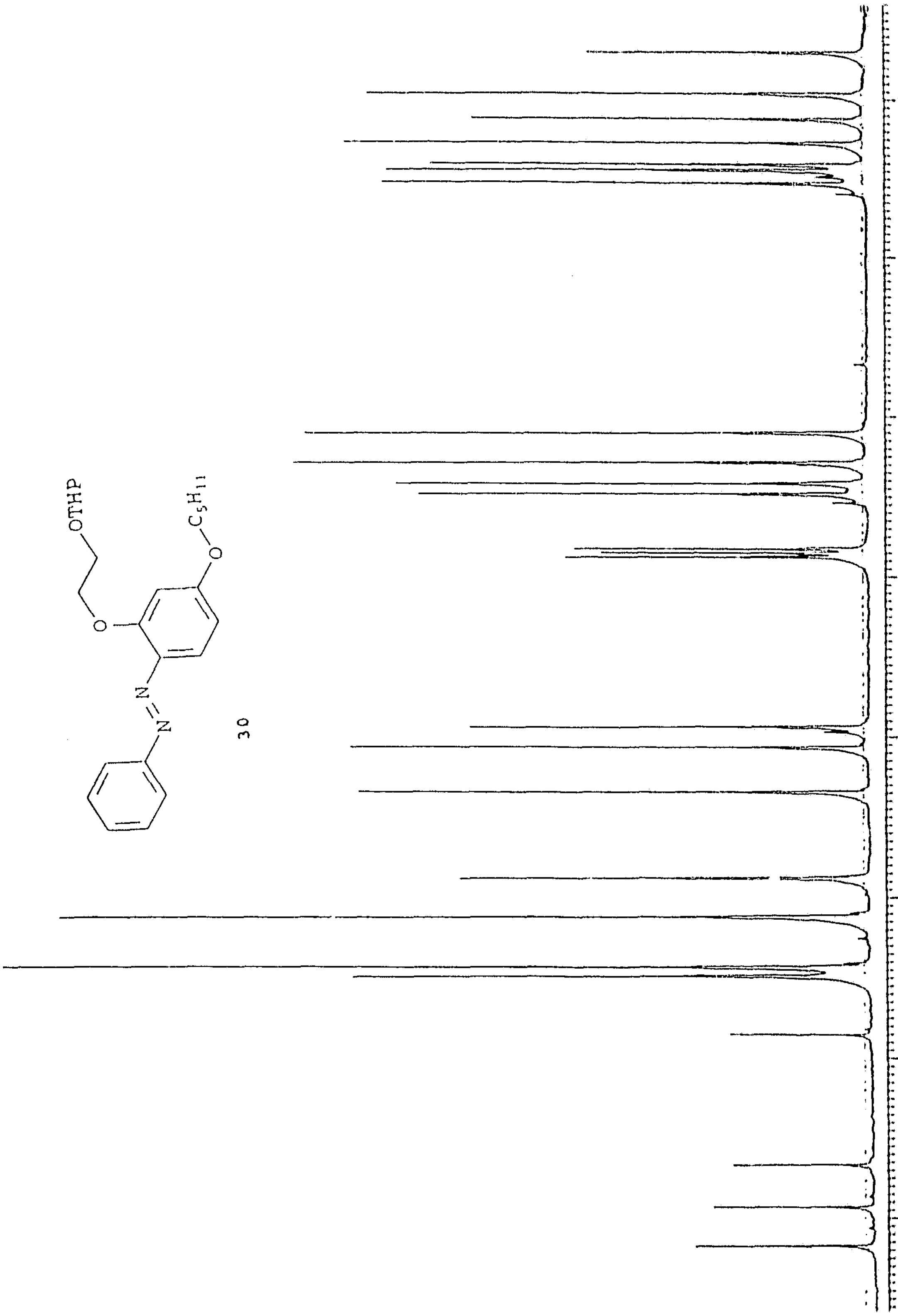

Figure 53. ^{13}C NMR spectrum of compound **30** in $CDCl_3$.

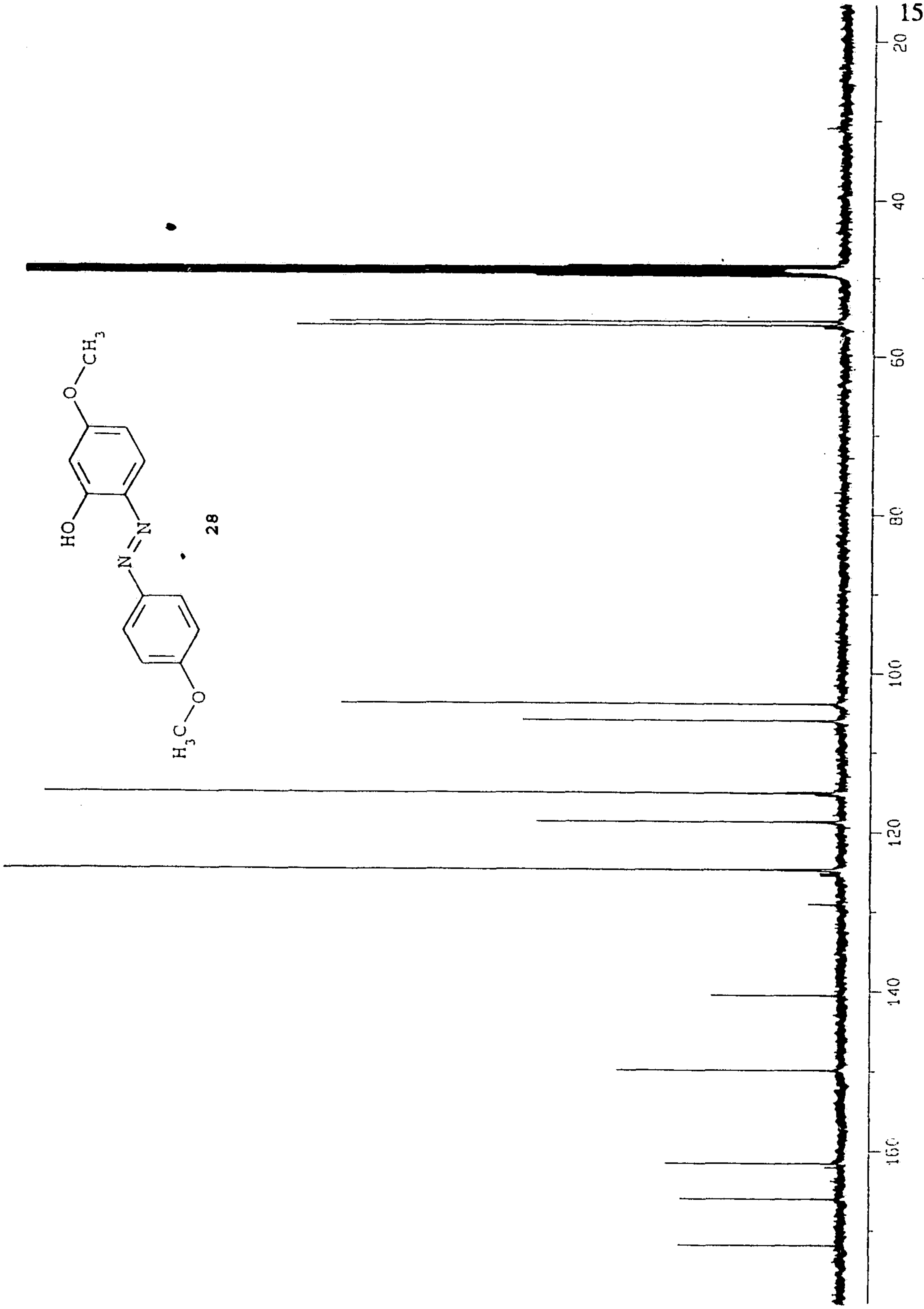

28

Figure 54. ^{13}C NMR spectrum of compound **28** in CD_3OD / CD_3O^-.

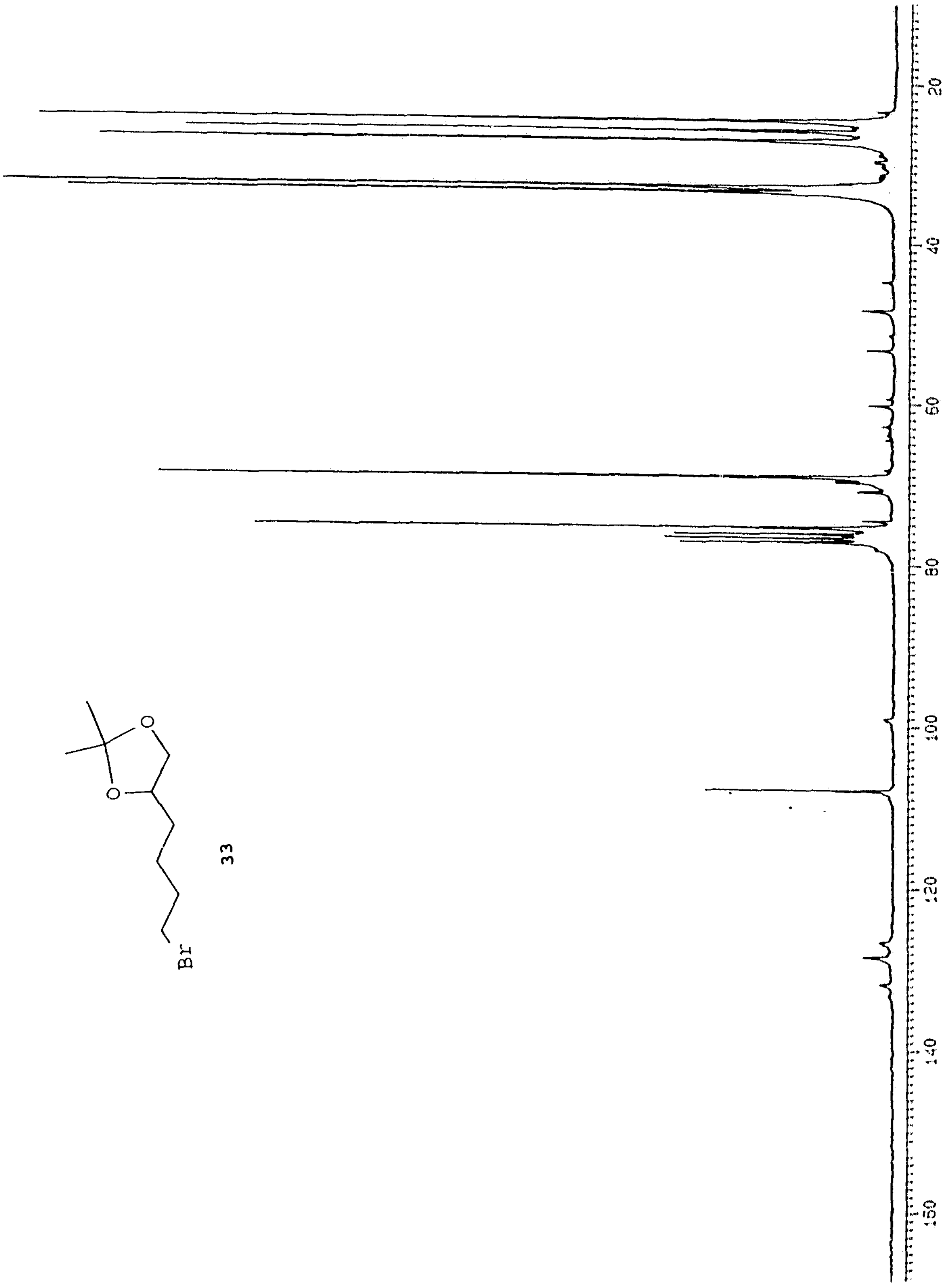

Figure 55. ^{13}C NMR spectrum of compound **33** in $CDCl_3$.

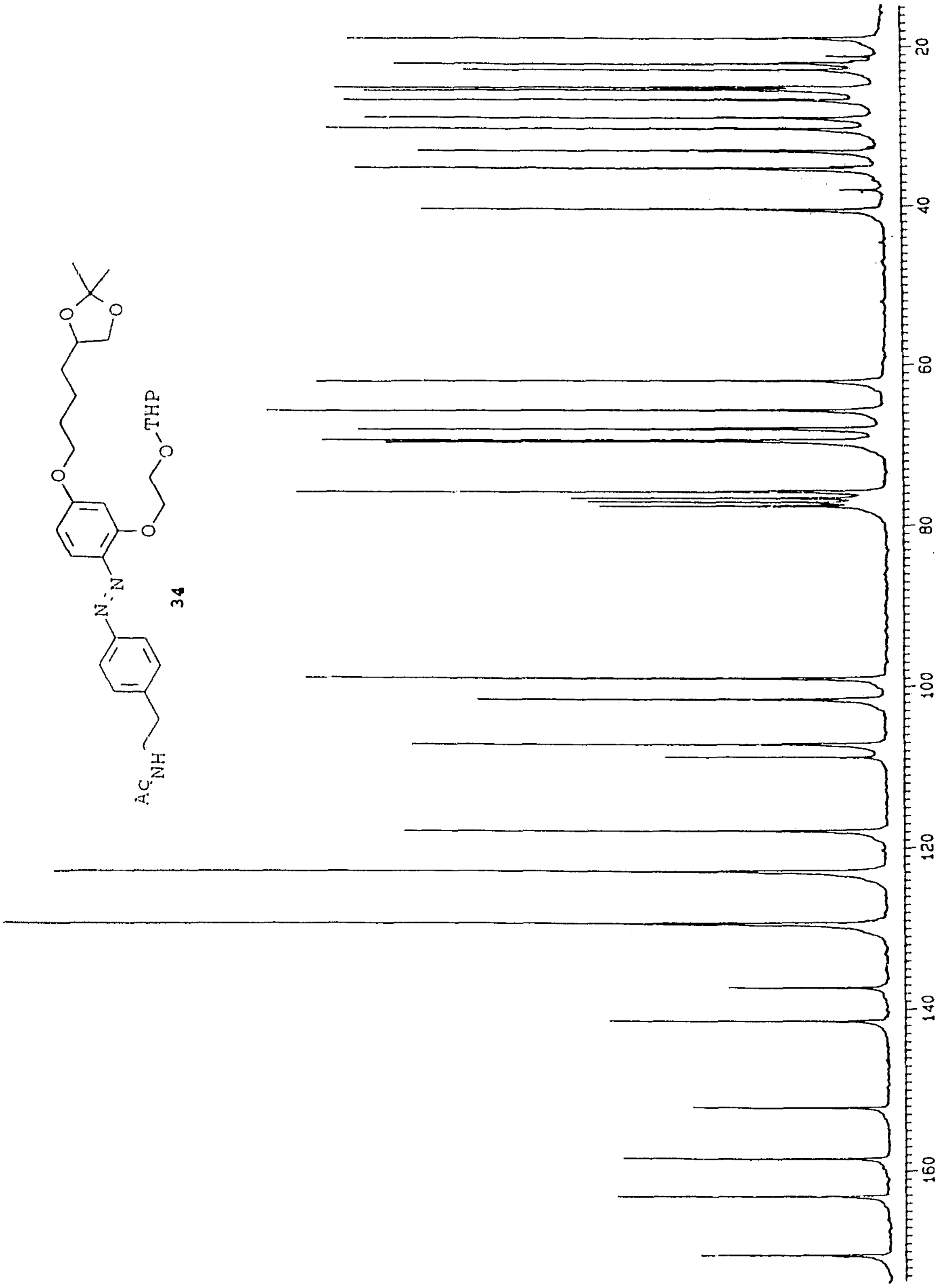

Figure 56. ^{13}C NMR spectrum of compound **34** in $CDCl_3$.

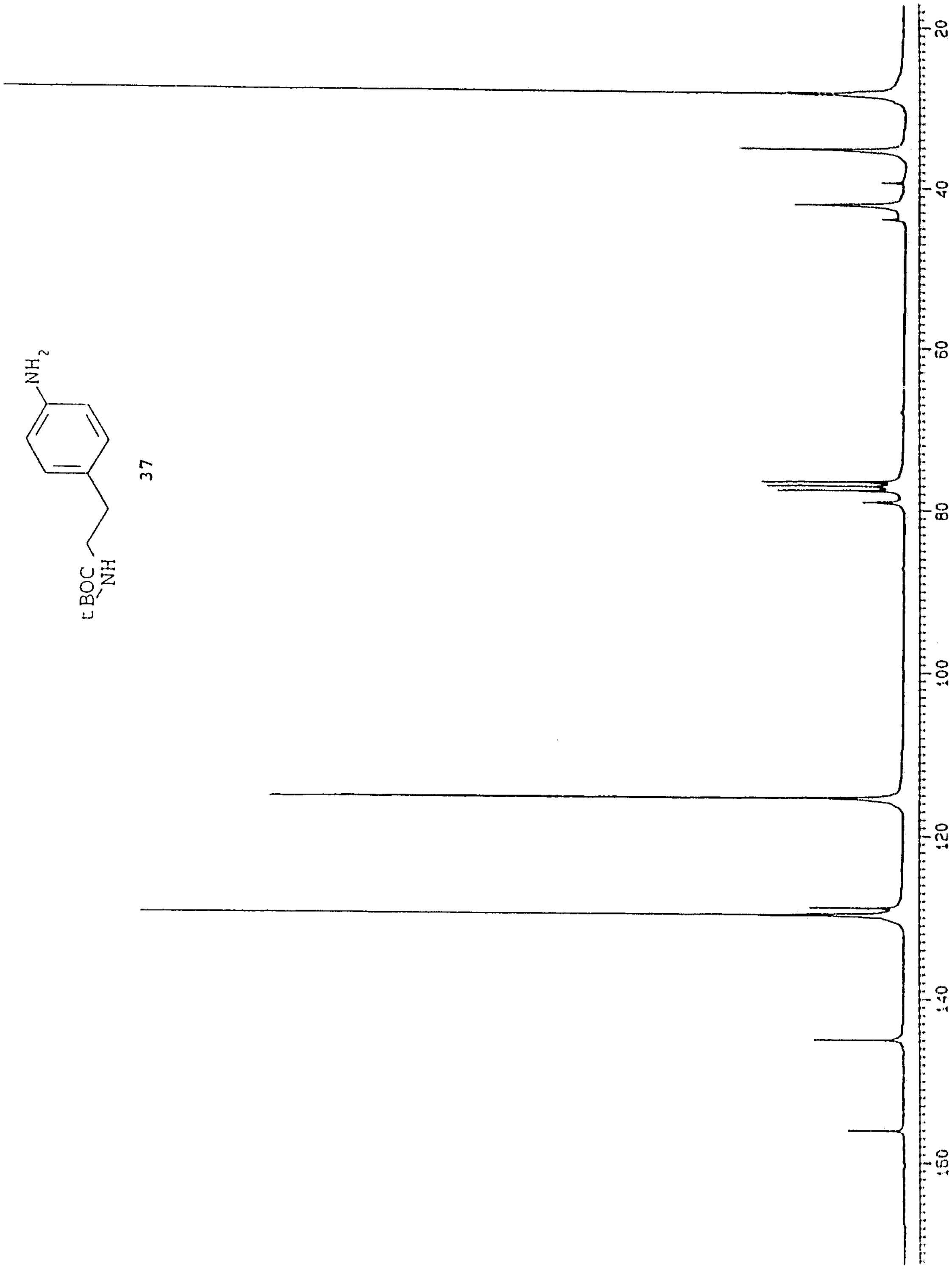

37

Figure 57. ^{13}C NMR spectrum of compound **37** in CDCl$_3$.

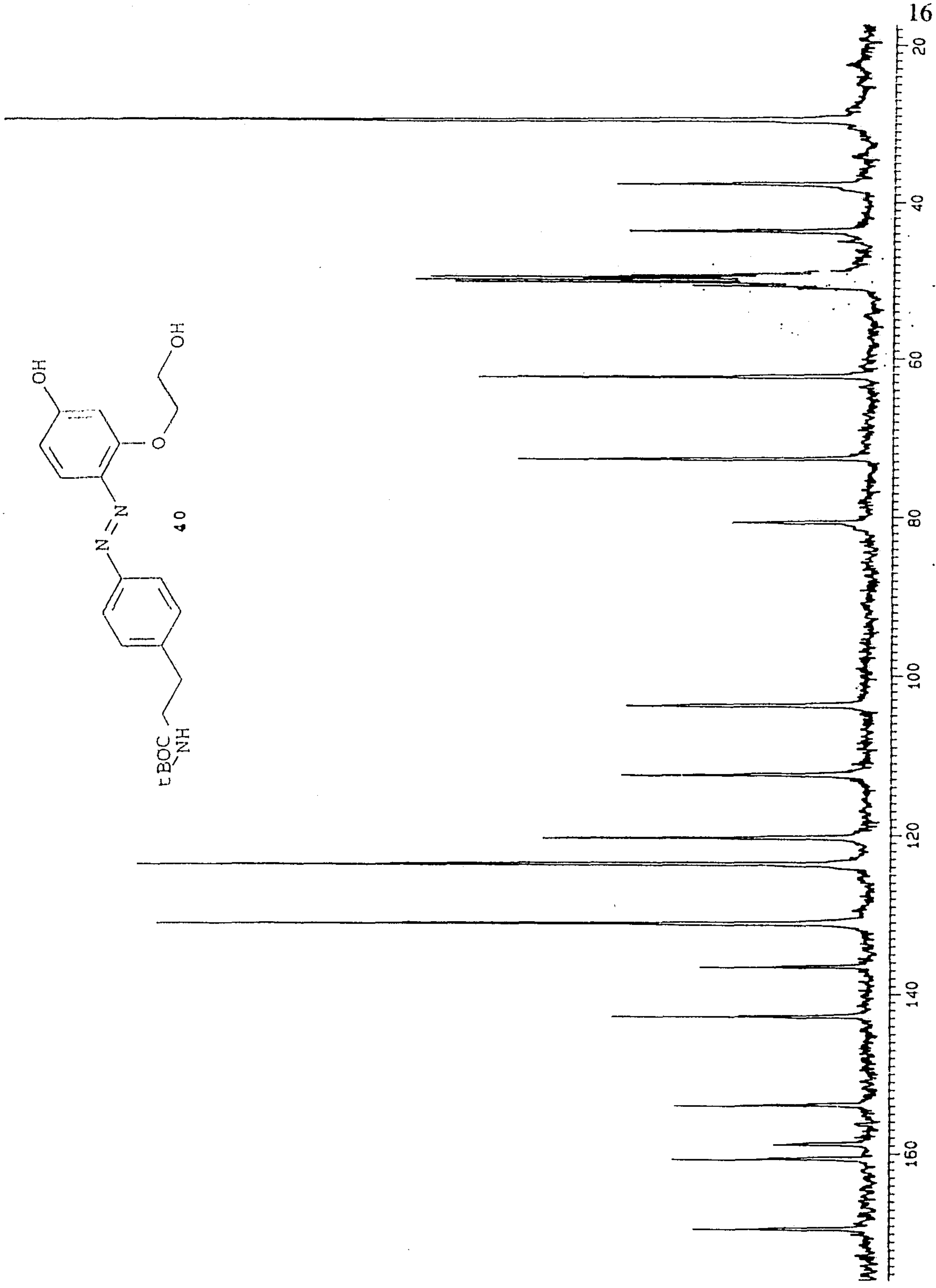

Figure 58. ^{13}C NMR spectrum of compound **40** in CD_3OD.

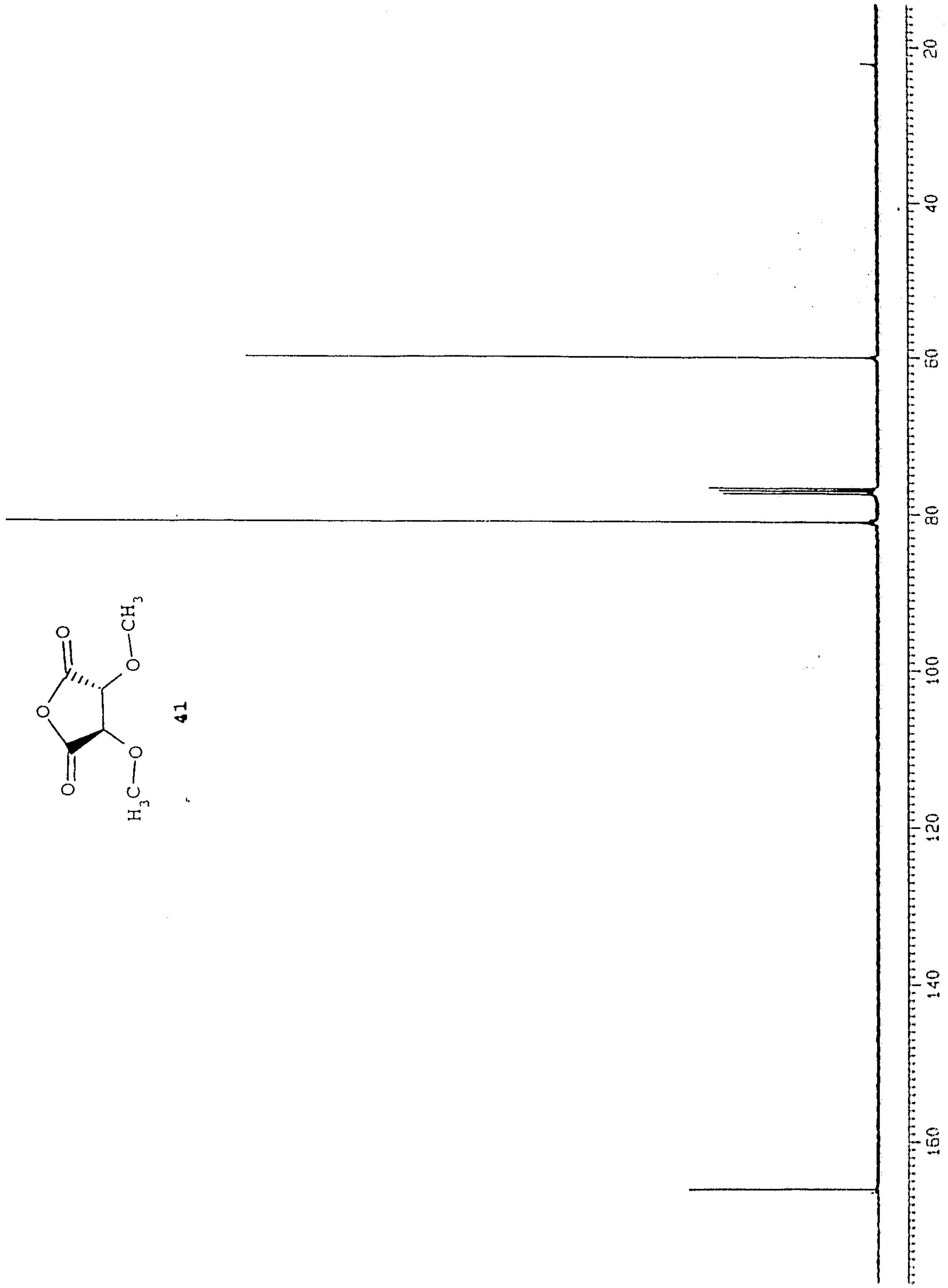

41

Figure 59. ^{13}C NMR spectrum of compound **41** in $CDCl_3$.

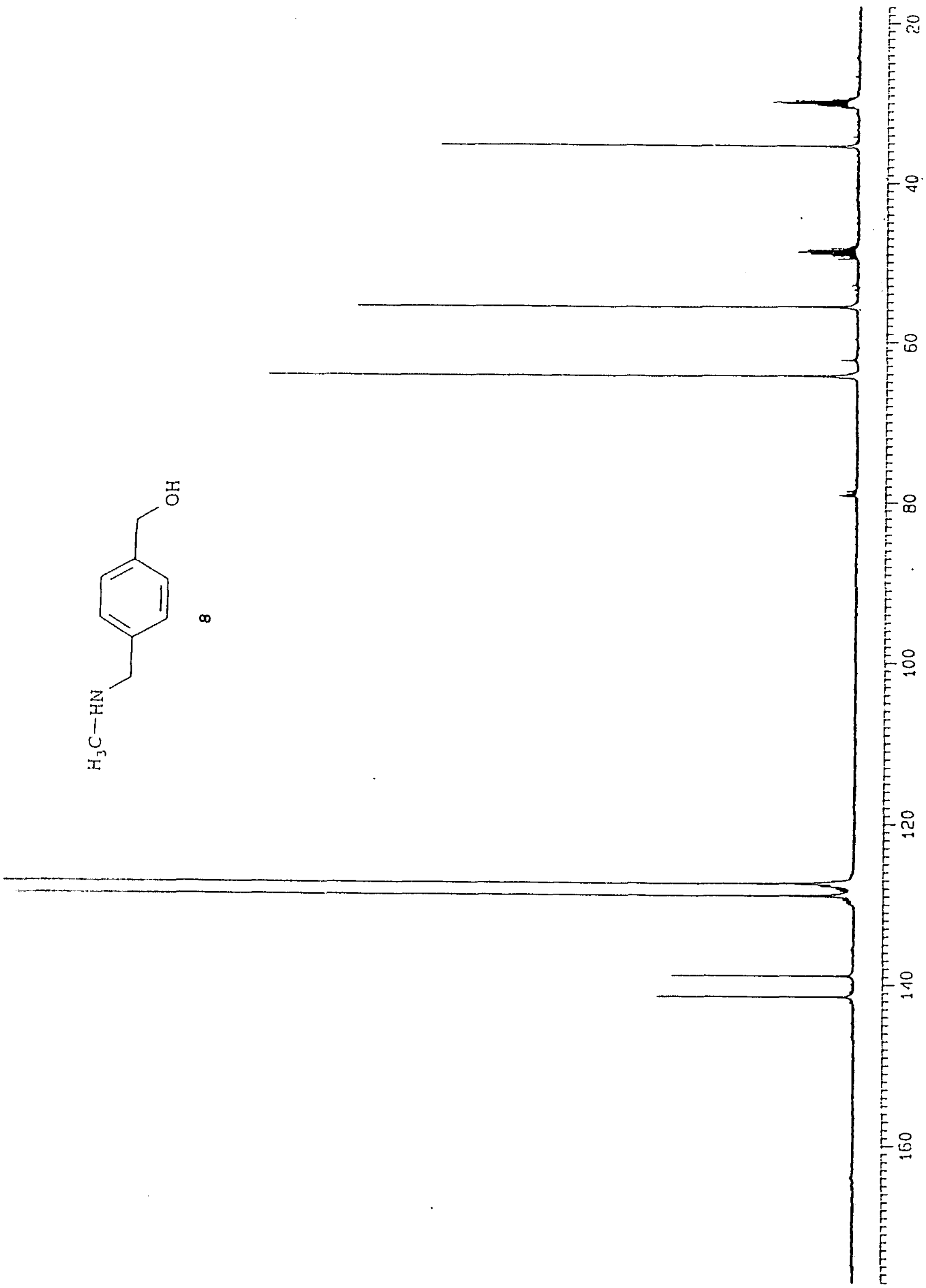

Figure 60. ^{13}C NMR spectrum of compound 8 in CD_3OD / acetone-d_6.

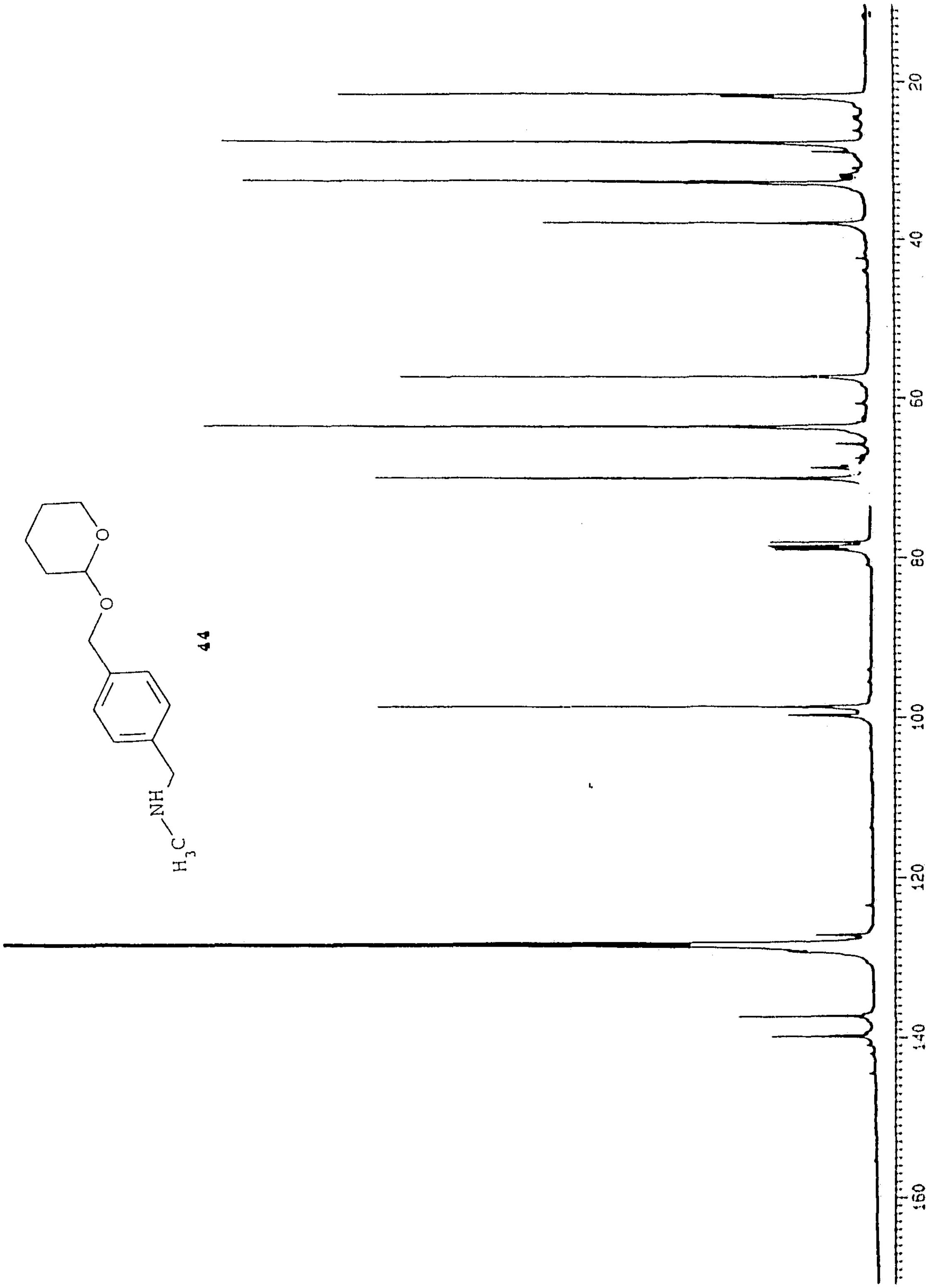

44

Figure 61. ^{13}C NMR spectrum of compound **44** in $CDCl_3$.

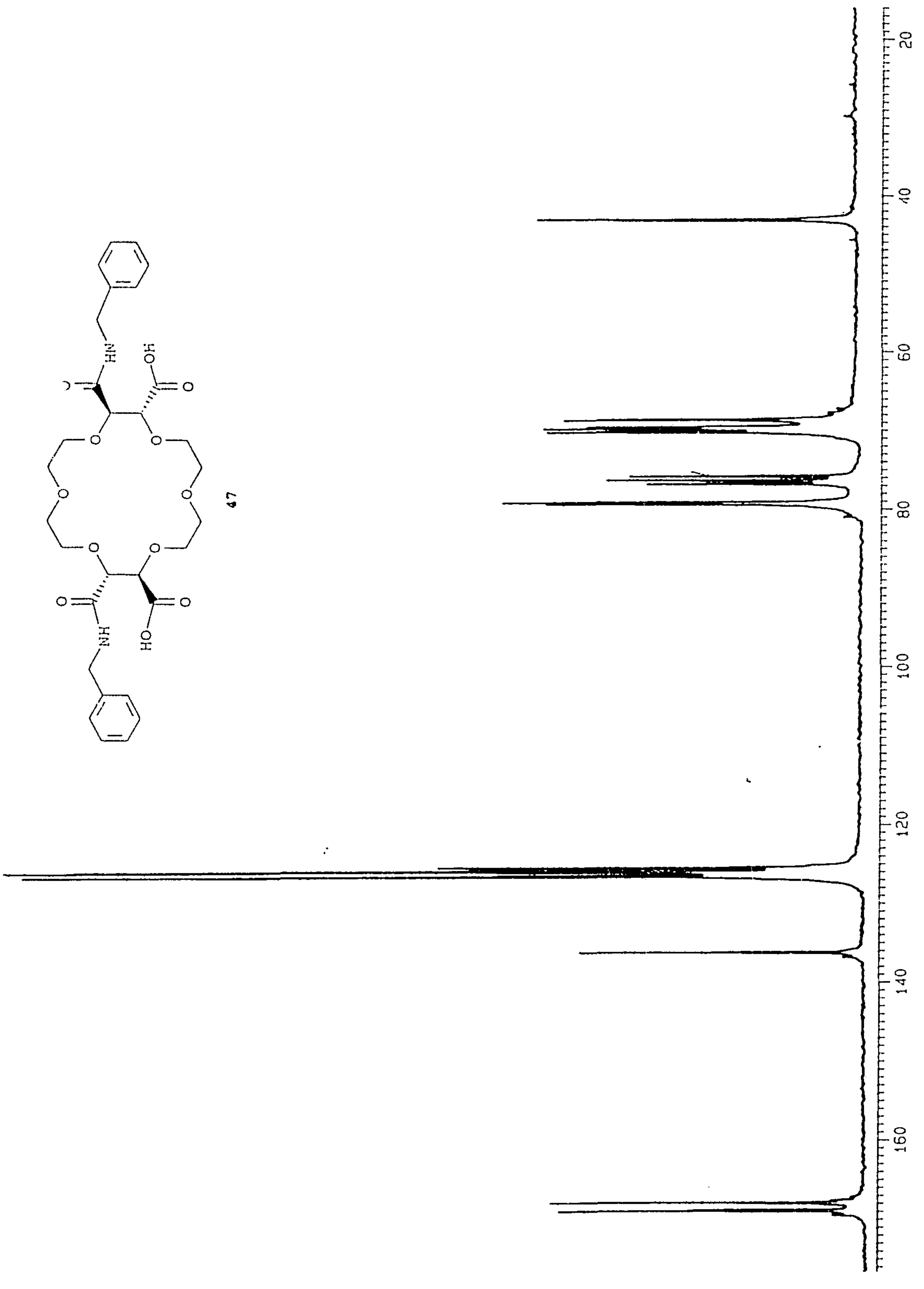

47

Figure 62. ^{13}C NMR spectrum of compound **47** in $CDCl_3$.

REFERENCES

1. (a) M.D. Houslay and K.K. Stanley, *Dynamics of Biological Membranes*, John Wiley and Sons, New York (1982). (b) R.N. Robertson, *The Lively Membranes*, Cambridge University Press, Cambridge (1983).

2. P.C. Jordan, *J. Phys. Chem.*, **91**, 6582 (1987).

3. (a) Y.A. Ovchinnikov, V.Y. Ivanov, and A.M. Skorb, *Membrane Active Complexones*, Elsevier, Amsterdam (1974). (b) J.N. Westley ed., *Polyether Antibiotics*, Marcel Dekker, New York (1982). (c) M. Dobler, *Ionophores and their structures*, J. Wiley and Sons, New York (1981).

4. T.M. Fyles, *Frontiers in Bioorganic Chemistry*, **1**, 71 (1990).

5. H. Tsukube, *Liquid Membranes: Chemical Applications*, T. Araki and H. Tsukube eds., CRC Press Inc., Boca Raton, Florida (1990). pp. 51 - 75.

6. P. Läuger, *J. Memb. Biol.*, **57**, 163 (1980) and references therein.

7. R. Henderson, J.M. Baldwin, T.A. Ceska, F. Zemlin, E. Beckmann, and K.H. Downing, *J. Mol. Biol.*, **213**, 899 (1990).

8. (a) D.W. Urry, *Topics in Current Chemistry*, **128** (1985), pp. 175 - 218. (b) B.A. Wallace and K. Ravikumar, *Science*, **241**, 182 (1988).

9. B. Roux and M. Karplus, *J. Am. Chem. Soc.*, **115**, 3250 (1993).

10. (a) A. Finkelstein and R. Holz, *Membranes*, G. Eisenman ed., Marcel Dekker, New York (1973), Vol. **2**, p. 377. (b) B. de Kruiiff and R.A. Demel, *Biochim. Biophys. Acta*, **339**, 37 (1974). (c) J. Bolard, *Biochim. Biophys. Acta*, **864**, 257 (1986).

11. T.M. Fyles and W.F. Van Straaten-Nijenhuis, *Ion Channel Models*, in *Comprehensive Supramolecular Chemistry*, D.N. Reinhoudt ed., Vol. **10**, in press.

12. C.J. Stankovic, S.H. Heinemann, and S.L. Schreiber, *J. Am. Chem. Soc.*, **112**, 3702 (1990).

13. G. Spach, Y. Merle, and G. Molle, *J. Chim. Phys. - Chim. Biol.*, **82**, 719 (1985).

14. A.W. Bernheimer and B. Rudy, *Biochim. Biophys. Acta*, **864**, 123 (1986).

15. K.S. Akerfeldt, J.D. Lear, Z.R.Wasserman, L.A. Chung, and W.F. Delgrado, *Acc. Chem. Res.*, **26**, 19 (1993).

16. M.S.P. Sansom, *Prog. Biophys. Mol. Biol.*, **55**, 139 (1991).

17. (a) T. Kunitake, *Ann. N.Y. Acad. Sci.*, **471**, 70 (1986). (b) J-H. Furhop and J. Mathieu, *Angew. Chem. Int'l. Ed'n. Engl.*, **23**, 100 (1984). (c) J-H. Furhop and U. Liman, *J. Am. Chem. Soc.*, **106**, 4643 (1984). (d) J-H. Furhop and D. Fritsch, *Acc. Chem. Res.*, **19**, 130 (1986). (e) F.M. Menger, D.S. Davis, R.A. Persichetti, and J-J. Lee, *J. Am. Chem. Soc.*, **112**, 2451 (1990). (f) F.M. Menger, *Angew. Chem. Int'l. Ed'n. Engl.*, **30**, 1086 (1991).(g) Y. Kobuke, K. Ueda, and M. Sokabe, *J. Am. Chem. Soc.*, **114**, 7618 (1992).

18. I. Tabushi, Y. Kuroda, and K. Yokota, *Tetrahedron Lett.*, **23**, 4601 (1982).

19. R.J.M. Nolte, A.J.M. Van Beijnen, J.G. Neeved, J.W. Zwinker, A.J. Verkley, and W. Drenth, *Isr. J. Chem.*, **24**, 297 (1984).

20. A. Nakano, Q. Xie, J.V. Mallen, L. Echegoyan and G.W. Gokel, *J. Am. Chem. Soc.*, **112**, 1287 (1990).

21. J.M. Lehn and P.G. Potvin, *Can. J. Chem.*, **66**, 195 (1988).

22. V.E. Charmichael, P.J. Dutton, T.M. Fyles, T.D. James, J.A. Swan, and M. Zojaji, *J. Am. Chem. Soc.*, **111**, 767 (1989).

23. (a) L. Jullien and J-M. Lehn, *Tetrahedron Lett.*, **29**, 3803 (1988). (b) L. Jullien and J-M. Lehn, *J. Incl. Phen. Mol. Recog. Chem.*, **12**, 55 (1992). (c) M.J. Pregel, L. Jullien, and J-M. Lehn, *Angew. Chem. Int'l. Ed'n. Engl.*, **31**, 1637 (1992). (d) J. Canceill, L. Jullien, L. Lacombe, and J-M. Lehn, *Helv. Chim. Acta*, **75**, 791 (1992). (e) L. Jullien, T. Lazrak, J. Canceill, L. Lacombe, and J-M. Lehn, *J. Chem. Soc, Perkin Trans. 2*, 3110 (1993).

24. (a) V. Ahsen, E. Yilmazer, M. Ertas, and Ö. Bekâroğlu, *J. Chem. Soc., Dalton Trans.*, 401 (1988). (b) N. Kobayashi and A.B.P. Lever, *J. Am. Chem. Soc.*, **109**, 7433 (1987).

25. N. Voyer, *J. Am. Chem. Soc.*, **113**, 1818 (1991).

26. A. Grove, M. Mutter, J.E. Rivier, and M. Montal, *J. Am. Chem. Soc.*, **115**, 5919 (1993).

27. K.S. Åkerfeldt, R.M. Kim, D. Camac, J.T. Groves, J.D. Lear, and W.F. De Grado, *J. Am. Chem. Soc.*, **114**, 9656 (1992).

28. T.D. James, *Doctoral Thesis*, University of Victoria, Victoria B.C., Canada (1991).

29. T.M. Fyles, T.D. James, A. Pryhitka, and M. Zojaji, *J. Org. Chem.*, **58**, 7456 (1993).

30. T.M. Fyles, T.D. James, and K.C. Kaye, *J. Am. Chem. Soc.*, **115**, 12315 (1993).

31. G.G. Cross, T.M. Fyles, T.D. James, and M. Zojaji, *Synlett.*, 449 (1993).

32. J.B. Hendrickson, *J. Am. Chem. Soc.*, **99**, 5439 (1977).

33. T.M. Fyles and R. Gandour, *J. Incl. Phen. Mol. Recog. Chem.*, **12**, 313 (1992).

34. P.J. Dutton, *Doctoral Thesis*, University of Victoria, Victoria B.C. Canada (1988).

35. (a) J-P. Behr, J-M. Girodeau, R.C. Hayward, J-M. Lehn, and J-P. Sauvage, *Helv. Chim. Acta*, **63**, 2096 (1980). (b) H. Dugas and M. Ptak, *J. Chem. Soc., Chem. Commun.*, 710 (1982). (c) H. Dugas, P. Keroack, and M. Ptak, *Can. J. Chem.*, **62**, 489 (1984).

36. G. Dijkstra, W.H. Kruizinga, and R.M. Kellogg, *J. Org. Chem.*, **52**, 4230 (1987).

37. J.H. Furhop, H.H. David, J. Mathieu, U. Liman, H.J. Winter, and E. Boeckema, *J. Am. Chem. Soc.*, **108**, 1795 (1986).

38. M. Zojaji, *Doctoral Thesis*, University of Victoria, Victoria B.C. Canada (1991).

39. L.M. Cameron, unpublished results.

40. K.C. Kaye, *Masters Thesis*, University of Victoria, Victoria B.C. Canada (1991).

41. *Single Channel Recording*, B. Sakmann and E. Neher eds., Plenum Press, New York (1983).

42. M.S.P. Sansom, unpublished results.

43. M. Hervé, B. Cybulska, C.M. Gary-Bobo, *European Biophysics Journal*, **12**, 121 (1985).

44. H.R. Mahler and E.H. Cordes, *Biological Chemistry*, 2nd Edn., Harper and Row, New York (1971).

45. G. Eisenman, *Ion Selective Electrodes*, National Bureau of Standards Special Publication **314** (1969) pp 1 - 54.

46. B. Hille, *Ionic Channels of Excitable Membranes*, Sinauer Associates Inc., Sunderland, Massachusetts (1984).

47. (a) J.F.W. McOmie ed., *Protective Groups in Organic Chemistry*, Plenum Press, London (1973). (b) T.W. Greene, *Protective Groups in Organic Synthesis*, J. Wiley and Sons, New York (1981).

48. (a) H.O. Kalinowski, D. Seebach, and G. Crass, *Angew. Chem. Int'l. Ed'n. Engl.*, **14**, 762 (1975). (b) J.M. Girodeau, J.M. Lehn and J.P. Sauvage, *Angew. Chem. Int'l. Ed'n. Engl.*, **14**, 764 (1975).

49. (a) V.V. Suresh, *Doctoral Thesis*, University of Victoria, Victoria B.C. Canada (1991). (b) T.M. Fyles, V.V. Suresh, F.R. Fronczek, and R.D. Gandour, *Tetrahedron Lett.*, **31**, 1101 (1990).

50. (a) W. Rettig, *Modern Models of Bonding and Delocalization*, J.F. Liebman and A. Greenberg eds., VCH Publishers (1988) p. 229. (b) V. Balzani and F. Scandola, *Supramolecular Chemistry*, Ellis Horwood Series in Physical Chemistry - Photo- and Radiation Chemistry, T.J. Kemp series ed., (1991) p. 202.

51. R.C. Bertelson, *Photochromism*, G.H. Brown ed., Wiley (1971) p. 45.

52. H. Rau, *Photoisomerization of Azobenzenes*, in "Photochemistry and Photophysics", J.F. Rabek ed., CRC Press, Boca Raton, Florida, (1990).

53. (a) T. Asano, T. Okada, S. Shinkai, K. Shigematsu, Y. Kusano, and O. Manabe, *J. Am. Chem. Soc.*, **103**, 5161 (1981). (b) T. Asano and T. Okada, *J. Org. Chem.*, **49**, 4387 (1984).

54. H. Rau and E. Lüddecke, *J. Am. Chem. Soc.*, **104**, 1616 (1982).

55. H. Rau, *J. Photochem.*, **26**, 221 (1984).

56. S. Monti, G. Orlandi, and P. Palmieri, *Chemical Physics*, **71**, 87 (1982).

57. (a) S. Shinkai, H. Kinda, and O. Manabe, *J. Am. Chem. Soc.*, **104**, 2933 (1982). (b) J-I. Anzai, Y. Suzuki, A. Ueno, and T. Osa, *Isr. J. Chem.*, **26**, 60 (1985).

58. K. Kano, Y. Tanaka, T. Ogawa, M. Shimomura, Y. Okahata, and T. Kunitake, *Chem. Lett.*, 421 (1980).

59. Y. Okahata, H.J. Lim, and S. Hachiya, *J. Chem. Soc. Perkin Trans. II*, 989 (1984).

60. S. Shinkai, H. Kinda, and O. Manabe, *J. Am. Chem. Soc.*, **104**, 2933 (1982).

61. S. Shinkai, T. Minami, Y. Kusano, and O. Manabe, *J. Am. Chem. Soc.*, **105**, 1851 (1983).

62. S. Shinkai, Y. Honda, K. Ueda, and O. Manabe, *Isr. J. Chem.*, **24**, 302 (1984).

63. S. Shinkai, T. Nakaji, Y. Nishida, T. Ogawa, and O. Manabe, *J. Am. Chem. Soc.*, **102**, 5860 (1980).

64. S. Shinkai, T. Kuono, Y. Kusano, and O. Manabe, *J. Chem. Soc. Perkin Trans. I*, 2741 (1982).

65. (a) S. Shinkai, K. Miyazaki, and O. Manabe, *Angew. Chem. Int'l. Ed'n. Engl.*, **24**, 866 (1985). (b) S. Shinkai, K. Miyazaki, and O. Manabe, *J. Chem. Soc. Perkin Trans. I*, 449 (1987).

66. (a) S. Shinkai, T. Ogawa, Y. Kusano, O. Manabe, K. Kikukawa, T. Goto, and T. Matsuda, *J. Am. Chem. Soc.*, **104**, 1960 (1982). (b) S. Shinkai, K. Shigematsu, M. Sato, and O. Manabe, *J. Chem. Soc. Perkin Trans. I*, 2735 (1982).

67. S. Shinkai, T. Minami, Y. Kusano, and O. Manabe, *J. Am. Chem. Soc.*, **104**, 1967 (1982).

68. S.Shinkai, T. Nakaji, T. Ogawa, K. Shigematsu, and O. Manabe, *J. Am. Chem. Soc.*, **103**, 111 (1981).

69. (a) S. Shinkai, M. Ishihara, K. Ueda, and O. Manabe, *J. Chem. Soc., Chem. Commun.*, 727 (1984). (b) S. Shinkai, M. Ishihara, K. Ueda, and O. Manabe, *J. Inclusion Phenomena*, **2**, 111 (1984). (c) S. Shinkai, M. Ishihara, K. Ueda, and O. Manabe, *J. Chem. Soc., Perkin Trans. II*, 511 (1985). (d) S. Shinkai, T. Yoshida, K. Miyazaki, and O. Manabe, *Bull. Chem. Soc. Jap.*, **60**, 1819 (1987).

70. *Rodd's Chemistry of Carbon Compounds*, 2nd Edn., S. Coffey ed., Vol. III Part C, Elsevier, Amsterdam (1973) p. 136.

71. J.P. Behr, C.J. Burrows, R. Heng, and J.M. Lehn, *Tetrahedron Lett.*, **26**, 215 (1985).

72. Ref. 70, p. 88.

73. Ref. 70, p. 21.

74. Ref. 70, p. 151.

75. Ref. 70, p. 152.

76. (a) G.L. Nelson and E.A. Williams, *Prog. Phys. Org. Chem.*, **12**, 229 (1976). (b)E. Pretsch, P. Clerc, J. Seibl, and W. Simon, *Tables of Spectral Data for Structure Determination of Organic Compounds*, 2nd Edn., Springer-Verlag, (1989).

77. L.W. Reeves, *Can. J. Chem.*, **38**, 748 (1960).

78. J.H. Bowie, G.E. Lewis, and R.G. Cooks, *J. Chem. Soc. B*, 621 (1967).

79. (a) J. Badger and R.G. Buttery, *J. Chem. Soc.*, 2243 (1954). (b) M.M. Shemyakin, V.I. Maimind, and B.K. Vaichunaite, *Izvest. Akad. Nauk S.S.S.R., Otdel. Khim. Nauk*, **1960**, 866 (1960) (C.A. **54**, 24474 (1960)). (c)M.M. Shemyakin, Ts.E. Agadzhanyan, V.I. Maimind, R.V. Kudryatsev, and D.N. Kursanov, *Doklady Akad. Nauk S.S.S.R.*, **135**, 346 (1960) (C.A. **55**, 11337 (1961)).

80. S. Oae, T. Maeda, and S. Kozuka, *Bull. Chem. Soc. Jap.*, **44**, 2498 (1971).

81. (a) H. Rau, *Angew. Chem. Int'l. Ed'n. Engl.*, **12**, 224 (1973). (b) J. Ronayette, R. Arnaud, P. Lebourgeois, and J. Lemaire, *Can. J. Chem.*, **52**, 1848 (1974).

82. J. Chin, *Acc. Chem. Res.*, **24**, 145 (1991).

83. J. Chin, M. Banaszczyk, V. Jubian, and X. Zhou, *J. Am. Chem. Soc.*, **111**, 186 (1989).

84. A.M. Calafat and L.G. Marzilli, *Inorg. Chem.*,**31**, 1719 (1992).

85. R.S. Brown, unpublished results.

86. K. Ziegler, H. Eberle, and H. Ohlinger, *Liebigs Ann. Chem.*, **504**, 94 (1933).

87. J.P. Behr, J.M. Lehn, D. Moras, and J.C. Thierry, *J. Am. Chem. Soc.*, **103**, 701 (1981).

88. D.M. Whitfield, *Doctoral Thesis*, University of Victoria, Victoria B.C., Canada (1983).

89. G.G. Cross, unpublished results.

90. F.M. Jones III and E.M. Arnett, *Thermodynamics of Ionization of Aliphatic Amines in Water*, in Progress in Physical Organic Chemistry, Volume 11, A. Streitweiser Jr. and R.W. Taft eds., Interscience (1974).

91. D.P.N. Satchell and I.I. Secemski, *J. Chem. Soc. B*, 1013 (1970).

92. J. March, *Advanced Organic Chemistry*, 3d Edn., John Wiley and Sons, New York, (1985) p. 916.

93. Ref. 91, p. 690.

94. (a) Ref. 91, p. 310. (b) T.W.G. Solomons, *Organic Chemistry*, 5th Edn., John Wiley and Sons, New York (1992) p. 236.

95. G.A. Rogers and T.C. Bruice, *J. Am. Chem. Soc.*, **96**, 2463 (1974).

96. (a) A.R. Ferscht and A.J. Kirby, *J. Am. Chem. Soc.*, **89**, 5960 (1967); **90**, 5818 (1968). (b) A.C. Satterthwaite and W.P. Jencks, *J. Am. Chem. Soc.*, **96**, 7018 (1974).

97. S.L. Johnson, *Adv. Phys. Org. Chem.*, **5**, 237 (1967) pp. 284 - 289.

98. D.P.N. Satchell and I.I. Secemski, *J. Chem. Soc. B*, 130 (1969).

99. I.H. Pitman and T. Higuchi, *J. Org. Chem.*, **40**, 378 (1975).

100. D.F. de Tar and C. Delahunty, *J. Am. Chem. Soc.*, **105**, 2734 (1983).

101. L.A. Frederick, T.M. Fyles, N.P. Gurprasad, and D.M. Whitfield, *Can. J. Chem.*, **59**, 1724 (1981).

102. (a)J-P. Behr and J-M. Lehn, *Helv. Chim. Acta*, **63**, 2112 (1980). (b)W. Bussman, J-M. Lehn, U. Oesch, P. Plumeré, and W. Simon, *Helv. Chim. Acta*, **64**, 657 (1981). (c) J-P. Behr, J-M. Lehn and P. Vierling, *Helv. Chim. Acta*, **65**, 1853 (1982). (d) J-P. Behr, M. Bergdoll, B. Chevrier, P. Dumas, J-M Lehn, and D. Moras, *Tetrahedron Lett.*, **28**, 1989 (1987).

103. A. Basak and H. Dugas, *Tetrahedron Lett.*, **27**, 3 (1986).

104. T.M. Fyles, C.A. McGavin, and D.M. Whitfield, *J. Org. Chem.*, **49**, 753 (1984).

105. P. Tundo and J.H. Fendler, *J. Am. Chem. Soc.*, **102**, 1760 (1980).

106. F. Diederich, *Cyclophanes*, Monographs in Supramolecular Chemistry, J.F. Stoddard ed., The Royal Society of Chemistry, Cambridge (1991).

107. C.D. Gutsche, *Calixarenes*, Monographs in Supramolecular Chemistry, J.F. Stoddard ed., The Royal Society of Chemistry, Cambridge (1989). pp 130 - 131.

108 Ref. 106, Section 2.4.

109. For example: (a) I. Tabushi, Y. Kuroda, and T. Mizutani, *J. Am. Chem. Soc.*, **108**, 4514 (1986). (b) R.C. Petter and J.S. Salek, *J. Am. Chem. Soc.*, **109**, 7897 (1987). (c) K. Takahashi, Y. Ohtsuka, and K. Hattori, *Chem. Lett.*, 2227 (1990). (d) M. Fukushima, T. Osa, and A. Ueno, *J. Chem. Soc., Chem. Commun.*, 15 (1991).

110. H. Diehl and J. Ellingboe, *Anal. Chem.*, **32**, 1120 (1960).

111. A. McKillop, R.A. Raphael, and E.C. Taylor, *J. Org. Chem.*, **35**, 1670 (1970).

112. P.A. Cruikshank and M. Fishman, *J. Org. Chem.*, **34**, 4060 (1969).

113. I. Felner and K. Schenker, *Helv. Chim. Acta*, **53**, 754 (1970).

114. R.V. Hoffman and J.M. Salvador, *J. Org. Chem.*, **57**, 4487 (1992).

115. T. Nishiguchi and Y. Iwakura, *J. Org. Chem.*, **35**, 1591 (1970).

116. H. Nakata, Y. Suzuki, M. Shibata, K. Takahashi, H. Konishi, N. Takeda, and A. Tatematsu, *Org. Mass Spectr.*, **25**, 649 (1990).

VITA

Surname: Cross

Given Names: Gordon Grant

Place of Birth: Deep River, Ontario

Date of Birth: February 5, 1951

Educational Institutions Attended

University of Toronto	1968 to 1973
University of Alberta	1973 to 1979

Degrees Awarded

B.Sc.	University of Toronto	1973
M.Sc.	University of Alberta	1979

Honours and Awards

E.R. Wood Memorial Scholarship (Victoria College, University of Toronto) 1968 - 1972
National Research Council Postgraduate Scholarship 1975 - 1978
British Columbia Science Council STARS Award 1989 - 1990
British Columbia Science Council STARS Award 1990 - 1991 (declined)
University of Victoria Fellowship 1990 - 1991

Publications

J.W. Bunting, J. Murphy, C.D. Meyers, and G.G. Cross, "The Hydrolysis of Benzoate Esters by Carboxypeptidase A and the pH Rate Profile for the Hydrolysis of *O*-Hippuryl-L-3-phenyllactic Acid", *Can. J. Chem.*, **52**, 2648 (1974).

G.G. Cross, "Synthesis and Acid Catalysed Hydrolysis of Adenine Nucleosides with an Acyclic Sugar", *M.Sc. Thesis*, University of Alberta (1979).

G.G. Cross, A. Fischer, G.N. Henderson, and T.A. Smyth, "*ipso* Nitration. XXIV. Nitration of 2-methylphenols. Formation and rearrangement of 6-methyl-6-nitrocyclohexa-2,4-dienones", *Can. J. Chem.*, **62**, 1446 (1984).

G.G. Cross, A. Fischer, and G.N. Henderson, "*ipso* Nitration. XXV. Nitration of di-*tert*-butylphenols, α-(3,5-di-*tert*-butylphenoxy)isobutyric acid, and 3,5-di-*tert*-butylphenoxyacetic acid: Formation of nitrodienones and nitrodienes containing a secondary nitro group", *Can. J. Chem.*, **62**, 2803 (1984).

R.G. Clewley, G.G. Cross, A. Fischer, and G.N. Henderson, "Formation of 4-Halo-4-nitrocyclohexa-2,5-dienones on Nitration of p-Halophenols and p-Halophenyl Acetates", *Tetrahedron*, **45**, 1299 (1988).

G.G. Cross, T.M. Fyles, T.D. James, and M. Zojaji, "Design and Synthesis of Artificial Ion Channels", *Synlett*, 449 (1993).

G.G. Cross, T.M. Fyles, and V.V. Suresh, "Ion Selective and Coated Wire Electrodes Containing Polymer Immobilized Ionophores Blended with Poly(vinyl chloride)", *Talanta*, **41**, 1589 (1994).

G.G. Cross, T.M. Fyles, P.J. Montoya-Pelaez, W.F. van Straaten-Nijenhuis, and X. Zhou, "Design, Synthesis, and Characterization of Gated Ion Transporters", in *Interfacial Design and Chemical Sensing*, ACS Symposium Series 561, T.E. Mallouk and D.J. Harrison eds. (1994).

PARTIAL COPYRIGHT LICENSE

I hereby grant the right to lend my thesis to users of the University of Victoria Library, and to make single copies only for such users or in response to a request from the Library of any other university, or similar institution, on its behalf or for one of its users. I further agree that permission for extensive copying of this thesis for scholarly purposes may be granted by me or a member of the University designated by me. It is understood that copying or publication of this thesis for financial gain shall not be allowed without my written permission.

Title of Thesis: Synthetic Study of a Photogated Ion Channel

Author:

GORDON GRANT CROSS

Nov. 16, 1994

DATE